



I. Synthesis of C4-Modified Tetracyclines II. Aldolizations of Pseudoephedrine Glycinamide and Applications Toward the Synthesis of Monocyclic β -Lactam Antibiotics

Citation

Sussman, Robin Judith. 2015. I. Synthesis of C4-Modified Tetracyclines II. Aldolizations of Pseudoephedrine Glycinamide and Applications Toward the Synthesis of Monocyclic β -Lactam Antibiotics. Doctoral dissertation, Harvard University, Graduate School of Arts & Sciences.

Permanent link

<http://nrs.harvard.edu/urn-3:HUL.InstRepos:17467383>

Terms of Use

This article was downloaded from Harvard University's DASH repository, and is made available under the terms and conditions applicable to Other Posted Material, as set forth at <http://nrs.harvard.edu/urn-3:HUL.InstRepos:dash.current.terms-of-use#LAA>

Share Your Story

The Harvard community has made this article openly available.
Please share how this access benefits you. [Submit a story](#).

[Accessibility](#)

I. Synthesis of C4-Modified Tetracyclines

II. Aldolizations of Pseudoephedrine Glycinamide and Applications

Toward the Synthesis of Monocyclic β -Lactam Antibiotics

A dissertation presented

by

Robin Judith Sussman

to

The Department of Chemistry and Chemical Biology

in partial fulfillment of the requirements

for the degree of

Doctor of Philosophy

in the subject of

Chemistry

Harvard University

Cambridge, Massachusetts

May 2015

© 2015 – Robin Judith Sussman

All rights reserved.

I. Synthesis of C4-Modified Tetracyclines

II. Aldolizations of Pseudoephedrine Glycinamide and Applications

Toward the Synthesis of Monocyclic β -Lactam Antibiotics

Abstract

Part one of this thesis describes the production of C4-modified tetracycline derivatives. Our synthetic strategy originally targeted SF2575, a C4-oxygenated tetracycline analog with antiproliferative properties, but was later amended to target antibacterial C4-oxygenated minocycline analogs. The C4-modified tetracyclines were accessed utilizing a strategy based on the Myers' platform to 6-deoxytetracyclines (Michael–Claisen cyclization between AB enone **71** and D-ring phenyl esters **44** or **84**) in addition to the 4th generation route to tetracycline key AB enone (Michael–Claisen cyclization between B-ring enone **8** and isoxazole **21**). The crucial enabling step along this route was the C4-epimerization of Boc bis-carbonate **82** to Boc bis-carbonate **83**. Five C4-modified tetracyclines were synthesized and their antibiotic properties were assessed.

Part two of this thesis describes the development of a new chiral glycine equivalent for aldol reactions, pseudoephedrine glycinamide ((*R,R*)-**179**), and an application of this methodology toward the production of C4-disubstituted monocyclic β -lactam antibiotics. Asymmetric aldolization of pseudoephedrine glycinamide with aldehydes and ketones produces *syn*- β -hydroxy- α -amino amides **180** with high diastereoselectivities and without the use of protecting groups. These aldol adducts can be transformed into enantiomerically enriched alcohols, ketones, and carboxylates, many of which enable powerfully simplified syntheses of various antibiotics.

Utilization of the newly developed methodology enabled access to β,β' -disubstituted- β -hydroxy- α -amino acids. Elaboration of these substrates provided novel C4-disubstituted monobactam analogs, an underrepresented class of β -lactam antibiotics. Four C4-disubstituted monocyclic β -lactam antibiotic candidates were synthesized and their antibiotic activities were assessed.

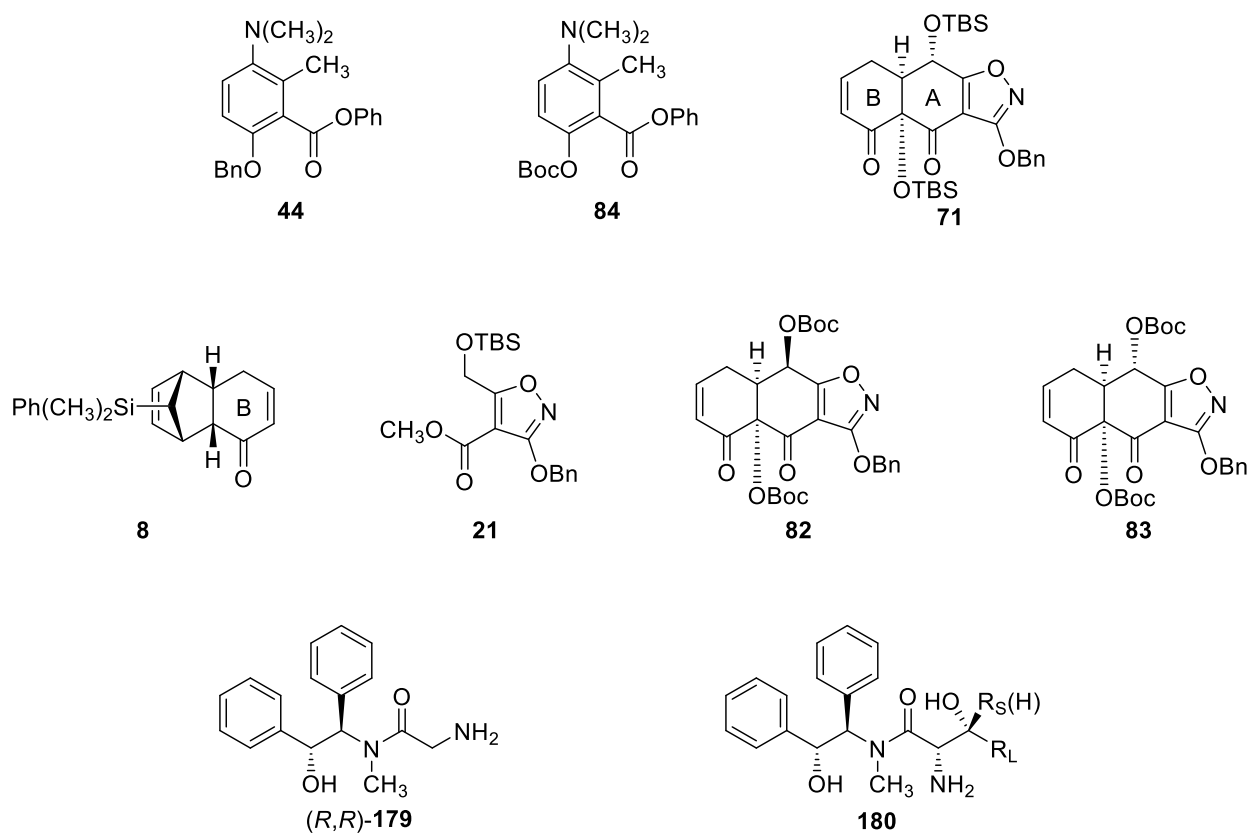


Table of Contents

Abstract	iii
Table of Contents	v
Acknowledgements	viii
List of Abbreviations	x
Chapter 1: Studies toward SF2575, a Tetracycline with Antiproliferative Activity	1
Introduction	2
Biological Activity	3
Structural Differences and Implications for Bioactivities	3
Synthetic Approaches to the Tetracyclines	5
Retrosynthetic Analysis of the SF2575 Core	10
Literature Precedent: Non-stabilized Phthalides in Michael–Claisen	
Cyclizations	12
Synthesis of SF2575 AB Enone 20	16
Attempted Michael–Claisen Cyclizations	19
Chapter 2: A New Direction: Synthesis of C4-Dedimethylamino-C4-Oxygenated	
Minocycline Analogs	25
Chemical Transformations of the 4-Position of the Tetracyclines	26
Potential Implications for Biological Activity	32
New Strategy: Epimerization at C4 and Synthesis of AB Enone 71	37
Synthesis of Analogs	41
Antibacterial Activity	44
Conclusions	46

Experimental Information	47
X-ray Data	92
Chapter 3: Pseudoephedrine Glycinamide as a Chiral Glycine Equivalent in Aldol	
Reactions	100
Introduction: β-Hydroxy-α-Amino Acids	101
An Overview on Asymmetric Aldol Reactions with Glycine	103
Synthesis of Pseudoephedrine Glycinamide	118
Aldolizations of Pseudoephedrine Glycinamide	120
Transformations of the Aldol Products	126
Transformations of the Carboxylate Products	131
Experimental Information	132
X-ray Data	188
Chapter 4: Synthesis of Monobactams through the Aldolization of Pseudoephedrine	
Glycinamide	200
Monocyclic β-Lactams (Monobactams)	201
Synthesis of C4-Disubstituted Monocyclic β-Lactams	210
Antibacterial Activity	216
Conclusions	218
Experimental Information	219
Appendix A. Catalog of Spectra	245

For all those who believed in me.

Acknowledgments

First, I would like to express my gratitude toward my research advisor, Professor Andrew Myers. Without his patience and guidance, I would not be presenting this thesis to you. His dedication to excellence and commitment to devoting resources to study challenging and relevant problems has directly shaped my experience. Additionally, he has taught me about the proper way to conduct research in a synthetic organic chemistry laboratory and I will carry those lessons with me as I continue in this field. I would also like to thank Professors Stuart Schreiber and Eric Jacobsen for serving on my Graduate Advising Committee and providing advice on life's challenges beyond the walls of the laboratory. I also owe a great debt of gratitude to my undergraduate advisor, Professor Barry Snider, who found a place for me in his group and encouraged me to pursue a graduate school degree. One of his graduate students, Olga Barykina, served as my first mentor and I am grateful for her guidance and support as I began to take an interest in synthetic organic chemistry.

The Myers group has been a wonderful place to learn, conduct research, engage in thoughtful conversations, and informally call home for the past six years. I am lucky to have been surrounded by colleagues and friends who share my excitement and interest in science. I enjoyed working with Dr. Dave Kummer, Dr. Amelie Dion, Dr. Peter Wright, Dr. Jonathan Mortison and Fan Liu on Team Tetracycline and Dr. Ian Seiple, Ziyang Zhang, Jaron Mercer and Claire Harmange on Team Pseudoephedrine Glycinamide. I am especially fortunate to have been able to share my work- and desk-space with two of the brightest chemists, Chong Si and Matthew Mitcheltree. Their patience with my never-ending stream of questions cannot be overstated. I gratefully acknowledge Dr. Dave Kummer for helping me settle in to graduate school and mentor me

through my first year and I am deeply indebted to Alex Zhurakovskiy, Fan Liu and Matthew Mitcheltree for reading and editing this thesis.

I would be remiss to not include acknowledgment of my family, especially my parents Phil and Janis Sussman, whose love and support has enabled me to complete this journey. Their patience and constant words of encouragement inspired me to continue and to exemplify my grandfather's favorite motto: "Keep up the good work!"

List of Abbreviations

Å	angstrom
A	adenine
Ac	acetyl
acac	acetylacetonate
<i>allo</i>	diastereomer (amino acid)
aq	aqueous
9-BBN	9-borabicyclo[3.3.1]nonane
Bn	benzyl
Boc	<i>tert</i> -butylcarbonate
Bu	butyl
C	cytosine
CAM	aqueous ceric ammonium molybdate solution
Cbz	carboxybenzyl
CDI	1,1'-carbonyldiimidazole
<i>cis</i>	<i>Lat.</i> , on the same side
cm ⁻¹	wavenumber
D	dextrorotatory
DABCO	1,4-diazabicyclo[2.2.2]octane
DBU	1,8-diazabicyclo[5.4.0]undec-7-ene
DCC	1,3-dicyclohexylcarbodiimide
de	diastereomeric excess
DEAD	diethyl diazenedicarboxylate

DIPEA	diisopropylethylamine
DMAP	4- <i>N,N</i> -dimethylaminopyridine
DMB	dimethoxybenzyl
DMF	<i>N,N</i> -dimethylformamide
DMSO	dimethyl sulfoxide
DNA	deoxyribonucleic acid
dppf	1,1'-bis(diphenylphosphino)ferrocene
dr	diastereomeric ratio
<i>E</i>	<i>Ger.</i> , entgegen
EDC	<i>N</i> -(3-dimethylaminopropyl)- <i>N'</i> -ethylcarbodiimide
ee	enantiomeric excess
ent-	enantiomeric
epi-	epimeric
equiv	equivalent
ESI	electrospray ionization
Et	ethyl
FDA	Food and Drug Administration
FTIR	Fourier transform infrared
G	guanine
g	gram
h	hour
HMPA	hexamethylphosphoramide
HPLC	high-pressure liquid chromatography

HRMS	high-resolution mass spectrometry
Hz	Hertz
IC ₅₀	fifty-percent maximal inhibitory concentration
<i>J</i>	coupling constant
KDA	potassium diisopropylamide
KHMDS	potassium hexamethyldisilazide
λ	wavelength
L	liter; levorotatory
LDA	lithium diisopropylamide
LiHMDS	lithium hexamethyldisilazide
M	molar
mg	milligram
μ g	microgram
MHz	megahertz
MIC	minimum inhibitory concentration
min	minute
mL	milliliter
μ L	microliter
mM	millimolar
μ M	micromolar
<i>m/z</i>	mass to charge ratio
mmol	millimole
μ mol	micromole

mol	mole
MS	molecular sieves; mass spectrometry
Ms	methanesulfonyl
<i>n</i> -Bu	normal-butyl
NaHMDS	sodium hexamethyldisilazide
NCS	<i>N</i> -chlorosuccinimide
nM	nanomolar
NMR	nuclear magnetic resonance
nOe	nuclear Overhauser effect
<i>p</i> -	<i>para</i>
Ph	phenyl
Phth	phthalimide
Piv-	pivaloyl
Pr	propyl
PMA	phosphomolybdic acid
ppm	parts per million
pyr	pyridine
rac-	racemic
<i>R</i>	rectus (Cahn–Ingold–Prelog system)
<i>R_f</i>	retention factor
RNA	ribonucleic acid
RP	reverse phase
<i>S</i>	sinister (Cahn–Ingold–Prelog system)

SAR	structure activity relationship(s)
SOCl ₂	thionyl chloride
sp.	species
TBDPS	<i>tert</i> -butyldiphenylsilyl
TBS	<i>tert</i> -butyldimethylsilyl
TBSCl	<i>tert</i> -butyldimethylsilyl chloride
TBSOTf	<i>tert</i> -butyldimethylsilyl trifluoromethanesulfonate
<i>t</i> -Bu	<i>tert</i> -butyl
Tet	tetracycline
TetA	tetracycline antiporter protein
TetR	tetracycline repressor protein
Tf	trifluoromethanesulfonyl
TFA	trifluoroacetic acid
THF	tetrahydrofuran
TIPS	triisopropylsilyl
TLC	thin-layer chromatography
TMS	trimethylsilyl
t _R	retention time
<i>trans</i>	<i>Lat.</i> , across
tRNA	transfer RNA
Ts	tosyl
UV	ultraviolet
Z	<i>Ger.</i> , zusammen

Chapter 1

Studies toward SF2575, a Tetracycline with Antiproliferative Activity

Introduction

SF2575 (also known as TAN 1518X, **1**) is a member of the tetracycline family and was isolated in 1992 from a Japanese soil sample containing *Streptomyces* sp. SF2575.¹ The structure was established by NMR and X-ray crystallographic studies, as well as by NMR analysis of its degradation products (Figure 1.1).² Unlike most natural tetracyclines, which exhibit broad-spectrum antibiotic activity, SF2575 displayed only weak antibacterial properties against select Gram-positive bacteria and was ineffective against Gram-negative pathogens. Two years later, TAN 1518A (**2**) and TAN 1518B (**3**) were isolated from a different Japanese soil sample containing the producing strain *Streptomyces* sp. AL-16012 and were similarly characterized.³ TAN 1518A exhibited weak antibiotic activity against Gram-positive and Gram-negative bacteria.

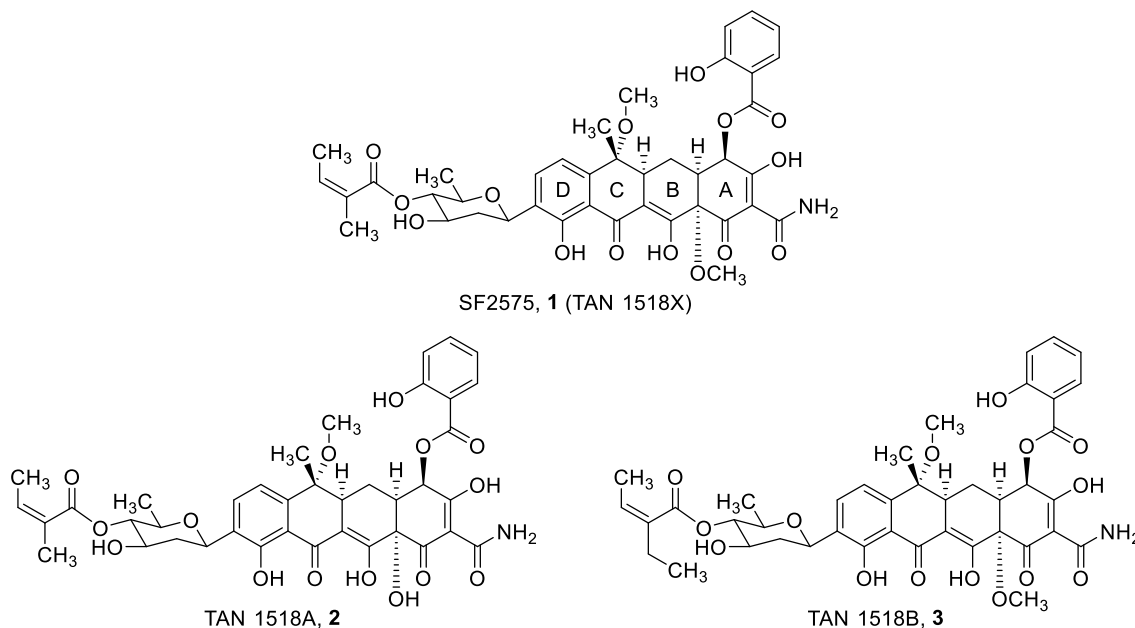


Figure 1.1: The TAN family of tetracyclines.

¹ Hatsu, M.; Sasaki, T.; Watabe, H.; Miyadoh, S.; Nagasawa, M.; Shomura, T.; Sezki, M.; Inouye, S.; Kondo, S. *J. Antibiot.* **1992**, *45*, 320–324.

² Hatsu, M.; Sasaki, T.; Gomi, S.; Kodama, Y.; Sezki, M.; Inouye, S.; Kondo, S. *J. Antibiot.* **1992**, *45*, 325–330.

³ Horiguchi, T.; Hayashi, K.; Tsubotani, S.; Iinuma, S.; Harada, S.; Tanida, S. *J. Antibiot.* **1994**, *47*, 545–556.

Biological Activity

Despite the lack of antibacterial efficacy, SF2575 and TAN1518A displayed unusual biological activities for tetracycline compounds – cytotoxicity.⁴ In fact, SF2575 exhibited activity against nearly every cell line in a 60-cell line screen performed by the National Cancer Institute (average IC₅₀ value of 11.2 nM). SF2575 and TAN 1518A were shown to inhibit DNA topoisomerase I, an enzyme which cuts the phosphate backbone of single- or double-stranded DNA before the DNA unwinds for replication and reseals the phosphate backbone afterward. Prevention of normal function of this enzyme disrupts DNA replication and causes cell apoptosis. DNA topoisomerase I is the target of many current anticancer medicines, including the camptothecin derivatives topotecan and irinotecan. The exact mechanism of action of the anticancer tetracyclines is unknown, but TAN 1518A was shown to interfere with DNA topoisomerase I in a different manner than the camptothecins.⁵ Access to a verified enzyme target through a new avenue allows for the development of a novel class of potential anticancer therapeutics and imparts the capacity to combat drug resistance. Therefore, detailed studies of DNA topoisomerase I inhibition by SF2575 and TAN 1518A was warranted. I decided to initiate the investigation by securing a synthetic approach to these compounds.

Structural Differences and Implications for Bioactivities

A structural side-by-side comparison of SF2575 with (–)-tetracycline (**4**) is shown in Figure 1.2. The SF2575 aglycon and tetracycline share the same 2-naphthacenecarboxamide skeleton. At C4, the (*R*)-dimethylamino group of tetracycline is replaced with an (*S*)-salicylate ester. The

⁴ Pickens, L. B.; Kim, W.; Wang, P.; Zhou, H.; Watanabe, K.; Gomi, S.; Tang, Y. *J. Am. Chem. Soc.* **2009**, *131*, 17677–17689.

⁵ The camptothecin antiproliferative agents bind to the topoisomerase I–DNA complex, preventing re-ligation and thereby causing DNA damage (See Schneider, E.; Hsiang, Y.-, H.; Liu, L. F. *Adv. Pharmacol.* **1990**, *21*, 149–183). In a biological screen, TAN 1518A did not stabilize the enzyme–DNA complex as did camptothecin (See Ref. 3).

C6 hydroxyl of SF2575 is methylated and its configuration is reversed. Additionally, SF2575 contains a glycosidic appendage, D-olivose 4'-angelate, at position C9. The lower periphery is conserved between the two compounds, except for the methylation of the hydroxyl at C12a on SF2575.

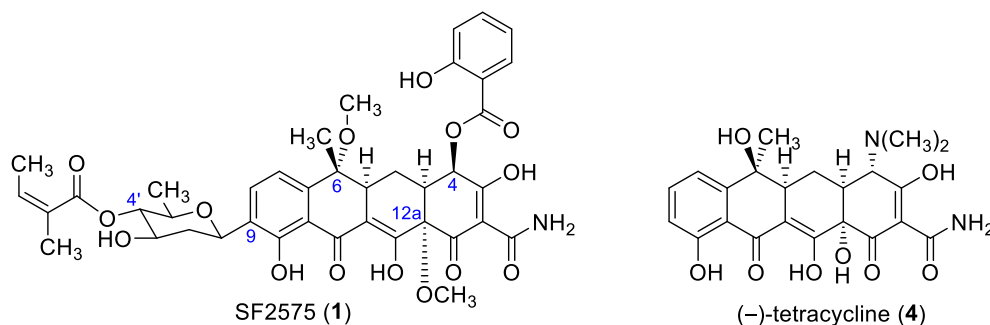


Figure 1.2: Comparison between SF2575 and tetracycline.

The loss of antibiotic activity in SF2575 was postulated to derive in part from the methylation of the C12a hydroxyl.⁴ It was well known that the lower periphery of tetracycline is actively involved in the binding to the 30S ribosomal subunit⁶ through coordination via a magnesium atom and through intricate hydrogen bonding to the phosphate backbone. The methyl group at C12a sterically interfered with these interactions as well as destroyed a hydrogen bond donor. Additionally, the (*R*)-dimethylamino moiety at C4 (empirically determined to be necessary for any antibacterial efficacy)⁷ was not present in the SF2575 scaffold and this also contributed to the loss of activity.

There is little data concerning the antiproliferative structure-activity relationships of SF2575.

Cleavage of the C4- and C4'-esters, both individually and collectively, are deleterious to the

⁶ (a) Brodersen, D. E.; Clemons, W. M. Jr.; Carter, A. P.; Morgan-Warren, R. J.; Wimberly, B. T.; Ramakrishnan, V. *Cell* **2000**, *103*, 1143–1154. (b) See Refs. 42 and 43 in Chapter 2.

⁷ Selected examples: (a) Mitscher, L. A. *The Chemistry of the Tetracycline Antibiotics*. Marcel Dekker, Inc: New York, 1978. (b) Nelson, M. L. The Chemistry and Cellular Biology of the Tetracyclines. In *Tetracyclines in Biology, Chemistry and Medicine*. Nelson, M., Hillen W., Greenwald, R. A., Eds.; Birkhäuser Verlag: Basel, Switzerland, 2001; 3–63. (c) Esse, R. C.; Lowery, J. A.; Tamorria, C. R.; Sieger, G. M. *J. Am. Chem. Soc.* **1964**, *86*, 3875–3877. (d) Dürckheimer, W. *Angew. Chem. Int. Ed. Engl.* **1975**, *14*, 721–774.

compound's potency.⁴ The scarcity of data is explained in part by the mode of production of SF2575 and its derivatives. SF2575 was isolated from fermentation broths, while its analogs have only been produced by engineered biosynthesis,^{4,8} and these methods are inherently limited in their generation of diverse scaffolds. Therefore, the goal of this project was to access anticancer tetracycline scaffolds as probes which would allow further investigation of SAR and lead to insights into the DNA topoisomerase I inhibition by tetracyclines.

Synthetic Approaches to the Tetracyclines

There are no published synthetic studies directed toward SF2575 (**1**), TAN 1518A (**2**) or TAN 1518B (**3**). On the other hand, multiple approaches have been developed toward various members of the tetracycline family. A detailed account of these strategies is outside the scope of this introduction; an overview will be presented. One approach, by Myers and coworkers, will be highlighted in greater detail, as it directly inspired the current goal (Scheme 1.1).

In 1962, R. B. Woodward, in collaboration with Pfizer scientists led by Lloyd Conover, reported the first total synthesis of (\pm)-sancycline (a tetracycline derivative with a single C4-(*R*)-dimethylamino substituent along the upper periphery), building the molecule in a linear fashion from the D-ring to the A-ring.⁹ Within the following five years, the Shemyakin¹⁰ and Muxfeldt¹¹ groups published their syntheses of (\pm)-tetracycline and (\pm)-oxytetracycline, respectively, both

⁸ (a) Pickens, L. B.; Sawaya, M. R.; Rasool, H.; Pashkov, I.; Yeates, T. O.; Tang, Y. *J. Biol. Chem.* **2011**, *286*, 41539–41551. (b) Pickens, L. B. Ph.D. Thesis, University of California Los Angeles, Los Angeles, CA, 2011. (c) Li, L.; Wang, P.; Tang, Y. *J. Antibiot.* **2014**, *67*, 65–70.

⁹ (a) Conover, L. H.; Butler, K.; Johnston, J. D.; Korst, J. J.; Woodward, R. B. *J. Am. Chem. Soc.* **1962**, *84*, 3222–3224. (b) Korst, J. J.; Johnston, J. D.; Butler, K.; Bianco, E. J.; Conover, L. H.; Woodward, R. B. *J. Am. Chem. Soc.* **1968**, *90*, 439–457.

¹⁰ Gurevich, A. I.; Karapetyan, M. G.; Kolosov, M. N.; Korobko, V. G.; Onoprienko, V. V.; Popravko, S. A.; Shemyakin, M. M. *Tetrahedron Lett.* **1967**, *8*, 131–134.

¹¹ Muxfeldt, H.; Rogalski, W. *J. Am. Chem. Soc.* **1965**, *87*, 933–934. (e) Muxfeldt, H.; Haas, G.; Hardtmann, G.; Kathawala, F.; Mooberry, J. B.; Vedejs, E. *J. Am. Chem. Soc.* **1979**, *101*, 689–701.

constructing the targets in a linear fashion from D to A. Thirty years later, Stork and coworkers disclosed an efficient synthesis of (\pm)-12a-deoxytetracycline,¹² again constructing their target in a stepwise manner from a CD-ring starting material to the A-ring.

Only two enantioselective syntheses of (–)-tetracycline are known. The first one was published by Tatsuda and coworkers¹³ in 2000 (34 steps, ~0.002% yield). Unlike the previous approaches, Tatsuda's synthesis began with an A-ring precursor and built up the carbon framework from right to left. Additionally, Tatsuda and coworkers utilized an interesting convergent coupling to form the C-ring (page 12).

The second report on the enantioselective production of (–)-tetracycline¹⁴ came from the Myers lab in 2005 (17 steps, ~1.1% yield). The Myers research group developed a convergent approach not only to tetracycline itself, but to the entire class of tetracycline antibiotics.¹⁵ The convergent nature of the synthesis greatly improved efficiency and overall yield, as well as enabled the production of a diverse set of analogs through modifications of the building blocks.

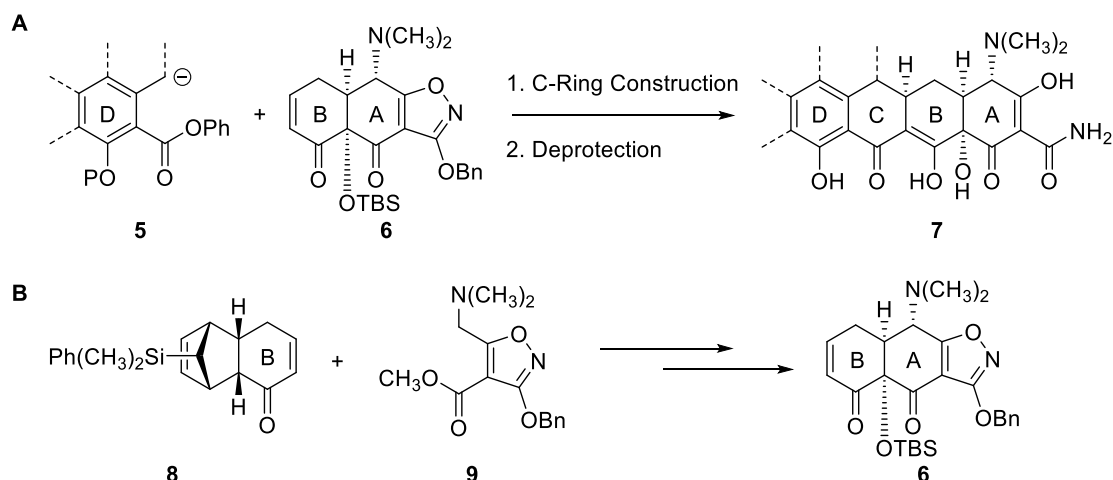
In 2005, Myers group researchers also reported the first total synthesis of 6-deoxytetracyclines employing this convergent strategy.^{15a} In 2008, the utility of the route was demonstrated, allowing expansive modifications of the D-ring coupling partners in the production of new tetracycline antibiotics.^{15b} Finally in 2011, Dr. Peter Wright extended the analog scope to include alterations of the key AB enone moiety.^{15c} The synthetic strategy for all these approaches was identical (Scheme 1.1, **A**).

¹² Stork, G.; La Clair, J. J.; Spargo, P.; Nargund, R. P.; Totah, N. *J. Am. Chem. Soc.* **1996**, *118*, 5304–5305.

¹³ Tatsuda, K.; Yoshimoto, T.; Gunji, H.; Okado, Y.; Takahashi, M. *Chem. Lett.* **2000**, *29*, 646–647.

¹⁴ Charest, M.; Siegel, D. R.; Myers, A. G. *J. Am. Chem. Soc.* **2005**, *127*, 8292–8293.

¹⁵ (a) Charest, M. G.; Lerner, C. D.; Brubaker, J. D.; Siegel, D. R.; Myers, A. G. *Science* **2005**, *308*, 395–398. (b) Sun, C.; Wang, Q.; Brubaker, J. D.; Wright, P. M.; Lerner, C. D.; Noson, K.; Charest, M.; Siegel, D. R.; Wang, Y-M.; Myers, A. G. *J. Am. Chem. Soc.* **2008**, *130*, 17913–17927. (c) Wright, P. M.; Myers, A. G. *Tetrahedron*, **2011**, *67*, 9853–9869.



Scheme 1.1: A: Myers convergent strategy to the tetracyclines; B: Myers convergent strategy to key AB enone 6.

The tetracyclic core was constructed from a stereoselective Michael–Claisen (also referred to as a Michael–Dieckmann¹⁶) cyclization between two coupling partners: a D-ring *ortho*-toluate anion **5** and key AB enone **6**. The resulting pentacyclic (or occasionally hexacyclic) intermediate was subjected to a two-step deprotection sequence, affording a tetracycline derivative **7**. This robust method tolerated substitution at a variety of positions which allowed for modifications at sites previously inaccessible by semi-synthesis or other means (Figure 1.3), and this platform has been utilized in the production of over 3000 fully synthetic analogs to date.¹⁷

¹⁶ A Claisen reaction is defined as a base mediated condensation between a nucleophilic ester enolate and an electrophilic ester carbonyl, thereby producing a β -keto ester. A Dieckmann cyclization is a subset of a Claisen reaction, in which the two esters are tethered and a cyclic β -keto ester is synthesized. See Kürti, L.; Czako, B. *Strategic Applications of Named Reaction in Organic Synthesis*. Elsevier, Inc: Amsterdam, 2005. p. 86. While it may be correct to classify the A- and the C-ring forming reactions as Michael–Dieckmann cyclizations, we decided to exclusively use the more general Michael–Claisen moniker.

¹⁷ (a) Clark, R. B.; He, M.; Fyfe, C.; Lofland, D.; O'Brien, W. J.; Plamondon, L.; Sutcliffe, J. A.; Xiao, X.-Y. *J. Med. Chem.* **2011**, *54*, 1511–1528. (b) Sun, C.; Hunt, D. K.; Clark, R. B.; Lofland, D.; O'Brien, W. J.; Plamondon, L.; Sutcliffe, J. A.; Xiao, X.-Y. *J. Med. Chem.* **2011**, *54*, 3704–3731. (c) Xiao, X.-Y.; Hunt, D. K.; Zhou, J.; Clark, R. B.; Dunwoody, N.; Fyfe, C.; Grossman, T. H.; O'Brien, W. J.; Plamondon, L.; Rönn, M.; Sun, C.; Zhang, W.-Y.; Sutcliffe, J. A. *J. Med. Chem.* **2012**, *55*, 597–605. (d) Clark, R. B.; Hunt, D. K.; He, M.; Achorn, C.; Chen, C.-L.; Deng, Y.; Fyfe, C.; Grossman, T. H.; Hogan, P. C.; O'Brien, W. J.; Plamondon, L.; Rönn, M.; Sutcliffe, J. A.; Zhu, Z.; Xiao, X.-Y. *J. Med. Chem.* **2012**, *55*, 606–622. (e) Clark, R. B.; He, M.; Deng, Y.; Sun, C.; Chen, C.-L.; Hunt, D. K.; O'Brien, W. J.; Fyfe, C.; Grossman, T. H.; Sutcliffe, J. A.; Achorn, C.; Hogan, P. C.; Katz, C. E.; Niu, J.; Zhang, W.-Y.; Zhu, Z.; Rönn, M.; Xiao, X.-Y. *J. Med. Chem.* **2013**, *56*, 8112–8138.

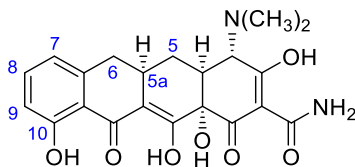
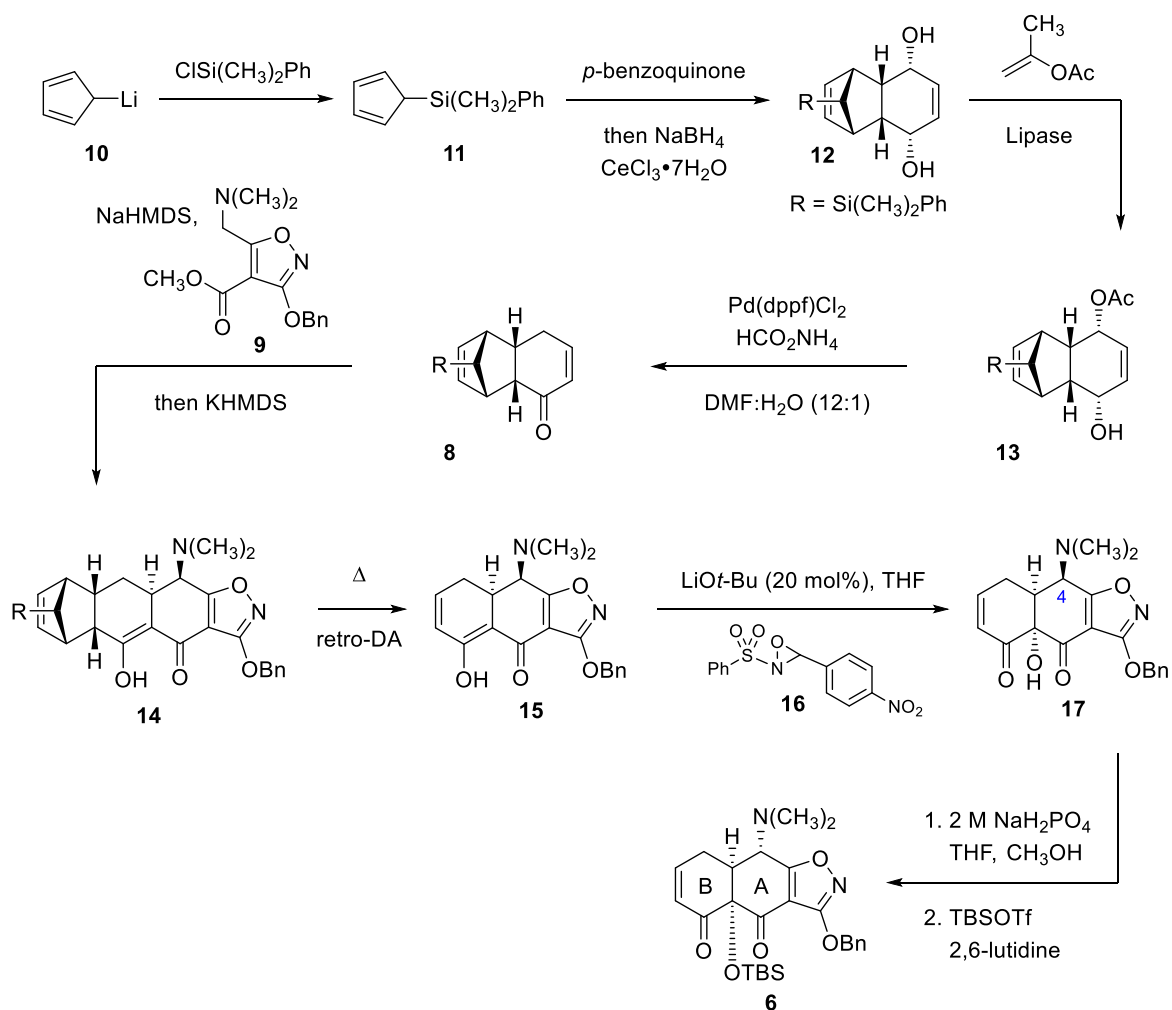


Figure 1.3: Sites of modifications of the tetracycline scaffold based on Myers convergent strategy.¹⁸

To obtain large quantities of the key tetracycline AB enone **6** for the production of additional analogs, a more scalable route was sought. In 2011, Dr. David Kummer, Dr. Derun Li and Dr. Amelie Dion developed the third and fourth generation routes to this key intermediate,¹⁹ taking advantage of a second stereoselective Michael–Claisen cyclization (summarized in Scheme 1.1, **B**, detailed in Scheme 1.2). This stereoselective cyclization brought together a dimethylamino isoxazole methyl ester **9** and a modified cyclohexenone **8** in a single operation to yield a single diastereomer of the Michael–Claisen adduct **14**, which was converted into AB enone **6** in four additional steps.

¹⁸ To date, no modifications to the C4-position have been disclosed utilizing this strategy. See Chapter 2.

¹⁹ Kummer, D. A.; Li, D.; Dion, A.; Myers, A. G. *Chem. Sci.* **2011**, 2, 1710–1718.



Scheme 1.2: Myers 4th generation route to the tetracycline AB enone **6**.

Lithiated cyclopentadiene **10** was trapped with phenyldimethylsilyl chloride to give silyl cyclopentadiene **11**, which then underwent a one-pot Diels–Alder cycloaddition with *p*-benzoquinone, followed by a Luche reduction to afford meso diol **12**. The diol **12** was subjected to enzymatic resolution with an Amano lipase, and the optically enriched acetate **13** then underwent a palladium-mediated rearrangement yielding silyl B-ring enone **8**. Treatment of this enone **8** with the sodium enolate of isoxazole methyl ester **9** followed by the addition of KHMDS afforded Michael–Claisen adduct **14** as a single diastereomer. The silyl cyclopentadiene auxiliary was removed (and then recycled) upon heating the adduct **14** to give

enol **15**. Oxidation of enol **15** with Davis oxaziridine **16** in the presence of catalytic lithium *tert*-butoxide produced hydroxy enone **17**. The dimethylamino group at C4 was epimerized upon treatment with a mildly acidic NaH₂PO₄ solution. The C12a hydroxyl was protected as a TBS ether, completing the synthesis of the key tetracycline AB enone **6**.

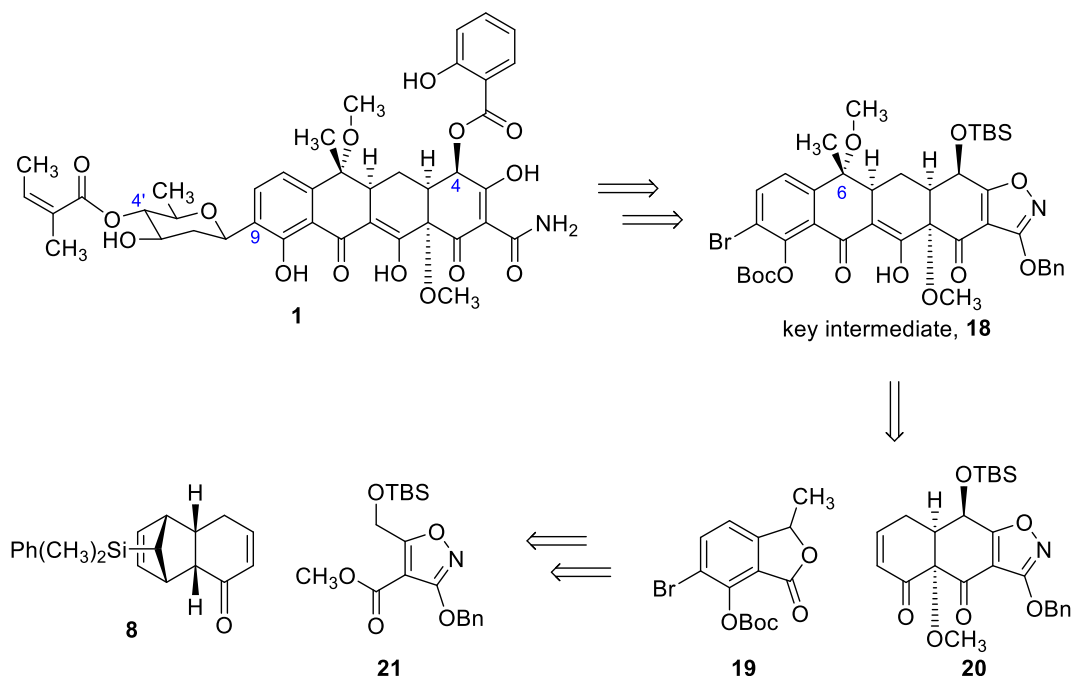
This route had a number of advantages over the previously reported methods.^{15a, 20} The chemistry was easily scalable, affording 41.6 g of **6** in a single batch in 35% overall yield. Many of the intermediates were crystalline and no column chromatography was required. Furthermore, the silyl cyclopentadiene **11** could be recovered and recycled through multiple iterations of this sequence.

Retrosynthetic Analysis of the SF2575 Core

Retrosynthetic analysis of the target SF2575 (**1**) was performed (Scheme 1.3). The salicylate ester at C4 and the C-aryl glycosidic appendage at C9 were the first logical disconnections, simplifying the structure to a fully functionalized SF2575 core **18**. This core was considered a key intermediate in our strategy to access not only the anticancer tetracycline family, but also a wider scope of analogs. Modifications of this diversifiable core were expected to produce a variety of scaffolds.

Compound **18** could be formed by a Michael–Claisen cyclization between a phthalide D-ring precursor **19** and an AB enone **20**, followed by methylation of the C6 hydroxyl. The AB enone **20** could itself be synthesized by another Michael–Claisen cyclization, this time utilizing isoxazole methyl ester **21** and the previously mentioned silyl B-ring enone **8** (*cf.* the 4th generation route to the tetracycline AB enone **6**).

²⁰ Brubaker, J. D.; Myers, A. G. *Org. Lett.* **2007**, *9*, 3523–3525.



Scheme 1.3: Retrosynthetic analysis of SF2575.

The retrosynthetic plan outlined above did not expound the construction of the glycosidic linkage at C9 or the salicylate ester at C4. Ample precedent is known for the syntheses of both C-aryl glycosides²¹ and salicylate esters.²² The main objective in presenting SF2575 as a synthetic target was to establish an initial aim in research and to introduce strategies and compounds which would ultimately lead to the achievement of a different goal (see Chapter 2).

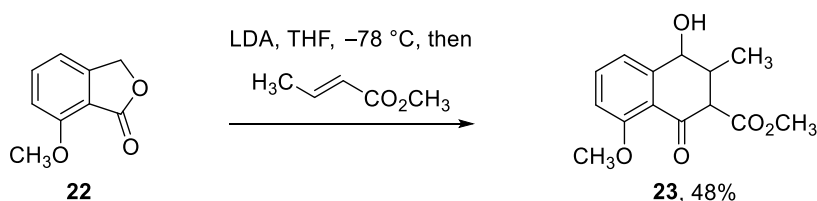
²¹ (a) Jaramillo, C.; Knapp, S. *Synthesis*, **1994**, 1–20. (b) Parker, K. *Pure Appl. Chem.* **1994**, 10/11, 2135–2138. (c) Suzuki, K. *Pure Appl. Chem.* **1994**, 10/11, 2175–2178. (d) Apsel B.; Bender, J. A.; Escobar, M.; Kaelin, D. E., Jr.; Lopez, O. D.; Martin, S. F. *Tetrahedron Lett.* **2003**, 44, 1075–1077. (e) Boyd, E.; Hallett, M. R.; Jones, R. V. H.; Painter, J. E.; Patel, P.; Quayle, P.; Waring, A. J. *Tetrahedron Lett.* **2006**, 47, 8337–8341.

²² (a) Gawronski, J. K.; Reddy, S. M.; Walborsky, H. M. *J. Am. Chem. Soc.* **1987**, 109, 6726–6730. (b) Nicolaou, K. C.; Nold, A. L.; Milburn, R. R.; Schindler, C. S.; Cole, K. P.; Yamaguchi, J. *J. Am. Chem. Soc.* **2007**, 129, 1760–1768. (c) Nojiri, A.; Kumagai, N.; Shibasaki, M. *J. Am. Chem. Soc.* **2008**, 130, 5630–5631. (d) Moriarty, L. M.; Lally, M. N.; Carolan, C. G.; Jones, M.; Clancy, J. M.; Gilmer, J. F. *J. Med. Chem.* **2008**, 51, 7991–7999. (e) DeBerardinis, A. M.; Madden, D. J.; Banerjee, U.; Sail, V.; Raccuia, D. S.; De Carlo, D.; Lemieux, S. M.; Meares, A.; Hadden, M. K. *J. Med. Chem.* **2014**, 57, 3724–3736.

Literature Precedent: Non-stabilized Phthalides in Michael–Claisen Cyclizations

Before experimenting with non-stabilized phthalides²³ as Michael–Claisen coupling partners, I investigated the viability of this strategy. Listed below are selected literature examples of the desired transformation, including some found only in Myers group theses.

The first example of a Michael–Claisen reaction utilizing a non-stabilized phthalide was disclosed by Broom and Sammes²⁴ in 1978 (Scheme 1.4). Treatment of compound **22** with LDA in THF at $-78\text{ }^{\circ}\text{C}$, followed by the addition of methyl crotonate, provided Michael–Claisen product **23** in 48% yield as a mixture of diastereomers. This instance showed that a phthalide enolate can attack a suitable Michael acceptor and then undergo a Claisen cyclization.

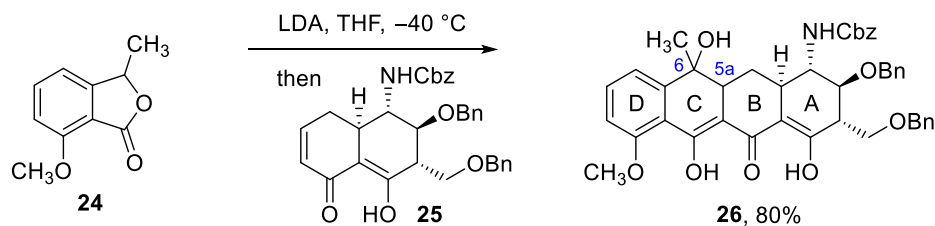


Scheme 1.4: First reported Michael–Claisen cyclization with a phthalide.

Another example of a Michael–Claisen cyclization with a phthalide coupling partner came from Tatsuta’s report in 2000 on the first enantioselective synthesis of (–)-tetracycline (Scheme 1.5).¹² Subjection of phthalide **24** to LDA in THF at $-40\text{ }^{\circ}\text{C}$, followed by the addition of enone **25** at the reduced temperature provided Michael–Claisen product **26** in 80% yield. The configuration of positions C5a or C6 was not discussed, however this was insignificant: the C6 hydroxyl was eliminated in the subsequent step, forming an aromatic CD-ring system and obviating any stereochemical data.

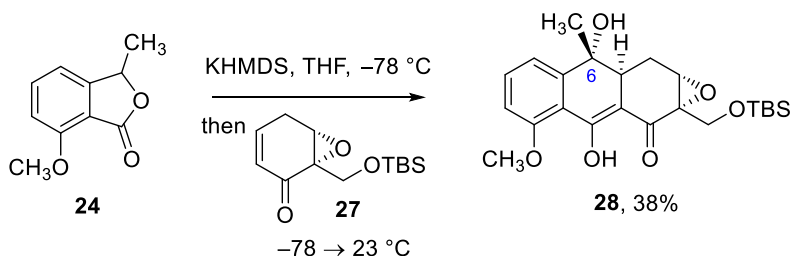
²³ The term “non-stabilized phthalide” includes substrates which lack strong electron withdrawing groups, for example phenylsulfonyl or cyano functionalities, at the benzylic position. More common Michael–Claisen cyclizations of stabilized phthalides typically afford aromatic quinone products and are known as Hauser annulations.

²⁴ Broom, N. J. P.; Sammes, P. G. *J. Chem. Soc., Chem. Commun.* **1978**, 162–164.



Scheme 1.5: Tatsuta's Michael–Claisen cyclization to form the tetracyclic core.

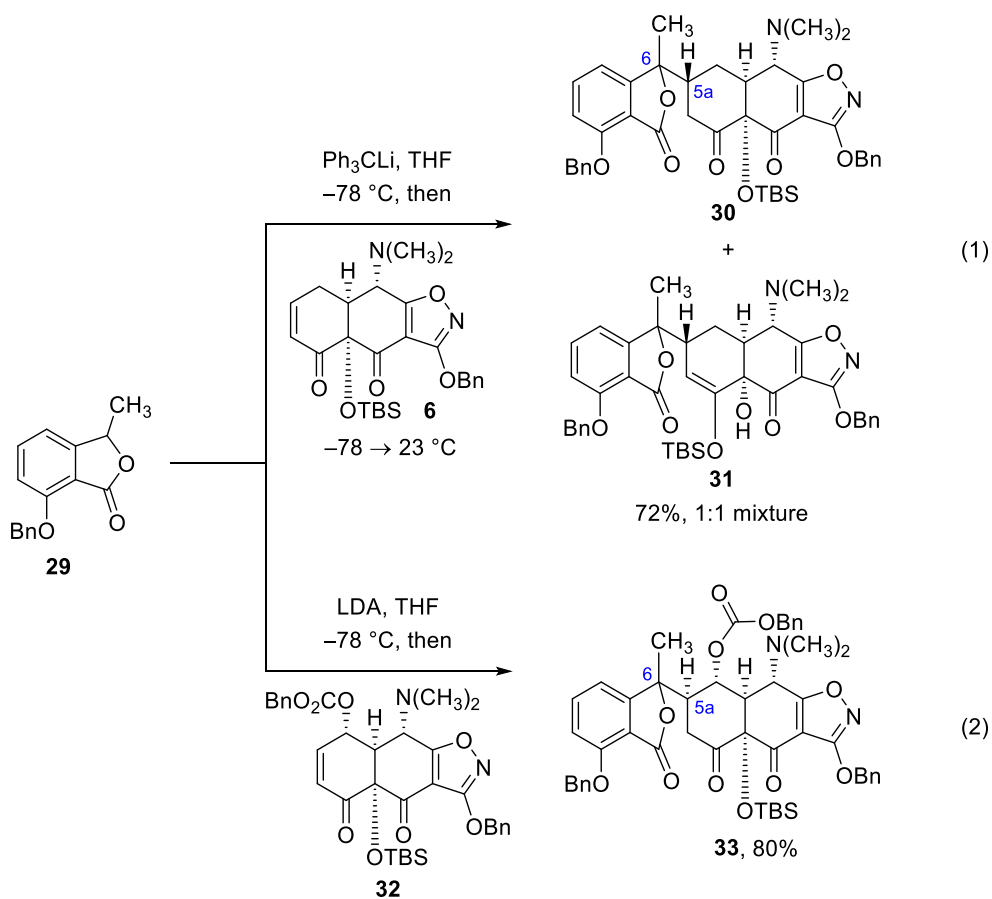
The Myers group began to study the feasibility of a Michael–Claisen strategy to build tetracycline C-rings with phthalide D-ring precursors in the late 1990s (Scheme 1.6). Dr. Cynthia Parrish discovered that treatment of phthalide **24** with KHMDS in THF at $-78\text{ }^{\circ}\text{C}$, followed by the addition of model AB enone system **27** provided Michael–Claisen product **28** in 38% yield.²⁵ The stereochemical outcome of the C6 position did not match that of tetracycline as shown by nOe experiments, but corresponded to the desired C6 configuration of SF2575. This example, in combination with Tatsuda's report, provided significant support for our pursuit of the SF2575 core using the aforementioned strategy.



Scheme 1.6: Michael–Claisen cyclization with phthalide **24** and model AB enone **27**.

However, further studies in the Myers lab revealed a noteworthy challenge. Reactions of the same phthalide precursor **29** with either the tetracycline AB enone **6** or a closely related derivative **32**, stopped at the Michael addition products (**30**, **31**, and **33**) and no Claisen cyclization occurred (Scheme 1.7).

²⁵ Parrish, C. A. Ph.D. Thesis, California Institute of Technology, Pasadena, CA, 1999.



Scheme 1.7: Attempted Michael–Claisen cyclizations with tetracycline AB enones **6** and **32**.

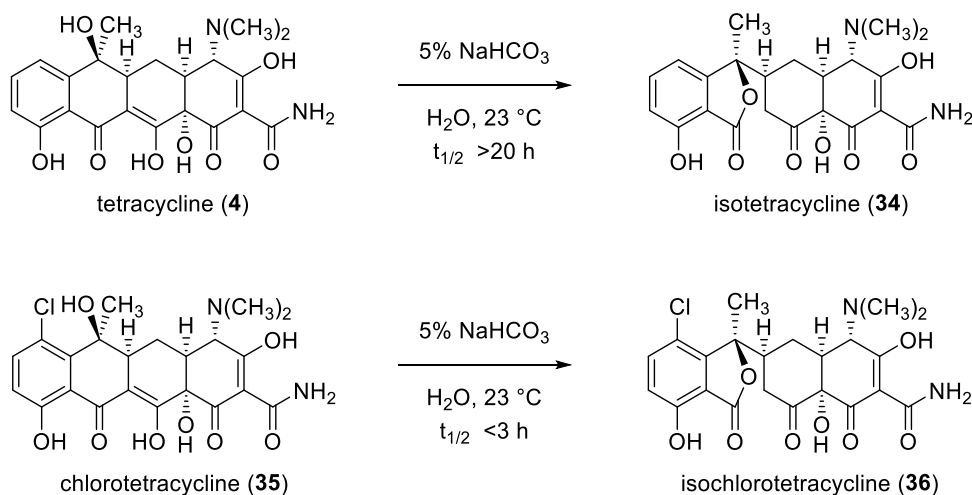
Dr. Dionicio Siegel found that deprotonation of phthalide **29** with trityl lithium in THF at $-78\text{ }^\circ\text{C}$, followed by the addition of the tetracycline AB enone **6** and warming to $23\text{ }^\circ\text{C}$, afforded Michael adduct **30** and silyl-transfer Michael adduct **31** in 72% as a 1:1 mixture (Scheme 1.7, equation 1).²⁶ The reaction could be optimized to produce exclusively compound **30** upon addition of $\text{MgBr}_2 \cdot \text{Et}_2\text{O}$ before quenching the reaction mixture. The configuration of the C5a position did not match that of tetracycline²⁷ and the orientation of C6 could not be established.

²⁶ Siegel, D. R. Ph.D. Thesis, Harvard University, Cambridge, MA, 2003.

²⁷ In all reported Michael–Claisen cyclizations with the tetracycline AB enone **6**, this is the only instance where the configuration of C5a was determined to be that of the undesired orientation. Therefore, we theorized that in this singular example, the C5a stereocenter was assigned erroneously.

Dr. Mark Charest discovered that deprotonation of phthalide **29** with LDA in THF at $-78\text{ }^{\circ}\text{C}$, followed by the addition of the tetracycline AB enone **32**, afforded only the Michael adduct **33** in 80% yield (Scheme 1.7, equation 2).²⁸ The configuration at the C5a position corresponded to the desired configuration in tetracyclines, but again there was no assignment of the stereochemical outcome at C6.

Stepwise Michael reactions, followed by Claisen cyclizations, were attempted. However no Claisen product was seen under a variety of conditions. It was known²⁹ that tetracycline and related compounds undergo retro-Claisen reactions under mildly basic conditions, yielding C-ring–opened compounds, such as isotetracycline (**34**) and isochlorotetracycline (**36**) (Scheme 1.8). These compounds closely resemble Michael adducts **30** and **33**, suggesting that the C-ring–opened lactones are the thermodynamic products of a reversible Claisen cyclization.



Scheme 1.8: Degradation of tetracycline and chlorotetracycline via retro-Claisen pathway.

While it was encouraging to see examples of non-stabilized phthalides undergoing Michael reactions and Michael–Claisen transformations, it was clear that the use of these compounds as

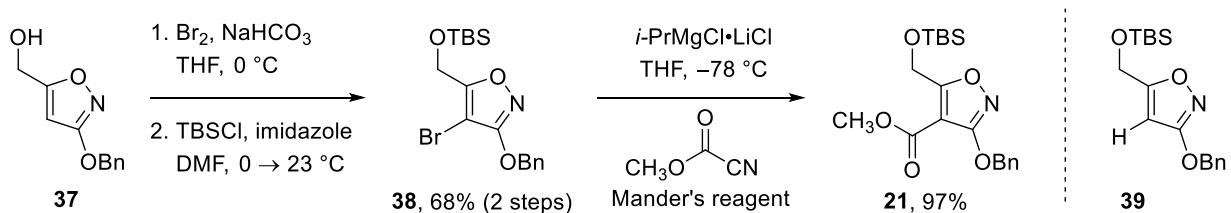
²⁸ Charest, M. G. Ph.D. Thesis, Harvard University, Cambridge, MA, 2004.

²⁹ Stephens, C. R.; Conover, L. H.; Pasternack, R.; Hochstein, F. A.; Moreland, W. T.; Regna, P. P.; Pilgrim, F. J.; Brunings, K. J.; Woodward, R. B. *J. Am. Chem. Soc.* **1954**, *76*, 3568–3575.

D-ring precursors had a potential challenge of its own: the cyclization to form the C-ring was not a guaranteed event. Enlightened and determined, I decided to study the synthesis of the tetracyclic core of SF2575.

Synthesis of SF2575 AB Enone 20

Using the 4th generation route to the tetracycline AB enone **6** as a guide and Dr. David Kummer as a mentor, I started by targeting isoxazole methyl ester **21** (Scheme 1.9). Bromination of known hydroxy isoxazole **37**¹⁷ with Br₂ in the presence of NaHCO₃ afforded an intermediate 3-benzyloxy-4-bromo-5-(hydroxymethyl)isoxazole (not shown). Sodium bicarbonate was a necessary additive to minimize the production of 4-bromo-1-butanol, the side-product arising from THF cleavage with HBr. Protection of the primary alcohol upon treatment with TBSCl and imidazole gave the *tert*-butyldimethylsilyl ether **38** in 68% yield over two steps. One-pot halogen-metal exchange with Knochel's *i*-PrMgCl•LiCl complex,³⁰ followed by trapping the metallated isoxazole with Mander's reagent (methyl cyanofornate) produced the desired isoxazole methyl ester **21** in 97% yield. While this method led to the release of toxic HCN gas upon workup, other reagents to install the carbomethoxy functionality (e.g. methyl chloroformate) were not as effective and significant amounts of isoxazole **39** were isolated.

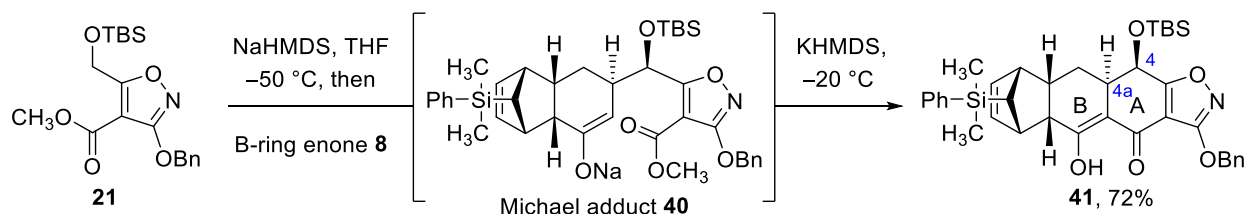


Scheme 1.9: Synthesis of isoxazole methyl ester **21**.

With isoxazole methyl ester **21** in hand, I explored the possibility of forming the A-ring by a Michael–Claisen cyclization (Scheme 1.10). Treatment of **21** with NaHMDS at –50 °C, followed

³⁰ Krasovskiy, A.; Knochel, P. *Angew. Chem., Int. Ed.* **2004**, *43*, 3333–3336.

by the addition of the silyl B-ring enone **8**, yielded intermediate Michael adduct **40** (based on TLC analysis of a quenched reaction sample, not characterized). Addition of a second equivalent of a different base, KHMDS,³¹ and warming the reaction mixture to $-20\text{ }^{\circ}\text{C}$ caused a stereoselective Claisen cyclization, producing Michael–Claisen adduct **41** as a ~15:1 mixture of diastereomers as determined by ^1H NMR analysis. Pure adduct **41** was obtained in 72% yield after flash column chromatography.



Scheme 1.10: Michael–Claisen cyclization to form the A-ring.

The stereochemistry of Michael–Claisen adduct **41** was assigned by analysis of the coupling constants of the C4 and C4a protons and comparison to Michael–Claisen adduct **14**. The bulky cyclopentenyl moiety effectively blocks the bottom π face of the B-ring enone **8**, and therefore the addition of the isoxazole methyl ester enolate occurs from the top face, setting the desired stereocenter at C4a (Scheme 1.10). As with the Michael–Claisen adduct **14**, the arrangement at the C4 stereocenter was of the (*S*)-configuration, which is the desired one for the SF2575 core. Future epimerization of this center would not be needed to target AB enone **20**.

Dr. David Kummer remarked in his thesis, when describing the stereochemical outcome of this reaction applied to the synthesis of compound **14**, “This is another example of high diastereocontrol in the creation of adjacent stereogenic sp^3 -centers by a Michael–Claisen cycloaddition (the other being formation of the C-ring <...>), suggesting that this powerful ring-

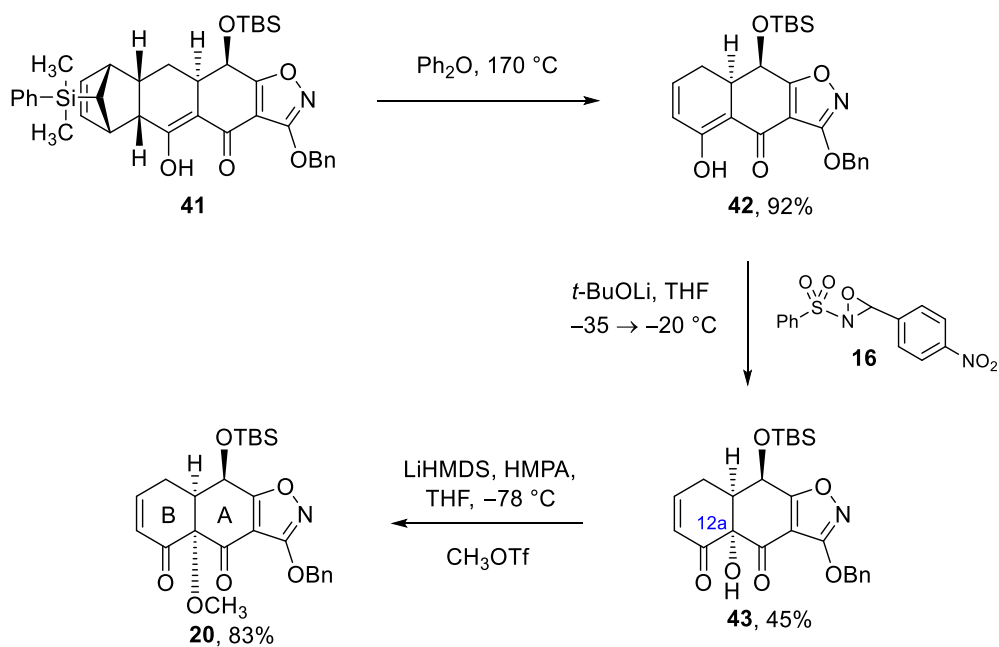
³¹ The second equivalent of base was necessary to deprotonate the Michael–Claisen adduct to prevent premature quenching of the intermediate enolate by the product or by methanol, a side-product. Optimization of this reaction sequence for the production of compound **14** was performed by Dr. David Kummer. The conditions found to yield the best result for that transformation were applied to these substrates (Scheme 1.10).

forming reaction may be more broadly applicable as a method for the stereocontrolled construction of 6-membered rings, a problem more typically addressed using Diels-Alder chemistry.”³² The additional example above supported his hypothesis of extending the scope of this methodology for the construction of 6-membered rings in a stereocontrolled manner.

Continuing toward the SF2575 AB enone (Scheme 1.11), I transformed the Michael–Claisen adduct **41** into enol **42** via a retro-Diels–Alder reaction upon brief heating in diphenylether in a pre-warmed oil bath at 170 °C (7 – 15 min, depending on the scale of the reaction), providing enol **42** in 92% yield. Treatment of enol **42** with Davis *p*-nitrophenyl oxaziridine **16** in the presence of a catalytic amount of *t*-BuOLi at reduced temperature afforded hydroxy enone **43** in 45% yield. This reaction produced a mixture of diastereomers at C12a, which transpired in the reduced yield.

Hydroxy enone **43** was just one step away from the desired SF2575 AB enone **20**. The C12a hydroxyl was deprotonated with LiHMDS in the presence of HMPA and the oxyanion was trapped with methyl triflate, affording AB enone **20** in 83% yield. Overall, the route to AB enone **20** was efficient and scalable, comparable to the 4th generation route to the tetracycline AB enone **6**. I obtained approximately 1 gram of **20** in a single batch in 16% overall yield starting with hydroxy isoxazole **37**.

³² Kummer, D. A. Ph.D. Thesis, Harvard University, Cambridge, MA, 2011.

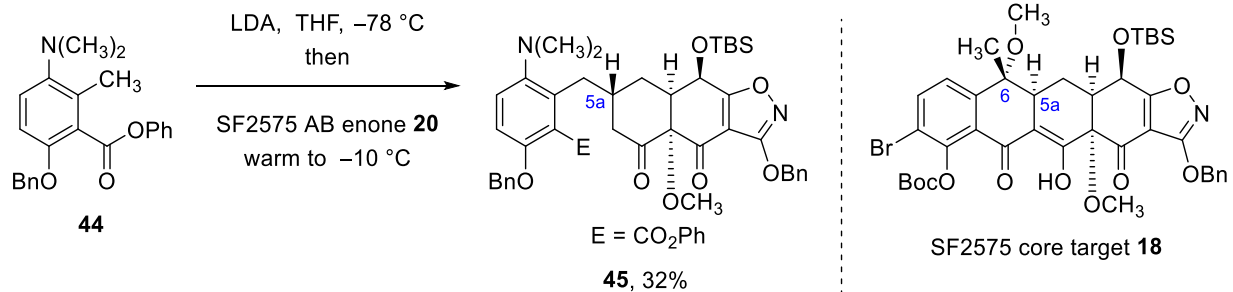


Scheme 1.11: Completion of the synthesis of AB enone **20**.

Attempted Michael–Claisen Cyclizations

With SF2575 AB enone **20** in hand, I attempted the formation of the C-ring by Michael–Claisen cyclization. Before testing the two novel coupling partners (the SF2575 AB enone and a phthalide D-ring precursor), I explored the cyclization between one known and one novel component. Analysis of the reaction products was expected to be straightforward because our lab has accumulated a wealth of data for this type of transformation.

First, the viability of the SF2575 AB enone **20** as a coupling partner was explored (Scheme 1.12). Treatment of the phenyl ester **44** (a minocycline D-ring precursor) with LDA at $-78\text{ }^\circ\text{C}$ produced a bright red *ortho*-toluate anion which was trapped with a solution of SF2575 AB enone **20** and the reaction mixture was allowed to warm slowly to $-10\text{ }^\circ\text{C}$. A single tractable product **45** was isolated in 32% yield, in addition to the recovered starting materials. ^1H NMR analysis, supplemented with mass spectrometry data, indicated that **45** was a Michael adduct and that the desired Claisen cyclization did not occur.



Scheme 1.12: Attempted Michael–Claisen cyclization with minocycline D-ring precursor **44**.

Single crystal X-ray crystallography allowed me to assign the relative configuration of **45** (Figure 1.4). The phenyl ester enolate addition occurred from the bottom π -face of the AB enone **20**, producing the undesired isomer at C5a.

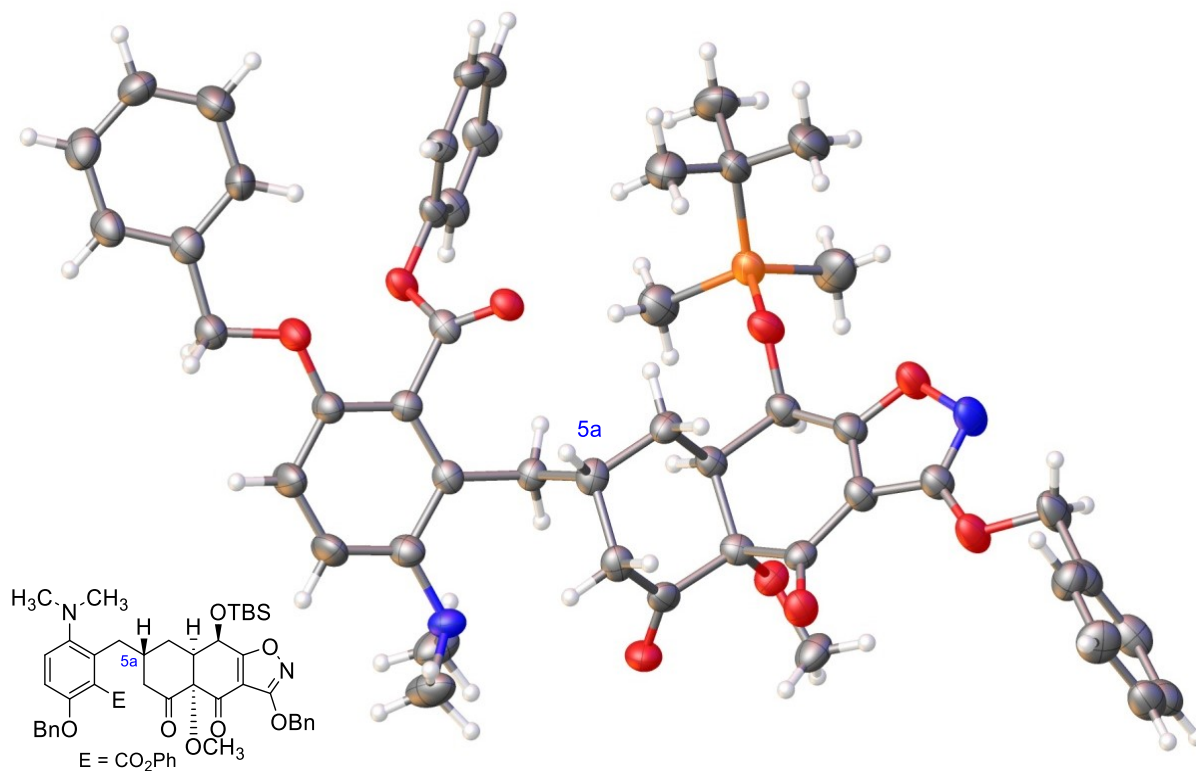


Figure 1.4: Crystal structure of Michael adduct **45**.

Upon closer scrutiny of the SF2575 AB enone **20**, I realized that it was not an ideal coupling partner for the synthesis of any tetracycline family members for two reasons (Figure 1.5). First, unlike the tetracycline AB enone **6**, it lacked the bulky *tert*-butyldimethylsilyl ether at C12a which would block the bottom π -face of the enone from nucleophilic attack. Second, the sp^3 -hybridized centers at C4a and C12a force **20** to adopt a bent conformation in which the large (*S*)-*tert*-butyldimethylsilyl ether at C4 occupies the space above the π -face of the enone, preventing the desired mode of addition. Presumably, the combination of these two factors explains the isolation of Michael adduct **45** with the undesired configuration at the C5a stereocenter.

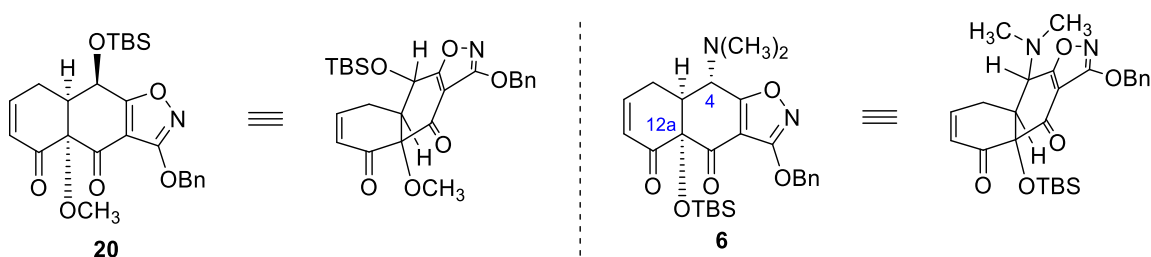
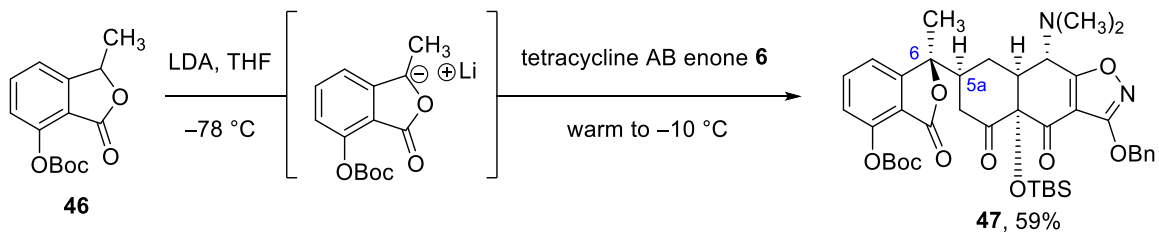


Figure 1.5: Rationale for the stereoselectivity of Michael additions to **20** and **6**.

Concurrently, the practicality of using phthalide D-ring precursors as Michael–Claisen coupling partners was also examined, with the tetracycline AB enone **6** as a model system (Scheme 1.13). Deprotonation of phthalide **46**²⁵ with LDA at -78 °C produced an orange anion which was trapped with a solution of tetracycline AB enone **6** and the reaction mixture was allowed to warm slowly to -10 °C. After quenching, workup and purification, a single product (**47**) was isolated in 59% yield. Again, ^1H NMR study and mass spectrometry data indicated the product was a Michael adduct.



Scheme 1.13: Attempted Michael–Claisen cyclization with phthalide **46**.

Similarly to compound **45**, Michael adduct **47** could be crystallized, and X-ray analysis confirmed the desired configuration of the C5a stereocenter (Figure 1.6), congruent with all tetracycline family members. However, the stereocenter at C6 was shown to have the tetracycline configuration, and not the one found in SF2575.

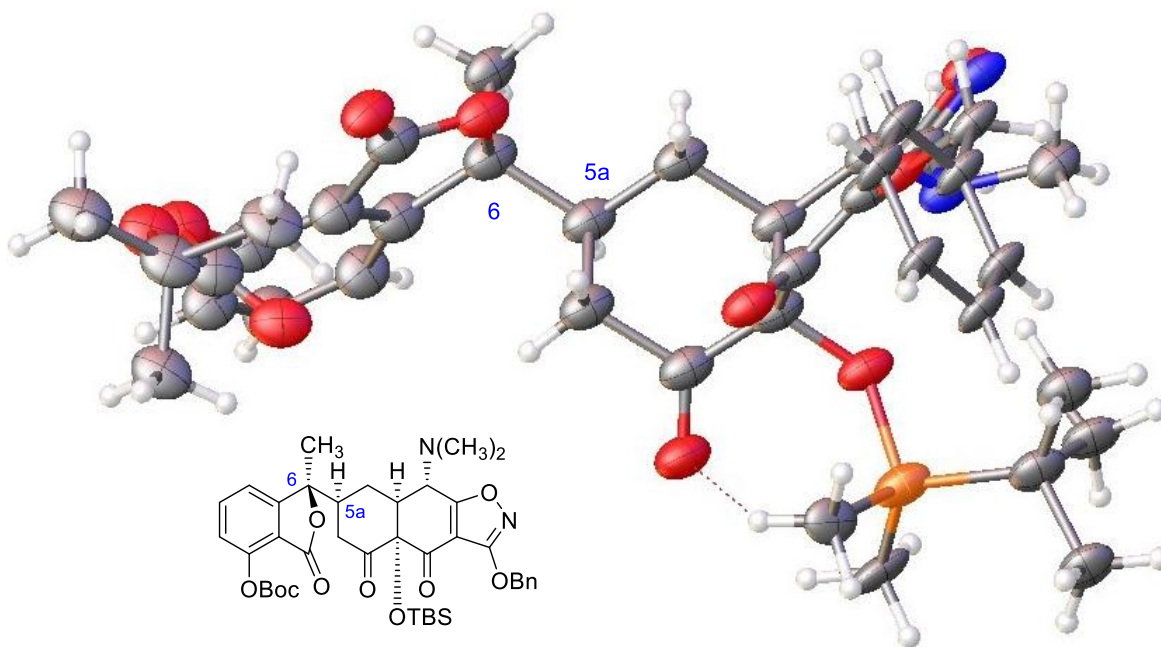


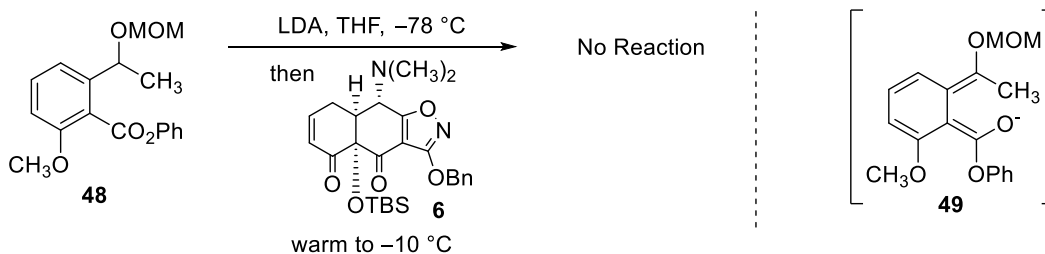
Figure 1.6: Crystal structure of the Michael adduct **47**.

While this was considered an unfavorable outcome in the context of targeting the SF2575 core **18**, there was another tempting application of this “negative” result. Michael adduct **47** required a single Claisen cyclization to form a protected version of tetracycline itself. If a one-

pot Michael–Claisen reaction or a stepwise Michael-then-Claisen sequence could be realized, then the most direct synthesis of (–)-tetracycline to date would be achieved.

Therefore, I executed extensive experimentation toward the tetracycline core. Direct Michael–Claisen cyclization with phthalide **46** was screened, using a variety of bases, reaction temperatures and other parameters. Additionally, a stepwise Michael-then-Claisen strategy was investigated, but I could not find conditions to effect the C-ring cyclization.³³ The earlier observations by Drs. Dionicio Siegel and Mark Charest³⁴ were replicated: phthalide D-rings are not suitable coupling partners with the tetracycline AB enone **6** to form tetracycline analogs due to the thermodynamic stability of the intermediate Michael adducts and the reversibility of the Claisen reaction.

In the final attempt to access either the tetracycline or SF2575 scaffold directly, I explored a Michael–Claisen cyclization with an open-chain D-ring precursor phenyl ester **48** (Scheme 1.14). Any cyclized product from the proposed transformation would be applied toward either SF2575 or tetracycline as a target, based on the stereochemical outcome at the C6 center. Treatment of phenyl ester **48** with LDA at $-78\text{ }^{\circ}\text{C}$, followed by the addition of tetracycline AB enone **6**, led to no reaction. Presumably, the reaction did not occur due to the inability to deprotonate the benzylic proton and to form the sterically hindered enolate **49**.



Scheme 1.14: Attempted Michael–Claisen cyclization with phenyl ester **48**.

³³ Only decomposition products and recovered starting materials were isolated from these experiments.

³⁴ See pages 13–15.

In summary, I synthesized an oxygenated AB enone (compound **20**) based on the Myers' 4th generation route to the tetracycline AB enone **6**. Attempted Michael–Claisen cyclizations utilizing the SF2575 AB enone **20** or the phthalide D-ring precursor **46** toward the SF2575 core **18** were unsuccessful. At this point, I considered that SF2575 was no longer a viable target using the aforementioned strategy, and another class of accessible compounds which would capitalize on the advances made was sought. With an approach to an oxygenated AB enone, I decided to investigate C4-oxygenated tetracyclines.

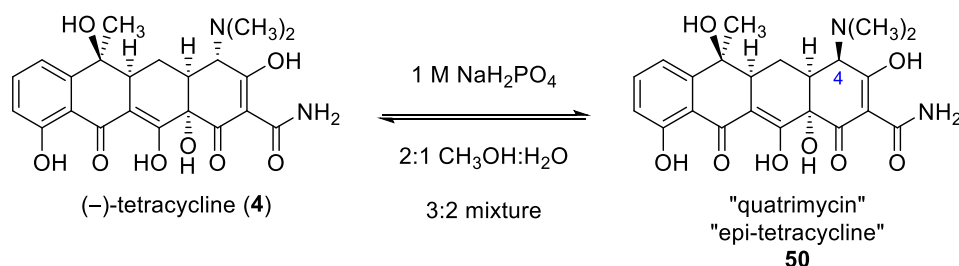
Chapter 2

A New Direction: Synthesis of C4-Dedimethylamino-C4-Oxygenated Minocycline Analogs

Chemical Transformations of the C4-Position of the Tetracyclines

Despite extensive study of tetracycline structure-activity relationships executed by many researchers over the past 60 years, influence of substitution at the C4 position has been largely neglected, simply noting that an (*R*)-dimethylamino substituent is essential for antibiotic activity.⁷ Only semi-synthetic modifications to the C4 position have been reported. They are described in detail below.

In the mid-1950s, two groups, one at Lederle Laboratories and another at Chas. Pfizer & Co, independently isolated and identified C4-epimerized tetracycline.³⁵ Upon treatment of tetracycline (**4**) with a solution of NaH₂PO₄ in a mixture of methanol and water, it equilibrated to a mixture with compound **50** in a 3:2 molar ratio (Scheme 2.1). The Lederle chemists named this new compound “quatrimycin,” while the Chas. Pfizer & Co. researchers labeled their product “epi-tetracycline.” The newly epimerized **50** demonstrated significantly reduced bioactivity (roughly 5%) compared to the parent tetracycline. This transformation was found to be general and was applied to other tetracycline family members (chlorotetracycline, oxytetracycline, etc.) and the reduced bioactivity of the C4-epimers was consistently observed.³⁶

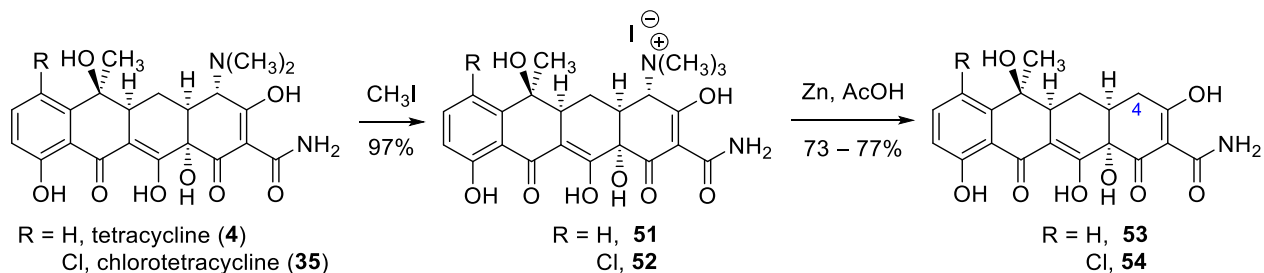


Scheme 2.1: Epimerization of tetracycline.

³⁵ (a) Doerschuk, A. P. Bitler, B. A.; McCormick, J. R. D. *J. Am. Chem. Soc.* **1955**, *77*, 4687. (b) Stephens, C. R.; Conover, L. H.; Gordon, P. N.; Pennington, F. C.; Wagner, R. L.; Brunings, K. J.; Pilgrim, F. J. *J. Am. Chem. Soc.* **1956**, *78*, 1515–1516. (c) McCormick, J. R. D.; Fox, S. M.; Smith, L. L.; Bitler, B. A.; Reichenthal, J.; Origoni, V. E.; Muller, W. H.; Winterbottom, R.; Doerschuk, A. P. *J. Am. Chem. Soc.* **1956**, *78*, 3547–3548.

³⁶ McCormick, J. R. D.; Fox, S. M.; Smith, L. L.; Bitler, B. A.; Reichenthal, J.; Origoni, V. E.; Muller, W. H.; Winterbottom, R.; Doerschuk, A. P. *J. Am. Chem. Soc.* **1957**, *79*, 2849–2858.

The Lederle Laboratory scientists also discovered a method to remove the dimethylamino functionality altogether (Scheme 2.2).³⁷ First, the tertiary amine was quaternized upon treatment with iodomethane. Addition of zinc dust to the methiodides **51** and **52** in acetic acid afforded the reduced compounds **53** and **54**, respectively. Both the quaternary salts and the dedimethylamino compounds lacked antibacterial activity.



Scheme 2.2: Synthesis of 4-dedimethylamino tetracyclines.

In 1964, the two competing groups at Chas. Pfizer & Co.³⁸ and at Lederle Laboratories,³⁹ also independently reported the isolation and identification a different class of tetracycline semi-synthetic derivatives – the 4,6-hemiketals **56** and **61** (Scheme 2.3 and Scheme 2.5). These interesting intermediates were further transformed into a narrow subset of C4-derivatives. These analogs served as empirical evidence that the (*R*)-dimethylamine at the C4-position was absolutely necessary for antibacterial activity.

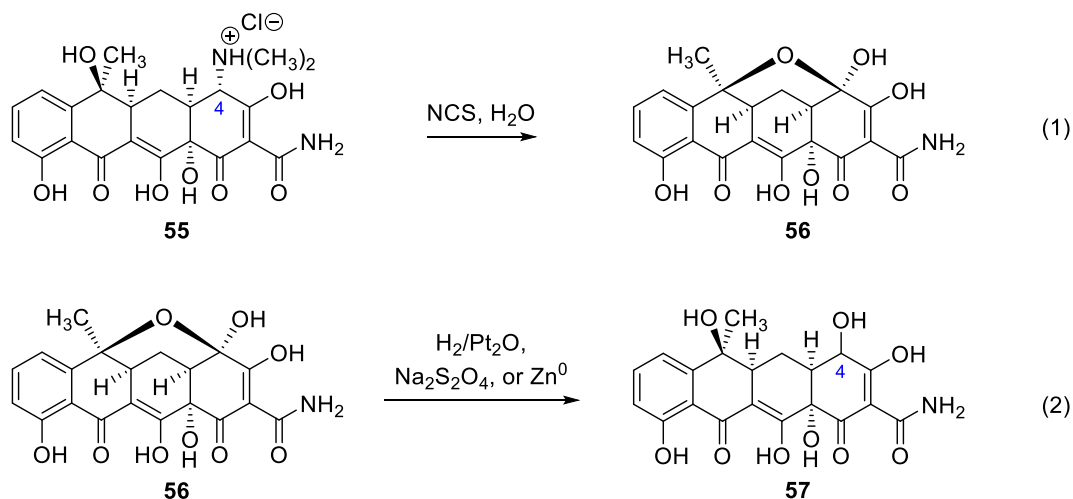
A scientist team at Chas. Pfizer & Co. found that treatment of tetracycline hydrochloride (**55**) with NCS in aqueous solvent afforded hemiketal **56** (Scheme 2.3, equation 1).³⁸ Reduction of the hemiketal was achieved under a variety of conditions – catalytic hydrogenation, sodium

³⁷ Boothe, J. H.; Bonvicino, G. E.; Waller, C. W.; Petisi, J. P. Wilkinson, R. W.; Broschard, R. B. *J. Am. Chem. Soc.* **1958**, *80*, 1654–1657.

³⁸ (a) Blackwood, R. K.; Stephens, C. R. *J. Am. Chem. Soc.* **1964**, *86*, 2736–2737. (b) Blackwood, R. K.; Stephens, C. R. *Can. J. Chem.* **1965**, *43*, 1382–1388.

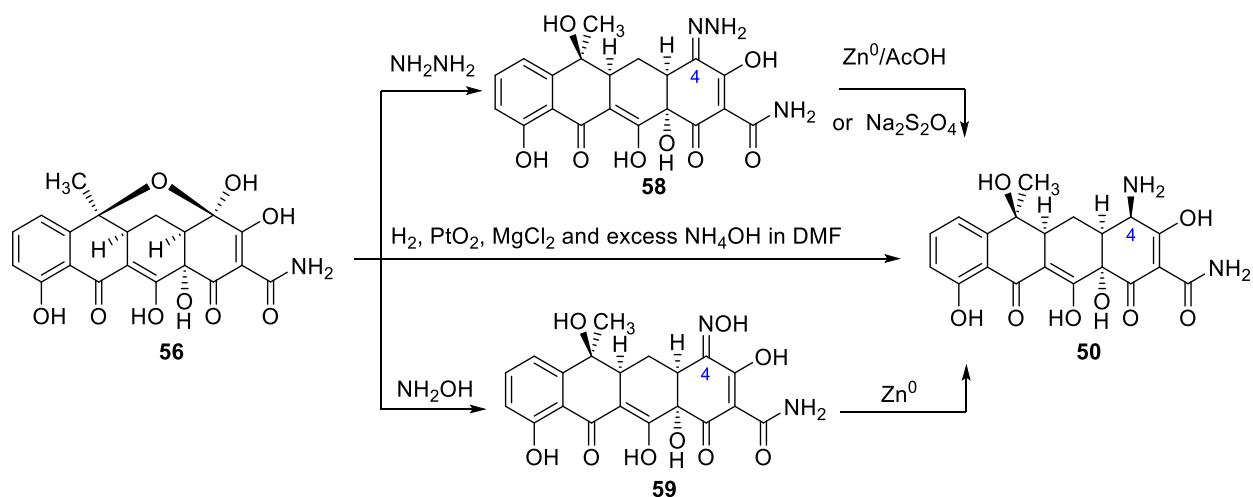
³⁹ (a) Esse, R. C.; Lowery, J. A.; Tamorria, C. R.; Sieger, G. M. *J. Am. Chem. Soc.* **1964**, *86*, 3874–3875. (b) Esse, R. C.; Lowery, J. A.; Tamorria, C. R.; Sieger, G. M. *J. Am. Chem. Soc.* **1964**, *86*, 3875–3877.

hydrosulfite reduction or zinc reduction – yielding C4-dedimethylamino-C4-hydroxytetracycline (**57**) (Scheme 2.3, equation 2). There was no discussion of the stereochemical configuration at the C4 center, nor was tetracycline **57** submitted for antibacterial screening.



Scheme 2.3: Synthesis of tetracycline 4,6-hemiketal **56** and reduction to alcohol **57**.

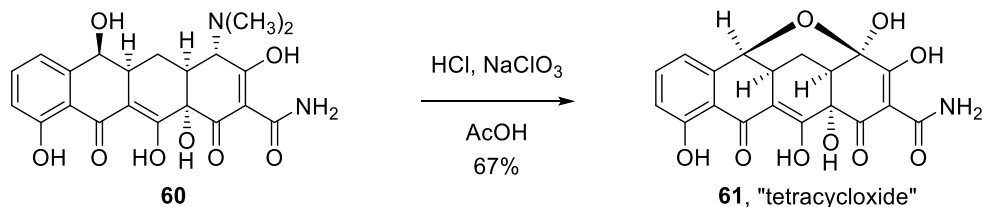
Additional transformations of hemiketal **56** were reported (Scheme 2.4).³⁸ Subjection of hemiketal **56** to hydrazine or hydroxylamine afforded the hydrazone **58** or oxime **59**, respectively. These derivatives were then both reduced to the free amine **50**. Amine **50** was also produced directly from reductive amination of hemiketal **56** using hydrogen, platinum oxide, and magnesium chloride in the presence of excess ammonium hydroxide. The exact stereochemical configuration of **50** was determined by degradation studies and compound **50**'s reduced antibacterial activity to be that of epi-tetracycline.



Scheme 2.4: Additional transformations of **56**.

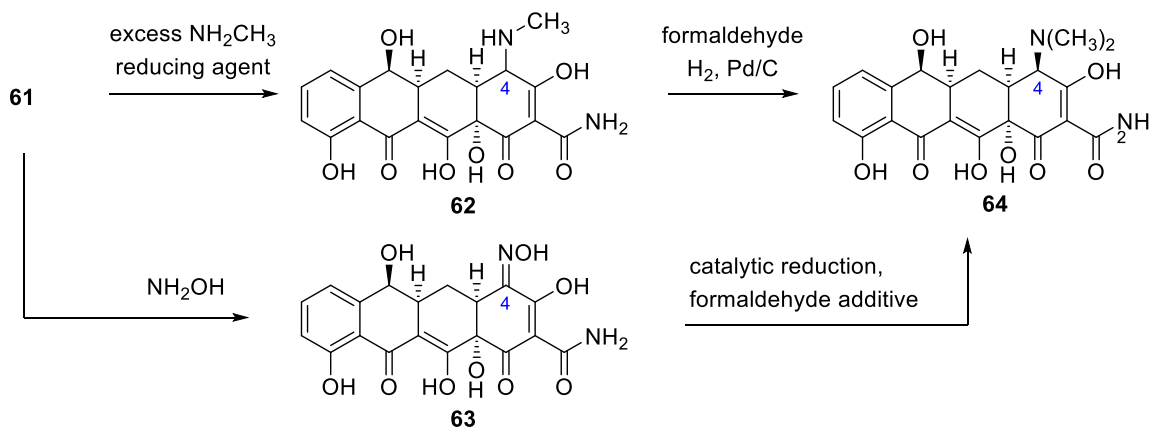
While studying 6-demethyltetracycline (**60**), a tetracycline derivative from fermentation broths of mutant *Streptomyces* bacteria,⁴⁰ the scientist team at Lederle Laboratory led by Dr. Robert Esse simultaneously published their synthesis and derivatization of the corresponding 6-demethyltetracycline-4,6-hemiketal (**61**).³⁹ 6-Demethyltetracycline (**60**), upon treatment with concentrated HCl and NaClO_3 in acetic acid, was transformed into the corresponding 4,6-hemiketal **61**, which was dubbed “tetracycloxide” (Scheme 2.5).

⁴⁰ McCormick, J. R. D.; Sjolander, N. O.; Hirsch, U.; Jensen, E. R.; Doerschuk, A. P. *J. Am. Chem. Soc.* **1957**, *79*, 4561–4563.



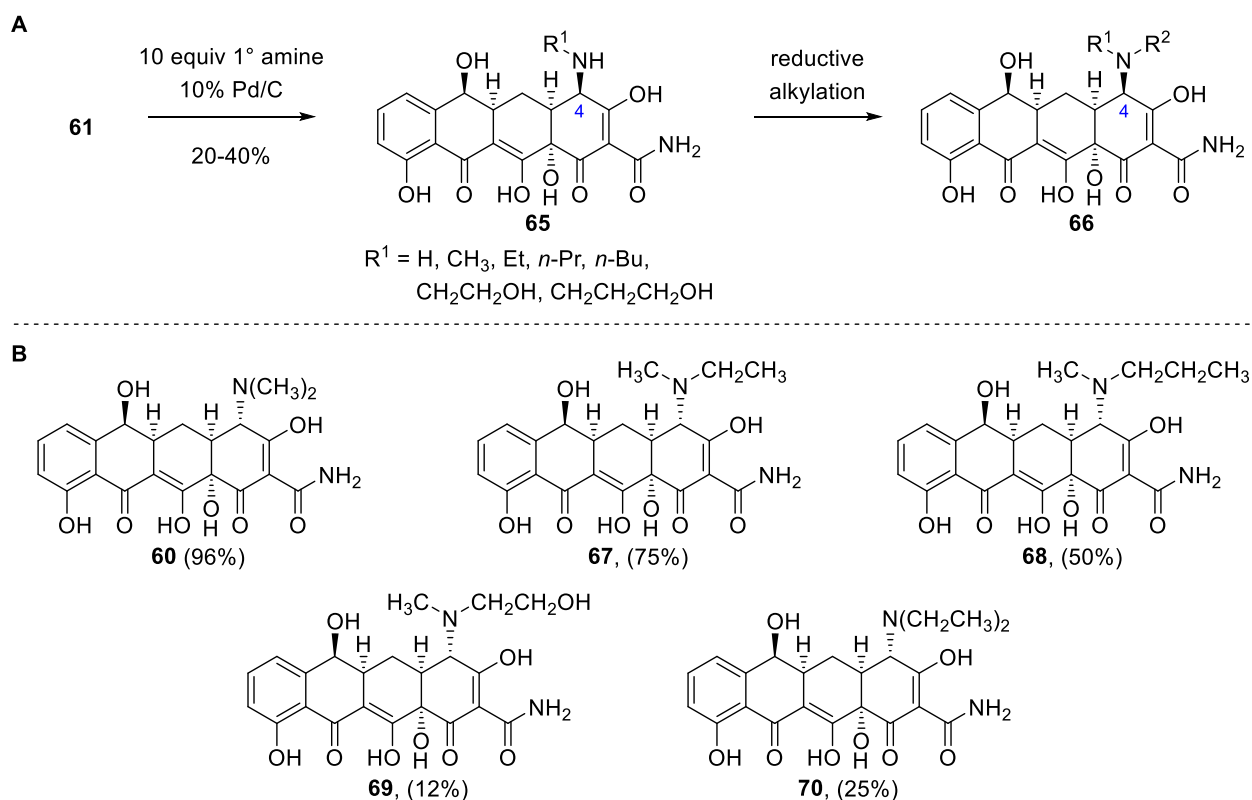
Scheme 2.5: Synthesis of 6-demethyltetracycline 4,6-hemiketal **61**.

Dr. Esse demonstrated that 6-demethyltetracycline (**60**) could be recovered from tetracycloxide **61** by two methods (Scheme 2.6). Reductive amination of tetracycloxide **61** with excess CH_3NH_2 afforded secondary amine **62**. An additional methyl group was installed using formaldehyde, H_2 , and Pd/C , resulting in **64**. Alternatively, tetracycloxide **61** could be transformed into oxime **63** upon reaction with hydroxylamine. Conversion back to the starting 6-demethyltetracycline (**60**) was realized after a catalytic reduction in the presence of formaldehyde. No explicit analysis of the configuration of the C4 stereocenter was mentioned in the initial report,^{39a} however a more detailed discussion of the stereochemical outcome was provided in the following report,^{39b} which suggested that epimeric **64** was initially formed, but was epimerized to **60**.



Scheme 2.6: Transformations of **61**.

Dr. Esse and the scientists at Lederle Laboratories utilized their tetracyclic intermediate **61** in the production of the C4-amino tetracycline analogs (Scheme 2.7), and screened these derivatives for biological activity, thereby generating the first reported SAR of the 4-position.^{39b} Reductive amination of tetracyclic **61** with ammonia and variety of aliphatic primary amines afforded secondary amine tetracyclines of the general structure **65** (Scheme 2.7, **A**). These amines were shown to have the *epi*-configuration at C4, and all attempts to epimerize them failed. A subset of amines **65** was reductively alkylated, yielding tertiary amines **66**. The tertiary amines **66** were also subjected to epimerization conditions, and 6-demethyltetracycline derivatives with the (*R*)-configuration at C4 (**67** – **70**) were isolated (Scheme 2.7, **B**).



Scheme 2.7: Strategy for the production of C4-tetracycline analogs (biological activity relative to tetracycline).

The antibacterial properties of both secondary amines **65** and C4-epimerized **60** and **67** – **70** were investigated (Scheme 2.7, **B**; antibacterial activity relative to tetracycline in parentheses).

Unsurprisingly, amines of the unnatural tetracycline configuration displayed weak antibacterial potencies. The C4-epimerized dialkyl analogs, however, retained much of the activity relative to tetracycline itself. In general, larger substituents on the amine led to greater reduction in activity.

These findings, made more than fifty years ago, comprise the known structure-activity relationships of the C4-position on tetracyclines. Tetracyclines are functionally dense molecules and semi-synthetic methods are limited in their ability to produce diversified analogs. Fully synthetic strategies, however, could access scaffolds unattainable by other means and represent the key to expanding the known SAR of the C4-position of tetracyclines. Based on the chemistry developed in Chapter 1, a C4-modified AB enone would achieve this exact goal.

Potential Implications for Biological Activity

Before proposing the synthesis of C4-modified tetracycline antibiotics, I considered the potential impact on both ribosomal and tetracycline repressor protein (TetR)⁴¹ affinities. Since tetracycline discovery, multiple studies⁴² have been devoted to the determination of the exact source of antibacterial action of the tetracycline family, including X-ray analysis of tetracycline bound to its target.^{6, 43} In the past three decades, incidence of antibiotic resistance (both in general and specifically to the tetracyclines) has spurred investigations of the underlying mechanisms. A brief review of the results will be presented here, including detailed analyses of the crystal structures of tetracycline bound to the 30S ribosomal subunit and bound to TetR.

⁴¹ Tetracycline repressor protein, TetR, contributes toward the primary mechanism of resistance to tetracyclines, energy-dependent efflux.

⁴² Selected examples: (a) Gale, E. F.; Folkes, J. P. *Biochem. J.* **1953**, *53*, 493–498. (b) Hash, J. H.; Wishnick, M.; Miller, P. A.; *J. Biol. Chem.* **1964**, *239*, 2070–2078. (c) Heman-Ackah, S. M. *Antimicrob. Agents Chemother.* **1976**, *10*, 223–228. (d) Weisblum, B.; Davies, J. *Bact. Rev.* **1968**, *32*, 493–528. (e) Gottesman, M. E. *J. Biol. Chem.* **1967**, *242*, 5564–5571. (f) Igarashi, K.; Kaji, A. *Eur. J. Biochem.* **1970**, *14*, 41–46.

⁴³ Crystallographic studies: (a) See Ref. 6 in Chapter 1. (b) Pioletti, M.; Schlünzen, F.; Harms, J.; Zarivach, R.; Glühmann, M.; Avila, H.; Bashan, A.; Bartels, H.; Auerbach, T.; Jacobi, C.; Hartsch, T.; Yonath, A.; Franceschi, F. *EMBO J.* **2001**, *20*, 1829–1839.

Tetracycline, coordinated to a Mg^{2+} atom, binds to the 30S subunit of the bacterial ribosome, inhibiting protein synthesis by preventing the docking of charged aminoacyl tRNA to the acceptor site on the ribosome. Once the tetracycline is bound, new amino acids are not able to attach and elongate the nascent polypeptide chain. Tetracycline is a bacteriostatic agent; cessation of protein synthesis does not immediately result in cell death. Also, tetracycline binding is reversible; removal of the tetracycline from the ribosome restores bacterial viability.

Tetracycline interacts with the 30S ribosomal subunit through several bonding interactions (Figure 2.1). The magnesium atom, coordinated to the keto-enol group spanning the B- and C-rings, creates an intermediate which establishes multiple contacts with the phosphate oxygens of RNA nucleotides G1197, G1198 and C1054. Additionally, an intricate hydrogen-bonding network exists between the lower periphery of tetracycline and the ribosomal residues C1054, G1196 and C1195. There is an apparent π -stacking interaction between the nucleoside base of C1054 and the D-ring of tetracycline, as well as two hydrogen bonds involving the A-ring enol, one with the sugar component of A965 and the other with the phosphate oxygen of G966.

The crystal structures succinctly explain the empirically determined SAR for the tetracycline family: the lower polar hemisphere must be conserved for biological activity, while the substitution of the northern non-polar periphery is well-tolerated.

We also considered how C4-modification of tetracycline antibiotics would impact resistance mechanisms.⁴⁴ There are three types of tetracycline resistance (in order of importance): efflux, ribosomal protection proteins (RPPs) and structural modifications. Inactivation of tetracyclines by structural alterations was not considered a clinically relevant mechanism of resistance due to its occurrence only in anaerobic bacteria under specific conditions.⁴⁵ Ribosomal protection proteins are postulated to bind to the tetracycline–ribosome complex at a distal location, causing a conformational change which dislodges the antibiotic without disrupting protein synthesis.⁴⁶ I realized that I could not predict *a priori* how modifications of the C4-position of tetracycline would affect these specific resistance mechanisms.

Energy-dependent tetracycline efflux constitutes the primary mode of resistance to the tetracyclines. This process is mediated by efflux pump (antiporter) proteins such as TetA and is regulated by a repressor protein, TetR. TetR controls TetA expression at the transcription level. Upon entry into a cell, a complex between TetR and tetracycline–Mg²⁺ forms. The affinity of the tetracycline–Mg²⁺ complex for TetR is 1000-fold greater than that for the ribosome.⁴⁷ This binding initiates the expression of the resistance protein (TetA) and tetracycline is pumped out of the cell.

⁴⁴ For an overview on tetracycline resistance, see: Thaker, M.; Spanogiannopoulos, P.; Wright, G. D. *Cell. Mol. Life Sci.* **2010**, *67*, 419–431. Tetracycline efflux: (a) Mendez, B.; Tachibana, C.; Levy, S. B. *Plasmid*, **1980**, *3*, 99–108. (b) Tovar, K.; Ernst, A.; Hillen, W. *Mol. Gen. Genet.* **1988**, *215*, 76–80. (c) Zhao, J.; Aoki, T. *Microbiol. Immunol.* **1992**, *36*, 1051–1060. (d) Schnappinger, D.; Hillen W.; *Arch. Microbiol.* **1996**, *165*, 359–369. Ribosomal protection proteins: (a) Burdett, V. *J. Biol. Chem.* **1991**, *266*, 2872–2877. (b) Sanchez-Pescador, R.; Brown, J. T.; Urden, M. S. *Nucl. Acids Res.* **1988**, *16*, 1218. (c) Taylor, D. E.; Chau, A. *Antimicrob. Agents Chemother.* **1996**, *40*, 1–5.

⁴⁵ Speer, B. S.; Bedzyk, L.; Salyers, A. A. *J. Bacteriol.* **1991**, *173*, 170–183.

⁴⁶ Connell, S. R.; Tracz, D. M.; Nierhaus, K. H.; Taylor, D. E. *Antimicrob. Agents Chemother.* **2003**, *47*, 3675–3681.

⁴⁷ (a) Hillen, W.; Gatz, C.; Altschmied, L.; Schollmeier, K.; Meier, I. *J. Mol. Biol.* **1983**, *169*, 707–721. (b) Takahashi, M.; Altschmied, L.; Hillen, W. *J. Mol. Biol.* **1986**, *187*, 341–348.

The three-dimensional structure of the tetracycline–Mg²⁺ complex bound to the TetR protein has been determined using X-ray crystallography (Figure 2.2, **B**)⁴⁸ and this provided an insight into the 1000-fold increase in binding affinity. As opposed to tetracycline’s ribosomal binding interactions which primarily engage the compound’s lower periphery (Figure 2.2, **A**), the TetR protein contacts surround the molecule and engage it as a whole. Of particular note, the asparagine-82 residue is involved in a hydrogen-bond with the dimethylamino substituent at C4. Interference with this constructive interaction should weaken tetracycline’s affinity for TetR. Additionally, the 6-hydroxyl functional group would not be present in the proposed C4-modified analogs, thus removing a second binding interaction and enabling the production of derivatives that may overcome TetR resistance.

⁴⁸ (a) Hinrichs, W.; Kisker, C.; Duvel, M.; Saenger, W. *Science*, **1994**, *264*, 418–420. (b) Kisker, C.; Hinrichs, W.; Tovar, K.; Hillen, W.; Saenger, W. *J. Mol. Biol.* **1995**, *247*, 260–280. (c) Orth, P.; Schnappinger, D.; Hillen, W.; Saenger, W.; Hinrichs, W. *Nature Struct. Biol.* **2000**, *7*, 215–219.

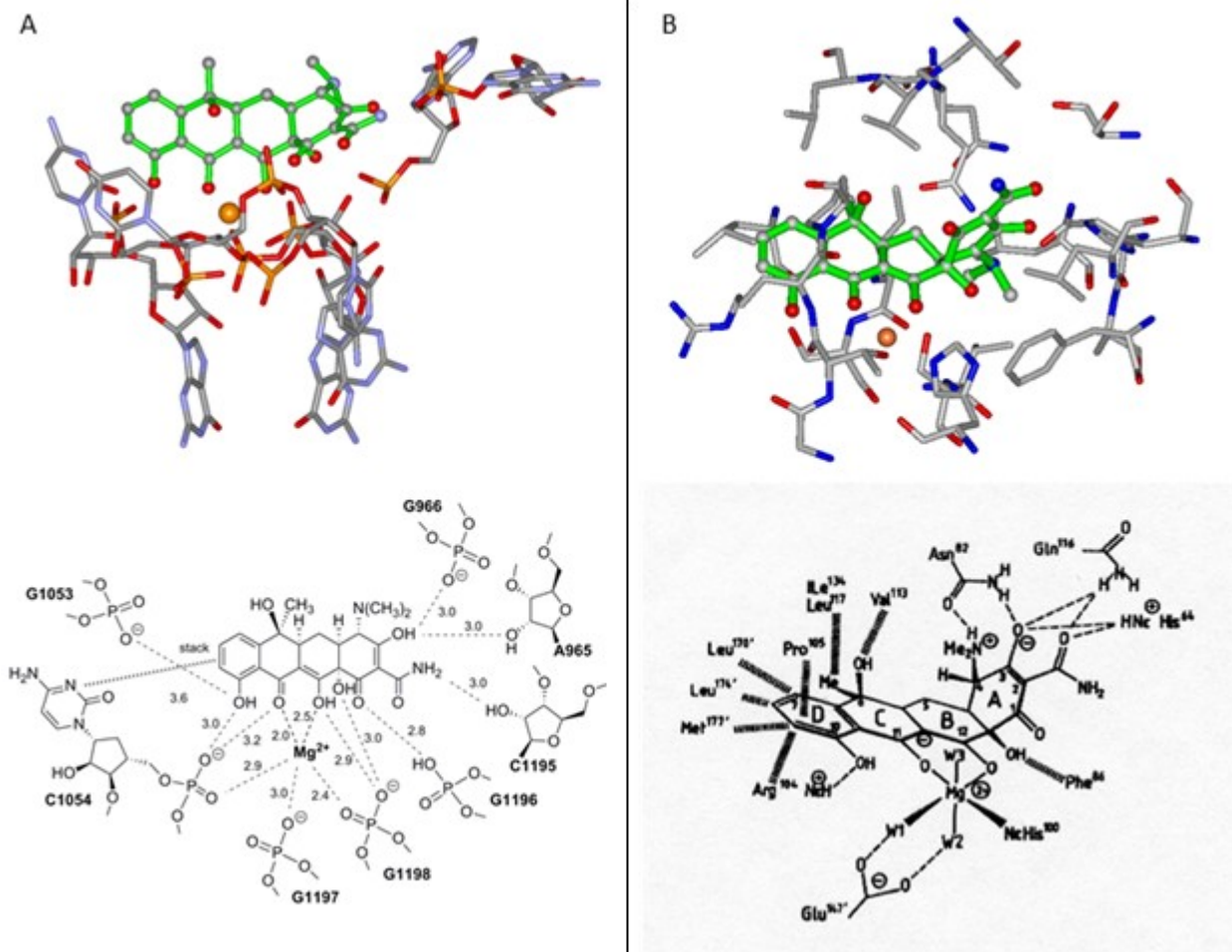


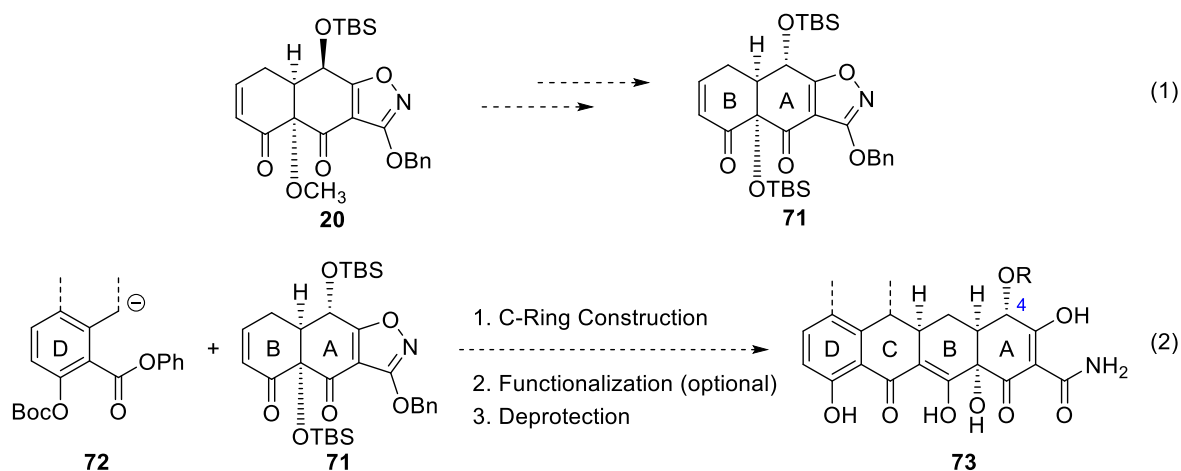
Figure 2.2: A. A different view of tetracycline (4) bound to the 30S subunit of the ribosome; magnesium atom shown in orange. B. Tetracycline (4) bound to the tetracycline repressor protein,⁴⁸ TetR; magnesium atom shown in orange.

Thus, I identified C4-modified tetracyclines as synthetic targets to probe the possibility of decreasing TetR affinity while maintaining antibacterial properties, thereby producing new antibiotic candidates.

New Strategy: Epimerization at C4 and Synthesis of AB Enone 71

I determined that AB enone **71** would be an appropriate key intermediate to access the C4-modified tetracycline derivatives (Scheme 2.8, equation 1). Myers' platform for the

tetracycline synthesis would make C4-dedimethylamino-C4-hydroxytetracycline analogs of the general scaffold **73** easily accessible (Scheme 2.8, equation 2).⁴⁹ Additionally, late stage functionalization of the free C4-hydroxyl group would lead to the production of a wider range of compounds including, but not limited to, ethers, esters, and carbamates. Furthermore, these C4-modified tetracyclines would be less likely to undergo epimerization reactions at biological pH, thereby potentially increasing the antibiotic activities of these compounds.



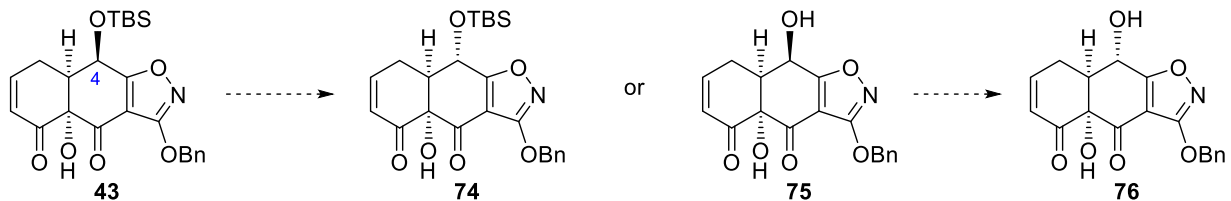
Scheme 2.8: Synthetic plan toward 4-dedimethylamino-4-hydroxytetracyclines.

To access AB enone **71** from the route to SF2575 AB enone **20**, I identified hydroxy enone **43** as a common intermediate. I would need to invert the configuration of the C4 stereocenter of AB enone **20** (Scheme 2.9) and protect the hydroxyl at C12a. Proposed strategies for the inversion of stereochemical configuration included: (1) direct epimerization of the hydroxy enone **43** or the diol **75**, (2) Mitsunobu reaction with a nucleophilic oxygenated substrate followed by saponification, and (3) activation of the free alcohol followed by displacement of the leaving group by an S_N2 reaction. The latter method would allow for an even wider AB enone substrate scope. For example, thiols, azides, and nitriles could be incorporated

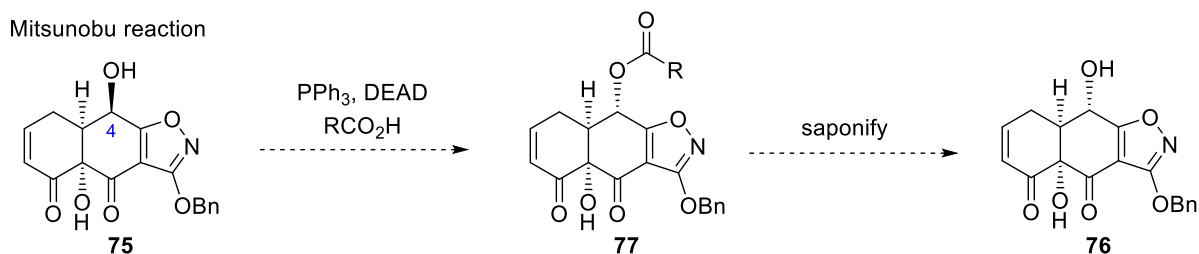
⁴⁹ See Chapter 1 for relevant background.

into the AB enone scaffold (and they themselves could be further modified), continually expanding the scope of SAR studies of the C4-position of tetracyclines.

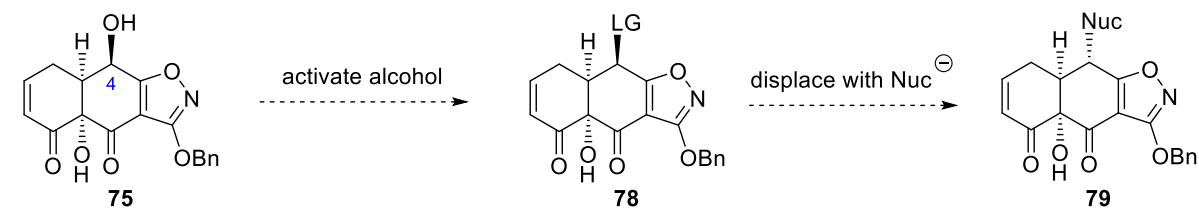
Direct epimerization



Mitsunobu reaction



$\text{S}_{\text{N}}2$ -displacement of a leaving group



Scheme 2.9: Strategies for epimerization of C4.

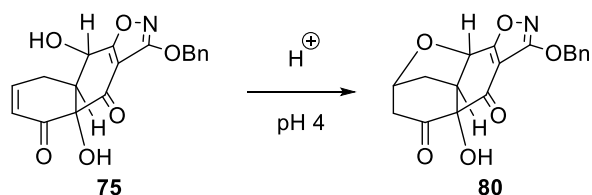
However, none of the proposed methods delivered any desired product. Under the well-precedented conditions for tetracycline epimerizations,⁵⁰ hydroxy enone **43** was either unreactive or decomposed. Under basic⁵¹ or acidic⁵² conditions, diol **75** was again either unreactive or unstable. Notably, treatment of diol **75** with a pH 4 buffer afforded cyclic ether **80** (Scheme 2.10) due to the addition of the hydroxyl into the Michael acceptor enone. Attempted Mitsunobu

⁵⁰ References cited in footnote 2 and (a) Yuen, P. H.; Sokoloski, T. D. *J. Pharm. Sci.* **1977**, *66*, 1648–1650. (b) Noseworthy, M. M. U.S. Patent 3,009,956, November 21, 1961.

⁵¹ Bases screened: pH 8 buffer, DBU, triethylamine, diisopropylamine or tetramethylguanidine at 23 °C for 24 h.

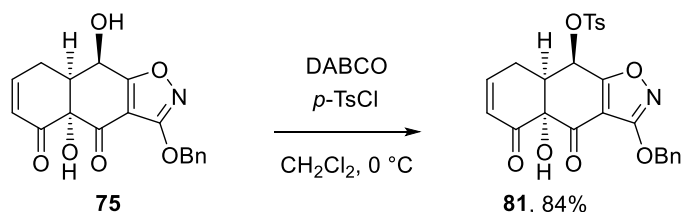
⁵² Acids screened: buffers ranging in pH from 4 to 6 at 23 °C for 24 h.

reactions were generally unsuccessful and the use of Brønsted acids (formic acid or *p*-nitrobenzoic acid) as sources of nucleophilic oxygen promoted the formation of cyclic ether **80**.



Scheme 2.10: Synthesis of cyclic ether **80**.

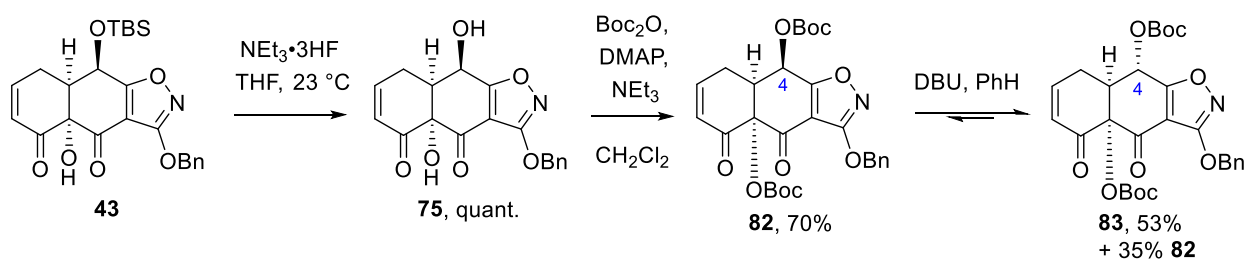
To investigate the activation and displacement strategy outlined in Scheme 2.9, I transformed the C4-hydroxyl into a tosylate by treatment with DABCO and *p*-tosyl chloride (Scheme 2.11). However, all attempts to displace the tosylate with a variety of nitrogen nucleophiles afforded only recovered starting materials or decomposition products. The AB ring system of **81** is highly oxygenated and further activation lowers the barrier for aromatization, the presumed decomposition pathway.



Scheme 2.11: Synthesis of tosylate **81**.

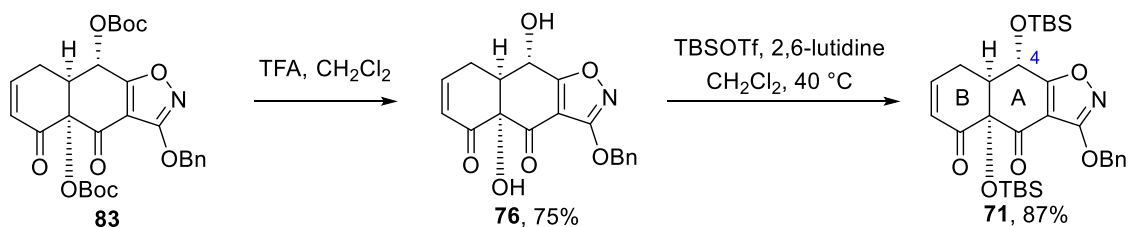
A pivotal breakthrough in the exploration of C4-epimerization was achieved upon the re-functionalization of diol **75** with an electron withdrawing group (Scheme 2.12). Diol **75** was transformed into the Boc bis-carbonate **82** in 70% yield under standard conditions. This carbonate **82** could be successfully epimerized by treatment with DBU. The electron withdrawing group stabilized the nascent partial negative charge which formed at the C4 center

upon treatment with DBU, allowing reprotonation to occur and establishing a thermodynamic equilibrium between **82** and **83**. This process was not without decomposition pathways, but recovered **82** could be resubjected to epimerization conditions, thus providing sufficient quantities of Boc bis-carbonate **83**.



Scheme 2.12: Synthesis and epimerization of Boc bis-carbonate **82**.

With a reliable method for epimerization of the C4-position, the remainder of the synthesis of AB enone **71** was straightforward (Scheme 2.13). Carbonate **83** was treated with trifluoroacetic acid, producing *syn* diol **76** in 75% yield. Both hydroxyls were easily protected upon reaction with TBS triflate and 2,6-lutidine at 40°C , delivering the AB enone **71** in 87% yield. Similarly to the 4th generation route to the tetracycline AB enone **6**, the method proved to be scalable and afforded ca. 1 gram of AB enone **71** in the largest batch.

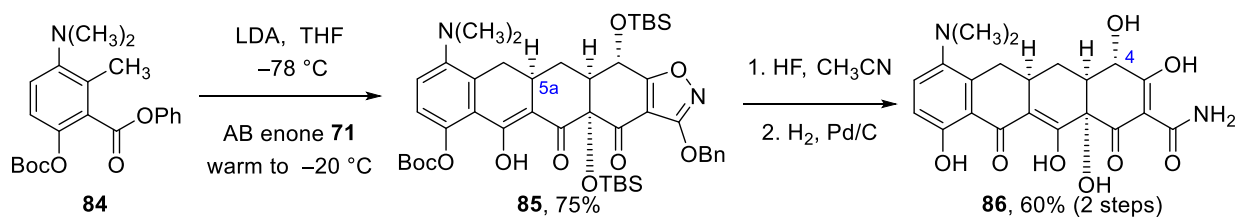


Scheme 2.13: Completion of the synthesis of AB enone **71**.

Synthesis of Analogs

Application of the Myers' platform for the construction of the 6-deoxytetracycline using the AB enone **71** afforded a number of C4-modified minocycline analogs. Gratifyingly, treatment of

minocycline D-ring phenyl ester **84**⁵³ with LDA at $-78\text{ }^{\circ}\text{C}$, followed by the addition of AB enone **71**, produced Michael–Claisen adduct **85** in 75% yield (Scheme 2.14). The stereochemical configuration of the C5a center matched the one found in natural tetracyclines. Subjection of Michael–Claisen adduct **85** to the standard two-step deprotection sequence (HF in acetonitrile, followed by H_2 , Pd/C) provided C4-dedimethylamino-C4-hydroxyminocycline (**86**) in 60% yield over the two steps.



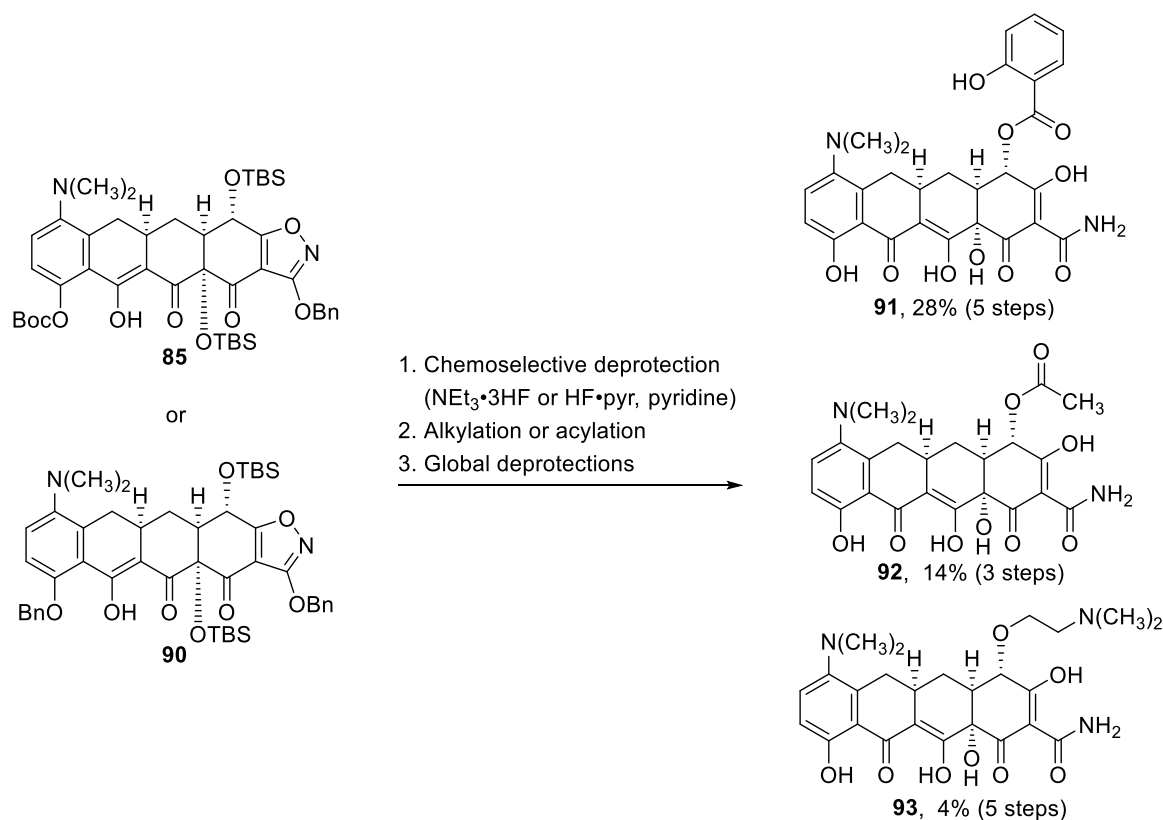
Scheme 2.14: Synthesis of 4-dedimethylamino-4-hydroxyminocycline (**86**).

C4-Dedimethylamino-C4-methoxyminocycline (**89**) was produced using a similar strategy (Scheme 2.15). Treatment of Michael–Claisen adduct **85** with HF removed the silyl and carbamate protecting groups, affording compound **87**. Addition of one equivalent of Meerwein’s salt⁵⁴ in the presence of Proton Sponge⁵⁵ produced methyl ether **88** in 78% yield. I presumed that the enolic hydroxyl groups at C10 and C12 were engaged in hydrogen bonding with the carbonyl at C11 and therefore, methylation occurred at the most accessible hydroxyl group, (C4 as opposed to C12a). This hypothesis was confirmed through nOe experiments. The addition of more than one equivalent of Meerwein’s salt resulted in a mixture of products which contained methylation at multiple sites. Hydrogenolysis of the isoxazole of compound **88** gave C4-dedimethylamino-C4-methoxyminocycline (**89**) in 75% yield.

⁵³ The decision to synthesize minocycline analogs was rooted in the availabilities of the *tert*-butylcarbonate D-ring precursor **84** and the benzyl ether D-ring precursor (compound **44**, page 20) in the lab.

⁵⁴ Trimethyloxonium tetrafluoroborate.

⁵⁵ 1,8-Bis(dimethylamino)naphthalene.



Scheme 2.15: Strategy for the synthesis of analogs **91**, **92**, and **93**.

Antibacterial Activity

Determination of minimum inhibitory concentration (MIC) values, a measure of antibiotic potency, was performed at Tetrphase Pharmaceuticals. The results are summarized in Table 2.1. In short, none of the C4-modified minocycline analogs demonstrated significant antibacterial properties, but some general trends were established. C4-Dedimethylamino-C4-hydroxyminocycline (**86**) was slightly more potent than the C4-methoxy analog **89** against both Gram-positive and Gram-negative strains. The ester derivatives **91** and **92** were both completely inactive against Gram-negative pathogens, but the bulkier salicyl ester **91** displayed greater efficacy against Gram-positive bacteria than the acetate **92**. The (2-dimethylamino)ethyl ether analog **93** was completely ineffective against the entire panel of bacteria.

Table 2.1: Minimum inhibitory concentration (MIC) values for minocycline and 4-modified minocycline analogs ($\mu\text{g/mL}$)

	GP				GN										
	tetM	tetK	tetM	tetM	tetM	tolC	tetM	tetA	KO	tetB	PA555	PA556	AB250	SM256	BC240
minocycline	0.031	8	≤ 0.016	16	16	4	0.25	0.25	8	4	32	0.25	8	0.5	4
4-OH-minocycline	32	>32	2	32	32	>32	4	16	>32	>32	>32	8	16	8	>32
4-OCH ₃ -minocycline	>32	>32	8	>32	>32	>32	16	32	>32	>32	>32	16	>32	32	>32
4-OAc-minocycline	16	16	4	32	32	>32	>32	>32	>32	>32	>32	>32	>32	32	>32
4-O-salicyl-minocycline	8	4	4	>32	>32	>32	>32	>32	>32	>32	>32	>32	>32	>32	>32
4-O-CH ₂ -CH ₂ -N(CH ₃) ₂ minocycline	>32	>32	>32	>32	>32	>32	>32	>32	>32	>32	>32	>32	>32	>32	>32
tigecycline	0.125	0.25	0.031	0.063	0.125	≤ 0.016	0.031	0.031	0.5	1	8	0.125	4	1	8

Abbreviations: GP: Gram-positive; GN: Gram-negative organisms: SA. *Staphylococcus aureus*; EF. *Enterococcus faecalis*; SP. *Streptococcus pneumoniae*,

EC. *Escherichia coli*; KP. *Klebsiella pneumoniae*; PA. *Pseudomonas aeruginosa*; AB. *Acinetobacter baumannii*; SM. *Stenotrophomonas maltophilia*; BC.

Burkholderia cenocepacia. resistance determinants: tetM: ribosomal protection proteins. tetA, tetB, tetK: tetracycline efflux proteins. KO: multiple efflux pump knockout. tolC: multiple efflux pump knockout.

Conclusions

While it was accepted in the scientific community that a basic amine of the (*R*)-configuration is necessary for tetracycline antibiotic potency, the crystal structure of tetracycline bound to the 30S subunit of the ribosome did not provide an explanation for this at the molecular level. The dimethylamino substituent did not engage in constructive binding interactions to the ribosome, but did engage in a hydrogen-bonding interaction with the tetracycline repressor protein, TetR, a protein responsible for tetracycline efflux from the cell. Thus, I identified C4-modified tetracyclines as synthetic targets to probe the possibility of decreasing TetR affinity while maintaining antibiotic activity.

To that end, I developed an epimerization strategy to enable synthesis of AB enone **71** from hydroxy enone **43** and I accessed five C4-modified minocycline derivatives via Michael–Claisen cyclizations on AB enone **71**. These compounds were screened against a panel of bacteria and were shown to possess poor bioactivity. At this point, I considered that the dimethylamino functionality must contribute to tetracyclines' antibacterial properties via an alternate mechanism (as opposed to concrete binding interactions).

Due to the simultaneous presence of the tertiary amine and the vinylogous carbamic acid on the A-ring, the tetracyclines exist primarily as zwitterionic compounds at physiological pH.⁵⁸ It has been theorized that both the zwitterionic form and a less polar, non-ionized species are required for biological activity.⁵⁹ The unionized structure may diffuse through permeable lipid membranes while the zwitterionic species actively binds the ribosomal subunit. This supposition potentially explains the poor bioactivities of our C4-modified minocycline analogs. They may display weak antibacterial potency in part due to their inefficient entry into the bacterial cell.

⁵⁸ At pH 7.4, only 7% of tetracycline exists in non-ionized form.

⁵⁹ Stezowski, J. J. *J. Am. Chem. Soc.* **1976**, *98*, 6012–6018.

General Experimental Procedures

All reactions were performed in flame-dried glassware fitted with rubber septa under a positive pressure of argon, unless otherwise noted. Air- and moisture-sensitive liquids were transferred via syringe or stainless steel cannula. Solutions were concentrated by rotary evaporation below 35 °C. Analytical thin-layer chromatography (TLC) was performed using glass plates pre-coated with silica gel (0.25 mm, 60 Å pore-size, 230–400 mesh, Merck KGA) impregnated with a fluorescent indicator (254 nm). TLC plates were visualized by exposure to ultraviolet light, then were stained by submersion in aqueous ceric ammonium molybdate (CAM) or potassium permanganate solutions followed by brief heating with a heat gun. Flash-column chromatography was performed as described by Still et al.,⁶⁰ employing silica gel (60 Å, 32–63 µm, standard grade, Dynamic Adsorbents, Inc.). Tetrahydrofuran, dichloromethane, and ether were purified by the method of Pangborn et al.⁶¹ The molarity of solutions of *n*-butyllithium was determined by titration against diphenylacetic acid as an indicator (average of three determinations).⁶²

Instrumentation

Proton nuclear magnetic resonance (¹H NMR) spectra and carbon nuclear magnetic resonance (¹³C NMR) spectra were recorded on Varian MERCURY 400 (400 MHz/100 MHz), Varian INOVA 500 (500 MHz/125 MHz), or Varian INOVA 600 (600 MHz/150 MHz) NMR spectrometers at 23 °C. Proton chemical shifts are expressed in parts per million (ppm, δ scale) and are referenced to residual protium in the NMR solvent (CHCl₃: δ 7.26, D₂HCO: δ 3.31).

⁶⁰ Still, W. C.; Khan, M.; Mitra, A. *J. Org. Chem.* **1978**, *43*, 2923–2925.

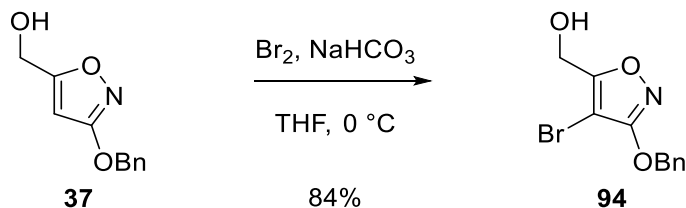
⁶¹ Pangborn, A. B.; Giardello, M. A.; Grubbs, R. H.; Rosen, R. K.; Timmers, F. J. *Organometallics* **1996**, *15*, 1518–1520.

⁶² W. G. Kofron, L. M. Baclawski, *J. Org. Chem.* **1976**, *41*, 1879–1880.

Carbon chemical shifts are expressed in parts per million (ppm, δ scale) and are referenced to the carbon resonance of the NMR solvent (CDCl_3 : δ 77.0, CD_3OD : δ 49.0). Data are represented as follows: chemical shift, multiplicity (s = singlet, d = doublet, t = triplet, q = quartet, dd = doublet of doublets, dt = doublet of triplets, td = triplet of doublets, m = multiplet and/or multiple resonances), integration, coupling constant (J) in Hertz. Infrared (IR) spectra were obtained using a Shimadzu 8400S FT-IR spectrometer. Data are represented as follows: frequency of absorption (cm^{-1}), intensity of absorption (vs = very strong, s = strong, m = medium, w = weak, br = broad). HPLC retention times were acquired using a Beckman System Gold instrument equipped with a Chiracel OD-H column (5 mm particle size, 4.6 mm x 250 mm). High-resolution mass spectra were obtained at the Harvard University Mass Spectrometry Facility using a Bruker micrOTOF-QII mass spectrometer. LC-MS analysis was performed on an Agilent 1260 Infinity instrument equipped with a 6120 quadrupole LC-MS. X-ray crystallographic analysis was performed at the Harvard University X-Ray Crystallographic Laboratory by Dr. Shao-Liang Zheng.

(For clarity, intermediates that have not been assigned numbers in the text are numbered sequentially in the Experimental Information beginning with 94.)

Bromoisoxazole **94**.

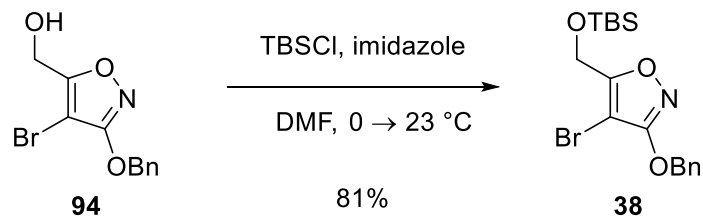


3-Benzyloxy-5-(hydroxymethyl)isoxazole (**37**) (19.8 g, 96.0 mmol, 1 equiv) was dissolved in tetrahydrofuran (200 mL) at 23 °C. Sodium bicarbonate⁶³ (20.3 g, 241 mmol, 2.5 equiv) was added to the reaction flask, producing a white slurry. The reaction flask was placed in an ice-water cooling bath. Bromine (12.4 mL, 241 mmol, 2.5 equiv) was added dropwise over 30 min, whereupon the reaction mixture darkened to red-orange in color. The reaction mixture continued to stir at 0 °C for 1 h before the cooling bath was removed. After a further hour of stirring at 23 °C, an additional portion of bromine (3.00 mL, 58.1 mmol, 0.6 equiv) was added dropwise. The reaction mixture was stirred for 2 h, and was quenched by the addition of saturated aqueous sodium thiosulfate solution (200 mL). Ethyl acetate (400 mL) was added, followed by an aqueous potassium phosphate buffer solution (pH 7.0, 600 mL). The layers were separated and the aqueous layer was extracted with ethyl acetate (2 × 500 mL). The combined organic layers were washed with saturated aqueous sodium chloride solution (750 mL). The washed solution was dried over sodium sulfate and the dried solution was filtered. The filtrate was concentrated and then dissolved in ethyl acetate (400 mL). The organic phase was filtered through a 2 inch pad of Celite, rinsing with additional ethyl acetate. The filtrate was concentrated and then dissolved in ethyl acetate (200 mL). The organic phase was filtered through a 2-inch pad of silica gel and Celite (1 inch of silica gel on top of 1 inch of Celite), rinsing with additional ethyl

⁶³ Sodium bicarbonate was added to neutralize hydrobromic acid. Hydrobromic acid reacts with the solvent, tetrahydrofuran, to form 4-bromobutanol in significant quantities. Addition of sodium bicarbonate greatly reduced the formation of this unwanted byproduct.

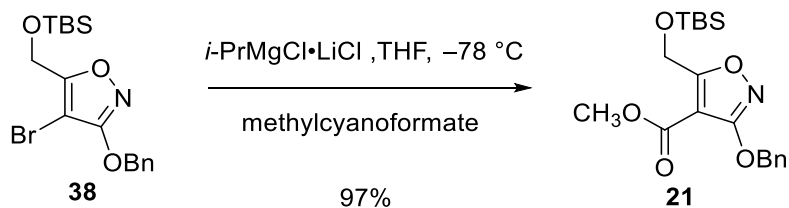
acetate. The filtrate was concentrated, yielding an oily residue, which was purified by flash-column chromatography (5→30% ethyl acetate–hexanes) to provide bromoisoxazole **94** (23.1 g, 84%) as a white solid. TLC: (50% ethyl acetate–hexanes) $R_f = 0.61$ (UV, CAM); ^1H NMR (500 MHz, CDCl_3) δ : 7.47 (d, 2H, $J = 7.3$ Hz), 7.42–7.36 (m, 3H), 5.33 (s, 2H), 4.68 (s, 2H), 2.11 (s, 1H); ^{13}C NMR (125 MHz, CDCl_3) δ : 168.5, 167.9, 135.1, 128.6, 128.6, 128.2, 83.9, 72.1, 55.3; FTIR (neat), cm^{-1} : 3369 (br), 3034 (m), 2931 (m), 1518 (s), 1359 (s), 1103 (s), 1016 (s), 694 (m); HRMS (ESI): Calcd for $(\text{C}_{11}\text{H}_{10}\text{BrNO}_3 + \text{Na})^+$: 305.9742; Found: 305.9738.

Silyl protected hydroxyisoxazole **38**.



Bromoisoxazole **94** (23.1 g, 81.0 mmol, 1 equiv) and imidazole (22.1 g, 325 mmol, 4 equiv) were dissolved in dimethylformamide (200 mL) and the yellow homogeneous reaction mixture was placed in an ice-water cooling bath. *tert*-Butyldimethylsilyl chloride (24.5 g, 162 mmol, 2 equiv) was added and the cooling bath was removed after 10 minutes. The reaction mixture was allowed to warm to 23 °C over 5 minutes. After 15 min at 23 °C, methanol (100 mL) was added to quench the reaction mixture. The quenched solution continued to stir for 20 minutes at 23 °C before it was poured into a 1:1 mixture of methyl *tert*-butyl ether:water (800 mL). The layers were separated and the aqueous layer was extracted with methyl *tert*-butyl ether (2 × 300 mL). The combined organic phase was washed with saturated aqueous sodium chloride solution (750 mL). The washed solution was dried over sodium sulfate and the dried solution was filtered. The filtrate was concentrated and the yellow oily residue was purified by flash-column chromatography on silica gel (2% ethyl acetate–hexanes) to provide silyl protected hydroxyisoxazole **38** (26.2 g, 81%) as a light yellow oil. TLC: (40% ethyl acetate–hexanes) R_f = 0.33 (UV, CAM); ^1H NMR (500 MHz, CDCl_3) δ : 7.47 (d, 2H, J = 6.8 Hz), 7.42–7.36 (m, 3H), 5.33 (s, 2H), 4.68 (s, 2H), 0.92 (s, 9H), 0.13 (s, 6H); ^{13}C NMR (125 MHz, CDCl_3) δ : 168.5, 168.2, 137.3, 128.6, 128.6, 128.2, 83.4, 71.9, 56.0, 25.7, 18.3, –5.4; FTIR (neat), cm^{-1} : 2929 (m), 2858 (m), 1519 (s), 1361 (s), 1105 (s), 908 (s), 835 (s), 731 (s); HRMS (ESI): Calcd for $(\text{C}_{17}\text{H}_{24}\text{BrNO}_3\text{Si} + \text{H})^+$: 400.0767; Found: 400.0762.

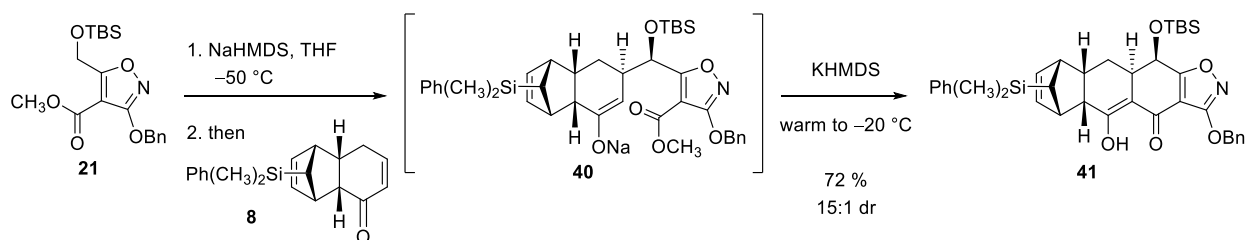
Isoxazole methyl ester **21**.



Silyl protected hydroxyisoxazole **38** (26.2 g, 65.6 mmol, 1 equiv) was dissolved in tetrahydrofuran (250 mL) in a 1-L, two-necked flask fitted with a graduated addition funnel and a septum with an argon inlet. The two-necked flask was placed in a 10 °C ice-water cooling bath. Isopropylmagnesium chloride–lithium chloride solution (1.3 M solution in tetrahydrofuran, 55.5 mL, 72.2 mmol, 1.1 equiv) was cannulated into the addition funnel, before dropwise addition into the reaction mixture over 15 minutes. Ice was added to the cooling bath to lower the temperature of the bath to 0 °C. Freshly distilled methyl cyanoformate (7.81 mL, 98.0 mmol, 1.5 equiv) was added slowly via syringe through the septum and the reaction mixture was slowly warmed to 23 °C over 1 h. The transparent, light brown solution darkened to yellow in color before a light yellow solid precipitated out of the solution. The reaction slurry was stirred at 23 °C for 2 h before saturated aqueous ammonium chloride solution (200 mL) and saturated aqueous sodium bicarbonate solution (400 mL) were added sequentially. Ethyl acetate (400 mL) was added and the layers were separated. The aqueous layer was extracted with ethyl acetate (2 × 300 mL). The combined organic extracts were washed with saturated aqueous sodium chloride solution (600 mL) and dried over sodium sulfate. The dried solution was filtered and the filtrate was concentrated to produce an orange solid. The orange solid was purified by flash-column chromatography (3→7% ethyl acetate–hexanes) to provide isoxazole methyl ester **21** (23.9 g, 97% yield) as a white solid. TLC: (10% ethyl acetate–hexanes) $R_f = 0.37$ (UV, CAM); ¹H NMR (500 MHz, CDCl₃) δ: 7.48 (d, 2H, $J = 7.3$ Hz), 7.41–7.34 (m, 3H), 5.36 (s, 2H), 5.00

(s, 2H), 3.84 (s, 3H), 0.92 (s, 9H), 0.12 (s, 6H); ^{13}C NMR (125 MHz, CDCl_3) δ : 177.2, 168.8, 161.3, 135.5, 128.5, 128.3, 127.8, 100.0, 71.8, 57.6, 51.8, 25.7, 18.3, -5.4; FTIR (neat), cm^{-1} : 2953 (m), 2857 (m), 1716 (s), 1510 (s), 1364 (s), 1113 (s), 835 (s); HRMS (ESI): Calcd for $(\text{C}_{19}\text{H}_{27}\text{NO}_5\text{Si} + \text{H})^+$: 378.1737; Found: 378.1731.

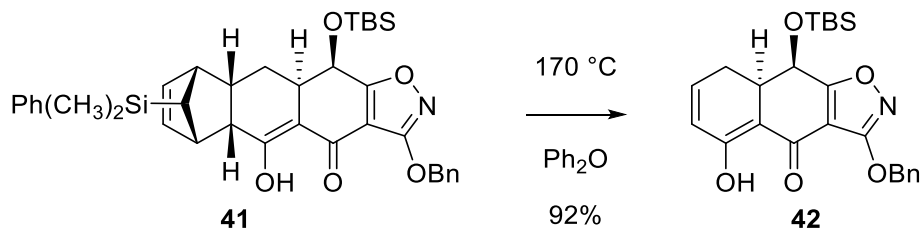
Michael-Claisen cyclization product **41**.



Isoxazole methyl ester **21** (7.98 g, 21.1 mmol, 1 equiv) was dissolved in tetrahydrofuran (70 mL) in a 500-mL 3-necked round-bottom flask equipped with two addition funnels and a septum with an argon inlet. The colorless solution was cooled to $-50\text{ }^{\circ}\text{C}$ in a dry ice–acetone cooling bath. A freshly prepared 1.0 M solution of sodium bis(trimethylsilyl)amide in tetrahydrofuran (21.4 mL, 21.1 mmol, 1.01 equiv) was cannulated into the first addition funnel and then added dropwise to the reaction mixture over 15 minutes. Upon addition of the basic solution, the reaction mixture darkened to yellow, then orange in color. The solution was stirred at $-50\text{ }^{\circ}\text{C}$ for 45 min. Enone **8**¹⁹ (6.54 g, 22.2 mmol, 1.05 equiv) was dissolved in tetrahydrofuran (30 mL) and added slowly to the reaction flask through the septum via syringe. The solution was stirred at $-50\text{ }^{\circ}\text{C}$ for 45 min. A freshly prepared 1.0 M solution of potassium bis(trimethylsilyl)amide in tetrahydrofuran (21.4 mL, 21.1 mmol, 1.01 equiv) was cannulated into the second addition funnel and was added dropwise to the reaction mixture over 15 minutes. The reaction mixture was allowed to warm to $-20\text{ }^{\circ}\text{C}$ over 60 min before aqueous potassium phosphate buffer solution (pH 7.0, 250 mL) was added. Ethyl acetate (300 mL) was added and the layers were separated. The aqueous layer was extracted with ethyl acetate ($2 \times 500\text{ mL}$). The combined organic extracts were dried over sodium sulfate and filtered. The filtrate was concentrated. The brown residue, a 15:1 mixture of diastereomers at C4, was purified by flash-column chromatography (1→5% ethyl acetate–hexanes) to provide the Michael-Claisen adduct **41** (9.85 g, 72%) as a light yellow foam as a single diastereomer. TLC: (20% ethyl acetate–hexanes) $R_f = 0.70$ (UV, CAM).

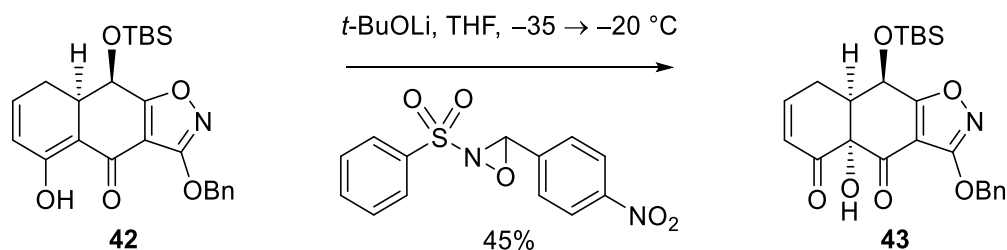
^1H NMR (500 MHz, CDCl_3) δ : 15.23 (s, 1H), 7.50 (d, 2H, $J = 7.3$ Hz), 7.44–7.33 (m, 8H), 5.93 (s, 2H), 5.38 (s, 2H), 4.43 (d, 2H, $J = 4.1$ Hz), 3.34 (br s, 1H), 2.99 (br s, 1H), 2.93 (dd, 1H, $J = 8.7$ Hz, 4.1 Hz), 2.78–2.74 (m, 1H), 2.57 (dt, 1H, $J = 12.0$ Hz, 4.1 Hz), 2.13 (td, 1H, $J = 13.2$ Hz, 7.6 Hz), 1.68 (dd, 1H, $J = 13.7$ Hz, 7.6 Hz), 1.36 (s, 1H), 0.80 (s, 9H), 0.20 (s, 6H), 0.11 (s, 3H), 0.00 (s, 3H); ^{13}C NMR (125 MHz, CDCl_3) δ : 183.4, 182.3, 179.0, 167.9, 139.6, 135.4, 135.2, 135.1, 133.5, 128.7, 128.5, 128.5, 128.4, 128.3, 127.7, 106.1, 104.1, 72.3, 63.3, 53.7, 52.5, 49.9, 45.2, 40.1, 37.3, 26.1, 25.6, 18.2, -1.5, -1.5, -4.9, -5.1; FTIR (neat), cm^{-1} : 3067 (m), 2955 (m), 2857 (m), 1641 (s), 1508 (s), 1329 (s), 908 (s), 727 (s); HRMS (ESI): Calcd for $(\text{C}_{37}\text{H}_{45}\text{NO}_5\text{Si}_2 + \text{H})^+$: 640.2909; Found: 640.2906.

Enol **42**.



The Michael-Claisen adduct **41** (10.7 g, 16.6 mmol, 1 equiv) was dissolved in diphenyl ether (166 mL) and placed in a warm water bath. To deoxygenate the solution, argon was bubbled through the stirring solution for 1 h. The reaction flask was removed from the water bath, dried and placed into a preheated 170 °C oil bath for 15 minutes. The colorless reaction mixture darkened to yellow as the reaction was heated. After 15 minutes, the reaction vessel was immediately placed in a 23 °C water bath. Once cooled, the entire reaction mixture was loaded onto a column and purified by flash-column chromatography (2 column volumes of hexanes to flush off the diphenyl ether, followed by 10→20% ethyl acetate–hexanes) to provide enol **42** (6.72 g, 92%) as a yellow oil. TLC: (20% ethyl acetate–hexanes) $R_f = 0.40$ (CAM); ^1H NMR (500 MHz, CDCl_3) δ : 15.1 (s, 1H), 7.49 (d, 2H, $J = 6.9$ Hz), 7.40–7.32 (m, 3H), 6.59 (m, 1H), 6.07 (dd, 1H, $J = 10.1$ Hz, 3.2 Hz), 5.39 (s, 2H), 4.70 (d, 1H, $J = 4.6$ Hz), 3.20 (m, 1H), 2.81 (m, 1H), 2.30 (dt, 1 H, $J = 17.4$ Hz, 6.4 Hz), 0.83 (s, 9H), 0.15 (s, 3H), 0.02 (s, 3H); ^{13}C NMR (125 MHz, CDCl_3) δ : 180.5, 177.3, 174.2, 167.8, 141.7, 135.1, 128.5, 128.5, 128.3, 124.7, 101.0, 95.7, 72.3, 62.5, 38.0, 25.6, 25.5, 18.2, –4.9, –5.2; FTIR (neat), cm^{-1} : 3034 (m), 2955 (m), 1645 (s), 1506 (s), 833 (s), 729 (s); HRMS (ESI): Calcd for $(\text{C}_{24}\text{H}_{29}\text{NO}_5\text{Si} + \text{H})^+$: 440.1893; Found: 440.1915.

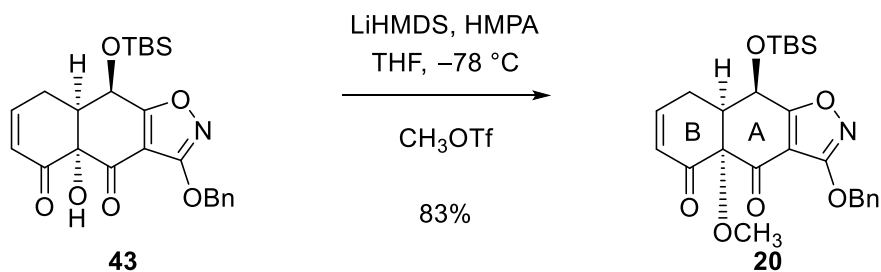
Hydroxy enone **43**.



Enol **42** (6.72 g, 15.3 mmol, 1 equiv) was dissolved in tetrahydrofuran (76 mL) and the reaction flask was placed in a $-35\text{ }^\circ\text{C}$ dry ice–acetone cooling bath. 3-(4-Nitrophenyl)-2-(phenylsulfonyl)-oxaziridine (7.02 g, 22.9 mmol, 1.5 equiv) was added in one portion, forming a yellow heterogeneous mixture. Lithium *tert*-butoxide solution (1.0 M in tetrahydrofuran, 3.06 mL, 3.10 mmol, 0.2 equiv) was added dropwise to the yellow slurry at $-35\text{ }^\circ\text{C}$. The reaction mixture was allowed to warm to $-20\text{ }^\circ\text{C}$ over 30 min. Saturated aqueous ammonium chloride solution (75 mL), water (100 mL) and ethyl acetate (100 mL) were added sequentially and the cooling bath was removed. The layers were separated and the aqueous phase was extracted with ethyl acetate ($3 \times 100\text{ mL}$). The combined organic extracts were washed with saturated aqueous sodium chloride solution (200 mL) and the washed extracts were dried over sodium sulfate. The dried organic phase was filtered and the filtrate was concentrated, producing an orange solid. The crude material was purified twice by flash-column chromatography (10→40% ethyl acetate–hexanes and then 50→90% dichloromethane–hexanes, followed by 3 column volumes of 20% ethyl acetate–hexanes) to provide hydroxy enone **43** (3.14 g, 45%) as a yellow foam. TLC: (20% ethyl acetate–hexanes) $R_f = 0.31$ (UV, CAM); $^1\text{H NMR}$ (500 MHz, CDCl_3) δ : 7.46 (d, 2H, $J = 7.3\text{ Hz}$), 7.39–7.34 (m, 3H), 7.02–6.99 (m, 1H), 6.24 (dd, 1H, $J = 10.3\text{ Hz}$, 2.4 Hz), 5.47 (d, 1H, $J = 5.4\text{ Hz}$), 5.35 (s, 2H), 4.58 (s, 1H), 2.97 (dt, 1H, $J = 10.9\text{ Hz}$, 5.6 Hz), 2.81–2.75 (m, 1H), 2.38–2.32 (m, 1H), 0.96 (s, 9H), 0.27 (s, 3H), 0.21 (s, 3H); $^{13}\text{C NMR}$ (125 MHz,

CDCl₃) δ : 194.7, 179.8, 167.8, 150.1, 134.8, 128.6, 128.5, 128.3, 128.2, 126.9, 105.2, 80.7, 72.4, 64.9, 48.0, 25.6, 25.4, 18.2, -4.9, -5.1; FTIR (neat), cm⁻¹: 3439 (br), 2930 (m), 1708 (s), 1608 (s), 1510 (s), 1256 (s), 837 (s), 729 (s); HRMS (ESI): Calcd for (C₂₄H₂₉NO₆Si + H)⁺: 456.1842; Found: 456.1825.

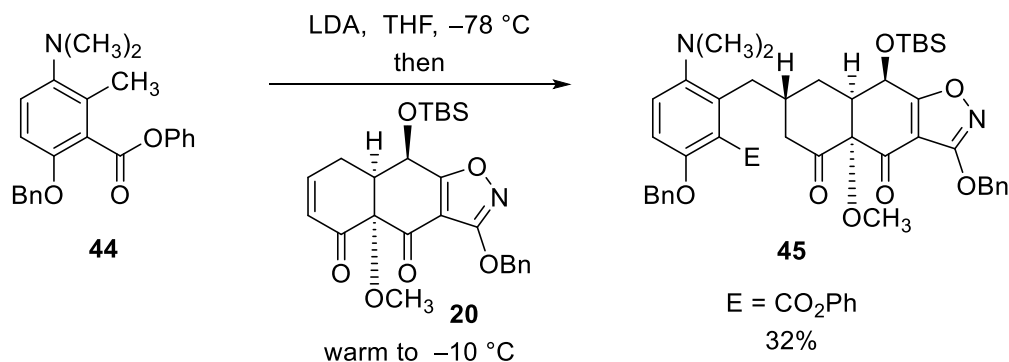
AB enone **20**.



A 50-mL round-bottom flask equipped with a stir bar was charged with tetrahydrofuran (10 mL) and placed in a $-78\text{ }^{\circ}\text{C}$ dry ice-acetone cooling bath. A lithium bis(trimethylsilyl)amide solution in tetrahydrofuran (1.0 M, 2.77 mL, 2.77 mmol, 1.2 equiv) and hexamethylphosphoramide (0.802 mL, 4.61 mmol, 2 equiv) were added sequentially. A solution of alcohol **43** (1.05 g, 2.31 mmol, 1 equiv) in tetrahydrofuran (10 mL) was added via cannula to the cooled reaction mixture, resulting in a brown homogenous solution. After stirring at $-78\text{ }^{\circ}\text{C}$ for 5 minutes, methyl triflate (0.522 mL, 4.61 mmol, 2 equiv) was added and the reaction mixture lightened to orange in color. The reaction mixture was stirred at $-78\text{ }^{\circ}\text{C}$ for 2 h and then was allowed to warm to $23\text{ }^{\circ}\text{C}$ over 15 min before quenching with saturated aqueous ammonium chloride solution (12 mL). Water (20 mL) and ethyl acetate (10 mL) were added and the layers were separated. The aqueous phase was extracted with ethyl acetate ($2 \times 50\text{ mL}$). The combined organic extracts were washed with saturated aqueous sodium chloride solution (100 mL) and the washed extracts were dried over sodium sulfate. The dried organic phase was filtered and the filtrate was concentrated. The crude material was purified by flash-column chromatography (5 \rightarrow 10% ethyl acetate–hexanes) to provide AB enone **20** (900 mg, 83%) as a yellow foam. TLC: (20% ethyl acetate–hexanes) $R_f = 0.46$ (UV, CAM); $^1\text{H NMR}$ (500 MHz, CDCl_3) δ : 7.47 (d, 2H, $J = 7.3\text{ Hz}$), 7.40–7.33 (m, 3H), 6.81 (ddd, 1H, $J = 10.1\text{ Hz}$, 5.5 Hz, 2.3 Hz), 6.08 (dd, 1H, $J = 10.1\text{ Hz}$, 2.3 Hz), 5.47 (br s, 1H), 5.38–5.33 (m, 2H), 3.57 (s, 3H), 3.12–3.07 (m, 1H), 2.75–

2.69 (m, 1H), 2.33–2.26 (m, 1H), 0.95 (s, 9H), 0.26 (s, 3H), 0.20 (s, 3H); ^{13}C NMR (125 MHz, CDCl_3) δ : 195.5, 185.9, 180.6, 167.7, 146.5, 134.8, 129.2, 128.6, 128.6, 128.3, 128.2, 86.5, 72.5, 65.0, 56.1, 48.1, 29.7, 25.6, 18.2, -4.9, -5.0; FTIR (neat), cm^{-1} : 3036 (m), 2932 (m), 1711 (s), 1510 (s), 1113 (s), 837 (s), 781 (s); HRMS (ESI): Calcd for $(\text{C}_{25}\text{H}_{31}\text{NO}_6\text{Si} + \text{Na})^+$: 492.1813; Found: 492.1829.

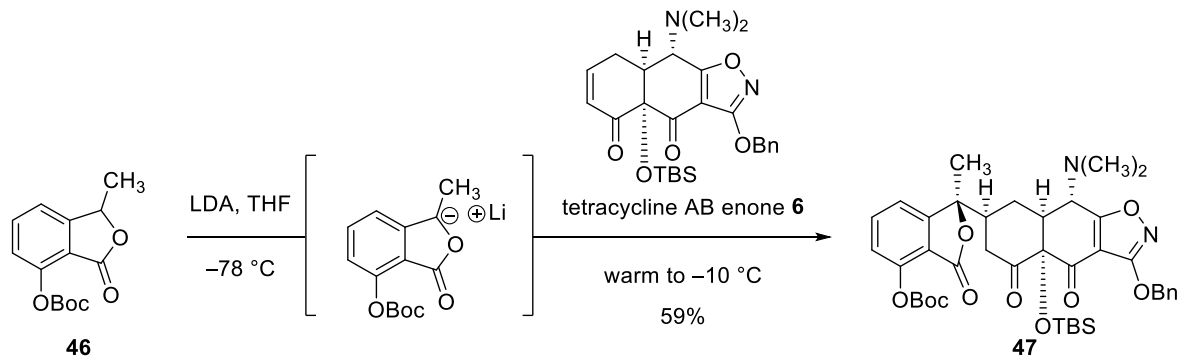
Michael adduct **45**.



A freshly prepared solution of lithium diisopropylamide in tetrahydrofuran (1.0 M, 106 μL , 106 μmol , 2 equiv) was added dropwise via syringe to a solution of phenyl ester **44** (39.0 mg, 106 μmol , 2 equiv) in tetrahydrofuran (1.5 mL) at $-78\text{ }^\circ\text{C}$ in a dry ice–acetone cooling bath, forming a bright red solution. The solution was stirred at $-78\text{ }^\circ\text{C}$ for 40 min. AB enone **20** (25.0 mg, 53.0 μmol , 1 equiv) was dissolved in tetrahydrofuran (0.5 mL) and added slowly to the reaction mixture. The reaction mixture was allowed to warm to $-10\text{ }^\circ\text{C}$ over 60 min before aqueous potassium phosphate buffer solution (pH 7.0, 6 mL) was added. Ethyl acetate (5 mL) was added and the layers were separated. The aqueous layer was extracted with ethyl acetate ($2 \times 5\text{ mL}$). The combined organic extracts were dried over sodium sulfate. The dried solution was filtered and the filtrate was concentrated. The residue was purified by flash-column chromatography (5 \rightarrow 15% ethyl acetate–hexanes) to provide the Michael adduct **45** as a light yellow foam (14.0 mg, 32%). Crystals were grown from slow evaporation of ethyl acetate and X-ray crystallographic analysis was performed in order to determine absolute stereochemistry of the Michael adduct, specifically determining the configuration of the C5a stereocenter. TLC: (20% ethyl acetate–hexanes) $R_f = 0.44$ (UV, CAM); $^1\text{H NMR}$ (600 MHz, CDCl_3) δ : 7.48 (d, 2H, $J = 7.2\text{ Hz}$), 7.43 (d, 2H, $J = 7.2\text{ Hz}$), 7.40–7.30 (m, 8H), 7.23–7.20 (m, 2H), 7.05 (d, 2H, $J = 7.6\text{ Hz}$), 6.88 (d, 1H, $J = 8.7\text{ Hz}$), 5.40 (d, 1H, $J = 5.7\text{ Hz}$), 5.35 (s, 2H), 5.09 (s, 2H), 3.44

(s, 3H), 3.01 (br s, 2H), 2.87 (br s, 1H), 2.61 (br s, 6H), 2.58–2.54 (m, 2H), 2.44–2.41 (m, 1H), 2.13–2.10 (m, 1H), 1.75–1.71 (m, 1H), 0.88 (s, 9H), 0.21 (s, 3H), 0.10 (s, 3H); FTIR (neat), cm^{-1} : 2931 (m), 2859 (m), 1734 (s), 1695 (s), 1479 (s), 1186 (s), 733 (s); HRMS (ESI): Calcd for $(\text{C}_{48}\text{H}_{54}\text{N}_2\text{O}_9\text{Si} + \text{H})^+$: 831.3677; Found: 831.3682.

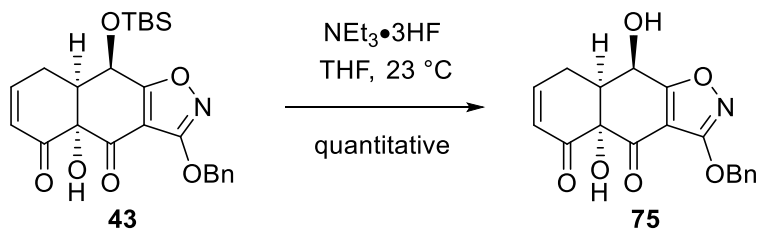
Michael adduct **47**.



A freshly prepared solution of lithium diisopropylamide in tetrahydrofuran (1.4 M, 444 μL , 0.622 mmol, 3 equiv) was added dropwise via syringe to a solution of phthalide **46**²⁵ (170 mg, 0.642 mmol, 3.1 equiv) in tetrahydrofuran (0.5 mL) at $-78\text{ }^{\circ}\text{C}$ in a dry ice–acetone cooling bath, forming a dark orange solution. The solution was stirred at $-78\text{ }^{\circ}\text{C}$ for 45 min. AB enone **6** (100 mg, 0.207 mmol, 1 equiv) was dissolved in tetrahydrofuran (0.5 mL) and added slowly to the reaction mixture. The reaction mixture was allowed to warm to $-10\text{ }^{\circ}\text{C}$ over 90 min before aqueous potassium phosphate buffer solution (pH 7.0, 6 mL) was added. Ethyl acetate (5 mL) was added and the layers were separated. The aqueous layer was extracted with ethyl acetate ($2 \times 10\text{ mL}$). The combined organic extracts were dried over sodium sulfate. The dried solution was filtered and the filtrate was concentrated. The residue was purified by flash-column chromatography (20 \rightarrow 50% ethyl acetate–hexanes) to provide the Michael adduct **47** (92 mg, 59%) as a light yellow foam. Crystals were grown from slow evaporation of a dichloromethane–hexanes solvent system and X-ray crystallographic analysis was performed in order to determine absolute stereochemistry of the Michael adduct, specifically determining the configuration of the C5a and C6 stereocenters. TLC: (20% ethyl acetate–hexanes) $R_f = 0.45$ (UV, CAM); $^1\text{H NMR}$ (600 MHz, CDCl_3) δ : 7.67 (t, 1H, $J = 7.8\text{ Hz}$), 7.48–7.47 (m, 2H), 7.40–7.37 (m, 2H), 7.35–7.33 (m, 1H), 7.23 (d, 1H, $J = 7.8\text{ Hz}$), 7.14 (d, 1H, $J = 7.8\text{ Hz}$), 5.37 (s, 2H), 3.49 (d, 1H, $J = 3.7\text{ Hz}$),

2.61–2.53 (m, 2H), 2.44 (s, 6H), 2.21–2.15 (m, 2H), 2.13–2.10 (m, 1H), 1.66 (s, 3H), 1.58 (s, 10H), 0.82 (s, 9H), 0.12 (s, 3H), –0.11 (s, 3H); ^{13}C NMR (125 MHz, CDCl_3) δ : 204.3, 187.2, 179.9, 167.8, 165.9, 153.5, 150.4, 149.1, 136.3, 135.0, 128.5, 128.5, 128.2, 122.6, 118.4, 118.1, 106.6, 86.9, 85.2, 84.9, 72.5, 64.3, 47.0, 43.5, 43.2, 39.9, 29.1, 27.6, 26.0, 24.2, 19.1, 11.4, –2.9, –3.0; FTIR (neat), cm^{-1} : 2934 (m), 1763 (s), 1233 (s), 1146 (s), 729 (s); HRMS (ESI): Calcd for $(\text{C}_{40}\text{H}_{50}\text{N}_2\text{O}_{10}\text{Si} + \text{H})^+$: 747.3313; Found: 747.3278.

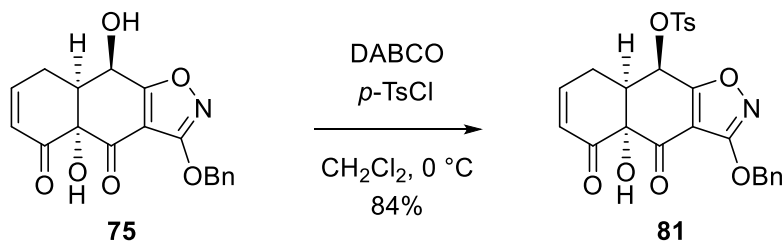
Diol **75**.



Alcohol **43** (3.14 g, 6.90 mmol, 1 equiv) was dissolved in tetrahydrofuran (69 mL) in a polypropylene reaction tube. Excess triethylamine trihydrofluoride (11.2 mL, 68.9 mmol, 10 equiv) was added and the reaction mixture was stirred at 23 °C for 16 h. The reaction mixture was quenched with the addition of an aqueous potassium phosphate buffer solution (pH 7.0, 90 mL). Ethyl acetate (150 mL) was added and the layers were separated. The aqueous layer was extracted with ethyl acetate (2 × 100 mL). The organic layers were combined and were washed with saturated aqueous sodium chloride solution (200 mL). The washed solution was dried over sodium sulfate and the dried solution was filtered. The filtrate was concentrated to provide diol **75** (2.35 g) as an orange foam in quantitative yield. The crude material was carried forward without further purification.⁶⁴ TLC: (50% ethyl acetate–hexanes) $R_f = 0.29$ (UV, CAM). ¹H NMR (600 MHz, CDCl₃) δ : 7.48–7.46 (m, 2H), 7.39–7.33 (m, 3H), 7.03–7.00 (m, 1H), 6.26–6.24 (m, 1H), 5.57 (d, 1H, $J = 5.3$ Hz), 5.36 (s, 2H), 4.57 (s, 1H), 3.14 (dt, 1 H, $J = 10.9$ Hz, 5.5 Hz), 2.90–2.85 (m, 1H), 2.65 (br s, 1 H), 2.37–2.31 (m, 1H). HRMS (ESI): Calcd for (C₁₈H₁₅NO₆ + H)⁺: 342.0972; Found: 342.0989.

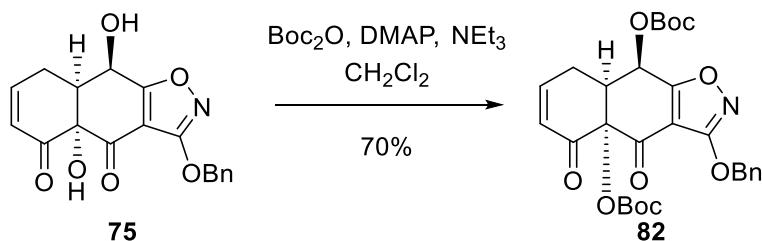
⁶⁴ Attempts to purify this alcohol by flash-column chromatography resulted in the formation of an unwanted cyclic ether, the byproduct of the addition of the C4-alcohol into the enone.

Tosylate **81**.



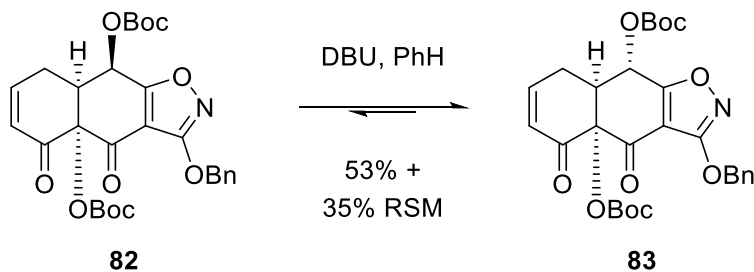
Diol **75** (100 mg, 0.29 mmol, 1 equiv) and DABCO (66 mg, 0.58 mmol, 2 equiv) were dissolved in dichloromethane (2.9 mL) and the homogeneous reaction mixture was placed in an ice-water cooling bath. *p*-Tosyl chloride (84 mg, 0.44 mmol, 1.5 equiv) was added portion-wise over 5 minutes and the reaction mixture continued to stir at 0 °C for 1 h. The reaction mixture was diluted with ether (10 mL) and filtered through a pad of Celite, rinsing with an additional portion of ether (10 mL). The ethereal filtrate was washed sequentially with a 2M hydrochloric acid solution (2 × 30 mL), a saturated aqueous sodium bicarbonate solution (2 × 30 mL), and water (30 mL). The organic phase was dried over sodium sulfate and the dried solution was filtered. The filtrate was concentrated and the yellow oily residue was purified by flash-column chromatography on silica gel (30→40% ethyl acetate–hexanes) to provide tosylate **81** (122 mg, 84%) as white foam. TLC: (50% ethyl acetate–hexanes) $R_f = 0.67$ (UV, CAM); ^1H NMR (600 MHz, CDCl_3) δ : 7.93–7.91 (m, 2H), 7.43 (d, 4H, $J = 7.3$ Hz), 7.37–7.33 (m, 3H), 7.01–6.98 (m, 1H), 6.24 (dt, 1H, $J = 10.2$ Hz, 1.4 Hz), 6.05 (d, 1H, $J = 5.9$ Hz), 5.31 (s, 2H), 4.57 (s, 1H), 3.36 (dt, 1H, $J = 10.2$ Hz, 5.5 Hz), 2.95–2.90 (m, 1H), 2.49 (s, 3H), 2.44–2.37 (m, 1H).

Boc bis-carbonate **82**.



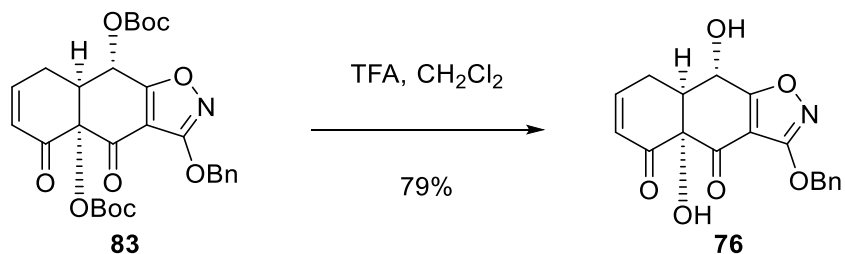
Crude diol **75** (2.64 g, 7.73 mmol, 1 equiv) was dissolved in dichloromethane (77 mL) and the reaction flask was placed in a 0 °C ice-water cooling bath. Triethylamine (3.23 mL, 23.2 mmol, 3 equiv) and dimethylaminopyridine (0.250 g, 2.07 mmol, 0.3 equiv) were added sequentially, followed by di-*tert*-butyl dicarbonate (3.59 mL, 15.5 mmol, 2 equiv). The cooling bath was removed and the reaction mixture was stirred at 23 °C for 5 minutes. The reaction mixture was concentrated and purified by flash-column chromatography (20→30% ethyl acetate–hexanes) to provide Boc bis-carbonate **82** (3.24 g, 77%) as a light yellow foam. TLC: (30% ethyl acetate–hexanes) $R_f = 0.47$ (UV, CAM); ^1H NMR (500 MHz, CDCl_3) δ : 7.45 (d, 2H, $J = 7.3$ Hz), 7.38–7.33 (m, 3H), 6.87 (ddd, 1H, $J = 10.3$ Hz, 5.9 Hz, 2.4 Hz), 6.23 (d, 1H, $J = 5.4$ Hz), 6.20 (dd, 1H, $J = 10.3$ Hz, 2.4 Hz), 5.35 (s, 2H), 4.10–4.06 (m, 1H), 2.83–2.76 (m, 1H), 2.42–2.35 (m, 1H), 1.54 (s, 9H), 1.49 (s, 9H); FTIR (neat), cm^{-1} : 2982 (m), 1751 (s), 1724 (s), 1274 (s), 1251 (s), 731 (s); HRMS (ESI): Calcd for $(\text{C}_{28}\text{H}_{31}\text{NO}_{10} + \text{Na})^+$: 564.1840; Found: 564.1835.

Epimerization of the Boc bis-carbonate **82** to Boc bis-carbonate **83**.



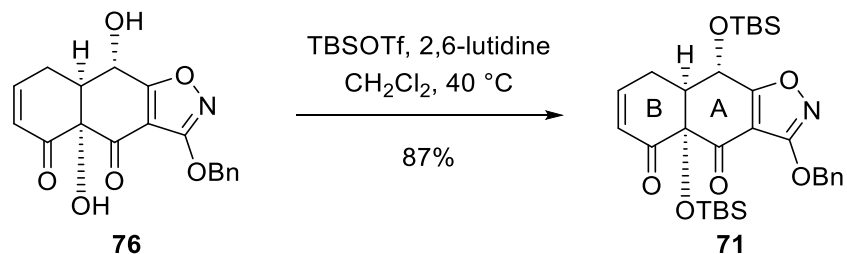
Boc bis-carbonate **82** (2.47 g, 4.56 mmol, 1 equiv) was dissolved in benzene (250 mL) in a 500-mL round-bottom flask. Argon was bubbled through the solution for 60 min before 1,8-diazabicycloundec-7-ene (0.34 mL, 2.28 mmol, 0.5 equiv) was added. Within the first minute, the reaction mixture darkened to yellow in color. After 15 min, saturated aqueous ammonium chloride solution (200 mL) was added and the layers were separated. The aqueous phase was extracted with ethyl acetate (3 × 150 mL). The combined organic extracts were washed with saturated aqueous sodium chloride solution (400 mL) and the washed extracts were dried over sodium sulfate. The dried organic phase was filtered and the filtrate was concentrated. The crude material was purified by flash-column chromatography (10→30% ethyl acetate–hexanes) to recover the starting material (866 mg, 35%) and to provide the C4-epimerized Boc bis-carbonate **83** (1.30 g, 53%) as a yellow foam. TLC: (30% ethyl acetate–hexanes) $R_f = 0.40$ (UV, CAM); $^1\text{H NMR}$ (600 MHz, CDCl_3) δ : 7.47 (d, 2H, $J = 7.3$ Hz), 7.39–7.33 (m, 3H), 6.91–6.89 (m, 1H), 6.24–6.22 (m, 1H), 5.78 (d, 1H, $J = 5.0$ Hz), 5.35 (s, 2H), 4.07–4.05 (m, 1H), 2.84–2.79 (m, 1H), 2.42–2.38 (m, 1H), 1.51 (s, 9H), 1.49 (s, 9H); FTIR (neat), cm^{-1} : 2982 (m), 1751 (s), 1724 (s), 1283 (s), 1254 (s), 731 (s); HRMS (ESI): Calcd for $(\text{C}_{28}\text{H}_{31}\text{NO}_{10} + \text{Na})^+$: 564.1840; Found: 564.1839.

Diol **76**.



C4-epimerized Boc bis-carbonate **83** (1.30 g, 2.40 mmol, 1 equiv) was dissolved in dichloromethane (24 mL) at 23 °C. Trifluoroacetic acid (1.85 mL, 24.0 mmol, 10 equiv) was added slowly and the reaction mixture continued to stir at 23 °C as consumption of starting material was monitored by TLC. When no starting material remained, saturated aqueous sodium bicarbonate solution (20 mL) was added carefully and the layers were separated. The aqueous phase was extracted with dichloromethane (3 × 15 mL). The combined organic extracts were washed sequentially with water (50 mL) and saturated aqueous sodium chloride solution (50 mL). The washed extracts were dried over sodium sulfate, the dried organic phase was filtered, and the filtrate was concentrated. The crude material was purified by flash-column chromatography (20→50% ethyl acetate–hexanes) to provide the C4-epimerized diol **76** (645 mg, 79%) as a yellow solid. TLC: (50% ethyl acetate–hexanes) $R_f = 0.30$ (UV, CAM); $^1\text{H NMR}$ (500 MHz, CDCl_3) δ : 7.49–7.47 (m, 2H), 7.40–7.34 (m, 3H), 6.95 (ddd, 1H, $J = 10.2$ Hz, 5.2 Hz, 2.7 Hz), 6.27–6.24 (m, 1H), 5.37 (s, 2H), 4.89 (br s, 1H), 4.70 (d, 1H, $J = 10.2$ Hz), 3.67 (br s, 1H), 3.04–3.02 (m, 1H), 2.80–2.74 (m, 1H), 2.30 (br s, 1H); FTIR (neat), cm^{-1} : 3462 (br), 3314 (br), 2934 (m), 1709 (s), 1514 (s), 735 (s); HRMS (ESI): Calcd for $(\text{C}_{18}\text{H}_{15}\text{NO}_6 + \text{H})^+$: 342.0972; Found: 342.0988.

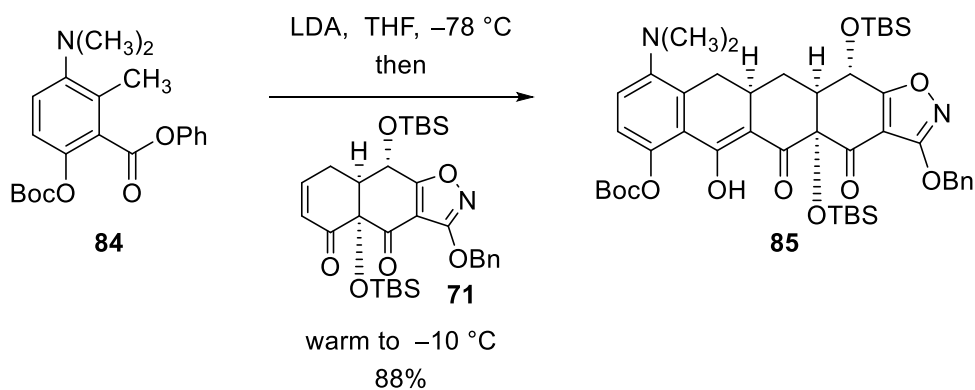
AB enone **71**.



A 50-mL round-bottom flask equipped with a stir bar was charged with diol **76** (846 mg, 2.48 mmol, 1 equiv), dichloromethane (12 mL), and 2,6-lutidine (0.866 mL, 7.44 mmol, 3 equiv) and was placed in a 0 °C ice-water cooling bath. *tert*-Butyldimethylsilyl trifluoromethanesulfonate (1.42 mL, 6.20 mmol, 2.5 equiv) was added dropwise by syringe to the ice-cooled solution. After 10 minutes, the cooling bath was removed and the reaction mixture was allowed to warm to 23 °C. After 10 minutes at 23 °C, the reaction flask was fitted with a reflux condenser and placed in a preheated 40 °C oil bath. After 3 h at 40 °C, the reaction flask was removed from the oil bath and methanol (40 mL) was added. The quenched reaction mixture continued to stir at 23 °C for 20 minutes before ethyl acetate (30 mL) and water (30 mL) were added. The layers were separated and the aqueous phase was extracted with ethyl acetate (3 × 30 mL). The combined organic extracts were washed with saturated aqueous sodium chloride solution (90 mL) and the washed extracts were dried over sodium sulfate. The dried organic phase was filtered and the filtrate was concentrated. The crude material was purified by flash-column chromatography (2→6% ethyl acetate–hexanes) to provide the AB enone **71** (1.23 g, 87%) as a white foam. TLC: (40% ethyl acetate–hexanes) $R_f = 0.71$ (UV, CAM); ¹H NMR (600 MHz, CDCl₃) δ : 7.50 (d, 1H, $J = 6.7$ Hz), 7.40–7.33 (m, 3H), 6.93–6.91 (m, 1H), 6.15 (dd, 1H, $J = 10.3$ Hz, 2.9 Hz), 5.37 (s, 2H), 4.79 (d, 1H, $J = 9.7$ Hz), 2.97–2.92 (m, 1H), 2.91–2.88 (m, 1H), 2.65–2.61 (m, 1H), 0.94 (s, 9H), 0.83 (s, 9H), 0.23 (s, 6H), 0.13 (s, 3H), 0.08 (s, 3H);

^{13}C NMR (125 MHz, CDCl_3) δ : 193.0, 187.0, 179.5, 167.5, 147.8, 134.9, 129.1, 128.5, 128.5, 128.4, 106.1, 83.1, 72.4, 64.5, 53.2, 26.0, 25.6, 24.8, 19.0, 18.0, -2.6, -4.0, -4.4, -4.9; FTIR (neat), cm^{-1} : 3036 (m), 2930 (m), 2859 (m), 1721 (s), 1512 (s), 1063 (s), 837 (s), 731 (s); HRMS (ESI): Calcd for $(\text{C}_{30}\text{H}_{43}\text{NO}_6\text{Si}_2 + \text{H})^+$: 570.2702; Found: 570.2695.

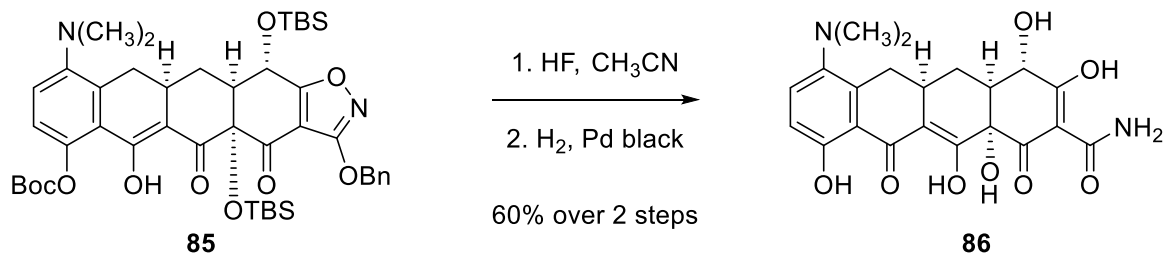
Michael-Claisen cyclization product **85**.



A freshly prepared solution of lithium diisopropylamide in tetrahydrofuran (1.0 M, 2.63 mL, 2.63 mmol, 3 equiv) was added dropwise via syringe to a solution of phenyl ester **84** (978 mg, 2.63 mmol, 3 equiv) in tetrahydrofuran (20 mL) at $-78\text{ }^{\circ}\text{C}$ in a dry ice–acetone cooling bath, forming a bright red solution. The solution was stirred at $-78\text{ }^{\circ}\text{C}$ for 20 min. AB enone **71** (500 mg, 0.877 mmol, 1 equiv) was dissolved in tetrahydrofuran (8 mL) and was added slowly to the reaction mixture over 5 minutes. The reaction mixture was allowed to warm to $-10\text{ }^{\circ}\text{C}$ over 90 min before aqueous potassium phosphate buffer solution (pH 7.0, 30 mL) was added. Ethyl acetate (20 mL) was added and the layers were separated. The aqueous layer was extracted with ethyl acetate ($3 \times 50\text{ mL}$). The combined organic extracts were dried over sodium sulfate. The dried solution was filtered and the filtrate was concentrated. The residue was purified by flash-column chromatography (2→15% ethyl acetate–hexanes) to provide the Michael-Claisen product **85** (657 mg, 88%) as a light yellow foam. TLC: (20% ethyl acetate–hexanes) $R_f = 0.50$ (UV, CAM); $^1\text{H NMR}$ (600 MHz, CDCl_3) δ : 15.87 (br s, 1H), 7.49 (d, 2H, $J = 7.5\text{ Hz}$), 7.40–7.32 (m, 3H), 7.22 (d, 1H, $J = 8.8\text{ Hz}$), 7.03 (d, 1H, $J = 8.8\text{ Hz}$), 5.41–5.37 (m, 2H), 4.84 (d, 1H, $J = 5.7\text{ Hz}$), 3.35–3.31 (m, 1H), 2.94–2.91 (m, 1H), 2.65 (s, 6H), 2.36–2.31 (m, 2H), 1.79–1.77 (m, 1H), 1.56 (s, 9H), 0.96 (s, 9H), 0.89–0.84 (m, 1H), 0.77 (s, 9H), 0.26 (s, 3H), 0.23 (s, 3H),

0.15 (s, 3H), 0.13 (s, 3H); ^{13}C NMR (125 MHz, CDCl_3) δ : 187.4, 184.0, 181.4, 178.3, 167.7, 152.1, 149.2, 145.3, 136.8, 135.1, 129.2, 128.5, 128.2, 124.1, 123.7, 122.0, 121.9, 107.9, 105.7, 83.7, 81.2, 72.3, 67.3, 50.8, 44.2, 33.3, 30.4, 27.7, 27.5, 25.9, 25.8, 19.0, 18.5, -3.2, -3.4, -4.2, -4.5; FTIR (neat), cm^{-1} : 2932 (m), 2859 (m), 1759 (s), 1512 (s), 1236 (s), 1142 (s), 835 (s), 729 (s); HRMS (ESI): Calcd for $(\text{C}_{45}\text{H}_{62}\text{N}_2\text{O}_{10}\text{Si}_2 + \text{H})^+$: 847.4016; Found: 847.4051.

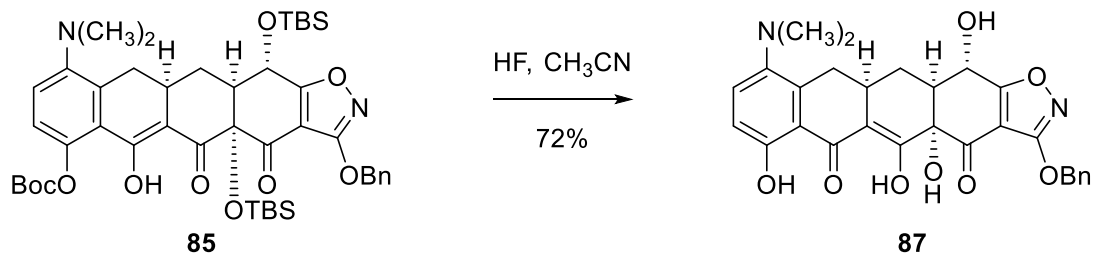
C4-dedimethylamino-C4-hydroxyiminocycline (**86**).



Concentrated aqueous hydrofluoric acid solution (48 wt%, 1 mL) was added to a solution of the Michael-Claisen cyclization product **85** (13 mg, 15 μ mol, 1 equiv) in acetonitrile (1 mL) in a polypropylene reaction vessel at 23 °C. The reaction vessel was then placed in a 35 °C oil heating bath for 20 h. Upon removal from the heating bath and cooling to 23 °C, the reaction mixture was poured into water (17 mL) containing dipotassium hydrogen phosphate trihydrate (3.3 g). The resulting mixture was extracted with ethyl acetate (4 \times 20 mL). The organic extracts were combined and the combined solution was dried over anhydrous sodium sulfate. The dried solution was filtered and the filtered solution was concentrated, affording a yellow solid. Methanol (1 mL) and 1,4-dioxane (1 mL) were added to the crude product, forming a yellow solution. Palladium black (5.7 mg, 54 μ mol, 3.5 equiv) was added in one portion at 23 °C. An atmosphere of hydrogen gas was introduced by briefly evacuating the flask, then backfilling with hydrogen (1 atm). The reaction mixture was stirred at 23 °C for 1 h, then was filtered through a cotton plug. The filtrate was concentrated, affording a yellow oil. The product was purified by reverse-phase HPLC (Agilent Extend-C18, 95:5 \rightarrow 60:40 water–acetonitrile + 0.1% trifluoroacetic acid) to afford C4-dedimethylamino-C4-hydroxyiminocycline (**86**, 4.0 mg, 60% over 2 steps). ¹H NMR (600 MHz, CD₃OD) δ : 7.73 (d, 1H, J = 9.0 Hz), 6.97 (d, 1H, J = 9.0 Hz), 4.24 (d, 1H, J = 7.1 Hz), 3.26–3.22 (m, 1H), 3.07 (s, 7H), 2.66 (t, 1 H, J = 14.8 Hz), 2.46 (td, 1H,

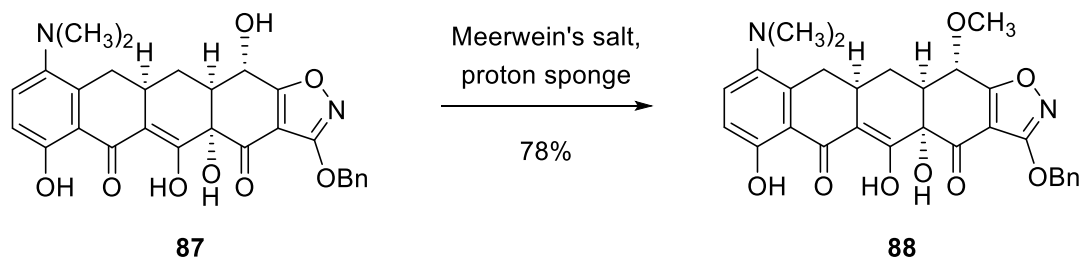
$J = 7.3$ Hz, 4.2 Hz), 2.37 – 2.34 (m, 1H), 1.87 – 1.86 (m, 1H); HRMS (ESI): Calcd for $(C_{21}H_{22}N_2O_8 + H)^+$: 431.1449 ; Found: 431.1466 .

Intermediate **87**.



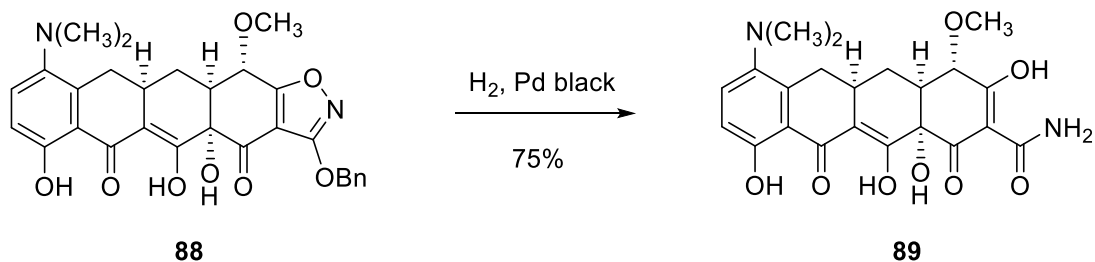
Concentrated aqueous hydrofluoric acid solution (48 wt%, 10 mL) was added to a solution of the Michael–Claisen cyclization product **85** (147 mg, 0.174 mmol, 1 equiv) in acetonitrile (12 mL) in a polypropylene reaction vessel at 23 °C. The reaction vessel was then placed in a 35 °C oil heating bath for 48 h. Additional concentrated aqueous hydrofluoric acid solution (48 wt%, 2 mL) was added and stirring continued at 35 °C oil bath for an additional 24 h. Upon removal from the heating bath and cooling to 23 °C, the reaction mixture was poured into a half saturated aqueous dipotassium hydrogen phosphate solution (75 mL). Additional water was added to dissolve the precipitate. The resulting mixture was extracted with ethyl acetate (4 × 50 mL). The organic extracts were combined and the combined solution was dried over anhydrous sodium sulfate. The dried solution was filtered and the filtered solution was concentrated, affording a yellow solid. The product was purified by reverse-phase HPLC (Agilent Extend-C18, 30:70→0:100 water–methanol) to afford intermediate **87** (65 mg, 72%). ¹H NMR (600 MHz, CDCl₃) δ: 14.92 (br s, 1H), 11.26 (s, 1H), 7.49 (d, 2H, *J* = 7.3 Hz), 7.40–7.34 (m, 3H), 7.31 (d, 1H, *J* = 8.8 Hz), 6.82 (d, 1H, *J* = 8.8 Hz), 5.41–5.37 (m, 2H), 4.70 (dd, 1H, *J* = 11.3 Hz, 1.9 Hz), 4.32 (br s, 1H), 3.70 (d, 1H, *J* = 11.3 Hz), 3.36 (dd, 1H, *J* = 14.5 Hz, 4.5 Hz), 2.92–2.88 (m, 1H), 2.85 (dt, 1H, *J* = 14.5 Hz, 1.9 Hz), 2.56 (s, 6H), 2.13–2.07 (m, 2H), 1.38–1.31 (m, 1H); HRMS (ESI): Calcd for (C₂₈H₂₆N₂O₈ + H)⁺: 519.1762; Found: 519.1767.

C4-dedimethylamino-C4-methoxyminocycline precursor **88**.



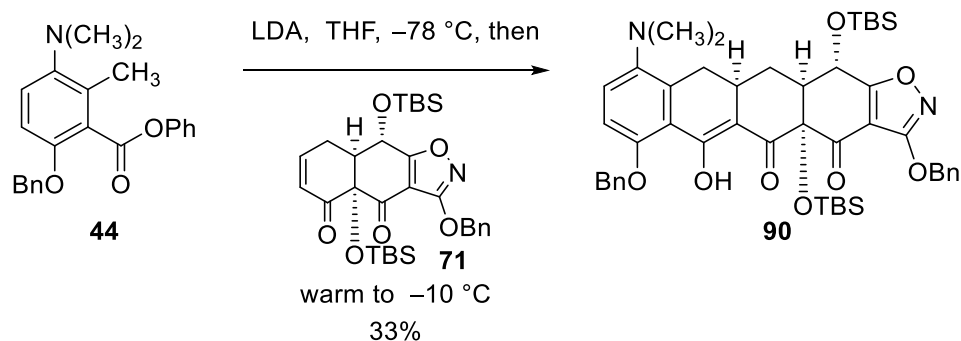
Trimethyloxonium tetrafluoroborate (1.4 mg, 9.6 μmol , 1 equiv) and 1,8-diaminonaphthalene (1.5 mg, 9.6 μmol , 1.0 equiv) were added to a solution of the intermediate **87** (5.0 mg, 9.6 μmol , 1 equiv) in dichloromethane (0.1 mL) at 23 $^{\circ}\text{C}$. The reaction mixture was stirred at 23 $^{\circ}\text{C}$ for 2 h before methanol (0.5 mL) and water (0.5 mL) were added to quench the reaction. A reverse-phase HPLC sample was prepared directly from the reaction mixture and was purified (Agilent Extend-C18, 30:70 \rightarrow 0:100 water-methanol) to afford C4-methyl ether **88** (4.0 mg, 78%) as a yellow solid. ^1H NMR (600 MHz, CDCl_3) δ : 12.67 (s, 1H), 7.51–7.48 (m, 2H), 7.41–7.35 (m, 3H), 7.29 (d, 1H, $J = 8.9$ Hz), 6.84 (d, 1H, $J = 8.9$ Hz), 5.40 (s, 2H), 4.66 (br s, 1H), 4.41 (br s, 1H), 3.99 (s, 3H), 3.82 (br s, 1H), 3.35 (dd, 1H, $J = 16.1$ Hz, 4.0 Hz), 3.02–2.96 (m, 1H), 2.78 (d, 1H, $J = 14.0$ Hz), 2.57 (s, 6H), 2.21 (dd, 1H, $J = 15.9$ Hz, 12.5 Hz), 2.08–2.05 (m, 1H); HRMS (ESI): Calcd for $(\text{C}_{29}\text{H}_{28}\text{N}_2\text{O}_8 + \text{H})^+$: 533.1918; Found: 533.1927.

C4-dedimethylamino-C4-methoxyminocycline (**89**).



Methanol (1 mL) and 1,4-dioxane (1 mL) were added to the C4-methyl ether **88** (4.0 mg, 7.5 μmol , 1 equiv), forming a yellow solution. Palladium black (2.8 mg, 26 μmol , 3.5 equiv) was added in one portion at 23 °C. An atmosphere of hydrogen gas was introduced by briefly evacuating the flask, then backfilling with hydrogen (1 atm). The reaction mixture was stirred at 23 °C for 1 h, then was filtered through a cotton plug. The filtrate was concentrated, affording a yellow film. The product was purified by reverse-phase HPLC (Agilent Extend-C18, 95:5→60:40 water–acetonitrile + 0.1% trifluoroacetic acid) to afford C4-dedimethylamino-C4-methoxyminocycline (**89**, 2.5 mg, 75%). HRMS (ESI): Calcd for $(\text{C}_{22}\text{H}_{24}\text{N}_2\text{O}_8 + \text{H})^+$: 445.1605; Found: 445.1615.

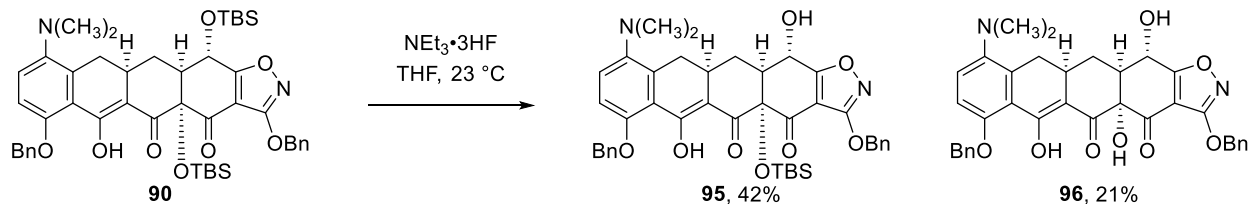
Michael-Claisen cyclization product **90**.



A freshly prepared solution of lithium diisopropylamide in tetrahydrofuran (1.0 M, 484 μL , 0.484 mmol, 3 equiv) was added dropwise via syringe to a solution of phenyl ester **44** (175 mg, 0.484 mmol, 3 equiv) in tetrahydrofuran (3.5 mL) at $-78\text{ }^{\circ}\text{C}$ in a dry ice–acetone cooling bath, forming a bright red solution. The solution was stirred at $-78\text{ }^{\circ}\text{C}$ for 20 min. AB enone **71** (92 mg, 0.161 mmol, 1 equiv) was dissolved in tetrahydrofuran (1 mL) and was added slowly to the reaction mixture over 2 minutes. The reaction mixture was allowed to warm to $-10\text{ }^{\circ}\text{C}$ over 60 min before aqueous potassium phosphate buffer solution (pH 7.0, 10 mL) was added. Ethyl acetate (15 mL) was added and the layers were separated. The aqueous layer was extracted with ethyl acetate ($3 \times 10\text{ mL}$). The combined organic extracts were dried over sodium sulfate. The dried solution was filtered and the filtrate was concentrated. The residue was purified by flash-column chromatography (2 \rightarrow 20% ethyl acetate–hexanes) to provide the Michael-Claisen product **90** (44 mg, 33%) as a light yellow foam. TLC: (20% ethyl acetate–hexanes) $R_f = 0.40$ (UV, CAM); $^1\text{H NMR}$ (600 MHz, CDCl_3) δ : 16.32 (s, 1H), 7.55 (d, 4H, $J = 7.3\text{ Hz}$), 7.39–7.34 (m, 5H), 7.31–7.29 (m, 1H), 7.15 (d, 1H, $J = 8.8\text{ Hz}$), 6.87 (d, 1H, $J = 8.8\text{ Hz}$), 5.42–5.37 (m, 2H), 5.23–5.14 (m, 2H), 4.82 (d, 1H, $J = 5.0\text{ Hz}$), 3.36–3.34 (m, 1H), 2.87–2.82 (m, 1H), 2.65–2.62 (m, 1H), 2.61 (s, 6H), 2.30–2.22 (m, 2H), 1.73–1.69 (m, 1H), 0.96 (s, 9H), 0.76

(s, 9H), 0.25 (s, 3H), 0.21 (s, 3H), 0.17 (s, 3H), 0.15 (s, 3H); HRMS (ESI): Calcd for $(C_{47}H_{60}N_2O_8Si_2 + H)^+$: 837.3966; Found: 837.3890.

Differentially deprotected intermediates **95** and **96**.



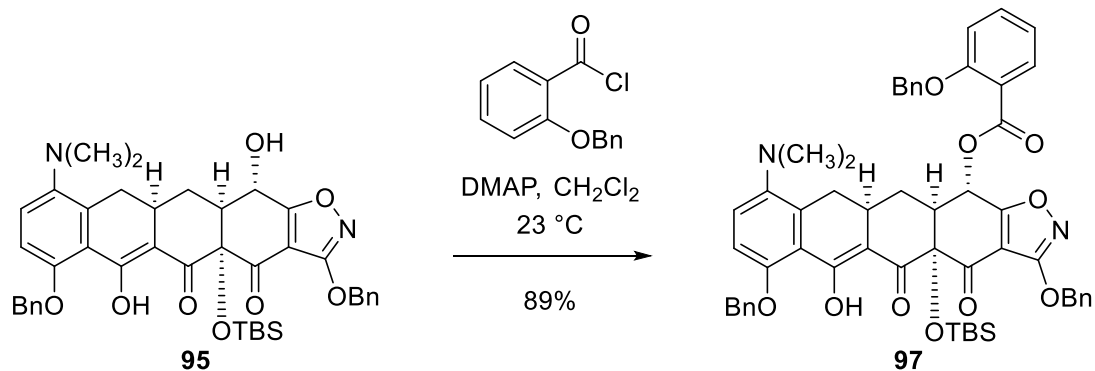
Triethylamine trihydrofluoride (50 μL , 0.31 mmol, 6.6 equiv) was added to a solution of the Michael–Claisen cyclization product **90** (39 mg, 47 μmol , 1 equiv) in tetrahydrofuran (1 mL) in a polypropylene reaction vessel at 23 °C. After 16 h at 23 °C, aqueous potassium phosphate buffer solution (pH 7.0, 2 mL) was added. Ethyl acetate (2 mL) was added and the layers were separated. The aqueous layer was extracted with ethyl acetate (2 \times 3 mL). The combined organic extracts were washed with saturated aqueous sodium chloride solution (10 mL) and the washed extracts were dried over sodium sulfate. The dried organic phase was filtered and the filtrate was concentrated, affording a yellow solid. The crude material was purified by reverse-phase HPLC (Agilent Extend-C18, 30:70 \rightarrow 0:100 water–methanol) to afford silyl intermediate **95** (14 mg, 42%) and desilylated intermediate **96** (6 mg, 21%).

Silyl intermediate 95: ^1H NMR (600 MHz, CDCl_3) δ : 16.59 (s, 1H), 7.53–7.48 (m, 4H), 7.40–7.30 (m, 6H), 7.16 (d, 1H, $J = 8.8$ Hz), 6.88 (d, 1H, $J = 8.8$ Hz), 5.44–5.38 (m, 2H), 5.24 (d, 1H, $J = 12.5$ Hz), 5.15 (d, 1H, $J = 12.5$ Hz), 4.63 (dd, 1H, $J = 10.9$ Hz, 1.5 Hz), 3.90 (d, 1H, $J = 10.9$ Hz), 3.23–3.21 (m, 1H), 2.81–2.78 (m, 1H), 2.57 (br s, 6H), 2.08–2.04 (m, 2H), 1.35–1.29 (m, 1H), 0.74 (s, 9H), 0.26 (s, 3H), 0.16 (s, 3H); HRMS (ESI): Calcd for $(\text{C}_{41}\text{H}_{46}\text{N}_2\text{O}_8\text{Si} + \text{H})^+$: 723.3096; Found: 723.3106.

Desilylated intermediate 96: ^1H NMR (600 MHz, CDCl_3) δ : 16.02 (s, 1H), 7.51–7.48 (m, 4H), 7.40–7.30 (m, 6H), 7.19 (d, 1H, $J = 8.9$ Hz), 6.91 (d, 1H, $J = 8.9$ Hz), 5.41–5.37 (m, 2H), 5.22

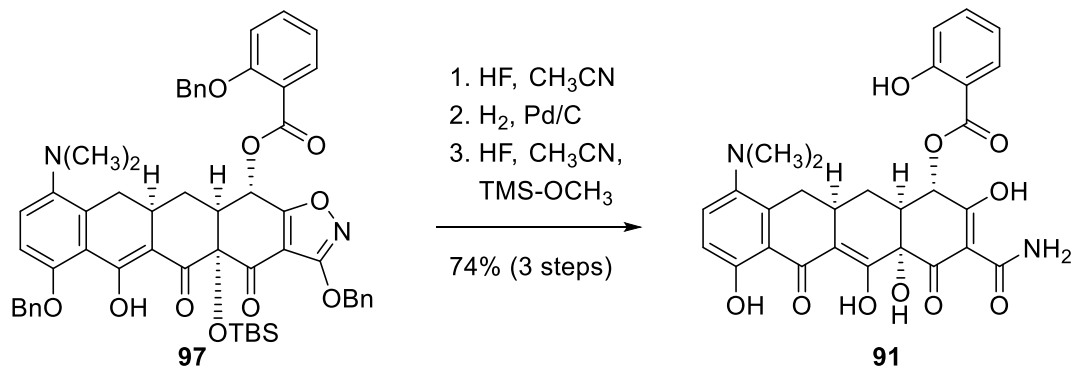
(d, 1H, $J = 12.1$ Hz), 5.13 (d, 1H, $J = 12.1$ Hz), 4.79 (br s, 1 H), 4.70 (s, 1H), 3.25 (dd, 1H, $J = 15.6, 4.1$ Hz), 2.81 (dt, 1H, $J = 13.5, 1.9$ Hz), 2.78–2.73 (m, 1H), 2.59 (s, 6H), 2.11–2.05 (m, 2H), 1.36–1.33 (m, 2H); HRMS (ESI): Calcd for $(C_{35}H_{32}N_2O_8 + H)^+$: 609.2237; Found: 609.2194.

Protected salicylate **97**.



4-Dimethylaminopyridine (4.7 mg, 39 μ mol, 4 equiv) and commercially available 2-benzyloxybenzoyl chloride (4.8 mg, 19 μ mol, 2 equiv) were dissolved in dichloromethane (50 μ L) at 23 °C. A solution of intermediate **95** (7.0 mg, 9.7 μ mol, 1 equiv) in dichloromethane (0.2 mL) was added and the reaction mixture continued to stir at 23 °C for 3 h. The reaction mixture was concentrated, loaded onto a column, and purified via flash-column chromatography (5 \rightarrow 30% ethyl acetate–hexanes) to provide the salicylate ester **97** (8.0 mg, 89%) as a light yellow foam. This material was carried forward without further purification.

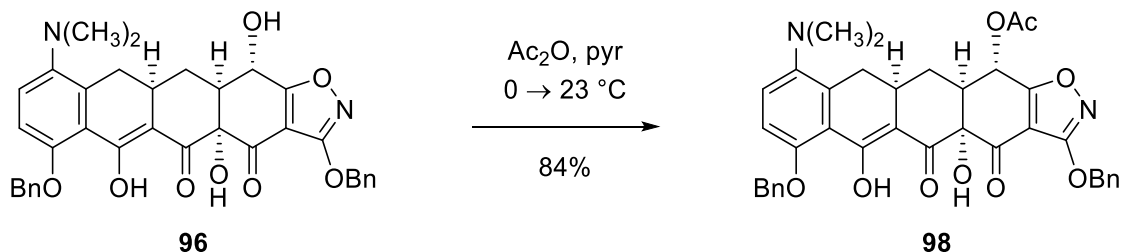
C4-dedimethylamino-C4-salicyloxyminocycline (**91**).



Concentrated aqueous hydrofluoric acid solution (48 wt%, 1 mL) was added to a solution of the salicylate ester **97** (8.0 mg, 8.6 μ mol, 1 equiv) in acetonitrile (1 mL) in a polypropylene reaction vessel at 23 °C. The reaction vessel was then placed in a 35 °C oil heating bath for 20 h. Upon removal from the heating bath and cooling to 23 °C, the reaction mixture was poured into water (17 mL) containing dipotassium hydrogen phosphate trihydrate (3.3 g). The resulting mixture was extracted with ethyl acetate (4 \times 20 mL). The organic extracts were combined and the combined solution was dried over anhydrous sodium sulfate. The dried solution was filtered and the filtered solution was concentrated, affording a yellow solid. Methanol (1 mL) and 1,4-dioxane (1 mL) were added to the crude product, forming a yellow solution. Palladium black (3.9 mg, 30 μ mol, 3.5 equiv) was added in one portion at 23 °C. An atmosphere of hydrogen gas was introduced by briefly evacuating the flask, then backfilling with hydrogen (1 atm). The reaction mixture was stirred at 23 °C for 3 h, then was filtered through a cotton plug. The filtrate was concentrated, affording a yellow oil. It was determined at this point that there was incomplete deprotection of the C12a silyl ether and therefore the crude material was dissolved in acetonitrile (1 mL) in a polypropylene reaction and additional concentrated aqueous hydrofluoric acid solution (48 wt%, 1 mL) was added at 23 °C. The reaction vessel was then placed in a 40 °C oil heating bath for 48 h. Upon removal from the heating bath and cooling to 23 °C, acetonitrile

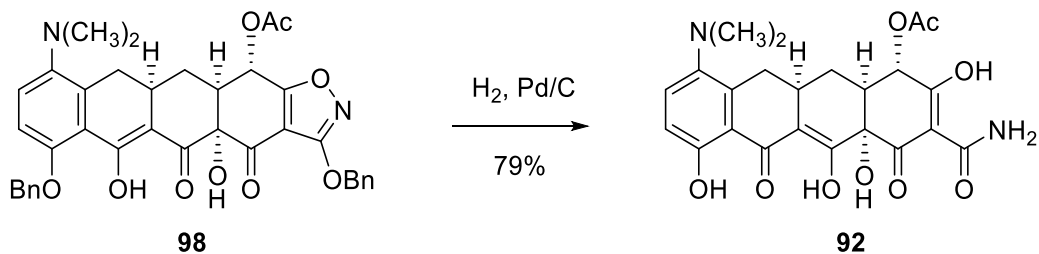
(3 mL) was added, followed by excess methoxytrimethylsilane (4.0 mL) to quench the hydrofluoric acid. The reaction mixture was concentrated and the residue was purified by reverse-phase HPLC (Agilent Extend-C18, 95:5→60:40 water–acetonitrile + 0.1% trifluoroacetic acid) to afford C4-dedimethylamino-C4-salicyloximinocycline (**91**, 3.5 mg, 74% over 3 steps). ¹H NMR (600 MHz, CD₃OD) δ: 7.96 (dd, 1H, *J* = 7.9 Hz, 1.8 Hz), 7.74 (d, 1H, *J* = 9.4 Hz), 7.55–7.52 (m, 1H), 7.00–6.95 (m, 3H), 5.79 (d, 1H, *J* = 6.7 Hz), 3.16 (dd, 1H, *J* = 15.5 Hz, 4.7 Hz), 3.06 (s, 6H), 2.80 (br s, 1H), 2.66–2.62 (m, 1H), 2.53–2.49 (m, 1H), 1.94 (s, 1H), 1.33 (br s, 1H); HRMS (ESI): Calcd for (C₂₈H₂₆N₂O₁₀ + H)⁺: 551.1660; Found: 551.1672.

Acetate **98**.



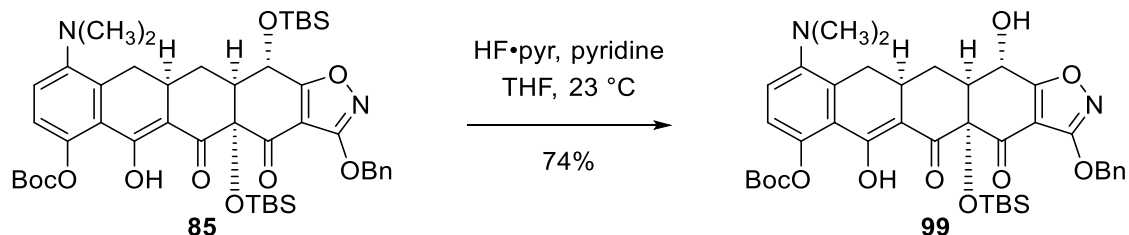
Desilylated intermediate **96** (6.0 mg, 9.9 μmol , 1 equiv) was dissolved in a 1:1 mixture of dichloromethane:pyridine (0.1 mL) and placed in an ice-water cooling bath. Acetic anhydride (1.0 μL , 11 μmol , 1.1 equiv) was added and the reaction mixture was slowly warmed to 23 $^\circ\text{C}$. After 12 h at 23 $^\circ\text{C}$, an additional portion of acetic anhydride (10 μL) was added. Upon complete consumption of starting material indicated by TLC, water (2 mL) and ethyl acetate (2 mL) were added. The layers were separated and the aqueous layer was extracted with ethyl acetate (2 \times 3 mL). The combined organic extracts were washed with saturated aqueous sodium chloride solution (10 mL) and the washed extracts were dried over sodium sulfate. The dried organic phase was filtered and the filtrate was concentrated, affording a yellow solid. The crude material was purified by reverse-phase HPLC (Agilent Extend-C18, 30:70 \rightarrow 0:100 water–methanol) to afford acetate **98** (5.4 mg, 84%). ^1H NMR (500 MHz, CDCl_3) δ : 16.11 (s, 1H), 7.49 (t, 4H, $J = 8.5$ Hz), 7.40–7.36 (m, 5H), 7.31–7.29 (m, 1H), 7.19 (d, 1H, $J = 9.2$ Hz), 6.90 (d, 1H, $J = 9.2$ Hz), 5.95 (d, 1H, $J = 2.7$ Hz), 5.41–5.36 (m, 2H), 5.22 (d, 1H, $J = 12.4$ Hz), 5.13 (d, 1H, $J = 12.4$ Hz), 3.30–3.27 (m, 1H), 2.82–2.75 (m, 2H), 2.60 (s, 6H), 2.29–2.24 (m, 1H), 2.20 (s, 3H), 2.17–2.11 (m, 1H), 1.48–1.41 (m, 1H); HRMS (ESI): Calcd for $(\text{C}_{37}\text{H}_{34}\text{N}_2\text{O}_9 + \text{H})^+$: 651.2337; Found: 651.2329.

C4-dedimethylamino-C4-acetoximinocycline (**92**).



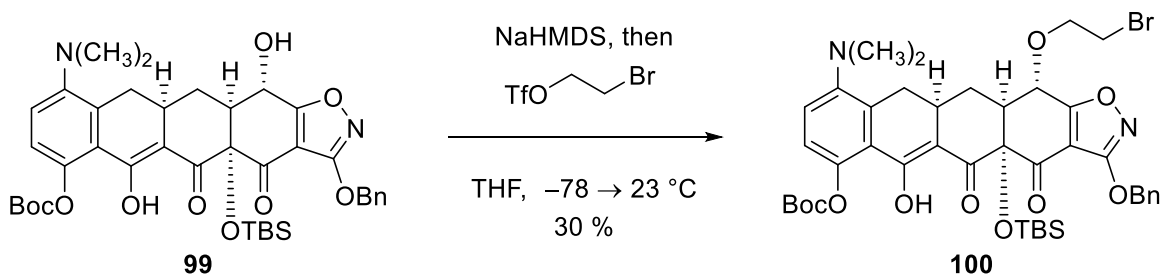
Methanol (1 mL) and 1,4-dioxane (1 mL) were added to the acetate **98** (5.4 mg, 8.3 μmol , 1 equiv), forming a yellow solution. Palladium black (3.1 mg, 29 μmol , 3.5 equiv) was added in one portion at 23 °C. An atmosphere of hydrogen gas was introduced by briefly evacuating the flask, then backfilling with hydrogen (1 atm). The reaction mixture was stirred at 23 °C for 1 h, then was filtered through a cotton plug. The filtrate was concentrated, affording a yellow film. The residue was purified by reverse-phase HPLC (Agilent Extend-C18, 95:5 \rightarrow 60:40 water–acetonitrile + 0.1% trifluoroacetic acid) to afford C4-dedimethylamino-C4-acetoximinocycline (**92**, 3.1 mg, 79%). HRMS (ESI): Calcd for ($\text{C}_{23}\text{H}_{24}\text{N}_2\text{O}_9 + \text{H}$) $^+$: 473.1555; Found: 473.1574.

Alcohol **99**.



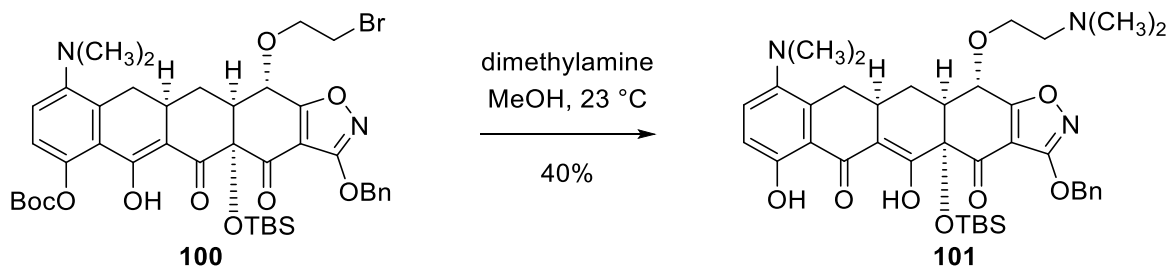
Hydrogen fluoride–pyridine complex (~70% solution of HF in pyridine, 1 mL) was added to a solution of the Michael–Claisen cyclization product **85** (114 mg, 0.135 mmol, 1 equiv) in tetrahydrofuran (9 mL), containing additional pyridine (0.5 mL). After 23 h at 23 °C, the reaction mixture was diluted with ethyl acetate (20 mL). Saturated aqueous sodium bicarbonate solution (20 mL) was added and the layers were separated. The organic layer was washed sequentially with additional portions of saturated aqueous sodium bicarbonate solution (2 × 50 mL) and saturated aqueous sodium chloride solution (50 mL). The washed extracts were dried over sodium sulfate, the dried organic phase was filtered, and the filtrate was concentrated, affording a yellow solid. The crude material was purified by reverse-phase HPLC (Agilent Extend-C18, 30:70→0:100 water–methanol) to afford alcohol **99** (73 mg, 74%). ¹H NMR (600 MHz, CDCl₃) δ: 16.19 (br s, 1H), 7.49–7.47 (m, 2H), 7.39–7.32 (m, 3H), 7.20 (d, 1H, *J* = 8.7 Hz), 7.01 (d, 1H, *J* = 8.7 Hz), 5.43–5.37 (m, 2H), 4.64 (dd, 1H, *J* = 10.8 Hz, 1.7 Hz), 3.79 (d, 1H, *J* = 10.8 Hz), 3.18 (dd, 1H, *J* = 15.3 Hz, 4.1 Hz), 2.82–2.77 (m, 2H), 2.61 (s, 6H), 2.12 (t, 1H, *J* = 14.6 Hz), 1.57 (s, 9H), 1.39–1.31 (m, 1H), 0.74 (s, 9H), 0.21 (s, 3H), 0.13 (s, 3H); HRMS (ESI): Calcd for (C₃₉H₄₈N₂O₁₀Si + H)⁺: 733.3151; Found: 733.3132.

2-Bromoethyl ether **100**.



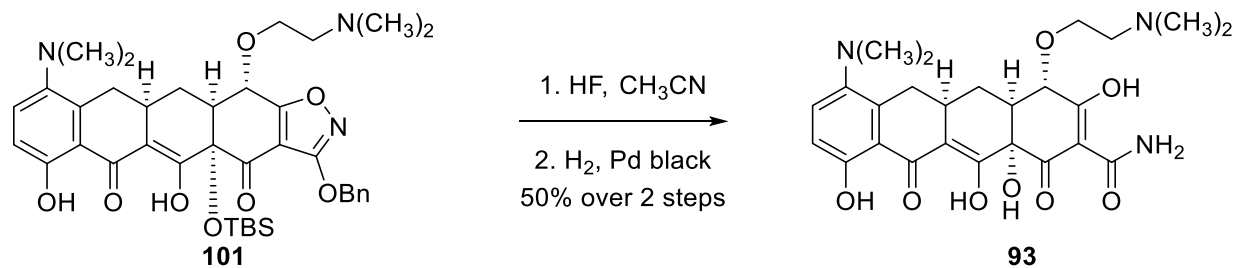
Alcohol **99** (17 mg, 23 μmol , 1 equiv) was dissolved in tetrahydrofuran (0.3 mL) and placed in a dry ice–acetone cooling bath. A sodium bis(trimethylsilyl)amide solution in tetrahydrofuran (1.0 M, 56 μL , 56 μmol , 2.4 equiv) was added, followed by 2-bromoethyl triflate (10.1 mg, 39 μmol , 1.7 equiv) at $-78 \text{ }^\circ\text{C}$. Upon consumption of the starting material, aqueous potassium phosphate buffer solution (pH 7.0, 2 mL) was added followed by ethyl acetate (2 mL). The layers were separated and the aqueous layer was extracted with ethyl acetate ($2 \times 3 \text{ mL}$). The combined organic extracts were washed with saturated aqueous sodium chloride solution (10 mL) and the washed extracts were dried over sodium sulfate. The dried organic phase was filtered and the filtrate was concentrated, affording a yellow oil. The crude material was purified via flash-column chromatography (10 \rightarrow 40% ethyl acetate–hexanes) to recover starting alcohol **99** (11 mg) and to provide the 2-bromoethyl ether **100** as a light yellow foam (6 mg, 30%). TLC: (20% ethyl acetate–hexanes) $R_f = 0.50$ (UV, CAM); $^1\text{H NMR}$ (600 MHz, CDCl_3) δ : 15.88 (br s, 1H), 7.49 (d, 2H, $J = 7.3 \text{ Hz}$), 7.39–7.33 (m, 3H), 7.22 (d, 1H, $J = 8.7 \text{ Hz}$), 7.03 (d, 1H, $J = 8.7 \text{ Hz}$), 5.40–5.36 (m, 2H), 4.62 (d, 1H, $J = 6.6 \text{ Hz}$), 4.49–4.46 (m, 1H), 3.92 (ddd, 1H, $J = 10.6 \text{ Hz}$, 7.8 Hz, 5.6 Hz), 3.56–3.53 (m, 2H), 3.35 (dd, 1H, $J = 15.5 \text{ Hz}$, 4.5 Hz), 2.97–2.92 (m, 1H), 2.78–2.76 (m, 1H), 2.65 (s, 6H), 2.39–2.33 (m, 2H), 1.95 (d, 1H, $J = 13.5 \text{ Hz}$), 1.55 (s, 9H), 0.78 (s, 9H), 0.17 (s, 3H), 0.14 (s, 3H); HRMS (ESI): Calcd for $(\text{C}_{41}\text{H}_{51}\text{BrN}_2\text{O}_{10}\text{Si} + \text{H})^+$: 839.2569; Found: 839.2533.

2-dimethylaminoethyl ether **101**.



2-Bromoethyl ether **100** (6.0 mg, 7.1 μmol , 1 equiv) was dissolved in methanol (1 mL). Approximately 1 mL of dimethylamine was condensed into the reaction flask by passage of a stream of dimethylamine gas over a coldfinger condenser. The coldfinger apparatus was then removed and the reaction flask was sealed with a yellow cap and Keck clip. The reaction mixture darkened to yellow and then green as it stirred for 16 h at 23 °C. The reaction mixture was then concentrated and the crude material was purified by reverse-phase HPLC (Agilent Extend-C18, 30:70 \rightarrow 0:100 water–methanol) to afford 2-dimethylaminoethyl ether **101** (2 mg, 40%). HRMS (ESI): Calcd for $(\text{C}_{38}\text{H}_{49}\text{N}_3\text{O}_8\text{Si} + \text{H})^+$: 704.3367; Found: 704.3341.

C4-dedimethylamino-C4-(2-dimethylaminoethoxy)minocycline (**93**).



Concentrated aqueous hydrofluoric acid solution (48 wt%, 1 mL) was added to a solution of the 2-dimethylaminoethyl ether **101** (2.5 mg, 3.6 μ mol, 1 equiv) in acetonitrile (1 mL) in a polypropylene reaction vessel at 23 °C. The reaction vessel was then placed in a 35 °C oil heating bath for 60 h. Upon removal from the heating bath and cooling to 23 °C, the reaction mixture was poured into water (17 mL) containing dipotassium hydrogen phosphate trihydrate (3.3 g). The resulting mixture was extracted with ethyl acetate (4 \times 20 mL). The organic extracts were combined and the combined solution was dried over anhydrous sodium sulfate. The dried solution was filtered and the filtered solution was concentrated, affording a yellow solid. Methanol (1 mL) and 1,4-dioxane (1 mL) were added to the crude product, forming a yellow solution. Palladium black (1.3 mg, 12 μ mol, 3.5 equiv) was added in one portion at 23 °C. An atmosphere of hydrogen gas was introduced by briefly evacuating the flask, then backfilling with hydrogen (1 atm). The reaction mixture was stirred at 23 °C for 1 h, then was filtered through a cotton plug. The filtrate was concentrated, affording a yellow oil. The product was purified by reverse-phase HPLC (Agilent Extend-C18, 95:5 \rightarrow 60:40 water–acetonitrile + 0.1% trifluoroacetic acid) to afford C4-dedimethylamino-C4-(2-dimethylaminoethoxy)minocycline (**93**, 1.0 mg, 50% over 2 steps). HRMS (ESI): Calcd for (C₃₂H₃₅N₃O₈ + H)⁺: 590.2497; Found: 590.2495.

X-Ray Crystallography

A crystal mounted on a diffractometer was collected data at 100 K. The intensities of the reflections were collected by means of a Bruker APEX II DUO CCD diffractometer ($\text{Cu}_{K\alpha}$ radiation, $\lambda=1.54178 \text{ \AA}$), and equipped with an Oxford Cryosystems nitrogen flow apparatus. The collection method involved 0.7° scans in ω at 30° , 68° and 105° in 2θ . Data integration down to 0.84 \AA resolution was carried out using SAINT V7.46 A⁶⁵ with reflection spot size optimization. Absorption corrections were made with the program SADABS.⁶⁵ The structure was solved by the direct methods procedure and refined by least-squares methods again F^2 using SHELXS-97 and SHELXL-97.⁶⁶ Non-hydrogen atoms were refined anisotropically, and hydrogen atoms were allowed to ride on the respective atoms. Crystal data as well as details of data collection and refinement are summarized in Table E1. The Ortep plots produced with SHELXL-97 program, and the other drawings were produced with Accelrys DS Visualizer 2.0.⁶⁷

⁶⁵ Bruker AXS APEX II, Bruker AXS, Madison, Wisconsin, 2009.

⁶⁶ Sheldrick, G. M. *Acta Cryst.* **2008**, *A64*, 112–122.

⁶⁷ Accelrys DS Visualizer v2.0.1, Accelrys Software. Inc., 2007.

Table E1: Experimental details.

Crystal data	
Chemical formula	C ₉₆ H ₁₀₈ N ₄ O ₁₈ Si ₂
M_r	1662.04
Crystal system, space group	Orthorhombic, $P2_12_12_1$
Temperature (K)	100
a, b, c (Å)	14.7418 (4), 22.4564 (6), 26.8138 (7)
V (Å ³)	8876.6 (4)
Z	4
Radiation type	Cu $K\alpha$
μ (mm ⁻¹)	0.94
Crystal size (mm)	0.20 × 0.18 × 0.05
Data collection	
Diffractometer	CCD area detector diffractometer
Absorption correction	Multi-scan <i>SADABS</i>
T_{\min}, T_{\max}	0.835, 0.955
No. of measured, independent and observed [$I > 2\sigma(I)$] reflections	88849, 15376, 14708
R_{int}	0.055
Refinement	
$R[F^2 > 2\sigma(F^2)], wR(F^2), S$	0.053, 0.125, 1.09
No. of reflections	15376
No. of parameters	1091
No. of restraints	0
H-atom treatment	H-atom parameters constrained
$\Delta\rho_{\max}, \Delta\rho_{\min}$ (e Å ⁻³)	0.43, -0.51
Absolute structure	Flack H D (1983), Acta Cryst. A39, 876-881
Flack parameter	0.03 (3)

Computer programs: *APEX2* v2009.3.0 (Bruker-AXS, 2009), *SAINT* 7.46A (Bruker-AXS, 2009), *SHELXS97* (Sheldrick, 2008), *SHELXL97* (Sheldrick, 2008), Bruker *SHELXTL*.

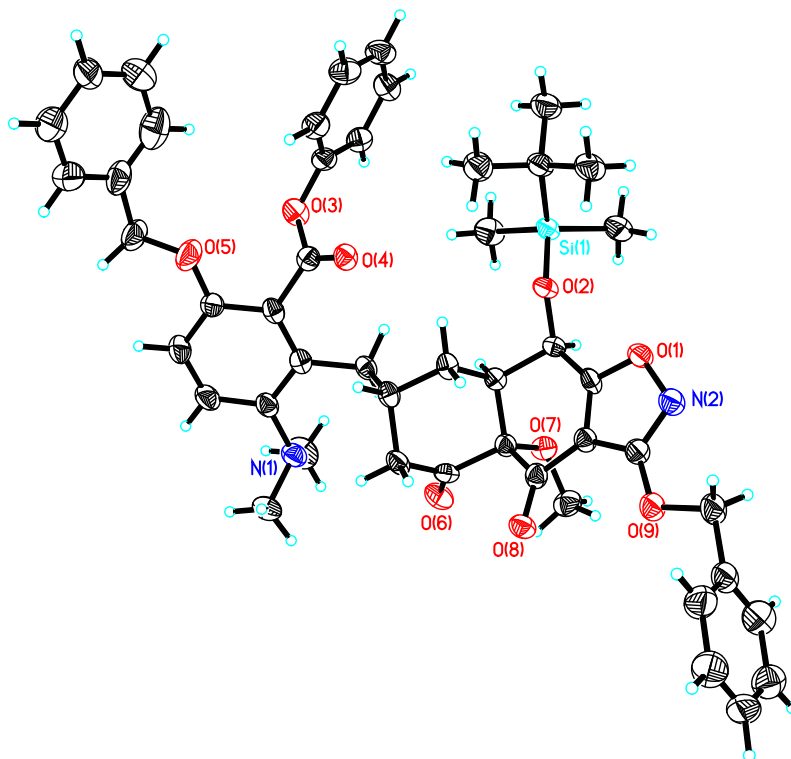


Figure E1: Perspective views showing 50% probability displacement.

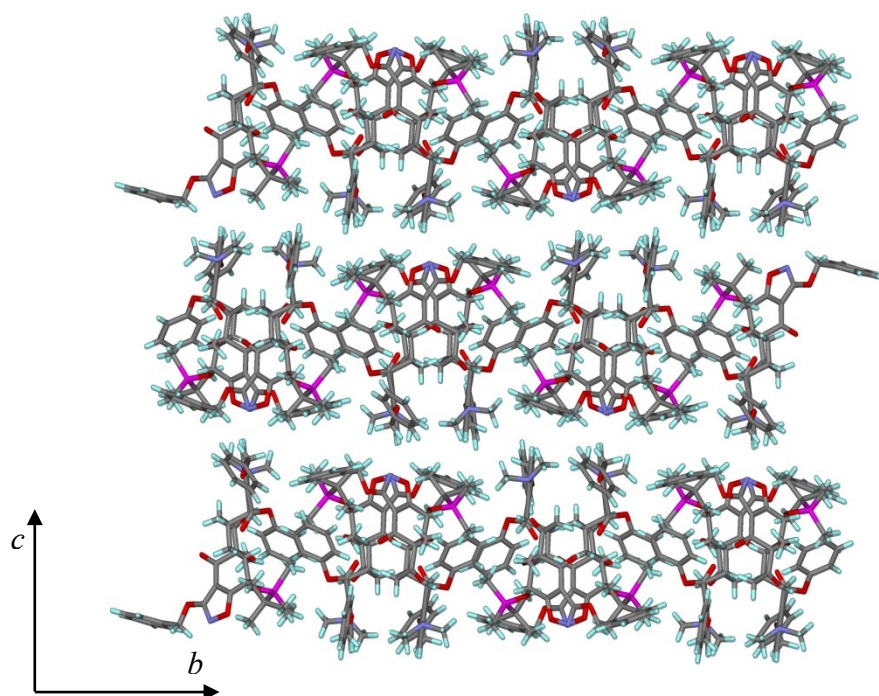
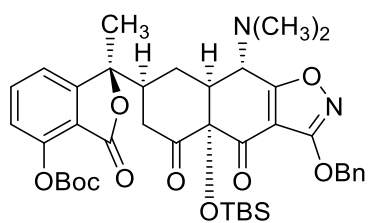


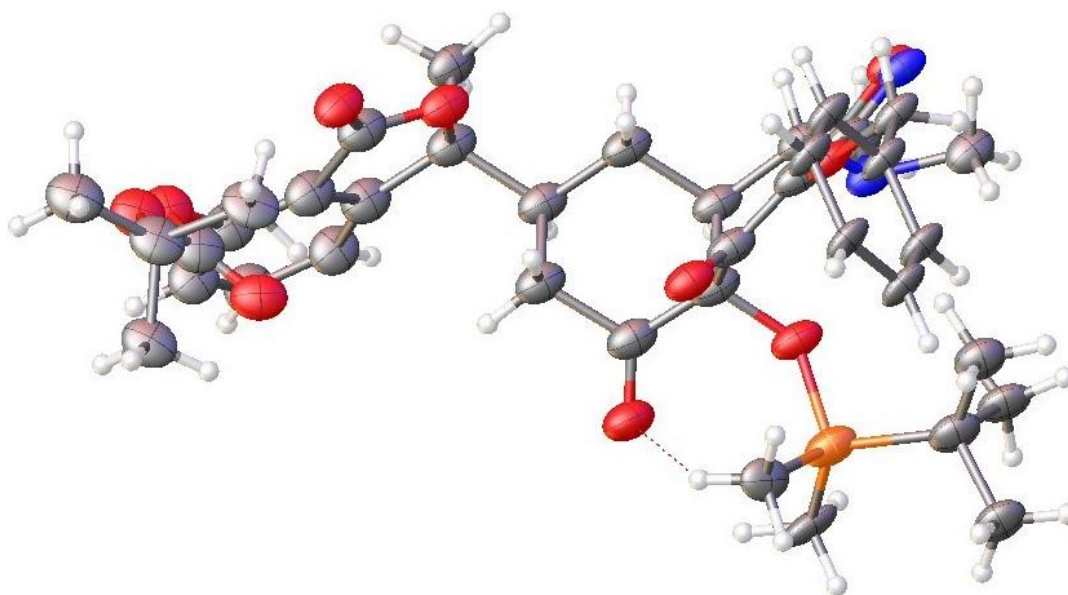
Figure E2: Three-dimensional supramolecular architecture viewed along the *a*-axis direction.

X-ray Crystallographic Laboratory Structure Report

Shao-Liang Zheng, Harvard University



47



X-Ray Crystallography

A crystal mounted on a diffractometer was collected data at 100 K. The intensities of the reflections were collected by means of a Bruker APEX II CCD along with the D8 Diffractometer (30 KeV, $\lambda = 0.413280 \text{ \AA}$), and equipped with an Oxford Cryosystems nitrogen open flow apparatus. The collection method involved 0.5° scans in Phi at -5° in 2θ . Data integration down to 0.82 \AA resolution was carried out using SAINT V7.46 A⁶⁵ with reflection spot size optimization. Absorption corrections were made with the program SADABS.⁶⁵ The structure was solved by the direct methods procedure and refined by least-squares methods again F^2 using SHELXS-97 and SHELXL-97.⁶⁶ Non-hydrogen atoms were refined anisotropically, and hydrogen atoms were allowed to ride on the respective atoms. Crystal data as well as details of data collection and refinement are summarized in Table E2. The Ortep plots produced with SHELXL-97 program, and the other drawings were produced with Accelrys DS Visualizer 2.0.⁶⁷

We thank Dr. Yu-Sheng Chen at ChemMatCARS, APS, for his assistance with single-crystal data. ChemMatCARS Sector 15 is principally supported by the National Science Foundation/Department of Energy under grant number NSF/CHE-0822838. Use of the Advanced Photon Source was supported by the U. S. Department of Energy, Office of Science, Office of Basic Energy Sciences, under Contract No. DE-AC02-06CH11357.⁶⁸

⁶⁸ See: <http://cars9.uchicago.edu/chemmat/pages/acknowledge.html>.

Table E2: Experimental details.

Crystal data	
Chemical formula	C ₈₀ H ₁₀₀ N ₄ O ₂₀ Si ₂
M_r	1493.82
Crystal system, space group	Monoclinic, $P2_1$
Temperature (K)	100
a, b, c (Å)	15.4569 (11), 15.5369 (11), 17.3009 (13)
β (°)	92.449 (1)
V (Å ³)	4151.1 (5)
Z	2
Radiation type	Synchrotron, $\lambda = 0.41328$ Å
μ (mm ⁻¹)	0.07
Crystal size (mm)	0.10 × 0.04 × 0.02
Data collection	
Diffractometer	Bruker D8 goniometer with CCD area detector diffractometer
Absorption correction	Multi-scan <i>SADABS</i>
T_{\min}, T_{\max}	0.993, 0.999
No. of measured, independent and observed [$I > 2\sigma(I)$] reflections	67406, 12514, 8468
R_{int}	0.086
Refinement	
$R[F^2 > 2\sigma(F^2)], wR(F^2), S$	0.067, 0.149, 1.09
No. of reflections	12514
No. of parameters	1454
No. of restraints	1010
H-atom treatment	H-atom parameters constrained
$\Delta\rho_{\max}, \Delta\rho_{\min}$ (e Å ⁻³)	0.83, -0.23
Absolute structure	Flack H D (1983), Acta Cryst. A39, 876-881
Flack parameter	0.3 (5)

Computer programs: *APEX2* v2009.3.0 (Bruker-AXS, 2009), *SAINT* 7.46A (Bruker-AXS, 2009), *SHELXS97* (Sheldrick, 2008), *SHELXL97* (Sheldrick, 2008), Bruker *SHELXTL*.

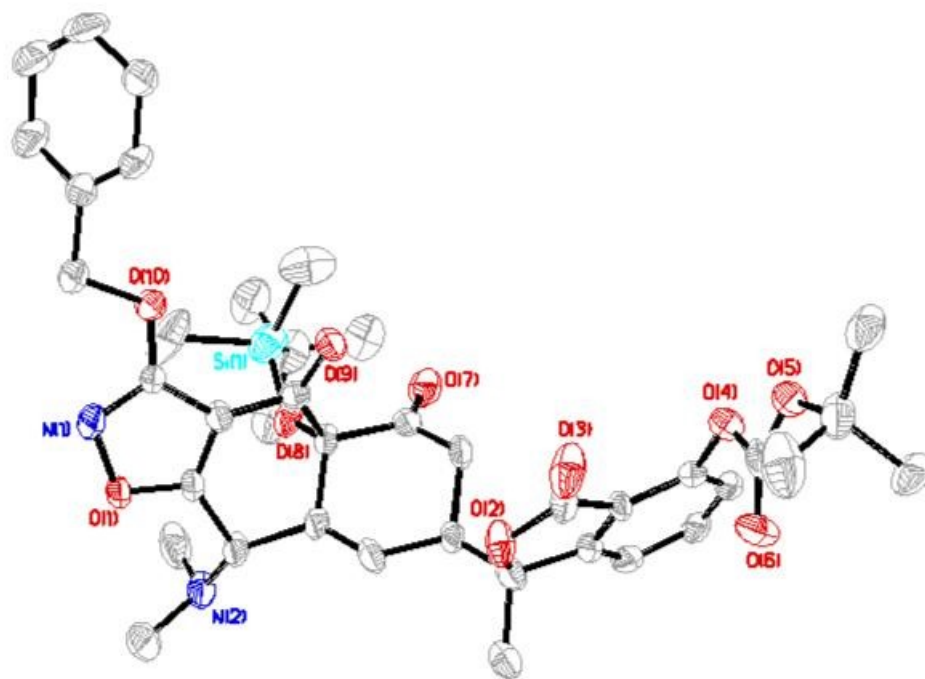


Figure E3: Perspective views showing 50% probability displacement.

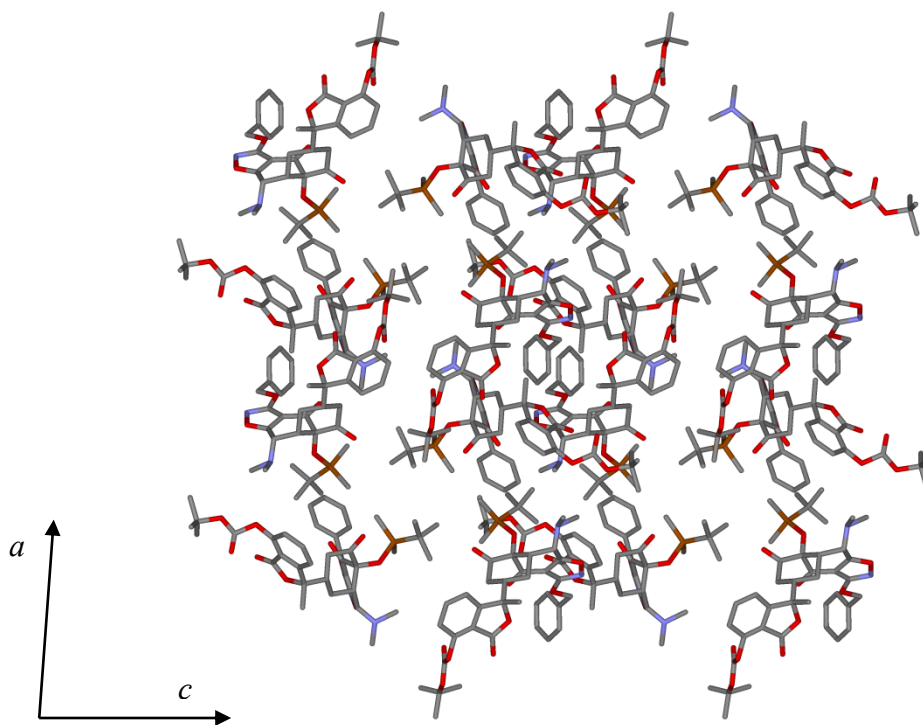


Figure E4: Three-dimensional supramolecular architecture viewed along the *b*-axis direction.

Chapter 3

Pseudoephedrine Glycinamide as a Chiral Glycine Equivalent in Aldol Reactions

Introduction: β -Hydroxy- α -Amino Acids

β -Hydroxy- α -amino acids, common chiral building blocks, are frequently found in biologically relevant molecules, including a wide range of antibiotics (Figure 3.1). Broad-spectrum antibiotics (chloramphenicol and thiamphenicol)⁶⁹ as well as antibacterials with specifically Gram-positive (solithromycin⁷⁰ and vancomycin⁷¹) or Gram-negative (aztreonam)⁷² activity feature either the β -hydroxy- α -amino acid motif itself or a derivative thereof. Antitumor antibiotic actinobolin⁷³ and nucleoside antibacterial polyoxin B⁷⁴ also contain the aforementioned scaffold.

⁶⁹ Review: Fisch, A.; Bryskier, A. *Antimicrob. Agents* **2005**, 925–929.

⁷⁰ Review: (a) Fernandes, P.; Pereira, D.; Jamieson, B.; Keedy, K. *Drugs Future*, **2011**, 36, 751–758. Discovery: (b) Lemaire, S.; Van Bambeke, F.; Tulkens, P. M. *Antimicrob. Agents Chemother.* **2009**, 53, 3734–3743.

⁷¹ Reviews: (a) Williams, D. H.; Bardsley, B. *Angew. Chem. Int. Ed.* **1999**, 38, 1172–1193. (b) Butler, M. S.; Hansford, K. A.; Blaskovich, M. A. T.; Halai, R.; Cooper, M. A. *J. Antibiot.* **2014**, 67, 631–634.

⁷² Review: Sykes, R. B.; Bonner, D. P. *Rev. Infect. Dis.* **1985**, 7 Suppl 4, S579–S593.

⁷³ Review: (a) Fraser-Reid, B.; Lopez, J. C. Actinobolin and Bactobolin: Chemical Aspects and Syntheses. In *Recent Progress in the Chemical Synthesis of Antibiotics*. Lukacs, G., Ohno, M., Eds.; Springer-Verlag: Berlin, Germany, **1990**; 285–319. See also: (b) Munk, M. E.; Sodano, C. S.; McLean, R. L.; Haskell, T. H. *J. Am. Chem. Soc.* **1967**, 89, 4158–4165. (c) Munk, M. E.; Nelson, D. B.; Antosz, F. J.; Herald, D. L., Jr.; Haskell, T. H. *J. Am. Chem. Soc.* **1968**, 90, 1087–1089. (d) Antosz, F. J.; Nelson, D. B.; Herald, D. L., Jr.; Munk, M. E. *J. Am. Chem. Soc.* **1970**, 92, 4933–4942. (e) Garigipati, R. S.; Tschaen, D. M.; Weinreb, S. M. *J. Am. Chem. Soc.* **1985**, 107, 7790–7792.

⁷⁴ (a) Isono, K.; Nagatsu, J.; Kawashima, Y.; Suzuki, S. *Agr. Biol. Chem.* **1965**, 29, 848–854. (b) Isono, K.; Asahi, K.; Suzuki, S. *J. Am. Chem. Soc.* **1969**, 91, 7490–7505. (c) Uchida, K.; Kato, K.; Yamaguchi, K.; Akita, H. *Heterocycles*, **2000**, 53 2253–2259.

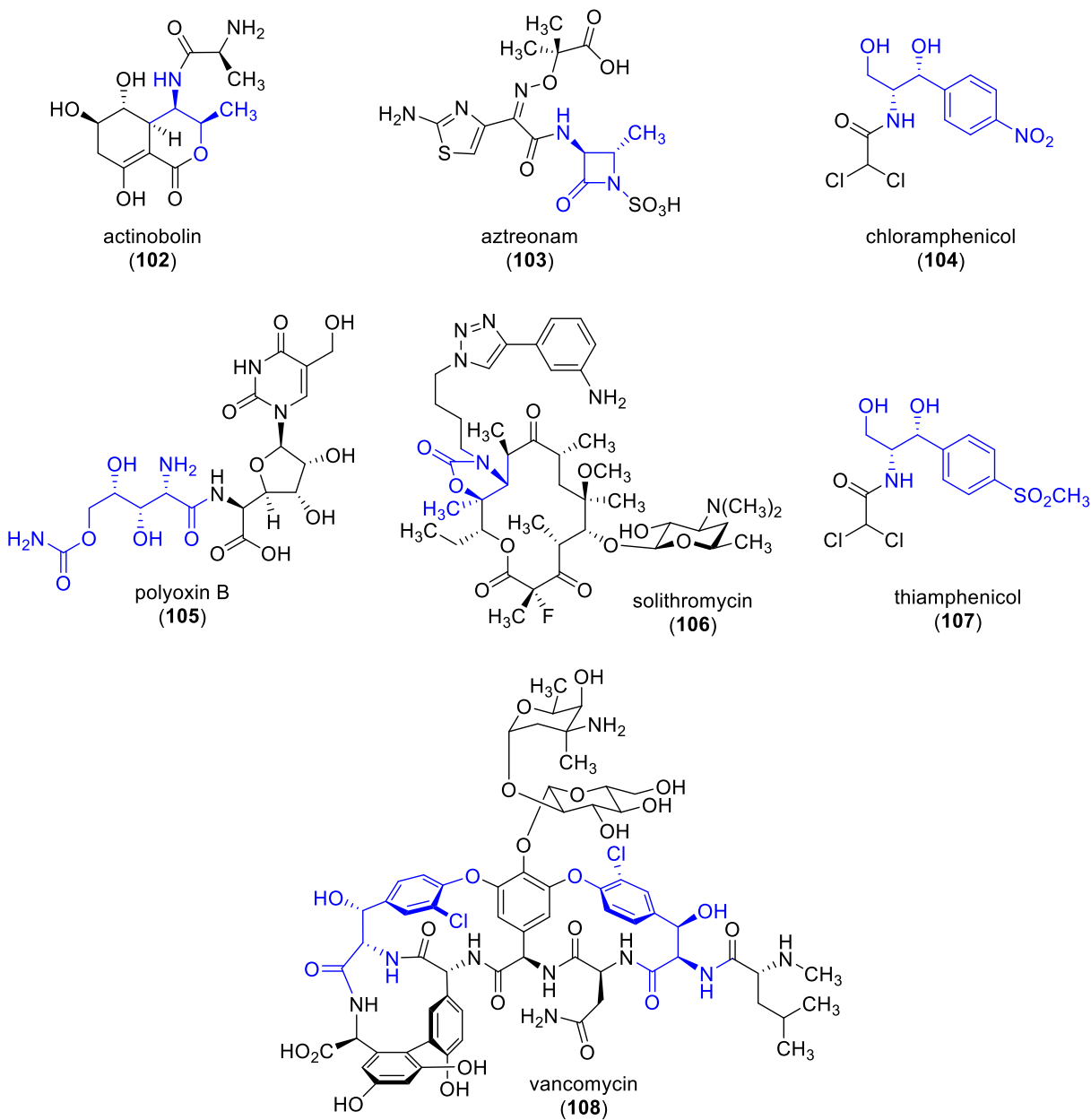


Figure 3.1: Antibiotics containing the β -hydroxy- α -amino acid motif (highlighted in blue).

Additionally, β,β' -disubstituted- β -hydroxy- α -amino acids, a type of non-proteinogenic amino acids, are often present in bioactive compounds, including fungicides,⁷⁵ HIV reverse

⁷⁵ (a) Takesako, K.; Ikai, K.; Haruna, F.; Endo, M.; Shimanaka, K.; Sono, E.; Nakamura, T.; Kato, I.; Yamaguchi, H. *J. Antibiot.* **1991**, *44*, 919–924. (b) Fujikawa, A.; In, Y.; Inoue, M.; Ishida, T.; Nemoto, N.; Kobayashi, Y.; Katakoa, R.; Ikai, K.; Takesako, K.; Kato, I. *J. Org. Chem.* **1994**, *59*, 570–578.

transcriptase inhibitors,⁷⁶ and β -lactam antibiotics.⁷⁷ These non-canonical amino acids are also attractive substrates for the *de novo* synthesis of peptides and peptidomimetics. Incorporation of the aforementioned amino acids into peptides results in greater conformational rigidity, which in turn provides enhanced activity and resistance to proteolytic degradation.⁷⁸

Overall, both β -hydroxy- α -amino acids and β,β' -disubstituted- β -hydroxy- α -amino acids are valuable targets due to their potential as chiral building blocks for chemical synthesis and their ubiquity in biologically significant systems.

An Overview on Asymmetric Aldol Reactions with Glycine

Historically, β -hydroxy- α -amino acids have been synthesized using various strategies, which can be divided into two general classes: (1) constructive transformations, which build the C–C bond between an α -carbon bearing a nitrogen substituent and a β -carbon bearing an oxygen substituent in a single operation (such as glycine aldol reactions), and (2) nonconstructive methodologies, which arrive at the desired functionality through alternate, generally less direct, means. Examples of nonconstructive strategies include Sharpless asymmetric aminohydroxylation of specific alkenyl esters,⁷⁹ multistep reactions via Garner aldehyde-type

⁷⁶ (a) Konish, M.; Ohkuma, H.; Sakai, F.; Tsuno, T.; Koshiyama, H.; Naito, T.; Kawaguchi, H. *J. Am. Chem. Soc.* **1981**, *103*, 1241–1243. (b) Boger, D. L.; Ledebor, M. W.; Kume, M.; Searcey, M.; Jin, Q. *J. Am. Chem. Soc.* **1999**, *121*, 11375–11383.

⁷⁷ Gordon, E. M.; Ondetti, M. A.; Pluscec, J.; Cimarusti, C. M.; Bonner, D. P. Sykes, R. B. *J. Am. Chem. Soc.* **1982**, *104*, 6053–6060. Also see Chapter 4.

⁷⁸ (a) Hruby, V. J.; Schwyzer, R., Eds. *Tetrahedron-Symposia-in-Print: Peptide Chemistry: Design and Synthesis of Peptides, Conformational Analysis and Biological Functions. Tetrahedron*, **1988**, *44*, 661–1006. (b) Giannis, A.; Kolter T. *Angew. Chem. Int. Ed. Engl.* **1993**, *32*, 1244–1267. (c) Robl, J. A.; Cimarusti, M. P.; Simpkins, L. M.; Weller, H. N.; Pan, Y. Y.; Malley, M.; DiMarco, J. D. *J. Am. Chem. Soc.* **1994**, *116*, 2348–2355. (d) Cardillo, G.; Gentilucci, L.; Tolomelli, A. *Mini-Rev. Med. Chem.* **2006**, *6*, 293–304.

⁷⁹ (a) Tao, B.; Schlingloff, G.; Sharpless, K. B. *Tetrahedron Lett.* **1998**, *39*, 2507–2510. (b) Morgan, A. J.; Masse, C. E.; Panek, J. S. *Org. Lett.* **1999**, *1*, 1949–1952. (c) Park, H.; Cao, B.; Joullie, M. M. *J. Org. Chem.* **2001**, *66*, 7223–7226.

intermediates,⁸⁰ asymmetric hydrogenation of α -amino- β -ketoesters,⁸¹ and others.⁸² Analyses of existing nonconstructive methodologies, as well as of chemoenzymatic glycine aldol reactions catalyzed by threonine aldolases⁸³ and hydroxymethylations of alanine equivalents,⁸⁴ are outside of the scope of this introduction.

A generic glycine aldol reaction is depicted in Scheme 3.1. A nucleophilic glycine enolate attacks an electrophilic carbonyl compound (aldehyde or ketone), affording a β -hydroxy- α -amino product in a single transformation. To impart asymmetry into these reactions, two strategies are primarily employed: (1) the use of a glycine equivalent derived from a chiral auxiliary, or (2) enantioselective catalysis.

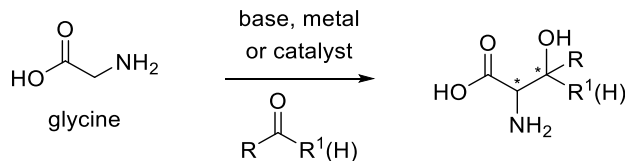
⁸⁰ (a) Williams, L.; Zhang, Z.; Shao, F.; Carroll, P. J.; Joullie, M. M. *Tetrahedron* **1996**, *52*, 11673–11694. (b) Blaskovich, M. A.; Evindar, G.; Rose, N. G. W.; Wilkinson, S.; Luo, Y.; Lajoie, G. A. *J. Org. Chem.* **1998**, *63*, 3631–3646. (c) Avenozza, A.; Cativiela, C.; Corzana, F.; Peregrina, J. M.; Zurbano, M. M. *Tetrahedron: Asymmetry* **2000**, *11*, 2195–2204. (d) Okamoto, N.; Hara, O.; Makino, K.; Hamada, Y. *J. Org. Chem.* **2002**, *67*, 9210–9215.

⁸¹ (a) Noyori, R.; Ikeda, T.; Ohkuma, T.; Widhalm, M.; Kitamura, M.; Takaya, H.; Akutagawa, S.; Sayo, N.; Saito, T.; Taketomi, T.; Kumobayashi, H. *J. Am. Chem. Soc.* **1989**, *111*, 9134–9135. (b) Coulon, E.; Cristina, M.; De, A. C.; Ratovelomanana-Vidal, V.; Genet, J.-P. *Tetrahedron Lett.* **1998**, *39*, 6467–6470. (c) Kuwano, R.; Okuda, S.; Ito, Y. *J. Org. Chem.* **1998**, *63*, 3499–3503. (d) Makino, K.; Goto, T.; Hiroki, Y.; Hamada, Y. *Angew. Chem. Int. Ed.* **2004**, *43*, 882–884. (e) Makino, K.; Hiroki, Y.; Hamada, Y. *J. Am. Chem. Soc.* **2005**, *127*, 5784–5785. (f) Seashore-Ludlow, B.; Villo, P.; Hacker, C.; Somfai, P. *Org. Lett.* **2010**, *12*, 5274–5277.

⁸² (a) Guanti, G.; Banfi, L.; Narisano, E. *Tetrahedron* **1988**, *44*, 5553–5562. (b) Genet, J. P.; Juge, S.; Mallart, S. *Tetrahedron Lett.* **1988**, *29*, 6765–6768. (c) Ruble, J. C.; Fu, G. C. *J. Am. Chem. Soc.* **1998**, *120*, 11532–11533. (d) Davis, F. A.; Srirajan, V.; Fanelli, D. L.; Portonovo, P. *J. Org. Chem.* **2000**, *65*, 7663–7666. (e) Hale, K. J.; Manaviazar, S.; Delisser, V. M. *Tetrahedron* **1994**, *50*, 9181–9188. (f) Rao, A. V. R.; Chakraborty, T. K.; Reddy, K. L.; Rao, A. S. *Tetrahedron Lett.* **1994**, *35*, 5043–5046. (g) Shao, H.; Goodman, M. *J. Org. Chem.* **1996**, *61*, 2582–2583. (h) Shao, H.; Rueter, J. K.; Goodman, M. *J. Org. Chem.* **1998**, *63*, 5240–5244. (i) Alker, D.; Hamblett, G.; Harwood, L. M.; Robertson, S. M.; Watkin, D. J.; Williams, C. E. *Tetrahedron* **1998**, *54*, 6089–6098. (j) Corey, E. J.; Lee, D.-H.; Choi, S. *Tetrahedron Lett.* **1992**, *33*, 6735–6738.

⁸³ (a) Vassilev, V. P.; Uchiyama, T.; Kajimoto, T.; Wong, C.-H. *Tetrahedron Lett.* **1995**, *36*, 4081–4084. (b) Kimura, T.; Vassilev, V. P.; Shen, G.-J.; Wong, C.-H. *J. Am. Chem. Soc.* **1997**, *119*, 11734–11742. (c) Dueckers, N.; Baer, K.; Simon, S.; Groeger, H.; Hummel, W. *Appl. Microbiol. Biotechnol.* **2010**, *88*, 409–424.

⁸⁴ (a) Ji, C.-B.; Liu, Y.-L.; Cao, Z.-Y.; Zhang, Y.-Y.; Zhou, J. *Tetrahedron Lett.* **2011**, *52*, 6118–6121. (b) Shirakawa, S.; Ota, K.; Terao, S. J.; Maruoka, K. *Org. Biomol. Chem.* **2012**, *10*, 5753–5755.



Scheme 3.1: A generalized glycine aldol reaction.

Auxiliary Based Approaches

Two pioneering discoveries in the field of asymmetric glycine aldol reactions were disclosed by the Schöllkopf and Seebach research groups in the early to mid-1980s (Scheme 3.2). Bis(lactim) ether **109**,⁸⁵ a masked chiral glycine equivalent derived in 4 steps from L-valine, was reported to undergo tin-mediated aldol transformations with a variety of aldehydes (or ketones⁸⁶), to afford a range of *syn*-aldol products **110** (Scheme 3.2, **A**), usually as a single diastereomer. The bis(lactim) ether auxiliary was removed upon treatment with strong acid, revealing *syn*- β -hydroxy- α -amino esters **111**. In some cases, the by-products of auxiliary cleavage complicated purification of the ester products.

Seebach's imidazolidinone auxiliary **112**⁸⁷ was prepared in two steps from glycine, methylamine, pivaldehyde, and benzoyl chloride. Treatment of this chiral glycine equivalent with LDA, followed by enolate trapping with an aldehyde (or acetone), provided *syn*-aldol adducts **113**, with transposition of the benzoyl group onto the secondary alcohol (Scheme 3.2, **B**). Aldol adducts were obtained in high yields ($\geq 75\%$) and good diastereoselectivities

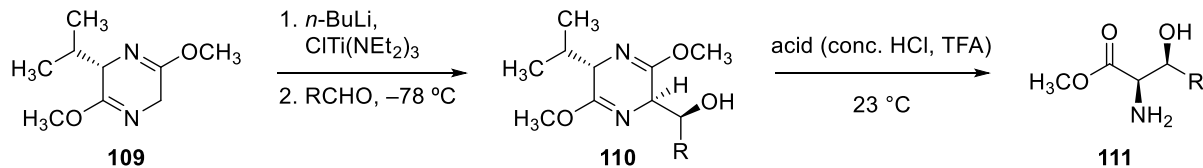
⁸⁵ (a) Schöllkopf, U.; Groth, U.; Gull, M. R.; Nozulak, J. *Liebigs Ann. Chem.* **1983**, 1133–1151. (b) Grauert, M.; Schöllkopf, U. *Liebigs Ann. Chem.* **1985**, 1817–1824. (c) Schöllkopf, U.; Nozulak, J.; Grauert, M. *Synthesis* **1985**, 55–56. (d) Schöllkopf, U.; Bardenhagen, J. *Liebigs Ann. Chem.* **1987**, 393–397. (e) Schöllkopf, U.; Tiller, T. Bardenhagen, J. *Tetrahedron* **1988**, *44*, 5293–5305. (f) Groth, U.; Schöllkopf, U.; Tiller, T. *Tetrahedron* **1991**, *47*, 2835–2842. (g) Modifications of the Schöllkopf method have been reported. See: Di, F. P.; Porzi, G.; Sandri, S. *Tetrahedron: Asymmetry* **1999**, *10*, 2191–2201.

⁸⁶ The ketones investigated were acetone, acetophenone and cyclohexanone. See Ref. 85a.

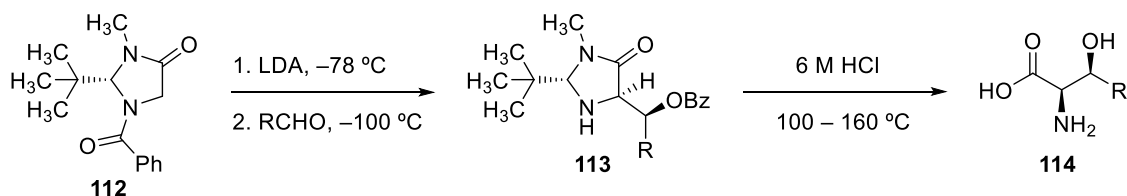
⁸⁷ Seebach, D.; Juaristi, E.; Miller, D. D.; Schickli, C.; Weber, T. *Helv. Chim. Acta* **1987**, *70*, 237–261.

($\geq 86:14$ *syn:anti* ratio). The auxiliary was cleaved under acidic conditions at elevated temperatures, liberating the *syn*- β -hydroxy- α -amino acids **114** in 54% to $\geq 98\%$ yield.

A. Schöllkopf bis(lactim) ether auxiliary

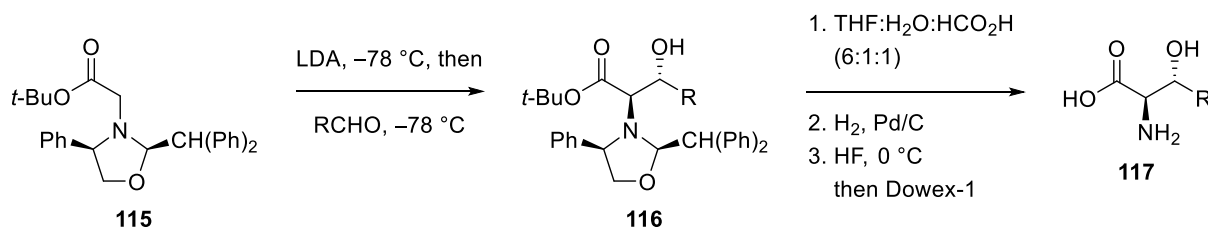


B. Seebach imidazolidinone auxiliary



Scheme 3.2: Schöllkopf and Seebach methodologies.

Researchers at Bristol-Myers Squibb transformed glycine *tert*-butyl ester into chiral oxazolidine **115** in an attempt to impart diastereoselectivity on the aldol transformation (Scheme 3.3).⁸⁸ Treatment of **115** with LDA, followed by the addition of an aldehyde (from a select subset of aliphatic and aromatic ones), afforded *anti*-aldol adducts **116** in $\geq 73\%$ yield and good selectivities ($\geq 90\%$ major isomer). Cleavage of the oxazolidine and the *tert*-butyl ester in three steps provided the β -hydroxy- α -amino acids **117**.



Scheme 3.3: BMS glycine aldol reaction via oxazolidine **115**.

⁸⁸ Iwanowicz, E. J.; Blomgren, P.; Cheng, P. T. W.; Smith, K.; Lau, W. F.; Pan, Y. Y.; Gu, H. H.; Malley, M. F.; Gougoutas, J. Z. *Synlett* **1998**, 664–666.

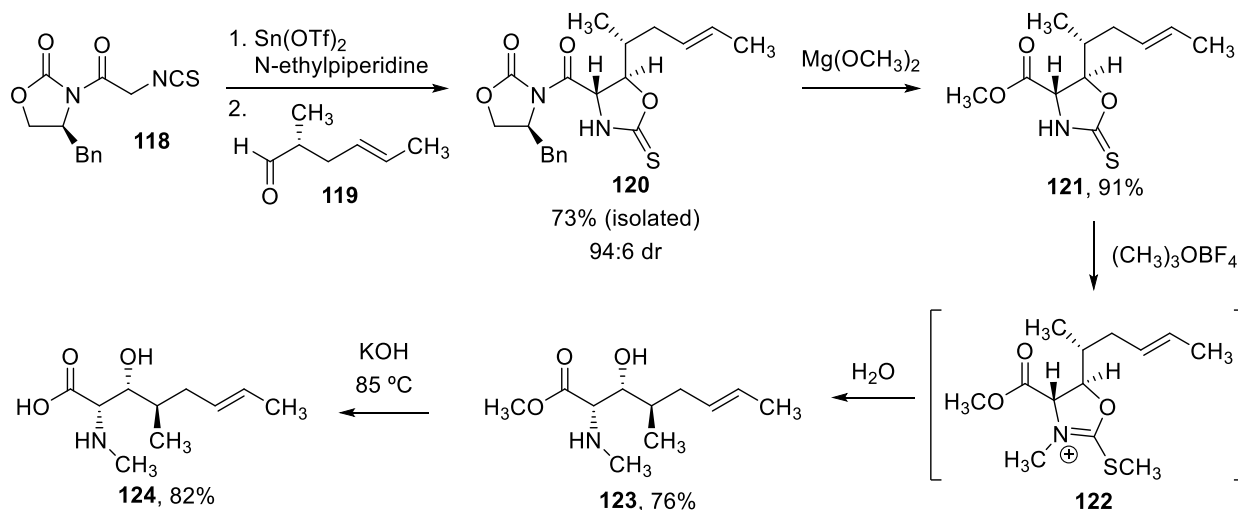
The Evans research group applied their oxazolidinone chiral auxiliary in the synthesis of *syn*- and *anti*- β -hydroxy- α -amino acids via Lewis acid-mediated aldol reactions (Scheme 3.4). Tin-mediated aldol reaction using α -isothiocyanato acyl oxazolidinone **118** as a chiral glycine equivalent⁸⁹ and aldehyde **119** afforded *syn*-thiocarbamate **120** (73%, dr 94:6; Scheme 3.4, **A**). The thiocarbamate effectively protected both of the *syn*-heteroatomic functionalities; however a multi-step sequence was necessary to convert **120** into methyl ester **123**. Saponification of methyl ester **123** afforded amino acid **124**, a component of the immunosuppressant cyclosporine.

To access *anti*- β -hydroxy- α -amino acids,⁹⁰ α -chloro acyl oxazolidinone **125** was utilized as a chiral glycine equivalent in a boron mediated aldol reaction with acetaldehyde, affording *syn*- β -hydroxy- α -chloro intermediate **126** as a 95:5 mixture of diastereomers and the major diastereomer was isolated in 67% yield (Scheme 3.4, **B**). The chloride was displaced with sodium azide (thereby installing the amino functionality and inverting the stereochemical configuration of the α -center). The auxiliary was cleaved through basic hydrolysis with LiOH and the azide was reduced to the amine with H₂ and Pd/C, producing *anti*- β -hydroxy- α -amino acid **127** in 57% over the three steps.

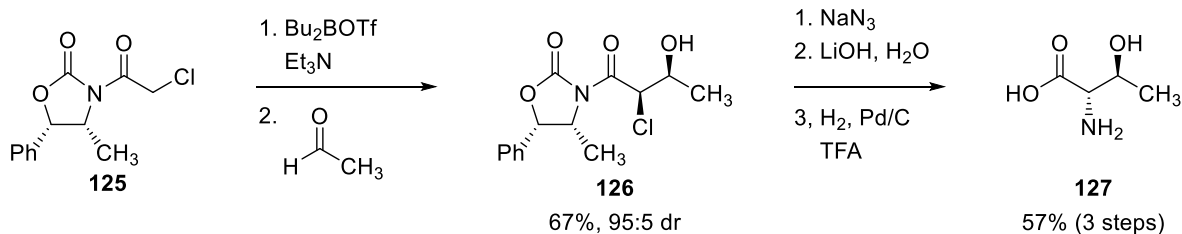
⁸⁹ (a) Evans, D. A.; Weber, A. E. *J. Am. Chem. Soc.* **1986**, *108*, 6757–6761. (b) Evans, D. A.; Weber, A. E. *J. Am. Chem. Soc.* **1987**, *109*, 7151–7157.

⁹⁰ This reaction is not in a strict sense a glycine aldol, but the desired β -hydroxy- α -amino acid motif was accessed. See: Evans, D. A.; Sjogren, E. B.; Weber, A. E. Conn, R. E. *Tetrahedron Lett.* **1987**, *28*, 39–42. Also, Corey and coworkers utilized a similar strategy for the synthesis of both *syn*- and *anti*- β -hydroxy- α -amino acids via an aldol reaction between an achiral α -bromo *tert*-butyl ester, an aldehyde, and a chiral boron catalyst (i.e. not by definition a glycine aldol). See Ref. 82j.

A. Evans *syn*-glycine aldol reaction



B. Evans *anti*- β -hydroxy- α -amino acid strategy



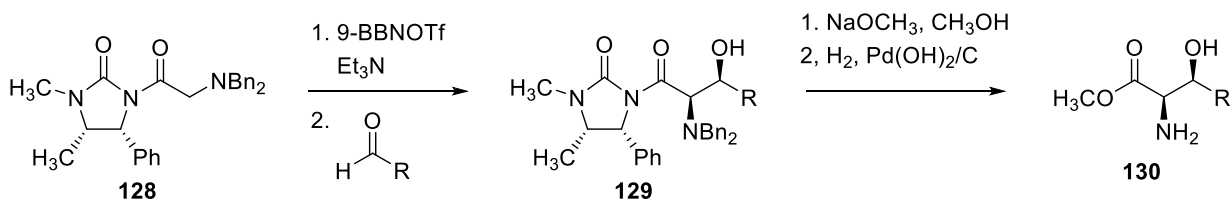
Scheme 3.4: Evans *syn*- and *anti*-glycine aldol strategies with oxazolidinones.

In addition to the oxazolidinone-based auxiliaries, related heterocycles have also been used to impart diastereoselectivity in Lewis acid-mediated aldol reactions (Scheme 3.5). Caddick and coworkers utilized an α -dibenzylamino acyl imidazolidinone **128** in a boron mediated aldolization with aldehydes (aliphatic, aromatic and heteroaromatic) to prepare *syn*- β -hydroxy- α -amino derivatives **129** (Scheme 3.5, A).⁹¹ The aldol adducts were isolated in 62 – 84% yield and $\geq 88\%$ de, and were converted into *syn*- β -hydroxy- α -amino esters upon methanolysis of the auxiliary and reductive cleavage of the benzyl protecting groups. Franck and others demonstrated that tin-mediated aldolization with α -azido acyl thiazolidinone **131** and a variety

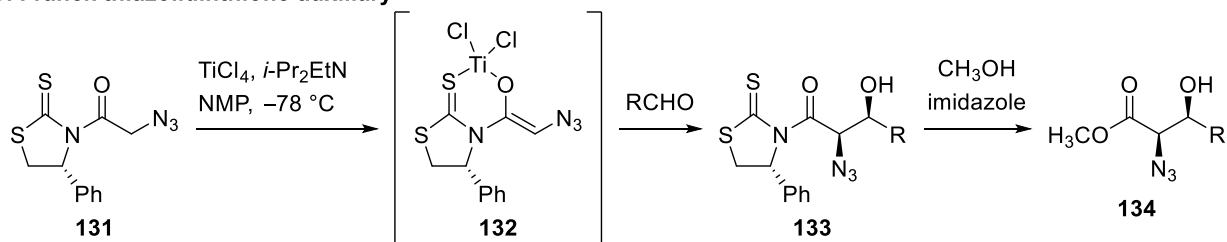
⁹¹ Caddick, S.; Parr, N. J.; Pritchard, M. C. *Tetrahedron Lett.* **2000**, *41*, 5963–5966.

of aldehydes provided *syn*-aldol adducts **133** in $\geq 60\%$ yield and $\geq 98:2$ dr (Scheme 3.5, **B**).⁹² Aldol adducts **133** were converted into the corresponding methyl esters **134** by treatment with imidazole in methanol. In some cases, auxiliary cleavage was accompanied by epimerization of the α -stereocenter.

A. Caddick imidazolidinone auxiliary



B. Franck thiazolidinthione auxiliary



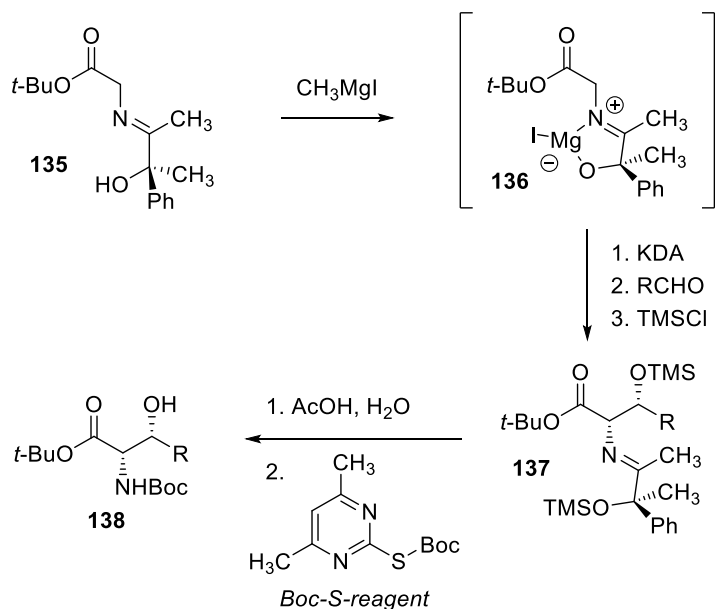
Scheme 3.5: Additional oxazolidinone-related scaffold strategies.

Chiral auxiliaries have also been attached to imines to impart selectivity in asymmetric glycine aldol reactions. An example of this method was reported by Mukaiyama and others in 1981 (Scheme 3.6).⁹³ Treatment of chiral imine **135** with CH_3MgI afforded a metal alkoxide **136**. Deprotonation of **136** with KDA, addition of an aldehyde (predominantly aryl), and global silylation with TMSCl afforded *syn*-aldol adducts **137**. Adducts **137** were converted into the *N*-Boc β -hydroxy- α -amino esters **138** upon reaction with aqueous acetic acid, followed by treatment with *S*-Boc-2-mercapto-4,6-dimethylpyrimidine (also known as Boc-S-reagent). The nature of the base for aldolization (KDA) was shown to be significant, as well as the presence of

⁹² Patel, J.; Clavé, G.; Renard, P.-Y.; Franck, X. *Angew. Chem. Int. Ed.* **2008**, *47*, 4224–4227.

⁹³ Nakatsuka, T.; Miwa, T.; Mukaiyama, T. *Chem. Lett.* **1981**, 279–282.

the free hydroxyl (to coordinate to magnesium). Aldol adducts were isolated in 46 – 67% yield, generally $\geq 75:25$ *syn:anti* selectivity, and approximately 70% optical purity. Aromatic aldehydes were shown to be superior substrates than aliphatic aldehydes.



Scheme 3.6: Imine as a chiral glycine equivalent.

Catalytic Asymmetric Approaches

A second strategy to impart selectivity into glycine aldol reactions employs *achiral* substrates with *chiral catalysts* as stereoinducing factors. To demonstrate examples of this method, several research groups have reacted aldehydes with optically inactive α -isothiocyanato acyl oxazolidinone **139** or **142** in the presence of asymmetric catalysts to afford diastereo- and enantioenriched products (Scheme 3.7). As with the Evans' approach, these reactions delivered thiocarbamates as products which required additional transformations to reveal the free amine and hydroxyl groups. Willis and coworkers utilized pyridine bis(oxazoline) catalyst **140** (Pybox), α -isothiocyanato acyl oxazolidinone **139**, and aryl aldehydes to synthesize *syn*-thiocarbamate esters **141** in $\geq 70\%$ yield, $\geq 80:20$ *syn:anti* selectivity and $\geq 86\%$ ee of the major diastereomer

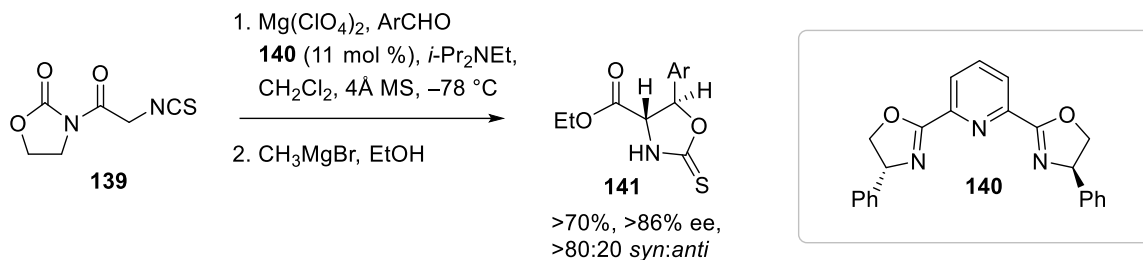
(Scheme 3.7, **A**).⁹⁴ Seidel and others showed that aldol reaction of achiral oxazolidinone **142**, thiourea catalyst **143**, and primarily aryl and heteroaryl aldehydes afforded *syn*-thiocarbamates **144** in $\geq 80\%$ yield, $\geq 80:20$ *syn:anti* selectivity, and $\geq 90\%$ ee of the major diastereomer (Scheme 3.7, **B**).⁹⁵ Aliphatic aldehydes were found to be less reactive with this system and afforded products in lower yields and lower selectivities. Lastly, Feng and coworkers employed achiral α -isothiocyanato acyl oxazolidinone **139**, Ni(acac)₂, ligand **145** and a wide range of predominantly aromatic and heteroaromatic aldehydes to access *syn*-thiocarbamate esters **146** in $\geq 80\%$ yield, $\geq 90:10$ *syn:anti* selectivity, and $\geq 90\%$ ee of the major diastereomer (Scheme 3.6, **C**).⁹⁶

⁹⁴ Willis, M. C.; Cutting, G. A.; Piccio, V. J.-D.; Durbin, M. J.; John, M. P. *Angew. Chem. Int. Ed.* **2005**, *44*, 1543–1545.

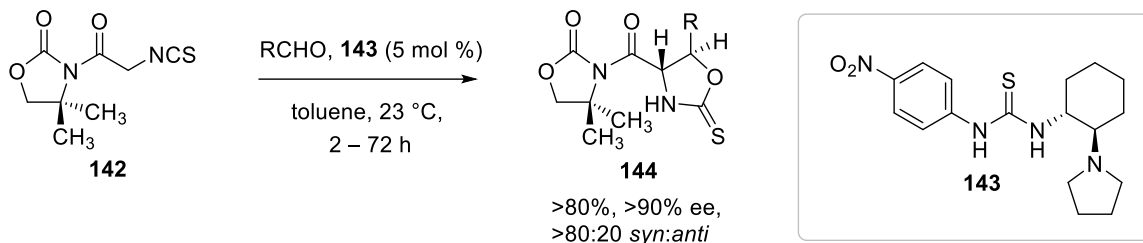
⁹⁵ (a) Li, L.; Klauber, E. G.; Seidel, D. *J. Am. Chem. Soc.* **2008**, *130*, 12248–12249. (b) Vecchione, M. K.; Li, L.; Seidel, D. *Chem. Commun.* **2010**, *46*, 4604–4606.

⁹⁶ Chen, X.; Zhu, Y.; Qiao, Z.; Xie, M.; Lin, L.; Liu, X.; Feng, X. *Chem. Eur. J.* **2010**, *16*, 10124–10129.

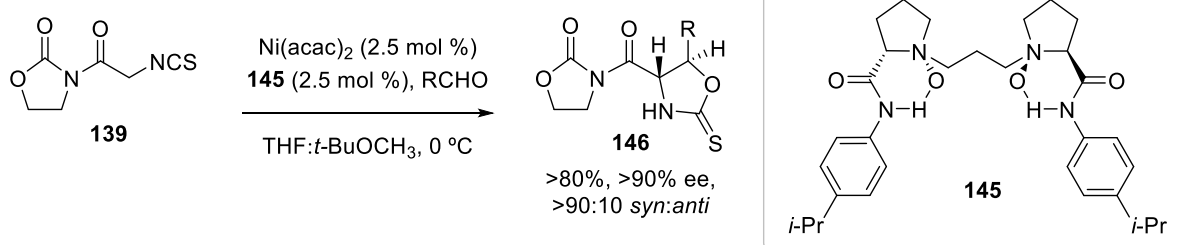
A. Willis Pybox Glycine Aldol



B. Seidel Thiourea Glycine Aldol



C. Feng Nickel-Catalyzed Glycine Aldol

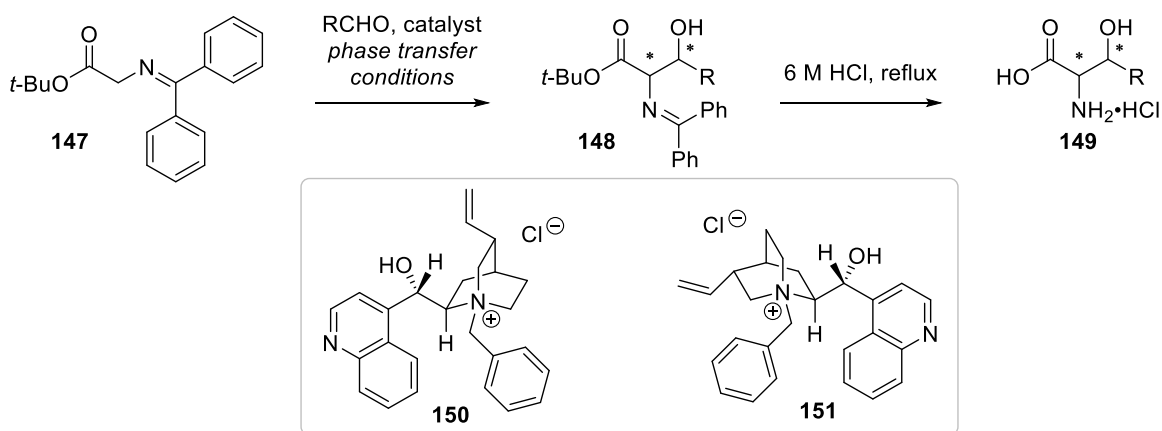


Scheme 3.7: Catalytic asymmetric glycine aldol reactions with isothiocyanate oxazolidinones **139** and **142**.

Achiral imines, commonly the Schiff bases of *tert*-butyl glycine esters, were also utilized in conjunction with chiral catalysts to afford diastereoenriched β -hydroxy- α -amino acids. The first description of such a transformation came from the Miller group in 1991,⁹⁷ and later the Shibasaki and Castle laboratories employed a similar strategy (Scheme 3.8). Treatment of imine **147** with a variety of aldehydes in the presence of cinchona alkaloid catalysts **150** or **151** under phase transfer conditions afforded β -hydroxy- α -amino esters **148** in 46 – 92% yield, with moderate 14 – 56% de. Medium- to long-chained alkyl and hydrophobic aryl aldehydes were the

⁹⁷ Gasparski, C. M.; Miller, M. J. *Tetrahedron* **1991**, *47*, 5367–5378.

best substrates for this reaction. The free β -hydroxy- α -amino acids were liberated by refluxing **148** in a 6M HCl solution. Shibasaki tuned his catalyst to favor the production of *anti*-aldol adducts⁹⁸ and Castle optimized his cinchona alkaloid catalyst to generate both *syn*- and *anti*-aldol adducts, albeit with modest diastereo- and enantioselectivities.⁹⁹



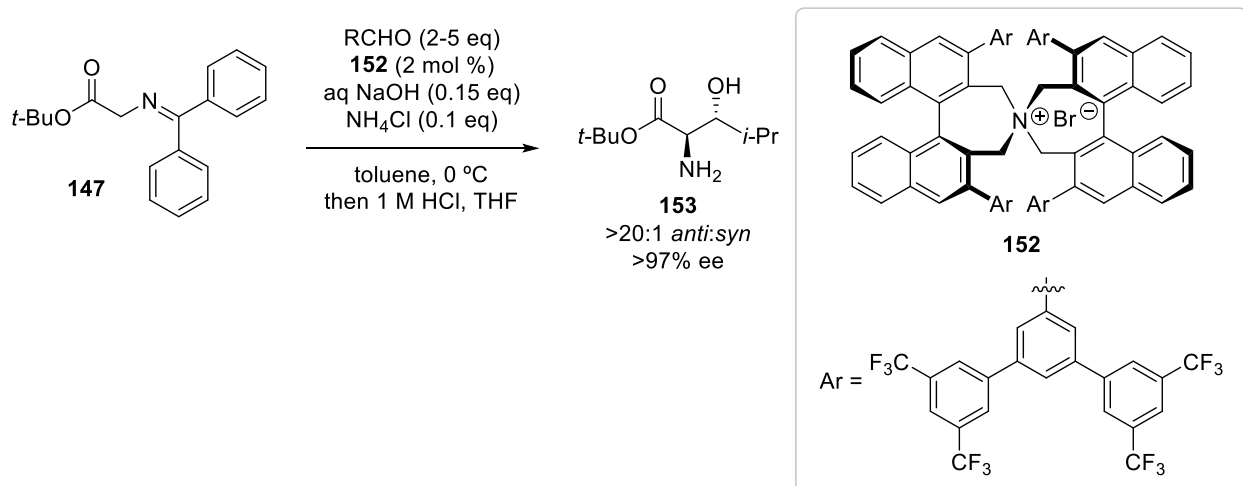
Scheme 3.8: Miller glycine aldol reaction with imine **147** and cinchona alkaloid derived catalysts **150** and **151**.

Utilizing chiral quaternary ammonium salts like **152** in aldol reactions of aliphatic aldehydes with the same imine **147**, Maruoka and coworkers effectively tuned the selectivity of their system to access *anti*- β -hydroxy- α -amino esters (Scheme 3.9).¹⁰⁰ The ester products such as **153** were isolated in $\geq 70\%$ yield, with $\geq 96:4$ *anti:syn* ratio and $\geq 97\%$ ee of the *anti* diastereomer. Aryl aldehydes were shown to be poor substrates for this system as little stereoselectivity was observed in the products of those transformations.

⁹⁸ Yoshikawa, N.; Shibasaki, M. *Tetrahedron* **2002**, *58*, 8289–8298.

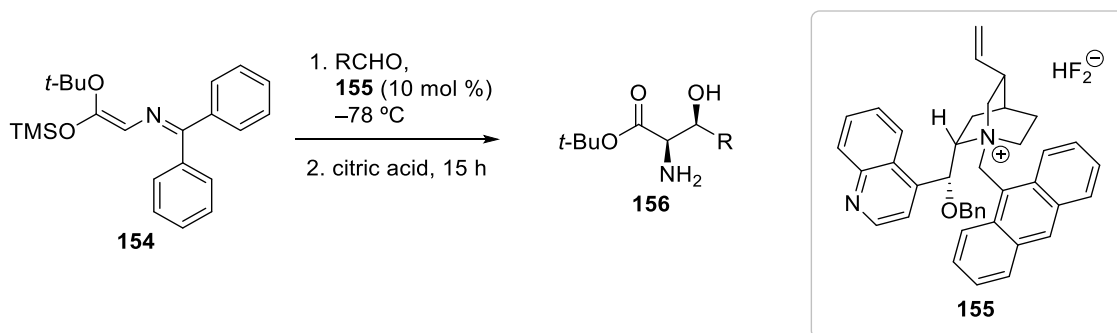
⁹⁹ (a) Mettath, S.; Srikanth, G. S. C.; Dangerfield, B. S.; Castle, S. L. *J. Org. Chem.* **2004**, *69*, 6489–6492. (b) Ma, B.; Parkinson, J. L.; Castle, S. L. *Tetrahedron Lett.* **2007**, *48*, 2083–2086.

¹⁰⁰ (a) Ooi, T.; Taniguchi, M.; Kameda, M.; Maruoka, K. *Angew. Chem. Int. Ed.* **2002**, *41*, 4542–4544. (b) Ooi, T.; Kameda, M.; Taniguchi, M.; Maruoka, K. *J. Am. Chem. Soc.* **2004**, *126*, 9685–9694. (c) Ooi, T.; Taniguchi, M.; Doda, K.; Maruoka, K. *Adv. Synth. Catal.* **2004**, *346*, 1073–1076.



Scheme 3.9: Maruoka *anti*-selective glycine aldol reaction with imine **147**.

In addition to the imine **147**, Corey and coworkers reported the use of trimethylsilyl ketene acetal **154** as an effective nucleophile in cinchona alkaloid catalyzed aldol reactions with aliphatic aldehydes (Scheme 3.10).¹⁰¹ *Syn*- β -hydroxy- α -amino esters **156** were isolated in ca. 70% yield, with *syn:anti* ratios ranging from 1:1 to 13:1 (α -branched aldehydes gave higher diastereoselectivities).



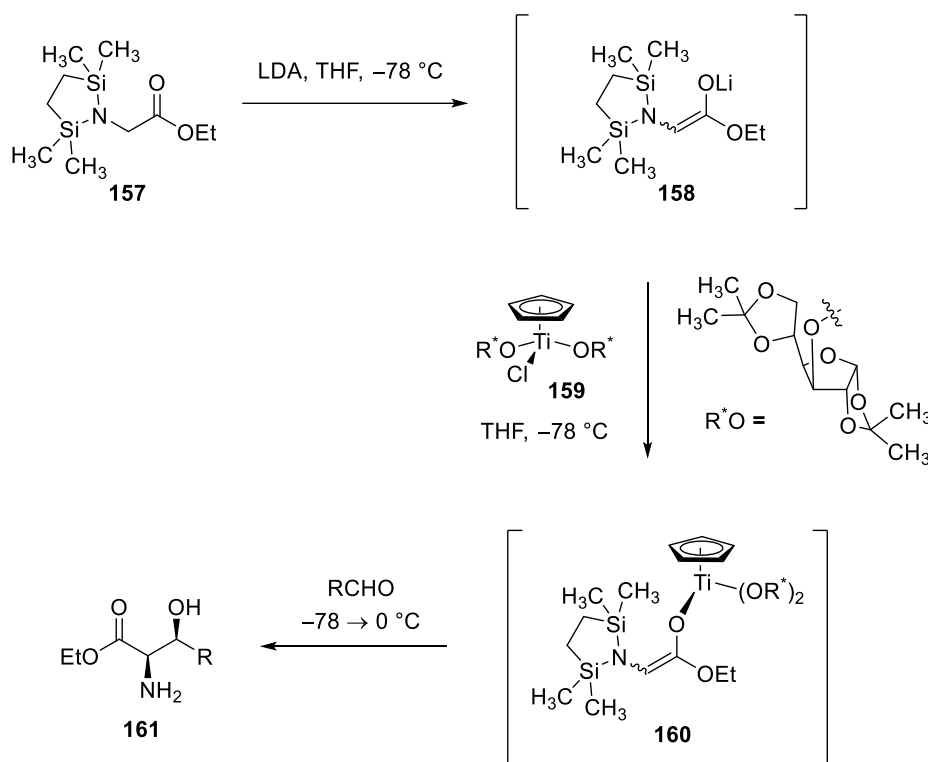
Scheme 3.10: Corey *syn*-glycine aldol with TMS-ketene acetal **154** catalyzed by cinchona alkaloid **155**.

Bold and coworkers utilized ethyl ester **157** as an achiral glycine equivalent (Scheme 3.11).¹⁰² Treatment of ethyl ester **157** with LDA, followed by addition of the titanium-

¹⁰¹ Horikawa, M.; Busch-Petersen, J.; Corey, E. J. *Tetrahedron Lett.* **1999**, *40*, 3843–3846.

¹⁰² Bold, G.; Duthaler, R. O.; Riediker, M. *Angew. Chem. Int. Ed. Engl.* **1989**, *28*, 497–498.

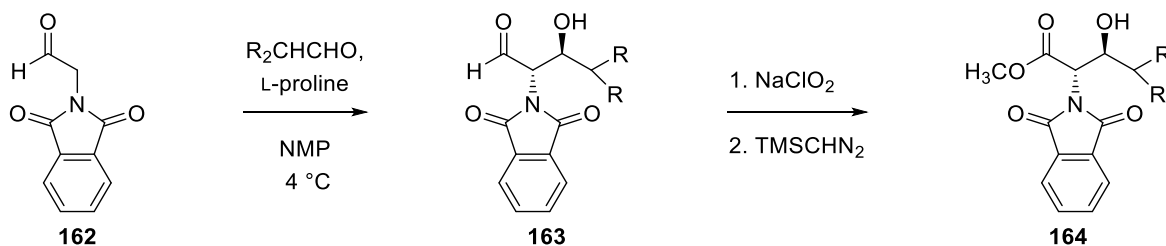
carbohydrate complex **159** and the aldehyde electrophile, afforded *syn*-aldol adducts **161** in 43 – 70% yield, usually $\geq 96\%$ de for the *syn*-diastereomer and generally $\geq 95\%$ ee.



Scheme 3.11: Bold *syn*-glycine aldol with ester **157** catalyzed by titanium-carbohydrate complex **159**.

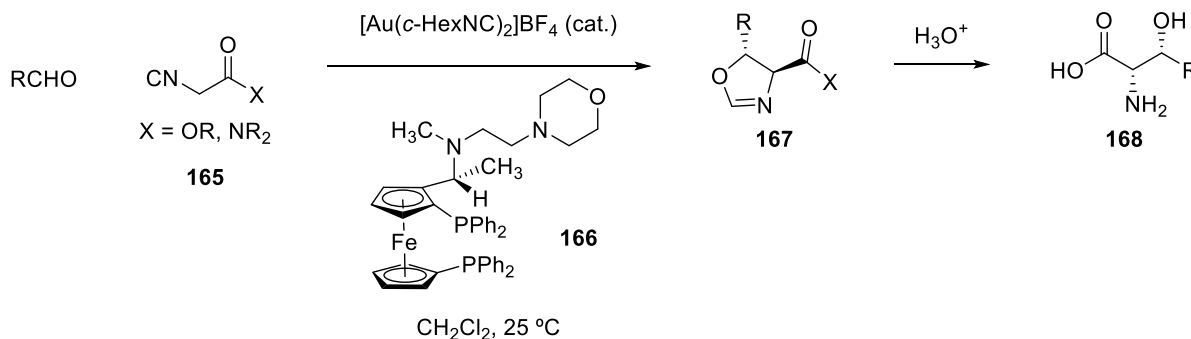
Barbas III and others reported the use of achiral amino aldehyde **162** as a glycine equivalent in an L-proline catalyzed aldol reaction with α -branched aldehydes (Scheme 3.12).¹⁰³ Aldol adducts were isolated as the corresponding methyl esters **164** in 62 – 75% yield, 1:1 – 16:1 *anti:syn* ratios and 86 – 98% ee. Despite good diastereo- and enantioselectivities, the narrow substrate scope of this transformation limits its application in the synthesis of *anti*- β -hydroxy- α -amino acids.

¹⁰³ Thayumanavan, R.; Tanaka, F.; Barbas III, C. F. *Org. Lett.* **2004**, *6*, 3541–3544.



Scheme 3.12: Barbas phthalimide method.

Oxazoline-4-carboxylates, other synthetically useful intermediates to access β -hydroxy- α -amino acids, can be converted into the desired scaffold upon treatment with strong acid. Ito, Hayashi and coworkers pioneered efforts to synthesize β -hydroxy- α -amino acids via oxazoline-4-carboxylates in the late 1980s. They found that treatment of α -isocyano esters and amides **165** with aldehydes in the presence of a gold(I) catalyst and ferrocenyphosphine ligand **166** afforded diastereoenriched oxazolines **167** (Scheme 3.13), which were hydrolyzed to produce *syn*- β -hydroxy- α -amino acids **168**.¹⁰⁴

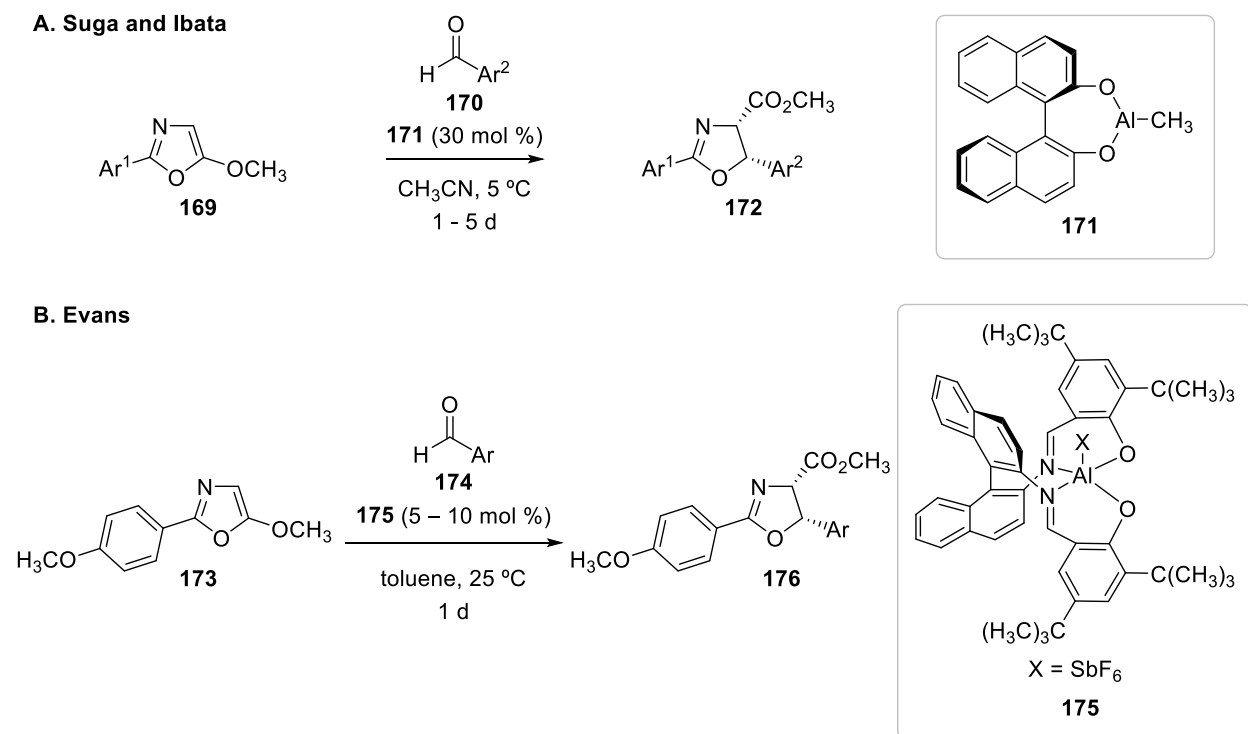


Scheme 3.13: Synthesis of β -hydroxy- α -amino acids via oxazoline-4-carboxylate **167**.

Oxazoline-4-carboxylates have also been constructed by the addition of 5-alkoxyoxazoles to aldehydes under catalysis by chiral aluminum catalysts **171** and **175**, as reported by Suga and

¹⁰⁴ (a) Ito, Y.; Sawamura, M.; Hayashi, T. *J. Am. Chem. Soc.* **1986**, *108*, 6405–6406. (b) Ito, Y.; Sawamura, M.; Shirakawa, E.; Hayashizaki, K.; Hayashi, T. *Tetrahedron Lett.* **1988**, *29*, 235–238. (c) Ito, Y.; Sawamura, M.; Shirakawa, E.; Hayashizaki, K.; Hayashi, T. *Tetrahedron* **1988**, *44*, 5253–5262. (d) Sawamura, M.; Nakayama, Y.; Kato, T.; Ito, Y. *J. Org. Chem.* **1995**, *60*, 1727–1732.

Ibata¹⁰⁵ and the Evans group,¹⁰⁶ respectively (Scheme 3.14). These systems were found to be highly efficient with aryl aldehydes.¹⁰⁷ Suga and Ibata isolated oxazoline-4-carboxylates **172** in 51 – 91% yield, generally $\geq 80:20$ *cis:trans* ratio, and 64 – 90% ee (Scheme 3.14, **A**), while the Evans group produced oxazoline-4-carboxylates **176** usually in $\geq 90\%$ yield, $\geq 90:10$ dr and $\geq 95\%$ ee (Scheme 3.14, **B**). Conversion of the oxazoline products into β -hydroxy- α -amino acids required a three step sequence and strongly acidic conditions.



Scheme 3.14: Oxazoline syntheses via aluminum catalysis

There are various synthetic avenues to access the β -hydroxy- α -amino acid scaffold, utilizing both chiral and achiral glycine equivalents. A wide range of aldehydes is tolerated as electrophiles, but in general, if a reagent system has been optimized for reaction with aliphatic

¹⁰⁵ Suga, H.; Ikai, K.; Ibata, T. *Tetrahedron Lett.* **1998**, *39*, 869–872.

¹⁰⁶ Evans, D. A.; Janey, J. M.; Magomedov, N.; Tedrow, J. S. *Angew. Chem. Int. Ed.* **2001**, *40*, 1884–1888.

¹⁰⁷ Heteroaromatic aldehydes, however, were not optimal substrates for this system, resulting in lower yields and lower diastereoselectivities.

aldehydes, it will lack selectivity with aromatic or heteroaromatic substrates. Alternatively, if both alkyl and aryl aldehydes are well-suited for a system, lower diastereoselectivities are seen for the aldol products. The use of certain chiral auxiliaries requires harsh conditions for their removal or requires further steps to reveal the hydroxyl and amino substituents. Lastly, none of the auxiliaries provide mainstream access to β,β' -disubstituted- β -hydroxy- α -amino acid derivatives, the products of a glycine aldolization with ketone electrophiles.¹⁰⁸

Synthesis of Pseudoephedrine Glycinamide

Expansion of the known chemistry of the pseudoephedrine¹⁰⁹ and pseudoephedrine¹¹⁰ auxiliaries to include glycine aldol reactions¹¹¹ was achieved through collaboration with Dr. Ian Seiple and Jaron Mercer, and with helpful insights from Ziyang Zhang.¹¹² Dr. Seiple found that pseudoephedrine glycinamide (**179**) could be synthesized in a two-step sequence or a one-pot

¹⁰⁸ In addition to the two instances mentioned previously where ketones were substrates for asymmetric glycine aldol reactions (Schöllkopf and Seebach), acetone and trifluoromethyl ketones have been used as electrophiles in asymmetric glycine aldol transformations via imine-metal complexes. For acetone, see (a) Belokon, Y. N.; Zel'tser, I. E.; Bakhmutov, V. I.; Saporovskaya, M. B.; Ryzhov, M. G.; Yanovskii, A. I.; Struchkov, Y. T.; Belikov, V. M. *J. Am. Chem. Soc.* **1983**, *105*, 2010–2017. For trifluoromethyl ketones, see (b) Soloshonok, V. A.; Avilov, D. V.; Kukhar, V. P. *Tetrahedron: Asymmetry* **1996**, *7*, 1547–1550. (c) Soloshonok, V. A.; Avilov, D. V.; Kukhar, V. P. *Tetrahedron* **1996**, *52*, 12433–12442.

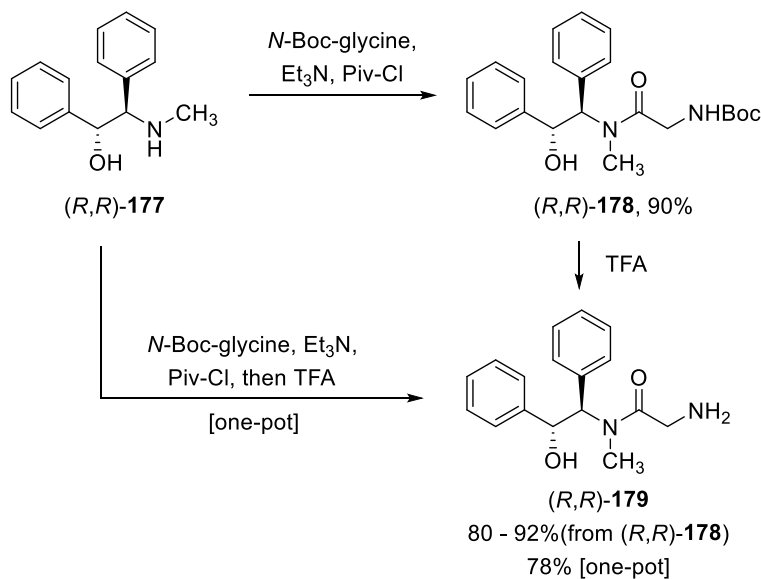
¹⁰⁹ (a) Myers, A. G.; Gleason, J. L.; Yoon, T. *J. Am. Chem. Soc.* **1995**, *117*, 8488–8489. (b) Myers, A. G.; Gleason, J. L.; Yoon, T.; Kung, D. W. *J. Am. Chem. Soc.* **1997**, *119*, 656–673. (c) Myers, A. G.; Schnider, P.; Kwon, S.; Kung, D. K. *J. Org. Chem.* **1999**, *64*, 3322–3327.

¹¹⁰ For practical, scalable syntheses of (*R,R*)- and (*S,S*)-pseudoephedrine, see: (a) Mellem, K. T.; Myers, A. G. *Org. Lett.* **2013**, *15*, 5594–5597. For the alkylation of pseudoephedrine amides, see: (b) Morales, M. R.; Mellem, K. T.; Myers, A. G. *Angew. Chem. Int. Ed.* **2012**, *51*, 4568–4571. For the synthesis and alkylation of pseudoephedrine alaninamide pivaldimine, see: (c) Hugelshofer, C. L.; Mellem, K. T.; Myers, A. G. *Org. Lett.* **2013**, *15*, 3134–3137.

¹¹¹ Aldolizations of pseudoephedrine amides (but not glycine aldol reactions) are well precedented. See: (a) Vicario, J. L.; Badía, D.; Domínguez, E.; Rodríguez, M.; Carrillo, L. *J. Org. Chem.* **2000**, *65*, 3754–3760. (b) Vicario, J. L.; Rodríguez, M.; Badía, D.; Carrillo, L.; Reyes, E. *Org. Lett.* **2004**, *6*, 3171–3174. (c) Rodríguez, M.; Vicario, J. L.; Badía, D.; Carrillo, L. *Org. Biomol. Chem.* **2005**, *3*, 2026–2030. (d) Ocejó, M.; Carrillo, L.; Vicario, J. S.; Badía, D.; Reyes, E. *J. Org. Chem.* **2011**, *76*, 460–470. (e) Kusuma, B. R.; Brandt, G. E. L.; Blagg, B. S. J. *Org. Lett.* **2012**, *14*, 6242–6245.

¹¹² Seiple, I. B.; Mercer, J. A. M.; Sussman, R. J.; Zhang, Z.; Myers, A. G. *Angew. Chem. Int. Ed.* **2014**, *53*, 4642–4647.

protocol from the appropriate enantiomers of pseudoephedrine (**177**) and *N*-Boc glycine, and then purified by either flash column chromatography or recrystallization from ethanol (Scheme 3.15). The free flowing, white crystalline solid was routinely produced on a 30-g scale and was found to be non-hygroscopic and easily handled in the laboratory environment.



Scheme 3.15: Synthesis of *(R,R)*-pseudoephedrine glycinamide (*(R,R)*-**179**).

Single crystal X-ray crystallography of *(R,R)*-pseudoephedrine glycinamide (*(R,R)*-**179**) allowed us to visualize its solid-state structure (Figure 3.2). Unlike pseudoephedrine glycinamide which could only be crystallized as a hydrate,¹⁰⁹ pseudoephedrine glycinamide contained no water or solvent molecules in its crystal lattice.

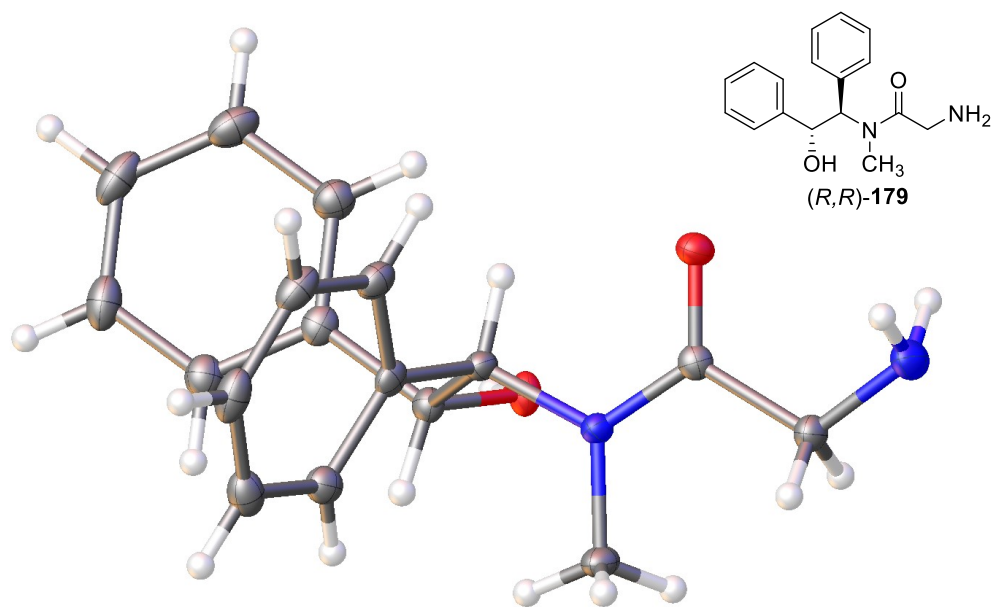


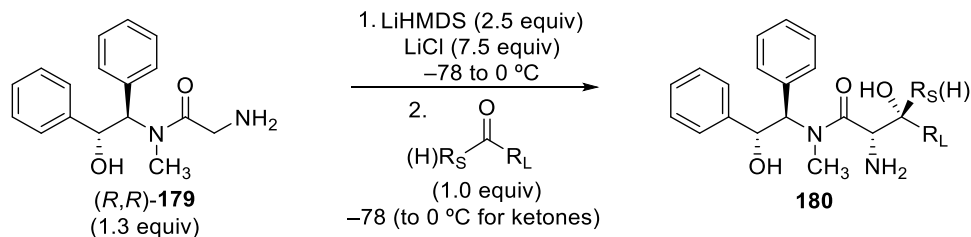
Figure 3.2: The crystal structure of (*R,R*)-pseudoephedrine glycinamide ((*R,R*)-179).

Aldolizations of Pseudoephedrine Glycinamide

In an advance with broad applications, Dr. Seiple discovered that asymmetric aldolization of pseudoephedrine glycinamide with aldehydes, and (surprisingly) ketones provided *syn*- β -hydroxy- α -amino amides with high diastereoselectivities,¹¹³ without the need of any protecting groups (Scheme 3.16). Jaron Mercer optimized the general reaction conditions: treatment of 1.3 equivalents of (*R,R*)-179 with 2.5 equivalents of LiHMDS in the presence of a saturating amount of LiCl¹¹⁴ in THF at -78 °C, followed by the addition of electrophile (and warming to 0 °C for ketone substrates) afforded *syn*- β -hydroxy- α -amino amides of the general scaffold **180**.

¹¹³ While pseudoephedrine glycinamide was shown to undergo stereoselective aldolizations with aldehydes, the yield and the selectivity of the reaction were inferior to the analogous reaction with pseudoephedrine glycinamide.

¹¹⁴ Lithium chloride was essential to solubilize the pseudoephedrine glycinamide enolate and to achieve high diastereoselectivities in aldolization reactions.



Scheme 3.16: Aldolization of *(R,R)*-**179** with aldehydes and ketones.

This reaction has the potential to produce up to four diastereomeric aldol adducts; however in every case, one isomer predominated. The minor diastereomers, typically comprising less than 15% of the isolated products, were not easily separated from each other and in many cases, were not studied in detail.¹¹⁵ In each case, the major diastereomer of **180** was purified by flash column chromatography and, in most cases, these were solids.

The stereochemical outcome of this highly selective transformation was rationalized by invoking a *Z* amide enolate (comparable to alkylation reactions of pseudoephedrine amide enolates) that proceeds through the closed Zimmerman–Traxler transition structure shown (Figure 3.3).

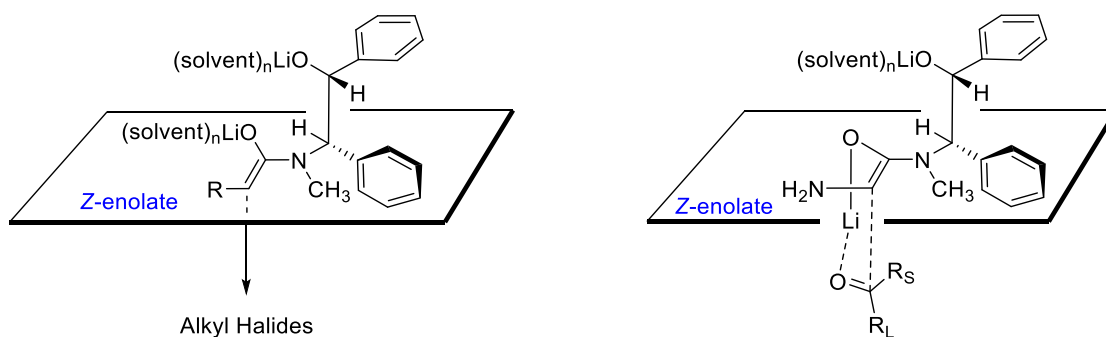


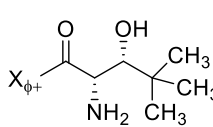
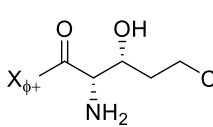
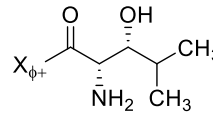
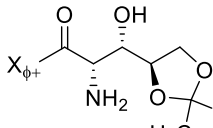
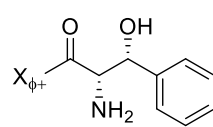
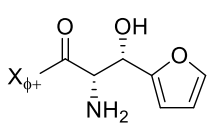
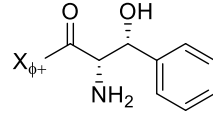
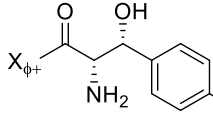
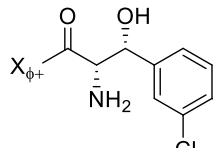
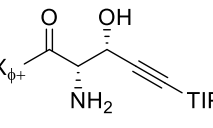
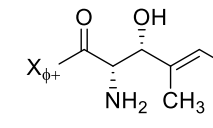
Figure 3.3: Rationale for the selectivity in aldolizations with *(R,R)*-**179**.

Jaron Mercer, Dr. Seiple and I screened a number of aldehydes with *(R,R)*-**179** (Table 3.1). Aliphatic aldehydes, including α -branched and α -tetrasubstituted, were good substrates.

¹¹⁵ We fully characterized the minor adduct from symmetric ketone substrates. See experimental section for details.

Aromatic and heteroaromatic, as well as alkenyl and alkynyl aldehydes were all demonstrated to be suitable electrophiles. In almost every case, the diastereomeric ratio¹¹⁶ was $\geq 80:20$ and pure product was isolated in 63 – 89% yield.

Table 3.1: Aldolization Adducts of Pseudoephedrine Glycinamide with Aldehydes.

Alkyl	
	181 , 89% 94:6 dr
	182 , 72% 83:17 dr
	183 , 77% 86:14 dr
	184 , 66% 89:11 dr
Aryl	
	185 , 80% 85:15 dr
	186 , 63% 79:21 dr
	187 , 78% 84:16 dr
	188 , 63% 81:19 dr
	189 , 75% 89:11 dr
Alkynyl/Alkenyl	
	190 , 75% 83:17 dr
	191 , 78% 79:21 dr

$X_{\phi+} = (R,R)\text{-177}$

*dr was determined by HPLC or ¹H NMR analysis.

¹¹⁶ The diastereomeric ratio is reported as major isomer:Σ(minor isomers) and was determined by HPLC or ¹H NMR analysis of crude reaction mixtures.

To establish the relative and absolute stereoselectivity of the reaction, we obtained crystals of aldol adduct **183** derived from (*R,R*)-**179** and isobutyraldehyde suitable for X-ray analysis. The solid-state structure of **183** confirmed the initial assignment of a *syn*-relationship between the amine and hydroxyl functionalities and revealed it to be stereochemically homologous to L-threonine (Figure 3.4). Also, aldol adducts **187** and **188** were successfully transformed into the antibiotics chloramphenicol and thiamphenicol, respectively,¹¹⁷ thereby forming a homologous series with **183**. The stereochemical configurations of the remaining aldehyde aldol adducts were assigned by analogy.

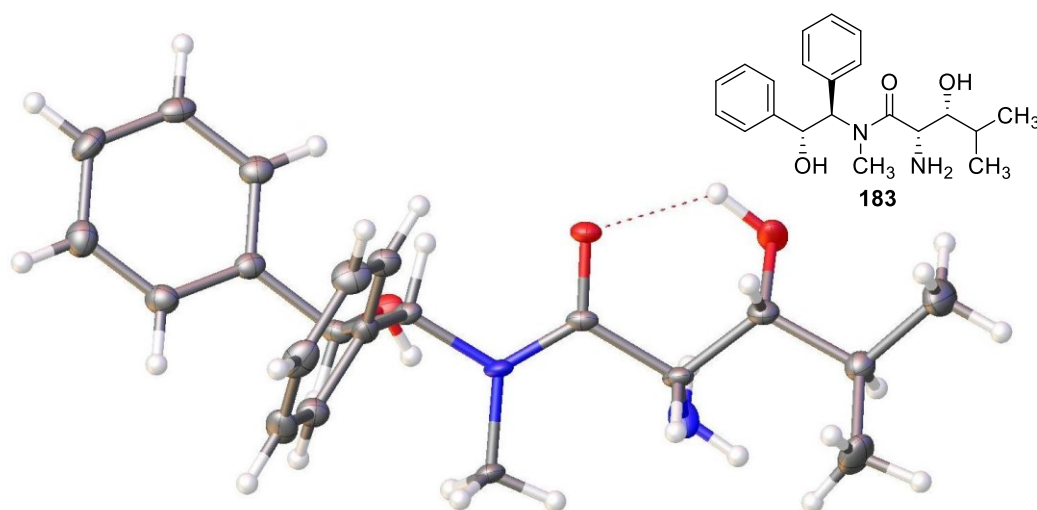
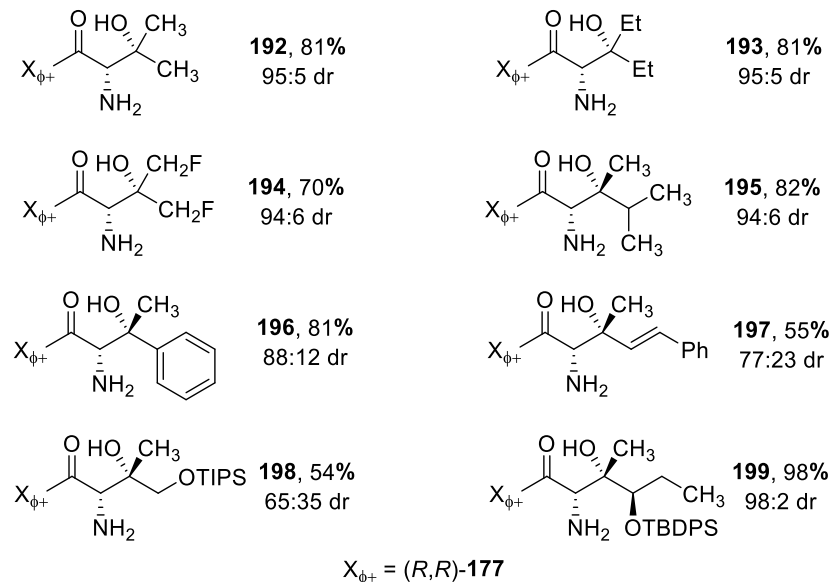


Figure 3.4: Crystal structure of aldol adduct **183**.

Jaron Mercer, Dr. Seiple and I also screened a number of symmetric and non-symmetric ketones with (*R,R*)-**179** (Table 3.2). Symmetric ketones afforded β -tetrasubstituted- α -amino amides, while non-symmetric ketones produced β,β' -disubstituted- β -hydroxy- α -amino amides, installing a tetrasubstituted stereocenter in a selective manner. The diastereomeric ratios were determined and reported as noted above and in most cases, the diastereomeric ratio was greater than those seen with aldehyde substrates.

¹¹⁷ See pages 129–130.

Table 3.2: Aldolization Adducts of Pseudoephedrine Glycinamide with Ketones.

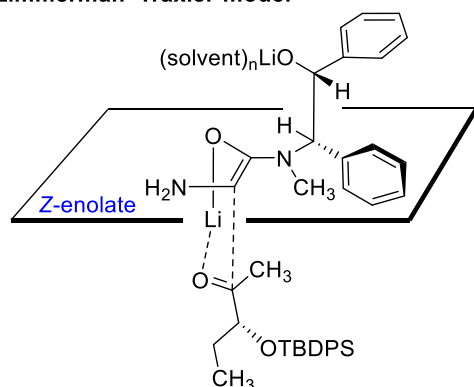


*dr was determined by HPLC or ^1H NMR analysis.

Pure products were isolated in 54 – 98% yield. The high yield and diastereoselectivity of adduct **199** presumably arose from the stereochemical matching of the diastereofacial preference of the enolate with the trajectory of Felkin-Anh addition into the chiral ketone substrate (Figure 3.5, **A** and **B**). In the absence of reinforcing stereochemical elements on the electrophile, the diastereoselectivity fell, as demonstrated by the lower dr of adduct **198**.¹¹⁸ The low yield of adduct **197** seemingly resulted from competitive 1,4-addition of the enolate to the enone electrophile.

¹¹⁸ A distribution of the four diastereomers was observed in a 65:20:9:6 ratio, as determined by ^1H NMR analysis.

A. Zimmerman-Traxler model



B. Felkin-Anh

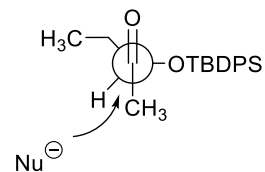


Figure 3.5: Rationale for high yield and diastereoselectivity seen in aldol adduct **199**.

Just as with **183**, we obtained crystals of aldol adduct **195** derived from (*R,R*)-**179** and methyl isopropyl ketone suitable for X-ray analysis (Figure 3.6). As expected, the solid-state structure of **195** was similar to that of aldol adduct **183**, with the methyl group serving as R_S . The stereochemical configurations of the remaining ketone aldol adducts were assigned by analogy.

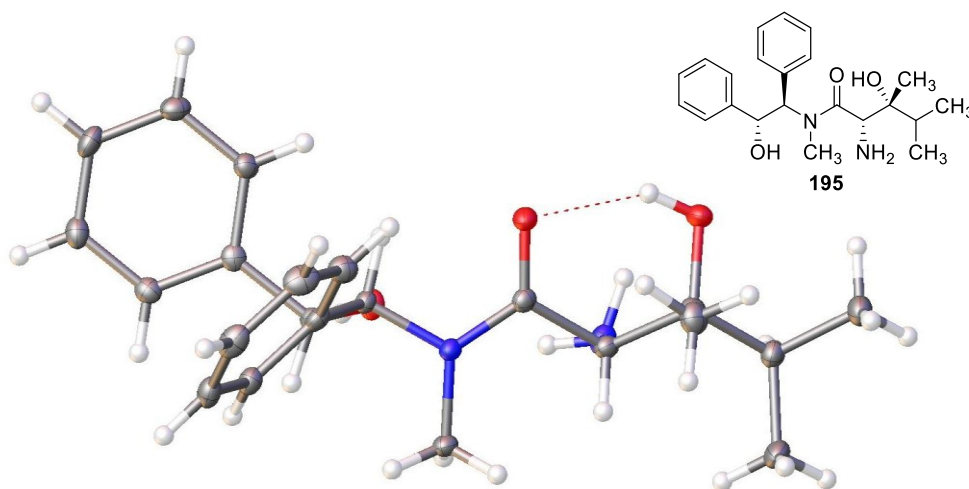


Figure 3.6: Crystal structure of aldol adduct **195**.

Most of the purified aldol adducts exist as two rotamers in solution; the presence of the two forms can be seen in the ^1H and ^{13}C NMR spectra. Rotameric relationships between peaks were

verified via saturation transfer experiments (1D gradient nOe experiments).¹¹⁹ Upon close examination of the ¹H NMR spectra for the purified aldol adducts from Tables 3.1 and 3.2, we could observe trace amounts of an impurity we identified as the N,O-acyl transfer product **200**,¹²⁰ in addition to the tertiary amide rotameric peaks (Figure 3.7). The presence of this product strongly suggested that these constitutional isomers were very close in energy to the tertiary amides. The intermediacy of the N,O-acyl transfer product was invoked to rationalize the ease with which the aldol adducts were directly transformed under unusually mild conditions and without protecting groups.

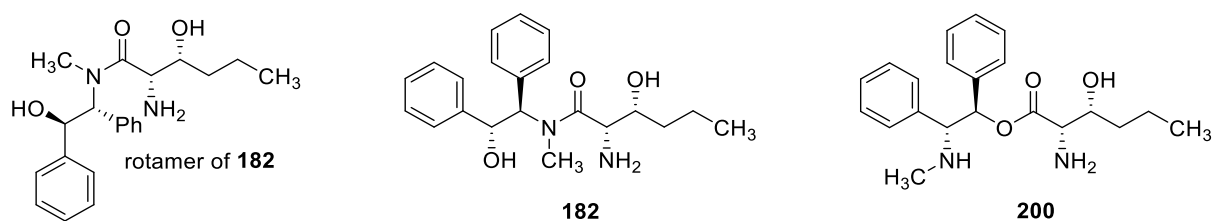


Figure 3.7: Rotamer and N,O-acyl transfer product **200** of aldol adduct **182**.

Transformations of the Aldol Products

Dr. Seiple and I developed exceptionally mild conditions to directly transform the aldol adducts **180** into enantiomerically enriched carboxylates and alcohols. Additionally, Dr. Seiple accessed enantioenriched ketones by a two-step sequence from the aldol adducts.¹²¹ All of these chiral building blocks enable streamlined access of various antibiotics.

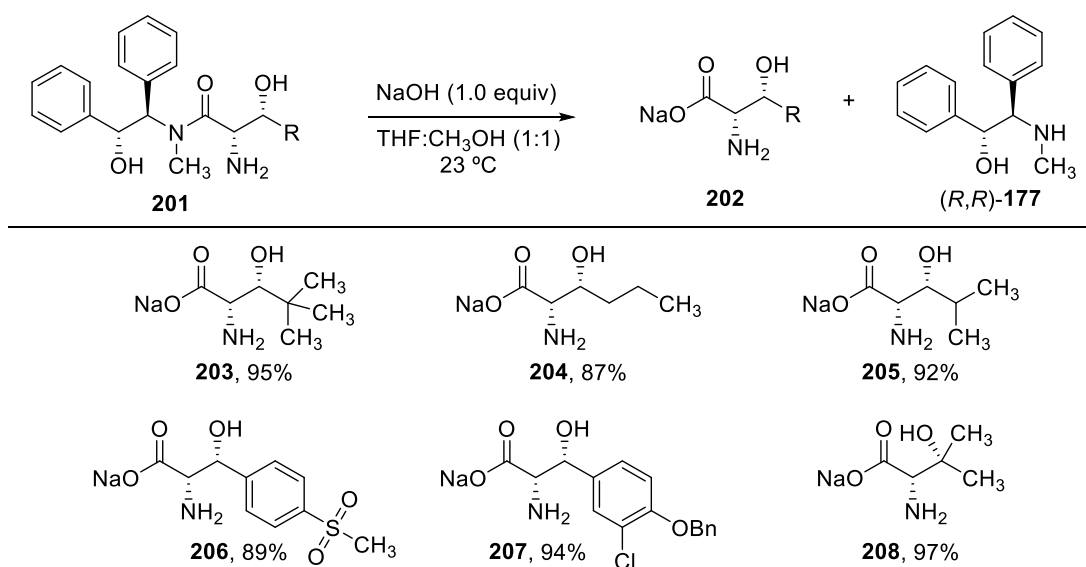
The tertiary amide aldol adducts were hydrolyzed upon treatment with 1 equivalent of NaOH in a 1:1 mixture of THF and methanol at 23 °C for several hours and the (*R,R*)-**177** auxiliary was

¹¹⁹ D. X. Hu, P. Grice, S. V. Ley, *J. Org. Chem.*, **2012**, *77*, 5198–5202. See experimental section for an example.

¹²⁰ Usually less than 5% of this impurity was present. See Ref. 109b and Myers, A. G.; Yang, B. H.; Chen, H.; McKinstry, L.; Kopecky, D. J.; Gleason, J. L. *J. Am. Chem. Soc.* **1997**, *119*, 6496–6511.

¹²¹ Formation of a cyclic carbamate from the β -hydroxy- α -amino amide aldol adduct, followed by Grignard addition to the amide afforded enantioenriched ketones.

recovered (Scheme 3.17).¹²² These conditions are exceedingly mild and are more consistent with saponification of an ester than hydrolysis of a tertiary amide. In contrast, hydrolysis of tertiary pseudoephedrine glycinamides required strongly acidic (9 N H₂SO₄) or basic (NaOH) conditions with heating.¹⁰⁹ I empirically determined that presence of methanol in the solvent system was crucial to avoid retroaldol fragmentation during the hydrolysis, an otherwise facile process. The resulting carboxylate salts were isolated in $\geq 87\%$ yield and $\geq 98\%$ ee.¹²³ Of note, carboxylate **207**, isolated in 94% yield and $\geq 98\%$ ee, was earlier reported as a key starting material in a synthesis of vancomycin developed by the Nicolaou group.¹²⁴



Scheme 3.17: Hydrolysis of aldol adducts under mildly basic conditions.

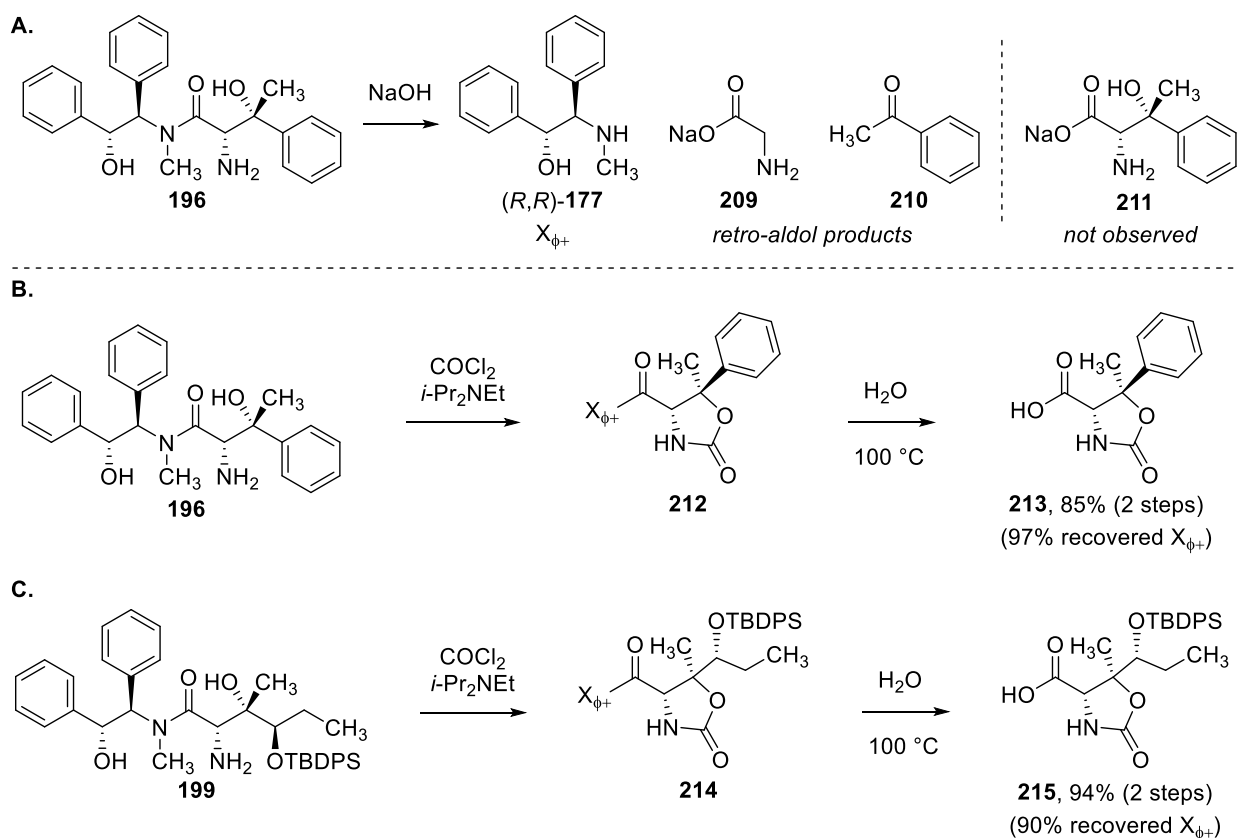
As previously mentioned, retroaldol fragmentation of the aldol adducts was a competitive process during hydrolysis. In the optimized method, we could minimize this decomposition

¹²² The (R,R)-177 pseudoephedrine auxiliary was recovered in $\geq 90\%$ yield in each case and in high purity.

¹²³ Enantiomeric excess was determined upon transformation of the carboxylates into Mosher amides and subsequent ¹H NMR analysis.

¹²⁴ Nicolaou, K. C.; Boddy, C. N. C.; Li, H.; Koumbis, A. E.; Hughes, R.; Natarajan, S.; Jain, N. F.; Ramanjulu, J. M.; Brase, S.; Solomon, M. E. *Chem. Eur. J.* **1999**, *5*, 2602–2621.

pathway, but certain aldol adducts still underwent noticeable retro-aldol fragmentation. For example, subjecting compound **196** to the optimized hydrolysis procedure afforded acetophenone (**210**), recovered (*R,R*)-**177**, and sodium glycinate (**209**) (Scheme 3.18, A). Searching to suppress this decomposition pathway, Dr. Seiple found that protection of the β -hydroxy group was necessary. He chose a cyclic carbamate as the protecting group because it can be easily introduced and cleaved under mild conditions.¹²⁵



Scheme 3.18: Carbamate strategy to overcome retroaldol fragmentation.

Treatment of aldol adducts **196** and **199** with phosgene in the presence of Hunig's base cleanly afforded carbamates **212** and **214**, respectively, after a biphasic extraction

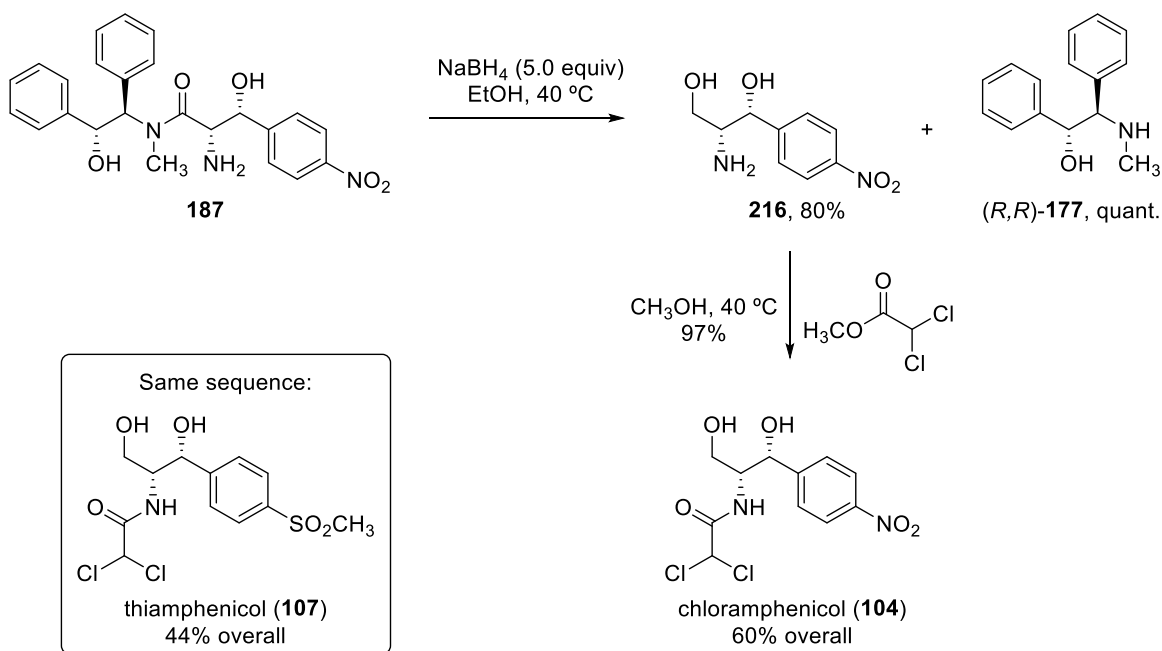
¹²⁵ (a) Jung, M. E.; Jung, Y. H. *Tetrahedron Lett.* **1989**, *30*, 6637–6640. (b) Di, G. M. C.; Misiti, D.; Zappia, G.; Delle, M. G. *Tetrahedron* **1993**, *49*, 11321–11328. (c) Williams, L.; Zhang, Z.; Ding, X.; Joullie, M. M. *Tetrahedron Lett.* **1995**, *36*, 7031–7034. (d) Delle, M. G.; Di, G. M. C.; Misiti, D.; Zappia, G. *Tetrahedron: Asymmetry* **1997**, *8*, 231–243. (e) Lab, T.; Chastanet, J.; Zhu, J. *Tetrahedron Lett.* **1997**, *38*, 1771–1772. (f) Tomasini, C.; Vecchione, A. *Org. Lett.* **1999**, *1*, 2153–2156.

(Scheme 3.18, **B** and **C**). The cleavage of the chiral auxiliary was achieved by heating the substrates in a mixture of 1,4-dioxane and water. Acid-base extraction yielded acids **213** and **215**, respectively, and the (*R,R*)-**177** auxiliary was recovered in $\geq 90\%$ yield. Carbamate **214** later became a pivotal building block in the synthesis of more than 240 novel macrolide antibiotics in the Myers lab.¹²⁶

Dr. Seiple and I also investigated alternative methods for auxiliary removal, specifically a reductive cleavage. We developed a methodology to directly reduce the tertiary amide to an alcohol, thereby providing enantioenriched 2-amino-1,3-diols (Scheme 3.19). Subjection of aldol adduct **187** to 5 equivalents of NaBH₄¹²⁷ in ethanol at 40 °C reductively cleaved the amide, producing the diol **216** in 80% yield and recovering the auxiliary in quantitative yield. Traditionally, reductions of pseudoephedrine amides are performed with a more reactive hydride donor lithium amidotrihydroborate (LAB). Attempts to reduce **187** with LAB gave the desired diol **216** in low yield, presumably due to product coordination to boron.

¹²⁶ Seiple, I. B.; Zhang, Z.; Wright, P. M.; Hog, D.; Jakubec, P.; Langlois, A.; Yabu, K.; Condakes, M.; Szczypiński, F.; Allu, S.; Kitamura, Y.; Wang, Y.; Myers, A. G., unpublished results.

¹²⁷ We are aware of only one other report on the use of sodium borohydride to reduce tertiary amides. See: Borkar, S. R.; Manjunath, B. N.; Balasubramaniam, S.; Aidhen, I. S. *Carbohydr. Res.* **2012**, 358, 23–30.



Scheme 3.19: Synthesis of chloramphenicol (**104**) and thiamphenicol (**107**).

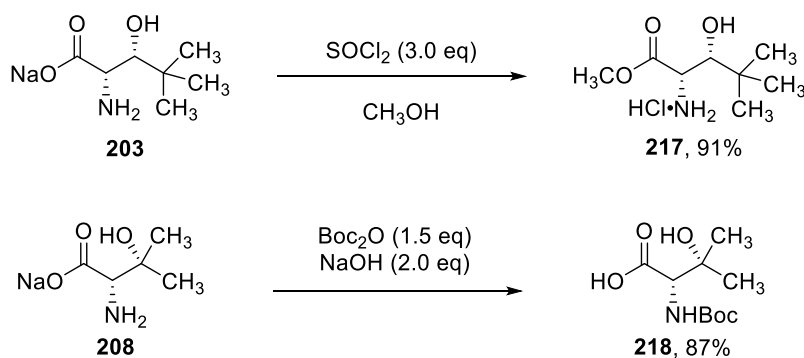
With the enantioenriched 2-amino-1,3-diols easily accessible, I investigated application of our methodology to the synthesis of chloramphenicol and thiamphenicol, two broad-spectrum antibiotics primarily used in developing countries and listed on the World Health Organization's List of Essential Medicines.¹²⁸ The synthesis of chloramphenicol was completed by acylation of the 2-amino-1,3-diol **216** with methyl dichloroacetate (Scheme 3.19), thereby providing the antibiotic in 3 steps and in 60% overall yield. Thiamphenicol was synthesized in an identical manner from *para*-methanesulfonylbenzaldehyde and (R,R)-**179** in three steps and 44% overall yield. Commercial routes to these antibiotics typically employ six linear steps, including a resolution.¹²⁹

¹²⁸ World Health Organization Model List of Essential Medicines, 18th edition: <http://www.who.int/medicines/publications/essentialmedicines/en/> (Accessed April, 2015).

¹²⁹ (a) Coppi, L.; Giordano, C.; Longoni, A.; Panossian, S. In: *Chirality in Industry II: Developments in the Commercial Manufacture and Applications of Optically Active Compounds*. Collins, A. N., Sheldrake, G., Crosby, J., Eds., John Wiley & Sons Ltd: West Sussex, England, **1998**, 353–362. (b) Bhat, S. V.; Nagasampagi, B. A.; Sivakumar, M. *Chemistry of Natural Products*, Springer: Berlin, **2005**; (c) Yunis, A. A. *Am. J. Med.* **1989**, *87*, 44N–48N.

Transformations of the Carboxylate Products

Lastly, Jaron Mercer and I transformed the β -hydroxy- α -amino carboxylates into protected amino acid precursors (esters and *N*-Boc acids, Scheme 3.20). Treatment of carboxylate **203** with acidic methanol afforded the hydrochloride salt of methyl ester **217** in 91% yield. Also, *N*-Boc amino acid **218** was synthesized from the carboxylate **208** upon addition of Boc_2O in the presence of NaOH . Amino acid **218** serves as a chiral building block in the synthesis of monocyclic β -lactam antibiotic BAL30072,¹³⁰ a fully synthetic antibiotic currently in Phase I clinical trials for the treatment of Gram-negative bacterial infections.



Scheme 3.20: Esterification and *N*-Boc protection of the carboxylates **203** and **208**.

In summary, we have developed methodology for asymmetric aldolization of pseudoephedrine glycinamide with aldehydes and ketones to produce *syn*- β -hydroxy- α -amino amides with high diastereoselectivities and without the use of protecting groups. These aldol adducts can be transformed into enantiomerically enriched alcohols, ketones, and carboxylates, many of which enable powerfully simplified syntheses of various antibiotics.

An extended application of this methodology in the synthesis of C4-disubstituted monobactam antibiotics will be discussed in greater detail in Chapter 4.

¹³⁰ See Ref. 146 in Chapter 4.

General Experimental Procedures

All reactions were performed in flame-dried glassware fitted with rubber septa under a positive pressure of argon, unless otherwise noted. Air- and moisture-sensitive liquids were transferred via syringe or stainless steel cannula. Solutions were concentrated by rotary evaporation below 35 °C. Analytical thin-layer chromatography (TLC) was performed using glass plates pre-coated with silica gel (0.25-mm, 60-Å pore size, 230–400 mesh, Merck KGA) impregnated with a fluorescent indicator (254 nm). TLC plates were visualized by exposure to ultraviolet light (UV), then were stained by submersion in a 10% solution of phosphomolybdic acid (PMA) in ethanol, followed by brief heating on a hot plate. Flash column chromatography was performed as described by Still et al.,⁶⁰ employing silica gel (60 Å, standard grade) purchased from Dynamic Adsorbents.

Materials

Commercial solvents and reagents were used as received with the following exceptions. Hexamethyldisilazane (HMDS) was distilled from calcium hydride under an atmosphere of dinitrogen at 760 mmHg. Dichloromethane, ethyl ether, dioxane, and tetrahydrofuran were purified by passage through Al₂O₃ under argon by the method of Grubbs et al.⁶¹ Aldehydes and ketones for use as electrophiles in aldol reactions were fractionally distilled immediately prior to use. The molarity of solutions of *n*-butyllithium was determined by titration against diphenylacetic acid as an indicator (average of three determinations).⁶²

Instrumentation

Proton nuclear magnetic resonance (^1H NMR) spectra and carbon nuclear magnetic resonance (^{13}C NMR) spectra were recorded on Varian MERCURY 400 (400 MHz/100 MHz), Varian INOVA 500 (500 MHz/125 MHz), or Varian INOVA 600 (600 MHz/150 MHz) NMR spectrometers at 23 °C. Proton chemical shifts are expressed in parts per million (ppm, δ scale) and are referenced to residual protium in the NMR solvent (CHCl_3 : δ 7.26, D_2HCO : δ 3.31). Carbon chemical shifts are expressed in parts per million (ppm, δ scale) and are referenced to the carbon resonance of the NMR solvent (CDCl_3 : δ 77.0, CD_3OD : δ 49.0). Data are represented as follows: chemical shift, multiplicity (s = singlet, d = doublet, t = triplet, q = quartet, dd = doublet of doublets, dt = doublet of triplets, sxt = sextet, m = multiplet, br = broad, app = apparent), integration, and coupling constant (J) in Hertz (Hz). Infrared (IR) spectra were obtained using a Shimadzu 8400S FT-IR spectrophotometer referenced to a polystyrene standard. Data are represented as follows: frequency of absorption (cm^{-1}), and intensity of absorption (s = strong, m = medium, br = broad). HPLC retention times were acquired using a Beckman System Gold instrument equipped with a Chiracel OD-H column (5 mm particle size, 4.6 mm x 250 mm). Melting points were determined using a Thomas Scientific capillary melting point apparatus. High-resolution mass spectra were obtained at the Harvard University Mass Spectrometry Facility using a Bruker micrOTOF-QII mass spectrometer. LC-MS analysis was performed on an Agilent 1260 Infinity instrument equipped with a 6120 quadrupole LC-MS. X-ray crystallographic analysis was performed at the Harvard University X-Ray Crystallographic Laboratory by Dr. Shao-Liang Zheng.

(For clarity, intermediates that have not been assigned numbers in the text are numbered sequentially in the Experimental Information beginning with 219.)

General Comments on NMR Spectra of Pseudoephedrine Amides

^1H NMR and ^{13}C NMR spectra of pseudoephedrine amides can be complicated by the presence of tertiary amide rotameric peaks in addition to N,O-acyl transfer product signals. Rotameric relationships between peaks were established via saturation transfer experiments (1D gradient nOe experiments) as described by Ley.¹¹⁹ The presence of N,O-acyl transfer products in NMR spectra was substrate- and pH-dependent. In some instances, HSQC analysis aided in determination of rotameric and N,O-acyl transfer product carbon assignments. Two annotated spectra are produced below (Figure 3.8).

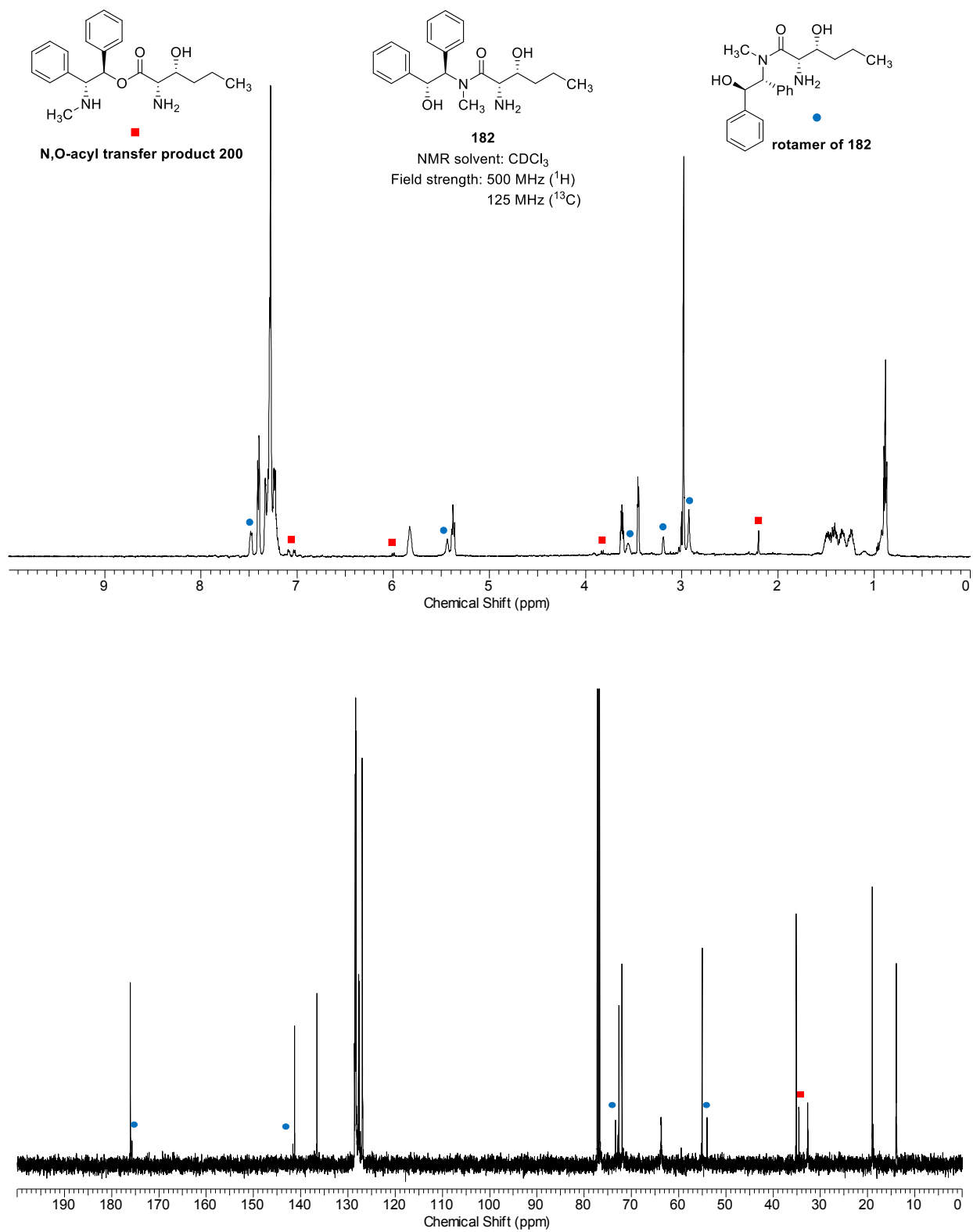
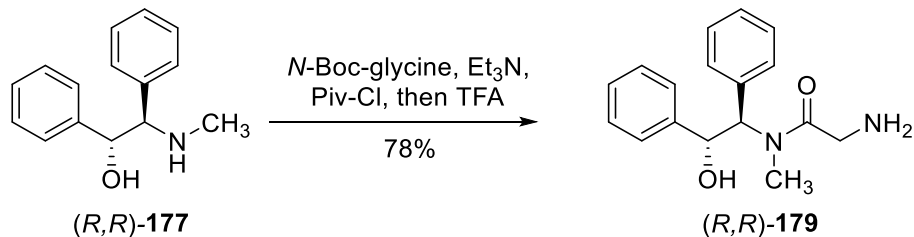


Figure 3.8. Annotated ¹H and ¹³C NMR spectra of aldol adduct **182**.

(*R,R*)-pseudoephedrine glycinamide (*R,R*)-179 – One-Pot Protocol.

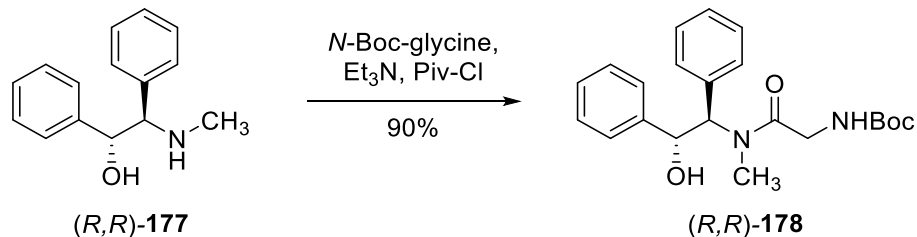


A solution of *N*-Boc-glycine (27.4 g, 156 mmol, 1.3 equiv) in dichloromethane (480 mL) in a 2-L round-bottom flask was cooled to 0 °C in an ice-water bath. Triethylamine (25.1 mL, 180 mmol, 1.5 equiv) was added dropwise over 2 minutes followed by pivaloyl chloride (17.73 mL, 144 mmol, 1.2 equiv) dropwise over 3 minutes. During the addition, a fine white solid precipitated from the solution. After 30 min, a second portion of triethylamine (25.1 mL, 180 mmol, 1.5 equiv) was added dropwise over 2 minutes, followed by finely powdered (*R,R*)-pseudoephedrine (27.3 g, 120 mmol, 1.0 equiv) in a single portion. The resulting mixture was allowed to stir at 0 °C for 45 minutes, at which point TLC analysis (10% methanol–dichloromethane + 1% saturated aqueous ammonium hydroxide solution) indicated complete consumption of pseudoephedrine. Trifluoroacetic acid (241 mL, 3123 mmol) was added (the first 15 mL was added carefully over 5 minutes, the remainder was added as a single portion), and the vessel was allowed to warm to 23 °C (CAUTION: gas evolution!). After 1.5 h, TLC analysis of the organic layer (mini-workup of 0.1 mL sample of the reaction mixture with dichloromethane/2 M NaOH, eluted with 10% methanol in dichloromethane + 1% saturated aqueous ammonium hydroxide solution) indicated complete consumption of the intermediate *N*-Boc glycinamide. The mixture was diluted with toluene (250 mL) and the volatiles were removed under reduced pressure at ≤ 30 °C. The clear yellow oil was dissolved in dichloromethane (500 mL), and the vessel was equipped with an internal thermometer and cooled in an ice water bath. The solution was stirred vigorously while 3 M aqueous sodium

hydroxide (~500 mL) was added slowly (~10 mL / min) so as to maintain an internal temperature of ≤ 15 °C, until the solution reached a pH of ~13-14. The mixture was transferred to a separatory funnel and the layers were separated. The aqueous layer was extracted with dichloromethane (300 mL), and the combined organic layers were dried with potassium carbonate (25 g), and were filtered through a sintered glass funnel. The filtrate was diluted with toluene (250 mL) and was concentrated under reduced pressure, and was further dried under high vacuum for 2 h. The solid was suspended in 200-proof ethanol (55 mL), and the mixture was equipped with a stir bar and brought to reflux with stirring. After 2 minutes, the solid fully dissolved, and the vessel was removed from heat and allowed to cool with constant stirring. Within 30 minutes, a white crystalline solid began to precipitate. Stirring was continued at 23 °C for 14 h and 0 °C for another 5 h. The mixture was filtered through a sintered glass funnel, and the resulting solid was washed with ethanol (2 × 15 mL) and diethyl ether (2 × 25 mL). Further drying at 0.1 mmHg provided (*R,R*)-pseudoephedrine glycinate (23.1 g, 68%). The filtrate was concentrated to provide a yellow foam that was recrystallized as before to provide a second crop of crystals (3.43 g, 10%) as a white crystalline solid (total: 26.6 g, 78%). Mp = 168–170 °C. TLC (10% methanol–dichloromethane + 0.5% saturated aqueous ammonium hydroxide solution): $R_f = 0.26$ (UV, PMA). ^1H NMR (3:1 ratio of rotamers, asterisk (*) denotes minor rotamer, 500 MHz, CDCl_3), δ : 7.35 (d, 2H, $J = 7.4$ Hz) 7.28–7.16 (m, 8H), 5.82 (d, 1H, $J = 8.8$ Hz), 5.30 (d, 1H, $J = 8.7$ Hz), 5.28* (d, 1H, $J = 7.8$ Hz), 4.87* (d, 1H, $J = 7.8$ Hz), 3.38* (dd, 2H, $J = 47.4$ Hz, 16.1 Hz), 3.27 (dd, 2H, $J = 34.1$ Hz, 17.1 Hz), 2.95* (s, 3H), 2.82 (s, 3H), 1.47 (br s, 2H). ^{13}C NMR (2:1 ratio of rotamers, asterisk (*) denotes minor rotamer, 125 MHz, CDCl_3), δ : 174.1, 173.6*, 141.7, 141.6*, 137.0, 136.5*, 128.5, 128.4*, 128.4, 128.3, 128.0*, 127.8*, 127.7, 127.6, 127.0*, 126.9, 72.9, 72.5*, 64.8*, 63.9, 43.5, 43.2*, 31.1, 29.6*.

^1H NMR (2:1 ratio of rotamers, asterisk (*) denotes minor rotamer, 400 MHz, CD_3OD), δ : 7.40–7.36 (m, 2H), 7.34–7.30 (m, 2H), 7.26–7.15 (m, 6H), 5.99 (d, 1H, $J = 9.5$ Hz), 5.38* (d, 1H, $J = 8.3$ Hz), 5.37 (d, 1H, $J = 9.5$ Hz), 5.02* (d, 1H, $J = 8.3$ Hz), 3.58 (dd, 2H, $J = 21.6$ Hz, 16.5 Hz), 3.42 (dd, 2H, $J = 29.9$ Hz, 17.8 Hz), 2.99 (s, 3H), 2.96* (s, 3H). ^{13}C NMR (2:1 ratio of rotamers, asterisk (*) denotes minor rotamer, 125 MHz, CD_3OD), δ : 175.1*, 174.9, 143.3*, 143.3, 138.6, 138.0*, 130.0*, 130.0, 129.4*, 129.3*, 129.3, 129.2, 128.9, 128.8*, 128.6*, 128.6, 128.5, 128.5*, 73.4*, 73.2, 66.2*, 63.8, 43.6, 43.5*, 30.3, 30.0*. FTIR (neat), cm^{-1} : 3356 (br), 3032 (m), 2976 (m), 1634 (s), 1452 (s), 1049 (s), 976 (s), 698 (s); HRMS (ESI): Calcd for $(\text{C}_{17}\text{H}_{20}\text{N}_2\text{O}_2 + \text{Na})^+$: 307.1417; Found: 307.1426.

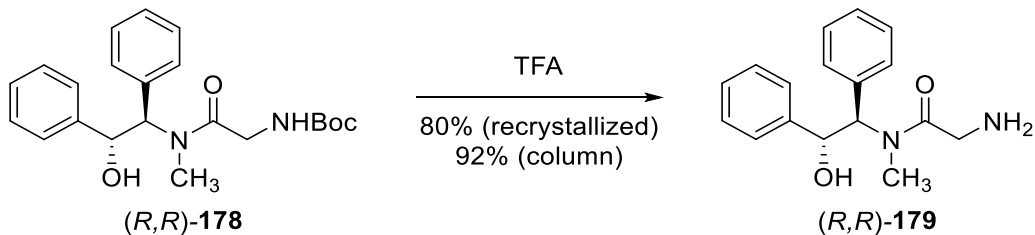
(*R,R*)-pseudoephedrine glycinamide (*R,R*)-**179** – Two-Pot Protocol: Step 1.



A solution of *N*-Boc-glycine (5.0 g, 28.6 mmol, 1.3 equiv) in dichloromethane (88 mL) in a 250-mL round-bottom flask was cooled to 0 °C in an ice-water bath. Triethylamine (3.99 mL, 28.6 mmol, 1.3 equiv) was added dropwise over 2 minutes followed by pivaloyl chloride (3.52 mL, 28.6 mmol, 1.3 equiv) dropwise over 5 minutes. During the addition, a fine white solid precipitated from the solution. After 30 min at 0 °C, a second portion of triethylamine (3.99 mL, 28.6 mmol, 1.3 equiv) was added dropwise over 2 minutes, followed by finely powdered (*R,R*)-pseudoephedrine (5.0 g, 22.0 mmol, 1.0 equiv) in a single portion. The resulting mixture was allowed to stir at 0 °C for 90 minutes, at which point TLC analysis (10% methanol–dichloromethane + 1% saturated aqueous ammonium hydroxide solution) indicated complete consumption of pseudoephedrine. 5% Aqueous sodium bicarbonate solution (67 mL) was added, and the layers were mixed vigorously and separated. The aqueous layer was extracted with dichloromethane (2 × 50 mL), and the combined organic layers were washed sequentially with water (70 mL) and saturated aqueous sodium chloride solution (70 mL). The washed organic phase was dried over sodium sulfate and filtered. The filtrate was concentrated and the crude solid was recrystallized from hot toluene (27 mL, ~3.3 mL per gram of theoretical product) to provide *N*-Boc-(*R,R*)-pseudoephedrine glycinamide as white crystals (7.59 g, 90%). Mp = 166–68 °C. TLC (10% methanol–dichloromethane + 0.5% saturated aqueous ammonium hydroxide solution): R_f = 0.43 (UV, PMA). ¹H NMR (multiple rotamers present, spectrum reported as observed, 500 MHz, CDCl₃), δ : 7.35 (d, 2H, J = 7.8 Hz) 7.31–7.21 (m, 13H), 5.72 (d,

1H, $J = 8.2$ Hz), 5.58 (br s, 0.3H), 5.51 (br s, 1.2H), 5.39 (d, 1H, $J = 8.1$ Hz), 5.33 (d, 0.3H, $J = 7.9$ Hz), 4.96 (d, 0.3H, $J = 8.0$ Hz), 4.91 (d, 0.1H, $J = 7.9$ Hz), 4.13–4.03 (br m, 0.7H), 3.94 (d, 2H, $J = 4.0$ Hz), 3.19 (br s, 0.9H), 2.99 (s, 0.9H), 2.87 (s, 3H), 1.45 (s, 12H). ^{13}C NMR (major rotamer reported, 125 MHz, CDCl_3), δ : 170.1, 155.7, 141.2, 136.5, 128.6, 128.5, 128.4, 127.9, 127.7, 126.8, 79.6, 73.3, 64.6, 42.8, 31.8, 28.3. FTIR (neat), cm^{-1} : 3420 (br), 2978 (m), 1703 (s), 1643 (s), 1167 (s), 909 (s), 727 (s), 698 (s); HRMS (ESI): Calcd for $(\text{C}_{22}\text{H}_{28}\text{N}_2\text{O}_4 + \text{H})^+$: 385.2122; Found: 385.2134.

(*R,R*)-pseudoephedrine glycinamide (*R,R*)-**179** – Two-Pot Protocol: Step 2.



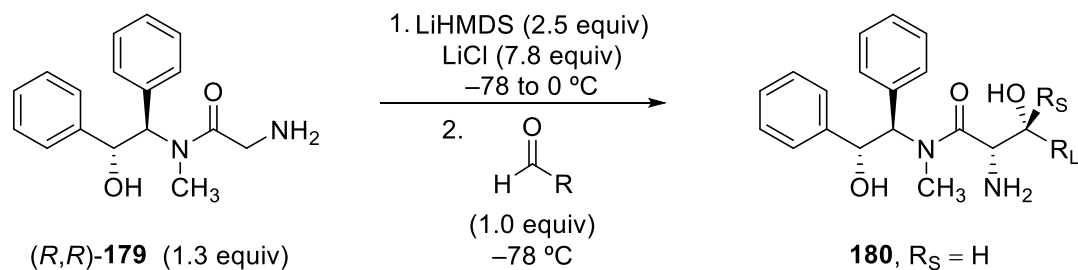
A solution of *N*-Boc-(*R,R*)-pseudoephedrine glycinamide (5.0 g, 13 mmol, 1.0 equiv) in dichloromethane (52 mL) in a 250-mL round-bottom flask was cooled to 0 °C in an ice-water bath. Trifluoroacetic acid (13 mL) was added slowly over 5 minutes. The colorless solution was allowed to stir at 0 °C for 5 minutes, before the cooling bath was removed and stirring was continued at 23 °C. After 1.5 h, TLC analysis of the organic layer (mini-workup of 0.1 mL sample of the reaction mixture with dichloromethane/1 M aqueous sodium hydroxide solution, eluted with 10% methanol–dichloromethane + 1% saturated aqueous ammonium hydroxide solution) indicated complete consumption of the starting material. The reaction mixture was concentrated in vacuo to provide a clear yellow oil. The oil was dissolved in dichloromethane (50 mL), and the vessel cooled in an ice water bath. The solution was stirred vigorously while 3 M aqueous sodium hydroxide (~30 mL) was added slowly by pipetful until the solution reached a pH of ~13-14. The mixture was transferred to a separatory funnel and the layers were separated. The aqueous layer was extracted with dichloromethane (2 × 40 mL), and the combined organic layers were dried with potassium carbonate (3 g), and were filtered through a sintered glass funnel. The filtrate was diluted with toluene (25 mL) and was concentrated under reduced pressure, and was further dried at 0.1 mmHg for 1 h. The solid was suspended in 200-proof ethanol (7 mL, ~1.7 mL ethanol per theoretical gram of product), and the mixture was equipped with a stir bar and brought to reflux with stirring. After 2 minutes, the solid had fully dissolved, and the vessel was removed from heat and allowed to cool to 23 °C with constant

stirring. Within 30 minutes, a white crystalline solid began to precipitate. Stirring was continued at 23 °C for 14 h and at 0 °C for another 5 h. The mixture was filtered through a sintered glass funnel, and the resulting solid was washed with cool (0 °C) ethanol (2 × 1.5 mL) and diethyl ether (2 × 2.5 mL). Further drying at 0.1 mmHg provided (*R,R*)-pseudoephedrine glycinate (2.13 g, 57%). The filtrate was concentrated to provide a yellow foam that was recrystallized as before with the exception that the recrystallized solid was only washed with multiple portions of ether to provide a second crop of (*R,R*)-pseudoephedrine glycinate (0.84 g, 23%) as a white crystalline solid (total: 2.97 g, 80%). Purification may also be performed by column chromatography on silica gel (10% methanol–dichloromethane + 0.5% saturated aqueous ammonium hydroxide solution). On a 3.95 mmol scale, this provided (*R,R*)-**179** as a white foam (3.64 mmol, 92%). Mp = 168–170 °C. TLC (10% methanol–dichloromethane + 0.5% saturated aqueous ammonium hydroxide solution): $R_f = 0.26$ (UV, PMA). $^1\text{H NMR}$ (3:1 ratio of rotamers, asterisk (*) denotes minor rotamer, 500 MHz, CDCl_3), δ : 7.35 (d, 2H, $J = 7.4$ Hz) 7.28–7.16 (m, 8H), 5.82 (d, 1H, $J = 8.8$ Hz), 5.30 (d, 1H, $J = 8.7$ Hz), 5.28* (d, 1H, $J = 7.8$ Hz), 4.87* (d, 1H, $J = 7.8$ Hz), 3.38* (dd, 2H, $J = 47.4$ Hz, 16.1 Hz), 3.27 (dd, 2H, $J = 34.1$ Hz, 17.1 Hz), 2.95* (s, 3H), 2.82 (s, 3H), 1.47 (br s, 2H). $^{13}\text{C NMR}$ (2:1 ratio of rotamers, asterisk (*) denotes minor rotamer, 125 MHz, CDCl_3), δ : 174.1, 173.6*, 141.7, 141.6*, 137.0, 136.5*, 128.5, 128.4*, 128.4, 128.3, 128.0*, 127.8*, 127.7, 127.6, 127.0*, 126.9, 72.9, 72.5*, 64.8*, 63.9, 43.5, 43.2*, 31.1, 29.6*.

$^1\text{H NMR}$ (2:1 ratio of rotamers, asterisk (*) denotes minor rotamer, 400 MHz, CD_3OD), δ : 7.40–7.36 (m, 2H), 7.34–7.30 (m, 2H), 7.26–7.15 (m, 6H), 5.99 (d, 1H, $J = 9.5$ Hz), 5.38* (d, 1H, $J = 8.3$ Hz), 5.37 (d, 1H, $J = 9.5$ Hz), 5.02* (d, 1H, $J = 8.3$ Hz), 3.58 (dd, 2H, $J = 21.6$ Hz, 16.5 Hz), 3.42 (dd, 2H, $J = 29.9$ Hz, 17.8 Hz), 2.99 (s, 3H), 2.96* (s, 3H). $^{13}\text{C NMR}$ (2:1 ratio of

rotamers, asterisk (*) denotes minor rotamer, 125 MHz, CD₃OD), δ : 175.1*, 174.9, 143.3*, 143.3, 138.6, 138.0*, 130.0*, 130.0, 129.4*, 129.3*, 129.3, 129.2, 128.9, 128.8*, 128.6*, 128.6, 128.5, 128.5*, 73.4*, 73.2, 66.2*, 63.8, 43.6, 43.5*, 30.3, 30.0*. FTIR (neat), cm⁻¹: 3356 (br), 3032 (m), 2976 (m), 1634 (s), 1452 (s), 1049 (s), 976 (s), 698 (s); HRMS (ESI): Calcd for (C₁₇H₂₀N₂O₂ + Na)⁺: 307.1417; Found: 307.1426.

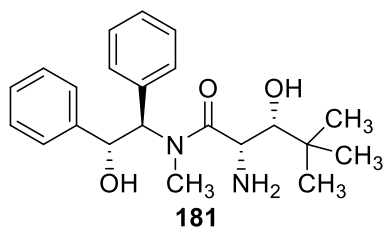
General Procedure for Aldolization of Pseudoephedrine Glycinamide (**179**) with Aldehydes.



A 25-mL round-bottom flask equipped with a stir bar was charged with anhydrous lithium chloride (331 mg, 7.80 mmol, 7.8 equiv). The vessel was heated with a gentle flame under vacuum (0.1 mmHg) for 2 minutes. After cooling to 23 °C in vacuo, the flask was backfilled with argon and *(R,R)*-pseudoephedrine glycinamide (370 mg, 1.30 mmol, 1.3 equiv) was added. Tetrahydrofuran (6.5 mL) was added by syringe and the reaction mixture was stirred at 23 °C until pseudoephedrine glycinamide had dissolved (~5 minutes); lithium chloride does not completely dissolve. The resulting suspension was cooled to -78 °C in a dry ice-acetone cooling bath and a freshly-prepared solution of lithium hexamethyldisilazide in tetrahydrofuran (1.0 M, 2.5 mL, 2.5 mmol, 2.5 equiv) was added dropwise. After 5 minutes, the reaction vessel was transferred to an ice-water bath and stirring was continued for 25 minutes. The vessel was re-cooled to -78 °C, and a solution of aldehyde in tetrahydrofuran (1.0 M, 1.0 mL, 1.0 mmol, 1.0 equiv) was added dropwise. Once the aldehyde was completely consumed as indicated by TLC (usually ≤ 30 minutes), a half-saturated aqueous ammonium chloride solution (0.10 mL) was added and the vessel was allowed to warm to 23 °C. The mixture was partitioned between half-saturated aqueous ammonium chloride solution (20 mL) and ethyl acetate (25 mL). The layers were separated, and the aqueous layer was extracted with ethyl acetate (2×25 mL). The combined organic extracts were washed with saturated aqueous sodium chloride solution (45 mL) and dried over sodium sulfate. The dried solution was filtered, and the filtrate was

concentrated. The diastereomeric ratio of the crude product was determined by NMR or HPLC analysis (*vide infra*). The residue was purified by flash column chromatography on silica gel.

Aldol adduct **181**.

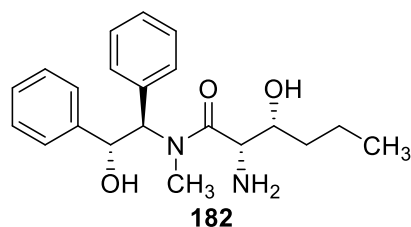


The general procedure for aldolization of pseudoephedrine glycinamide (*R,R*)-**179** with aldehydes (p. 144) was followed.

The diastereomeric ratio of the crude product residue was determined to be 94:6 by HPLC analysis (Agilent Extend-C18,

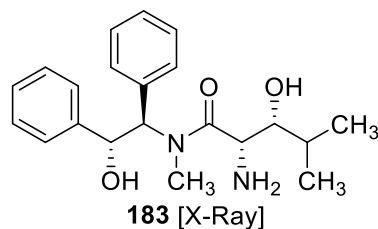
85:15→65:35 water:acetonitrile + 0.1% trifluoroacetic acid, 0.5 mL/min, $\lambda = 220$ nm, t_R (minor) = 18.5 min, t_R (major) = 20.8 min, t_R (minor) = 22.7 min). The residue was purified by flash column chromatography (2→4% methanol–dichloromethane + 0.5% saturated aqueous ammonium hydroxide solution) to provide the title compound as a white foam (330 mg, 89%). Mp = 53–55 °C. TLC (10% methanol–dichloromethane + 0.5% saturated aqueous ammonium hydroxide solution): $R_f = 0.43$ (UV, PMA). ^1H NMR (7:1 ratio of rotamers; major rotamer reported, 500 MHz, CDCl_3), δ : 7.39 (d, 2H, $J = 7.8$ Hz) 7.28–7.19 (m, 8H), 5.89 (d, 1H, $J = 8.8$ Hz), 5.34 (d, 1H, $J = 8.8$ Hz), 3.71 (m, 1H), 3.30 (d, 1H, $J = 3.9$ Hz), 2.95 (s, 3H), 0.89 (s, 9H). ^{13}C NMR (major rotamer reported, 125 MHz, CDCl_3), δ : 176.6, 141.2, 136.2, 128.6, 128.3, 128.2, 127.7, 127.5, 126.9, 76.6, 72.9, 63.5, 50.7, 34.7, 32.5, 26.5. FTIR (neat), cm^{-1} : 3356 (br), 3063 (m), 2955 (m), 1616 (s), 1479 (s), 1308 (s), 909 (s), 729 (s); HRMS (ESI): Calcd for $(\text{C}_{22}\text{H}_{30}\text{N}_2\text{O}_3 + \text{H})^+$: 371.2329; Found: 371.2330.

Aldol adduct **182**.



The general procedure for aldolization of pseudoephedrine glycinamide (*R,R*)-**179** with aldehydes (p. 144) was followed. The diastereomeric ratio of the crude product residue was determined to be 83:17 by HPLC analysis (Agilent Extend-C18, 85:15→65:35 water:acetonitrile + 0.1% trifluoroacetic acid, 0.5 mL/min, $\lambda = 220$ nm, t_R (minor) = 16.2 min, t_R , t_R (major) = 19.2 min). The residue was purified by flash column chromatography (3→5% methanol–dichloromethane + 0.3→0.5% saturated aqueous ammonium hydroxide solution, followed by a second column of 7% methanol–ethyl acetate + 0.5% saturated aqueous ammonium hydroxide solution) to provide the title compound as a white foam (257 mg, 72%). Mp = 48–50 °C. TLC (10% methanol–dichloromethane + 0.5% saturated aqueous ammonium hydroxide solution): $R_f = 0.25$ (UV, PMA). ¹H NMR (10:1 ratio of rotamers; major rotamer reported, 500 MHz, CDCl₃), δ : 7.41 (d, 2H, $J = 7.3$ Hz) 7.29–7.20 (m, 8H), 5.94 (d, 1H, $J = 8.8$ Hz), 5.33 (d, 1H, $J = 9.3$ Hz), 3.64 (m, 1H), 3.51 (d, 1H, $J = 4.9$ Hz), 2.98 (s, 3H), 1.50–1.44 (m, 1H), 1.42–1.37 (m, 1H), 1.35–1.28 (m, 1H), 1.25–1.18 (m, 1H), 0.87 (t, 3H, $J = 6.8$ Hz). ¹³C NMR (major rotamer reported, 125 MHz, CDCl₃), δ : 176.1, 141.3, 136.6, 128.5, 128.4, 128.3, 127.8, 127.7, 127.0, 72.7, 72.0, 63.7, 55.0, 35.1, 32.7, 19.1, 14.0. FTIR (neat), cm⁻¹: 3366 (br), 3032 (m), 2872 (m), 1616 (s), 1327 (s), 909 (s), 729 (s), 696 (s); HRMS (ESI): Calcd for (C₂₁H₂₈N₂O₃ + H)⁺: 357.2173; Found: 357.2175.

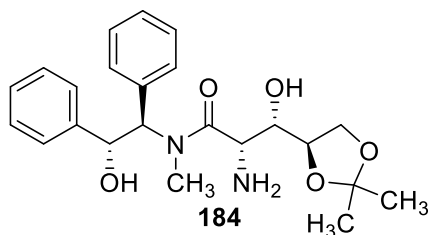
Aldol adduct **183**.



The general procedure for aldolization of pseudoephedrine glycinamide (*R,R*)-**179** with aldehydes (p. 144) was followed. The diastereomeric ratio of the crude product residue was determined to be 86:14 by HPLC analysis (Agilent Extend-C18,

85:15→65:35 water:acetonitrile + 0.1% trifluoroacetic acid, 0.5 mL/min, $\lambda = 220$ nm, t_R (minor) = 16.0 min, t_R (major) = 17.0 min). The residue was purified by flash column chromatography (2→7% methanol–ethyl acetate + 0.5% saturated aqueous ammonium hydroxide solution) to provide the title compound as a white foam (275 mg, 77%). Mp = 129–131 °C. TLC (10% methanol–dichloromethane + 0.5% saturated aqueous ammonium hydroxide solution): $R_f = 0.44$ (UV, PMA). ^1H NMR (6:1 ratio of rotamers; major rotamer reported, 500 MHz, CDCl_3), δ : 7.36 (d, 2H, $J = 7.3$ Hz) 7.24–7.15 (m, 8H), 5.86 (d, 1H, $J = 8.7$ Hz), 5.32 (d, 1H, $J = 9.2$ Hz), 3.63 (d, 1H, $J = 4.1$ Hz), 3.31 (dd, 1H, $J = 6.9$ Hz, 4.1 Hz), 2.93 (s, 3H), 1.66 (m, 1H), 0.92 (d, 3H, $J = 6.4$ Hz), 0.87 (d, 3H, $J = 6.9$ Hz). ^{13}C NMR (major rotamer reported, 125 MHz, CDCl_3), δ : 175.9, 141.3, 136.5, 128.5, 128.3, 128.2, 127.6, 127.5, 127.1, 76.6, 72.3, 63.3, 52.2, 32.2, 29.8, 19.3, 18.1. FTIR (neat), cm^{-1} : 3362 (br), 2961 (s), 1620 (m), 1452 (s), 1057 (s), 909 (s), 729 (s), 698 (s); HRMS (ESI): Calcd for $(\text{C}_{21}\text{H}_{28}\text{N}_2\text{O}_3 + \text{Na})^+$: 379.1992; Found: 379.1989.

Aldol adduct **184**.

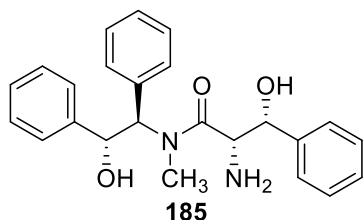


The general procedure for aldolization of pseudoephedrine glycinamide (*R,R*)-**179** with aldehydes (p. 144) was followed.

The diastereomeric ratio of the crude product residue was determined to be 89:11 by ^1H NMR. The residue was

purified by flash column chromatography (1→6% methanol–dichloromethane + 0.5% saturated aqueous ammonium hydroxide solution) to provide the title compound as a white foam (273 mg, 66%). Mp = 51–53 °C. TLC (10% methanol–dichloromethane + 0.5% saturated aqueous ammonium hydroxide solution): R_f = 0.39 (UV, PMA). ^1H NMR (12:1 ratio of rotamers; major rotamer reported, 500 MHz, CDCl_3), δ : 7.38 (d, 2H, J = 7.4 Hz) 7.31–7.21 (m, 8H), 5.65 (d, 1H, J = 7.9 Hz), 5.44 (d, 1H, J = 8.3 Hz), 4.12 (m, 1H), 4.04–3.96 (m, 2H), 3.90 (br s, 1H), 3.47 (d, 1H, J = 8.3 Hz), 3.01 (s, 3H), 1.33 (s, 3H), 1.32 (s, 3H). ^{13}C NMR (major rotamer reported, 125 MHz, CDCl_3), δ : 175.9, 141.3, 136.4, 128.6, 128.4, 128.3, 127.8, 127.7, 126.9, 109.3, 74.7, 73.0, 72.9, 67.6, 64.6, 51.2, 33.0, 26.6, 25.1. FTIR (neat), cm^{-1} : 3364 (br), 3063 (m), 2986 (m), 1626 (s), 1211 (s), 1061 (s), 729 (s), 698 (s); HRMS (ESI): Calcd for $(\text{C}_{23}\text{H}_{30}\text{N}_2\text{O}_5 + \text{Na})^+$; 437.2047. Found: 437.2026.

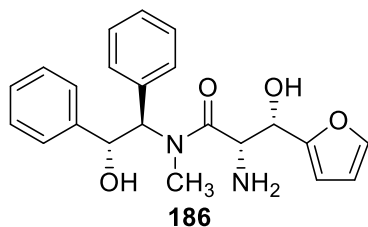
Aldol adduct **185**.



The general procedure for aldolization of pseudoephedrine glycinamide (*R,R*)-**179** with aldehydes (p. 144) was followed. The diastereomeric ratio of the crude product residue was determined to be 85:15 by HPLC analysis (Agilent Extend-C18, 85:15→65:35

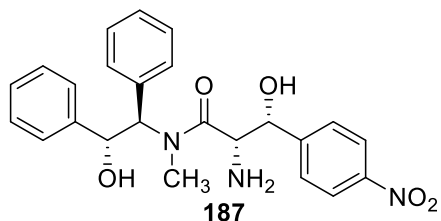
water:acetonitrile + 0.1% trifluoroacetic acid, 0.5 mL/min, $\lambda = 220$ nm, t_R (minor) = 19.2 min, t_R (minor) = 21.3 min, t_R (major) = 22.2 min). The residue was purified by flash column chromatography (2→5% methanol–dichloromethane + 0.5% saturated aqueous ammonium hydroxide solution) to provide the title compound as a white foam (311 mg, 80%). Mp = 63–65 °C. TLC (10% methanol–dichloromethane + 0.5% saturated aqueous ammonium hydroxide solution): $R_f = 0.35$ (UV, PMA). ^1H NMR (4:1 ratio of rotamers; asterisk (*) denotes minor rotamer, 500 MHz, CDCl_3), δ : 7.47* (d, 3H, $J = 7.3$ Hz), 7.34 (d, 3H, $J = 8.0$ Hz), 7.25–7.14 (m, 8H), 7.12–7.08 (m, 2H), 7.04–7.01 (m, 2H), 5.98 (d, 1H, $J = 9.1$ Hz), 5.35* (br s, 1H), 5.19 (dd, 1H, $J = 9.0$ Hz, 5.1 Hz), 4.77* (br s, 1H), 4.61 (dd, 1H, $J = 7.0$ Hz, 3.0 Hz), 3.61 (dd, 1H, $J = 7.0$ Hz, 4.2 Hz), 3.39* (d, 1H, $J = 2.0$ Hz), 2.92* (br s, 3H), 2.45 (s, 3H). ^{13}C NMR (major rotamer reported, 125 MHz, CDCl_3), δ : 174.8, 141.1, 140.1, 136.1, 128.7, 128.7, 128.3, 128.2, 127.7, 127.6, 127.4, 127.2, 126.3, 74.8, 72.3, 61.9, 57.9, 30.8. FTIR (neat), cm^{-1} : 3366 (br), 3032 (m), 1618 (s), 1452 (s), 1051 (s), 907 (s), 727 (s), 696 (s); HRMS (ESI): Calcd for $(\text{C}_{24}\text{H}_{26}\text{N}_2\text{O}_3 + \text{Na})^+$:413.1836; Found: 413.1839.

Aldol adduct **186**.



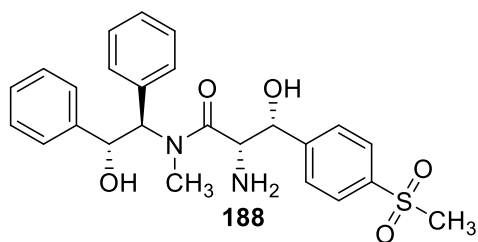
The general procedure for aldolization of pseudoephedrine glycinamide (*R,R*)-**179** with aldehydes (p. 144) was followed. The diastereomeric ratio of the crude product residue was determined to be 79:21 by HPLC analysis (Agilent Extend-C18, 85:15→65:35 water:acetonitrile + 0.1% trifluoroacetic acid, 0.5 mL/min, $\lambda = 220$ nm, t_R (minor) = 14.1 min, t_R (minor) = 15.5 min, t_R (major) = 17.1 min). The residue was purified by flash column chromatography (1→10% methanol–ethyl acetate + 0.5% saturated aqueous ammonium hydroxide solution) to provide the title compound as a white foam (240 mg, 63%). Mp = 64–66 °C. TLC (10% methanol–dichloromethane + 0.5% saturated aqueous ammonium hydroxide solution): $R_f = 0.30$ (UV, PMA). ^1H NMR (6:1 ratio of rotamers; major rotamer reported, 500 MHz, CDCl_3), δ : 7.36 (d, 2H, $J = 7.3$ Hz), 7.25–7.11 (m, 10H), 6.19 (s, 1H), 5.95 (d, 1H, $J = 8.8$ Hz), 5.27 (d, 1H, $J = 8.8$ Hz), 4.70 (d, 1H, $J = 6.8$ Hz), 4.01 (d, 1H, $J = 6.8$ Hz), 3.22 (br s, 2H), 2.71 (s, 3H). ^{13}C NMR (125 MHz, CDCl_3), δ : 174.3, 152.8, 141.8, 141.1, 136.2, 128.7, 128.3, 128.1, 127.7, 127.4, 127.3, 110.2, 107.9, 72.1, 68.9, 62.2, 55.2, 30.9. FTIR (neat), cm^{-1} : 3356 (br), 3032 (m), 2974 (m), 1624 (s), 1059 (s), 909 (s), 727 (s), 698 (s); HRMS (ESI): Calcd for $(\text{C}_{22}\text{H}_{24}\text{N}_2\text{O}_4 + \text{Na})^+$: 403.1628; Found: 403.1612.

Aldol adduct **187**.



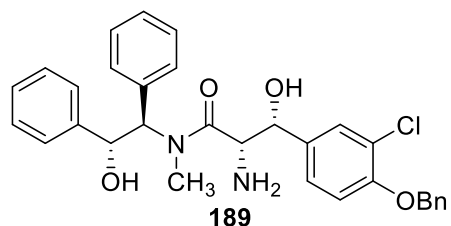
The general procedure for aldolization of pseudoephedrine glycinamide (*R,R*)-**179** with aldehydes (p. 144) was followed with the exception that the reaction was performed on a 2 mmol scale. The diastereomeric ratio of the crude product residue was determined to be 84:16 by HPLC analysis (Agilent Extend-C18, 82:18→72:28 water:acetonitrile + 0.1% trifluoroacetic acid, 0.5 mL/min, $\lambda = 220$ nm, t_R (minor) = 12.3 min, t_R (minor) = 24.2 min, t_R (major) = 25.5 min). The residue was purified by flash column chromatography (2→6% methanol–ethyl acetate + 0.5% saturated aqueous ammonium hydroxide solution) to provide the title compound as a yellow solid (681 mg, 78%). Mp = 127–129 °C. TLC (10% methanol–dichloromethane + 0.5% saturated aqueous ammonium hydroxide solution): $R_f = 0.40$ (UV, PMA). ^1H NMR (9:1 ratio of rotamers; major rotamer reported, 500 MHz, CD_3OD), δ : 7.74 (d, 2H, $J = 8.8$ Hz), 7.33 (d, 2H, $J = 8.8$ Hz), 7.28 (d, 2H, $J = 6.8$ Hz), 7.17–7.09 (m, 6H), 7.02 (d, 2H, $J = 7.3$ Hz), 5.89 (d, 1H, $J = 10.2$ Hz), 5.18 (d, 1H, $J = 10.2$ Hz), 4.62 (d, 1H, $J = 8.8$ Hz), 3.89 (d, 1H, $J = 8.3$ Hz), 2.64 (s, 3H). ^{13}C NMR (125 MHz, CD_3OD), δ : 174.8, 149.8, 148.5, 142.8, 137.8, 130.3, 129.1, 129.1, 128.8, 128.8, 128.7, 128.7, 124.2, 77.2, 73.0, 63.3, 59.0, 30.8. FTIR (neat), cm^{-1} : 3354 (br), 3032 (m), 2859 (s), 1622 (s), 1519 (s), 1346 (s), 908 (s), 727 (s); HRMS (ESI): Calcd for $(\text{C}_{24}\text{H}_{25}\text{N}_3\text{O}_5 + \text{Na})^+$: 458.1686; Found: 458.1677.

Aldol adduct **188**.



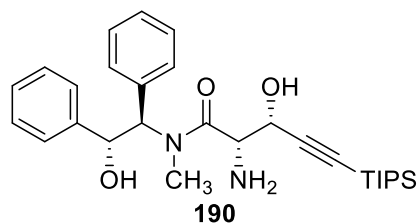
The general procedure for aldolization of pseudoephedrine glycinamide (*R,R*)-**179** with aldehydes (p. 144) was followed with the exceptions that the reaction was performed on a 2 mmol scale and that the electrophile was dissolved in 5 mL of tetrahydrofuran (0.2 M) due to the poor solubility of the starting aldehyde in tetrahydrofuran. The diastereomeric ratio of the crude product residue was determined to be 81:19 by ¹H NMR analysis. The residue was purified by flash column chromatography (2→4% methanol–ethyl acetate + 0.5% saturated aqueous ammonium hydroxide solution) to provide the title compound as a white solid (295 mg, 63%). Mp = 136–138 °C. TLC (10% methanol–dichloromethane + 0.5% saturated aqueous ammonium hydroxide solution): R_f = 0.26 (UV, PMA). ¹H NMR (8:1 ratio of rotamers; major rotamer reported, 500 MHz, CD₃OD), δ: 7.49 (d, 2H, *J* = 8.8 Hz), 7.37 (d, 2H, *J* = 8.3 Hz), 7.32 (d, 2H, *J* = 8.3 Hz), 7.21–7.09 (m, 8H), 5.97 (d, 1H, *J* = 10.2 Hz), 5.21 (d, 1H, *J* = 9.8 Hz), 4.61 (d, 1H, *J* = 8.3 Hz), 3.83 (d, 1H, *J* = 8.3 Hz), 2.95 (s, 3H), 2.54 (s, 3H). ¹³C NMR (125 MHz, CD₃OD), δ: 174.9, 148.8, 142.9, 141.1, 137.8, 130.4, 129.4, 129.1, 128.8, 128.8, 128.7, 128.6, 128.2, 76.8, 72.9, 63.2, 59.1, 44.5, 30.6. FTIR (neat), cm⁻¹: 3291 (br), 3063 (m), 2924 (s), 1622 (s), 1304 (s), 1148 (s), 700 (s); HRMS (ESI): Calcd for (C₂₅H₂₈N₂O₅S + Na)⁺: 491.1611; Found: 491.1635.

Aldol adduct **189**.



The general procedure for aldolization of pseudoephedrine glycinamide (*R,R*)-**179** with aldehydes (p. 144) was followed. The diastereomeric ratio of the crude product residue was determined to be 89:11 by ^1H NMR. The residue was purified by flash column chromatography (2 \rightarrow 10% methanol–ethyl acetate + 0.5% saturated aqueous ammonium hydroxide solution) to provide the title compound as a white foam (398 mg, 75%). Mp = 94–97 °C. TLC (10% methanol–dichloromethane + 0.5% saturated aqueous ammonium hydroxide solution): R_f = 0.38 (UV, PMA). ^1H NMR (10:1 ratio of rotamers; major rotamer reported, 500 MHz, CD_3OD), δ : 7.44–7.32 (m, 8H), 7.20–7.12 (m, 6H), 7.01 (d, 2H, J = 8.3 Hz), 6.85 (dd, 1H, J = 8.3 Hz, 2.0 Hz), 6.52 (d, 1H, J = 8.8 Hz), 5.96 (d, 1H, J = 9.8 Hz), 5.23 (d, 1H, J = 9.8 Hz), 4.98 (dd, 2H, J = 18.4 Hz, 12.2 Hz), 4.45 (d, 1H, J = 8.8 Hz), 3.82 (d, 1H, J = 8.3 Hz), 2.63 (s, 3H). ^{13}C NMR (125 MHz, CD_3OD), δ : 175.0, 155.0, 142.9, 138.1, 137.8, 135.8, 130.3, 129.6, 129.4, 129.2, 129.2, 129.0, 128.8, 128.7, 128.5, 128.2, 127.4, 123.8, 114.7, 76.7, 73.0, 71.6, 62.8, 59.1, 30.9. FTIR (neat), cm^{-1} : 3356 (br), 3032 (m), 2930 (m), 1616 (s), 1497 (s), 1256 (s), 1059 (s), 698 (s); HRMS (ESI): Calcd for $(\text{C}_{31}\text{H}_{31}\text{ClN}_2\text{O}_4 + \text{H})^+$: 531.2051; Found: 531.2059.

Aldol adduct **190**.



The general procedure for aldolization of pseudoephedrine glycinamide (*R,R*)-**179** with aldehydes (p. 144) was followed.

The diastereomeric ratio of the crude product residue was determined to be 83:17 by ^1H NMR. The residue was purified

by flash column chromatography (1→5% methanol–ethyl acetate + 0.5% saturated aqueous ammonium hydroxide solution) to provide the title compound as a white foam (372 mg, 75%).

Mp = 56–58 °C. TLC (10% methanol–dichloromethane + 0.5% saturated aqueous ammonium

hydroxide solution): R_f = 0.33 (UV, PMA). ^1H NMR (2:1 ratio of rotamers; asterisk (*) denotes

minor rotamer peaks, 500 MHz, CDCl_3), δ : 7.64* (d, 2H, J = 7.8 Hz) 7.38–7.19 (m, 10H), 5.88

(d, 1H, J = 8.3 Hz), 5.58* (br s, 1H), 5.52* (d, 1H, J = 4.9 Hz), 5.37 (d, 1H, J = 8.8 Hz), 4.61

(d, 1H, J = 4.4 Hz), 4.34* (br s, 1H), 3.81 (d, 1H, J = 3.9 Hz), 3.06 (s, 3H), 2.96* (br s, 1H),

2.84* (s, 3H), 1.11–1.00 (m, 21H). ^{13}C NMR (2:1 rotamer ratio, asterisk (*) denotes minor

rotamer peaks, 125 MHz, CDCl_3), δ : 174.8*, 174.0, 141.7*, 141.1, 136.9*, 136.3, 128.9*, 128.7,

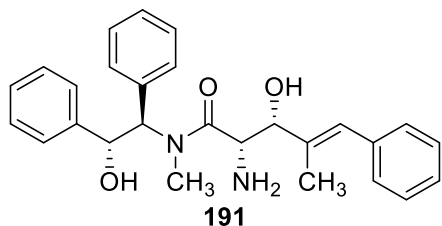
128.6*, 128.5*, 128.5, 128.4, 128.1*, 128.1, 127.9, 127.7*, 127.1, 126.6*, 105.6*, 105.3, 87.0,

85.8*, 73.8*, 72.9, 65.1*, 64.2, 64.0, 56.1, 55.2*, 32.9, 18.6, 18.5, 11.1*, 11.0*. FTIR (neat),

cm^{-1} : 3366 (br), 3032 (m), 2864 (s), 1626 (s), 1057 (s), 909 (s), 731 (s), 698 (s); HRMS (ESI):

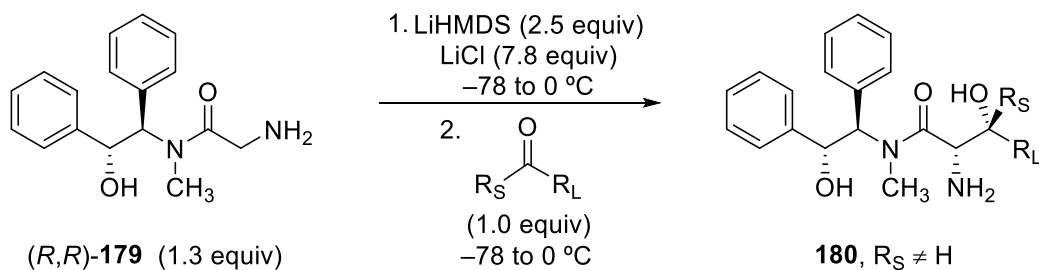
Calcd for $(\text{C}_{29}\text{H}_{42}\text{N}_2\text{O}_3\text{Si} + \text{H})^+$: 495.3037; Found: 495.3029.

Aldol adduct **191**.



The general procedure for aldolization of pseudoephedrine glycinamide (*R,R*)-**179** with aldehydes (p. 144) was followed. The diastereomeric ratio of the crude product residue was determined to be 79:21 by ^1H NMR. The residue was purified by flash column chromatography (2 \rightarrow 7% methanol–ethyl acetate + 0.5% saturated aqueous ammonium hydroxide solution) to provide the title compound as a white foam (335 mg, 78%). TLC (10% methanol–dichloromethane + 0.5% saturated aqueous ammonium hydroxide solution): R_f = 0.45 (UV, PMA). ^1H NMR (5:1 ratio of rotamers; major rotamer reported, 500 MHz, CDCl_3), δ : 7.39 (d, 2H, J = 8.2 Hz), 7.27–7.15 (m, 8H), 7.11–7.01 (m, 5H), 6.52 (s, 1H), 6.09 (d, 1H, J = 9.2 Hz), 5.27 (d, 1H, J = 9.2 Hz), 4.19 (d, 1H, J = 6.4 Hz), 3.70 (d, 1H, J = 6.4 Hz), 2.93 (s, 3H), 1.79 (s, 3H). ^{13}C NMR (125 MHz, CDCl_3), δ : 175.4, 141.2, 137.1, 136.2, 135.5, 129.0, 128.7, 128.4, 128.0, 127.9, 127.8, 127.6, 127.1, 126.4, 77.1, 72.7, 62.6, 53.7, 31.9, 14.5. FTIR (neat), cm^{-1} : 3362 (br), 3032 (m), 1622 (s), 1452 (s), 1057 (s), 907 (s), 727 (s), 696 (s); HRMS (ESI): Calcd for $(\text{C}_{27}\text{H}_{30}\text{N}_2\text{O}_3 + \text{Na})^+$: 453.2149; Found: 453.2156.

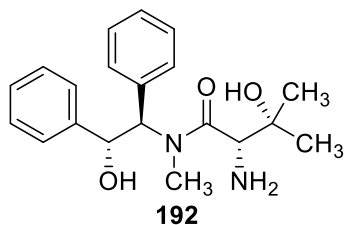
General Procedure for Aldolization of Pseudoephedrine Glycinamide (**179**) with Ketones.



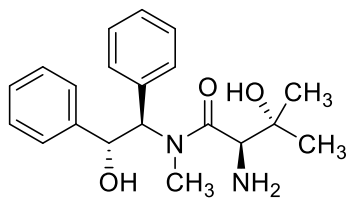
A 25-mL round-bottom flask equipped with a stir bar was charged with anhydrous lithium chloride (331 mg, 7.80 mmol, 7.8 equiv). The reaction vessel was heated with a gentle flame under vacuum (0.1 mmHg) for 2 minutes. After cooling to 23 °C in vacuo, the flask was backfilled with argon and (*R,R*)-pseudoephedrine glycinamide (370 mg, 1.30 mmol, 1.3 equiv) was added. Tetrahydrofuran (6.5 mL) was added by syringe and the reaction mixture was stirred at ambient temperature until pseudoephedrine glycinamide had dissolved (~5 minutes); lithium chloride does not completely dissolve. The resulting suspension was cooled to -78 °C in a dry ice-acetone cooling bath and a freshly-prepared solution of lithium hexamethyldisilazide in tetrahydrofuran (1.0 M, 2.5 mL, 2.5 mmol, 2.5 equiv) was added dropwise. After 5 minutes, the reaction vessel was transferred to an ice-water bath and stirring continued for 25 minutes. The vessel was re-cooled to -78 °C, and a solution of ketone in tetrahydrofuran (1.0 M, 1.0 mL, 1.0 mmol, 1.0 equiv) was added dropwise. After 30 minutes at -78 °C, the reaction vessel was transferred to an ice-water cooling bath and stirring continued at to 0 °C. Once the ketone was completely consumed as indicated by TLC (usually ≤ 30 minutes), the mixture was partitioned between half-saturated aqueous ammonium chloride solution (20 mL) and ethyl acetate (25 mL). The layers were separated, and the aqueous layer was extracted with ethyl acetate (2 \times 25 mL). The combined organic extracts were washed with saturated aqueous sodium chloride solution (45 mL) and dried over sodium sulfate. The dried solution was filtered, and the filtrate was

concentrated. The diastereomeric ratio of the crude product was determined by NMR or HPLC analysis (*vide infra*). The residue was purified by flash column chromatography on silica gel.

Aldol adduct **192**.



The general procedure for aldolization of pseudoephedrine glycinamide (*R,R*)-**179** with ketones (p. 156) was followed with the exception that the reaction was performed on a 3 mmol scale. The diastereomeric ratio of the crude product residue was determined to be 95:5 by HPLC analysis (Agilent Extend-C18, 85:15→65:35 water:acetonitrile + 0.1% trifluoroacetic acid, 0.5 mL/min, $\lambda = 220$ nm, t_R (major) = 14.4 min, t_R (minor) = 18.0 min). The residue was purified by flash column chromatography (2→4% methanol–dichloromethane + 0.2→0.4% saturated aqueous ammonium hydroxide solution) to provide both the minor diastereomer (characterized below) and the title compound as a white foam (746 mg, 73%). TLC (10% methanol–dichloromethane + 0.5% saturated aqueous ammonium hydroxide solution): $R_f = 0.49$ (UV, PMA). ^1H NMR (6:1 ratio of rotamers; major rotamer reported, 500 MHz, CDCl_3), δ : 7.41 (d, 2H, $J = 7.7$ Hz), 7.29–7.20 (m, 8H), 6.03 (d, 1H, $J = 8.6$ Hz), 5.32 (d, 1H, $J = 8.7$ Hz), 3.42 (s, 1H), 3.00 (s, 3H), 1.15 (s, 3H), 1.11 (s, 3H). ^{13}C NMR (major rotamer reported, 125 MHz, CDCl_3), δ : 176.6, 142.3, 136.5, 128.6, 128.4, 128.3, 127.8, 127.6, 127.0, 72.7, 71.7, 62.9, 56.9, 32.9, 26.9, 25.6. FTIR (neat), cm^{-1} : 3366 (br), 3032 (m), 2974 (s), 1614 (s), 1454 (m), 910 (s), 729 (s), 698 (s); HRMS (ESI): Calcd for $(\text{C}_{20}\text{H}_{26}\text{N}_2\text{O}_3 + \text{H})^+$: 343.2016; Found: 343.2026.

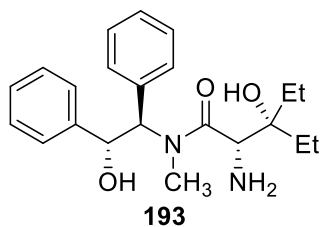


192 (minor diastereomer)

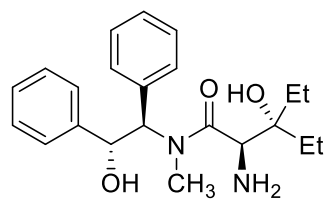
The minor diastereomer was isolated as a white foam (19 mg, 5%). TLC (10% methanol–dichloromethane + 0.5% saturated aqueous ammonium hydroxide solution): $R_f = 0.60$ (UV, PMA).

^1H NMR (1:1 ratio of rotamers, 500 MHz, CDCl_3), δ : 7.41 (d, 2H, $J = 7.4$ Hz), 7.33–7.19 (m, 8H), 6.08 (d, 1H, $J = 8.4$ Hz), 5.36 (d, 1H, $J = 8.4$ Hz), 5.35 (d, 1H, $J = 10.0$ Hz), 5.22 (d, 1H, $J = 10.0$ Hz), 3.71 (s, 1H), 3.52 (s, 1H), 3.04 (s, 3H), 2.92 (s, 3H), 1.31 (s, 3H), 1.29 (s, 3H), 1.19 (s, 3H), 1.12 (s, 3H). ^{13}C NMR (1:1 ratio of rotamers; asterisk (*) denotes rotamer peaks, 125 MHz, CDCl_3), δ : 176.2*, 174.7, 142.0*, 141.0, 136.5*, 135.7, 128.7*, 128.6 (2C), 128.5*, 128.5 (2C), 128.2, 127.9*, 127.9, 127.6*, 127.1, 127.0*, 72.8*, 72.5, 71.8*, 71.6, 65.7, 62.5*, 57.6, 56.3*, 32.7*, 28.0, 27.5, 27.3*, 25.9, 24.9*. FTIR (neat), cm^{-1} : 3362 (br), 3032 (m), 2974 (s), 1616 (s), 1452 (m), 910 (s), 729 (s) 698 (s); HRMS (ESI): Calcd for $(\text{C}_{20}\text{H}_{26}\text{N}_2\text{O}_3 + \text{H})^+$: 343.2016; Found: 343.2027.

Aldol adduct **193**.



The general procedure for aldolization of pseudoephedrine glycinamide (*R,R*)-**179** with ketones (p. 156) was followed. The diastereomeric ratio of the crude product residue was determined to be 95:5 by HPLC analysis (Agilent Extend-C18, 85:15→65:35 water:acetonitrile + 0.1% trifluoroacetic acid, 0.5 mL/min, $\lambda = 220$ nm, t_R (minor) = 17.0 min, t_R (major) = 19.4 min). The residue was purified by flash column chromatography (1→3% methanol–dichloromethane + 0.5% saturated aqueous ammonium hydroxide solution) to provide both the minor diastereomer (characterized below) and the title compound as a white foam (300 mg, 81%). Mp = 51–53 °C. TLC (10% methanol–dichloromethane + 0.5% saturated aqueous ammonium hydroxide solution): $R_f = 0.47$ (UV, PMA). ^1H NMR (12:1 ratio of rotamers; major rotamer reported, 500 MHz, CDCl_3), δ : 7.41 (d, 2H, $J = 7.3$ Hz), 7.32–7.20 (m, 8H), 5.98 (d, 1H, $J = 8.3$ Hz), 5.34 (d, 1H, $J = 8.3$ Hz), 3.53 (s, 1H), 3.01 (s, 3H), 1.59–1.50 (m, 2H), 1.38–1.27 (m, 2H), 0.80–0.76 (m, 6H). ^{13}C NMR (125 MHz, CDCl_3), δ : 177.2, 141.3, 136.5, 128.5, 128.4, 128.4, 127.8, 127.7, 127.0, 76.7, 72.7, 62.8, 53.1, 32.9, 27.8, 25.2, 7.6, 7.5. FTIR (neat), cm^{-1} : 3366 (br), 3032 (m), 2969 (s), 1610 (s), 1452 (m), 908 (s), 727 (s), 698 (s); HRMS (ESI): Calcd for $(\text{C}_{22}\text{H}_{30}\text{N}_2\text{O}_3 + \text{Na})^+$: 393.2149; Found: 393.2129.



193 (minor diastereomer)

The minor diastereomer was isolated as a white foam (10 mg, 3%).

TLC (10% methanol–dichloromethane + 0.5% saturated aqueous ammonium hydroxide solution): $R_f = 0.53$ (UV, PMA). ^1H NMR

(1.5:1 ratio of rotamers; asterisk (*) denotes minor rotamer peaks,

500 MHz, CDCl_3), δ : 7.42 (d, 2H, $J = 7.8$ Hz), 7.34–7.18 (m, 8H), 6.00* (d, 1H, $J = 7.8$ Hz),

5.42* (d, 1H, $J = 7.8$ Hz), 5.33 (d, 1H, $J = 10.3$ Hz), 5.22 (d, 1H, $J = 10.3$ Hz), 3.84 (s, 1H),

3.55* (s, 1H), 3.05* (s, 3H), 2.91 (s, 3H), 1.73–1.67 (m, 2H), 1.58–1.48 (m, 2H), 1.29–1.23*

(m, 2H), 0.91 (m, 3H), 0.81* (t, 3H, $J = 7.3$ Hz). ^{13}C NMR (1.5:1 ratio of rotamers; asterisk (*)

denotes minor rotamer peaks, 125 MHz, CDCl_3), δ : 177.1*, 174.8, 142.2, 141.1*, 136.7*, 135.7,

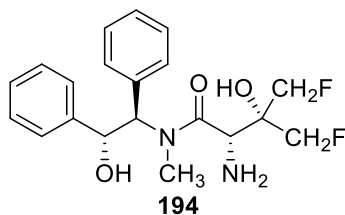
128.8, 128.6, 128.6*, 128.6, 128.5*, 128.3, 128.3*, 127.9*, 127.8, 127.7*, 127.0, 126.7, 76.2*,

75.8, 73.2*, 71.8, 65.9, 62.6*, 53.3*, 52.7, 33.2, 29.8*, 28.0*, 27.7, 25.6, 25.3*, 7.9, 7.7, 7.6*,

7.5*. FTIR (neat), cm^{-1} : 3374 (br), 3032 (m), 2967 (s), 1608 (s), 1452 (m), 910 (s), 731 (s)

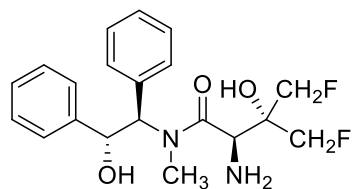
698 (s); HRMS (ESI): Calcd for $(\text{C}_{22}\text{H}_{30}\text{N}_2\text{O}_3 + \text{Na})^+$: 393.2149; Found: 393.2159.

Aldol adduct **194**.



The general procedure for aldolization of pseudoephedrine glycinamide (*R,R*)-**179** with ketones (p. 156) was followed. The diastereomeric ratio of the crude product residue was determined to be 94:6 by HPLC analysis (Agilent Extend-C18, 85:15→65:35

water:acetonitrile + 0.1% trifluoroacetic acid, 0.5 mL/min, $\lambda = 220$ nm, t_R (minor) = 12.9 min, t_R (major) = 15.3 min). The residue was purified by flash column chromatography (1→3% methanol–dichloromethane + 0.5% saturated aqueous ammonium hydroxide solution) to provide both the minor diastereomer (characterized below) and the title compound as a white foam (264 mg, 70%). Mp = 46–49 °C. TLC (10% methanol–dichloromethane + 0.5% saturated aqueous ammonium hydroxide solution): $R_f = 0.37$ (UV, PMA). ^1H NMR (3:1 ratio of rotamers; asterisk (*) denotes minor rotamer peaks, 500 MHz, CD_3OD), δ : 7.41 (d, 2H, $J = 8.3$ Hz), 7.38* (d, 2H, $J = 8.3$ Hz), 7.31 (d, 2H, $J = 6.8$ Hz), 7.25–7.16 (m, 6H), 6.02 (d, 1H, $J = 9.3$ Hz), 5.55* (d, 1H, $J = 9.7$ Hz), 5.42 (d, 1H, $J = 9.3$ Hz), 5.32* (d, 1H, $J = 9.7$ Hz), 4.78–4.60* (m, 3H), 4.60–4.54 (m, 1H), 4.50–4.44 (m, 2H), 4.39–4.34 (m, 1H), 4.27–4.25* (m, 2H), 4.08 (s, 1H), 3.16 (s, 3H), 3.03* (s, 3H). ^{13}C NMR (3:1 ratio of rotamers; asterisk (*) denotes minor rotamer peaks, 125 MHz, CD_3OD), δ : 175.8, 175.7*, 143.1, 143.0*, 138.3, 137.9*, 130.1, 129.9*, 129.5*, 129.3*, 129.3, 129.2, 129.0*, 128.9*, 128.8, 128.7, 128.7, 128.6*, 84.8 (dd, $J = 173.0$ Hz, 5.5 Hz), 84.2 (dd, $J = 172.1$ Hz, 3.7 Hz), 76.7* (dd, $J = 17.4$ Hz, 16.5 Hz), 75.6 (dd, $J = 17.4$ Hz, 16.5 Hz), 73.5*, 73.3, 67.1*, 63.6, 52.4*, 52.3, 32.3. FTIR (neat), cm^{-1} : 3364 (br), 3032 (m), 2969 (m), 1613 (s), 1452 (s), 1017 (s), 909 (s), 698 (s); HRMS (ESI): Calcd for $(\text{C}_{20}\text{H}_{24}\text{F}_2\text{N}_2\text{O}_3 + \text{Na})^+$: 401.1647; Found: 401.1634.



194 (minor diastereomer)

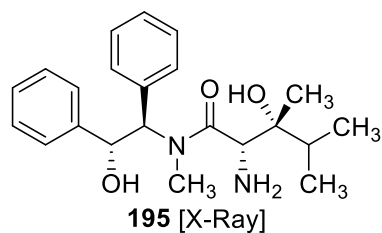
The minor diastereomer was isolated as a white foam (19 mg, 5%).

TLC (10% methanol–dichloromethane + 0.5% saturated aqueous ammonium hydroxide solution): $R_f = 0.37$ (UV, PMA). ^1H NMR

(1.5:1 ratio of rotamers; asterisk (*) denotes minor rotamer peaks,

500 MHz, CD_3OD), δ : 7.48* (d, 1H, $J = 7.2$ Hz), 7.44 (d, 2H, $J = 7.4$ Hz), 7.37* (d, 2H, $J = 7.44$ Hz), 7.29–7.16 (m, 8H), 6.16 (d, 1H, $J = 9.3$ Hz), 5.55* (d, 1H, $J = 8.6$ Hz), 5.41* (d, 1H, $J = 8.6$ Hz), 5.40 (d, 1H, $J = 9.3$ Hz), 4.71–4.67* (m, 2H), 4.63–4.57 (m, 2H), 4.54–4.49 (m, 1H), 4.48* (dd, 1H, $J = 9.8$ Hz, 2.0 Hz), 4.45–4.39 (m, 1H), 4.34* (br s, 1H) 4.32* (dd, 1H, $J = 9.8$ Hz, 1.8 Hz), 4.10 (br s, 1H), 3.13 (s, 3H), 2.85* (s, 3H). ^{13}C NMR (asterisk (*) denotes minor rotamer peaks, 125 MHz, CD_3OD), δ : 177.0*, 175.5, 143.4*, 143.0, 137.9, 137.4*, 130.7, 130.3, 130.0*, 129.9*, 129.5*, 129.3, 129.3, 129.2*, 128.9*, 128.7*, 128.7, 128.6, 84.3 (dd, $J = 173.0$ Hz, 5.5 Hz), 84.1 (dd, $J = 172.1$ Hz, 3.7 Hz), 75.8 (app t, $J = 16.5$ Hz), 72.9, 71.6*, 66.6, 63.2*, 52.3, 52.1*, 31.9, 26.0*. FTIR (neat), cm^{-1} : 3374 (br), 3032 (m), 2924 (m), 1614 (s), 1454 (s), 1018 (s), 976 (s), 700 (s); HRMS (ESI): Calcd for $(\text{C}_{20}\text{H}_{24}\text{F}_2\text{N}_2\text{O}_3 + \text{Na})^+$: 401.1647; Found: 401.1639.

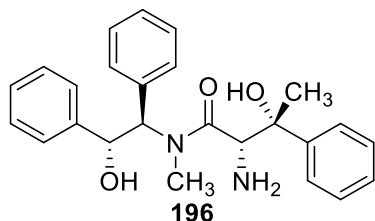
Aldol adduct **195**.



The general procedure for aldolization of pseudoephedrine glycinamide (*R,R*)-**179** with ketones (p. 156) was followed. The diastereomeric ratio of the crude product residue was determined to be 94:6 by HPLC analysis (Agilent Extend-C18, 85:15→65:35

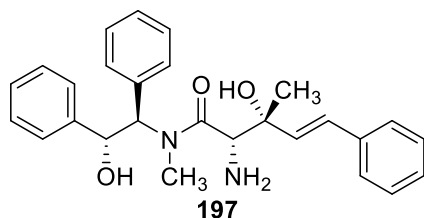
water:acetonitrile + 0.1% trifluoroacetic acid, 0.5 mL/min, $\lambda = 220$ nm, t_R (minor) = 19.5 min, t_R (major) = 21.5 min, t_R (minor) = 24.3 min). The residue was purified by flash column chromatography (2→4% methanol–dichloromethane + 0.2→0.4% saturated aqueous ammonium hydroxide solution) to provide the title compound as a white foam (302 mg, 82%). Mp = 112–114 °C. TLC (10% methanol–dichloromethane + 0.5% saturated aqueous ammonium hydroxide solution): $R_f = 0.28$ (UV, PMA). ^1H NMR (6:1 ratio of rotamers; major rotamer reported, 500 MHz, CDCl_3), δ : 7.43 (d, 2H, $J = 7.8$ Hz), 7.36–7.23 (m, 8H), 5.99 (d, 1H, $J = 8.3$ Hz), 5.40 (d, 1H, $J = 8.3$ Hz), 4.78 (br s, 1H), 3.62 (s, 1H), 3.03 (s, 3H), 2.10 (septet, 1H, $J = 6.8$ Hz), 0.95 (d, 3H, $J = 6.8$ Hz), 0.89 (s, 3H), 0.80 (d, 3H, $J = 6.8$ Hz). ^{13}C NMR (125 MHz, CDCl_3), δ : 177.6, 141.2, 136.4, 128.9, 128.6, 128.5, 127.9, 127.8, 126.9, 75.4, 73.0, 62.8, 53.3, 33.0, 32.0, 18.5, 17.5, 16.2. FTIR (neat), cm^{-1} : 3375 (br), 3032 (m), 2962 (m), 1611 (s), 1454 (s), 1096 (s), 910 (s), 698 (s); HRMS (ESI): Calcd for $(\text{C}_{22}\text{H}_{30}\text{N}_2\text{O}_3 + \text{Na})^+$: 393.2149; Found: 393.2163.

Aldol adduct **196**.



The general procedure for aldolization of pseudoephedrine glycinamide (*R,R*)-**179** with ketones (p. 156) was followed. The diastereomeric ratio of the crude product residue was determined to be 88:12 by HPLC analysis (Agilent Extend-C18, 85:15→65:35 water:acetonitrile + 0.1% trifluoroacetic acid, 0.5 mL/min, $\lambda = 220$ nm, t_R (minor) = 22.5 min, t_R (major) = 24.3 min). The residue was purified by flash column chromatography (2→4% methanol–ethyl acetate + 0.5% saturated aqueous ammonium hydroxide solution, followed by 2→4% methanol–dichloromethane + 0.2→0.4% saturated aqueous ammonium hydroxide solution) to provide the title compound as a white foam (350 mg, 86%). TLC (10% methanol–dichloromethane + 0.5% saturated aqueous ammonium hydroxide solution): $R_f = 0.54$ (UV, PMA). ^1H NMR (4:1 ratio of rotamers; major rotamer reported, 500 MHz, CDCl_3), δ : 7.39–7.35 (m, 5H), 7.25–7.18 (m, 10H), 6.09 (d, 1H, $J = 9.3$ Hz), 5.22 (d, 1H, $J = 9.3$ Hz), 3.65 (s, 1H), 2.78 (s, 3H), 1.43 (s, 3H). ^{13}C NMR (major rotamer reported, 125 MHz, CDCl_3), δ : 175.7, 144.3, 141.0, 136.3, 128.7, 128.4, 128.3, 128.2, 127.8, 127.7, 127.2, 126.9, 125.3, 75.3, 72.4, 62.5, 58.2, 31.8, 26.1. FTIR (neat), cm^{-1} : 3368 (br), 3032 (m), 2980 (s), 1615 (s), 1449 (m), 909 (s), 729 (s), 698 (s); HRMS (ESI): Calcd for $(\text{C}_{25}\text{H}_{28}\text{N}_2\text{O}_3 + \text{Na})^+$: 427.1992; Found: 427.2010.

Aldol adduct **197**.

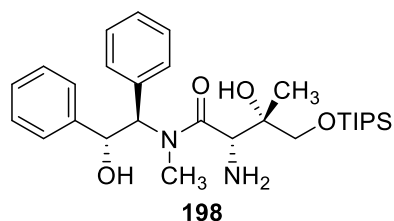


The general procedure for aldolization of pseudoephedrine glycinamide (*R,R*)-**179** with ketones (p. 156) was followed.

The diastereomeric ratio of the crude product residue was determined to be 79:21 by HPLC analysis (Agilent Extend-

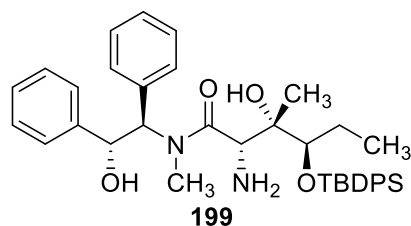
C18, 73:27 water:acetonitrile + 0.1% trifluoroacetic acid, 0.5 mL/min, $\lambda = 220$ nm, t_R (minor) = 23.7 min, t_R (minor) = 32.7 min, t_R (major) = 36.8 min). The residue was purified by flash column chromatography (1→3% methanol–dichloromethane + 0.5% saturated aqueous ammonium hydroxide solution, followed by 10% methanol–ethyl acetate + 0.5% saturated aqueous ammonium hydroxide solution) to provide the title compound as a white foam (238 mg, 55%). Mp = 70–72 °C. TLC (10% methanol–dichloromethane + 0.5% saturated aqueous ammonium hydroxide solution): $R_f = 0.30$ (UV, PMA). ^1H NMR (6:1 ratio of rotamers; major rotamer reported, 500 MHz, CDCl_3), δ : 7.40 (d, 2H, $J = 7.8$ Hz), 7.34–7.18 (m, 13H), 6.73 (d, 1H, $J = 16.1$ Hz), 6.07 (d, 1H, $J = 8.8$ Hz), 5.93 (d, 1H, $J = 16.1$ Hz), 5.31 (d, 1H, $J = 8.8$ Hz), 3.63 (s, 1H), 3.00 (s, 3H), 1.26 (s, 3H). ^{13}C NMR (125 MHz, CDCl_3), δ : 175.3, 141.1, 136.5, 136.4, 132.1, 129.6, 128.6, 128.5, 128.5, 128.4, 127.8, 127.7, 127.5, 127.2, 126.4, 74.4, 72.3, 62.7, 56.9, 32.3, 24.8. FTIR (neat), cm^{-1} : 3364 (br), 3030 (m), 2976 (m), 1616 (s), 1062 (s), 907 (s), 727 (s), 694 (s); HRMS (ESI): Calcd for $(\text{C}_{27}\text{H}_{30}\text{N}_2\text{O}_3 + \text{H})^+$: 431.2329; Found: 431.2326.

Aldol adduct **198**.



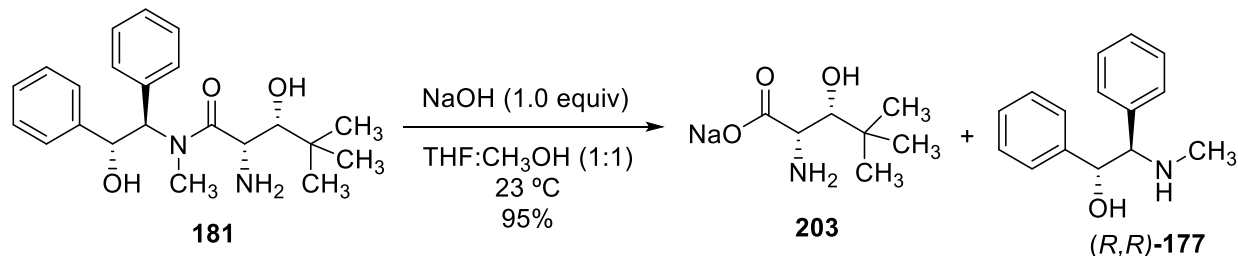
The general procedure for aldolization of pseudoephedrine glycinamide (*R,R*)-**179** with ketones (p. 156) was followed with the exception that the reaction was performed on a 15 mmol scale. The diastereomeric ratio of the crude product residue was determined to be 65:35 by ¹H NMR. The residue was purified by flash column chromatography (1→3% methanol–dichloromethane + 0.5% saturated aqueous ammonium hydroxide solution) to provide the title compound as a white foam (4.20 g, 54%). TLC (10% methanol–dichloromethane + 0.5% saturated aqueous ammonium hydroxide solution): *R_f* = 0.60 (UV, PMA). ¹H NMR (4:1 ratio of rotamers; major rotamer reported, 600 MHz, CD₃OD), δ: 7.41 (d, 2H, *J* = 7.6 Hz), 7.32 (d, 2H, *J* = 7.6 Hz), 7.23–7.15 (m, 6H), 6.11 (d, 1H, *J* = 10.0 Hz), 5.39 (d, 1H, *J* = 10.0 Hz), 3.99 (s, 1H), 3.76 (d, 1H, *J* = 9.4 Hz), 3.36 (d, 1H, *J* = 9.4 Hz), 3.17 (s, 3H), 1.16 (s, 3H), 1.10–1.05 (m, 21H). ¹³C NMR (major rotamer reported, 125 MHz, CD₃OD), δ: 177.0, 143.0, 138.4, 130.2, 129.3, 129.2, 128.8, 128.7, 128.7, 75.5, 73.1, 68.9, 63.3, 54.2, 31.9, 22.3, 18.5, 13.1. FTIR (neat), cm⁻¹: 3379 (br), 3032 (m), 2943 (s), 1614 (s), 1462 (m), 1098 (s), 881 (s) 698 (s); HRMS (ESI): Calcd for (C₂₉H₄₆N₂O₄Si₂ + Na)⁺: 537.3119; Found: 537.3111.

Aldol adduct **199**.



The general procedure for aldolization of pseudoephedrine glycinamide (*R,R*)-**179** with ketones (p. 156) was followed with the exceptions that the reaction was performed on a 5.9 mmol scale, the solution of electrophile was added at 0 °C as opposed to -78 °C and the workup was performed with water instead of half saturated aqueous ammonium chloride solution. The diastereomeric ratio of the crude product residue was determined to be $\geq 98:2$ by ^1H NMR. The residue was purified by flash column chromatography (2% methanol-dichloromethane + 0.2% saturated aqueous ammonium hydroxide solution) to provide the title compound as a white foam (3.59 g, 98%). Mp = 56–60 °C. TLC (5% methanol-dichloromethane + 0.5% saturated aqueous ammonium hydroxide solution): R_f = 0.30 (UV, PMA). ^1H NMR (15:1 ratio of rotamers; major rotamer reported, 500 MHz, CDCl_3), δ : 7.77 (d, 2H, J = 6.8 Hz), 7.70 (d, 2H, J = 6.8 Hz), 7.42–7.35 (m, 8H), 7.27–7.18 (m, 8H), 6.03 (d, 1H, J = 8.8 Hz), 5.31 (d, 1H, J = 8.8 Hz), 4.91 (br s, 1H), 3.92 (s, 1H), 3.84 (dd, 1H, J = 5.9 Hz, 4.9 Hz), 2.94 (s, 3H), 1.79–1.74 (m, 1H), 1.41–1.36 (m, 1H), 1.10 (s, 3 H), 0.98 (s, 9H). 0.58 (t, 3H, J = 7.8 Hz). ^{13}C NMR (125 MHz, CDCl_3), δ : 177.8, 141.1, 136.6, 135.9, 135.7, 134.4, 133.1, 129.8, 129.5, 128.5, 128.5, 128.4, 127.8, 127.7, 127.7, 127.4, 127.1, 76.4, 76.1, 72.7, 62.5, 52.6, 32.6, 27.0, 25.0, 19.5, 19.3, 12.1. FTIR (neat), cm^{-1} : 3372 (br), 3071 (m), 2934 (s), 2857 (s), 1608 (s), 1105 (m), 909 (s), 698 (s); HRMS (ESI): Calcd for $(\text{C}_{38}\text{H}_{48}\text{N}_2\text{O}_4\text{Si} + \text{Na})^+$: 647.3276; Found: 647.3278.

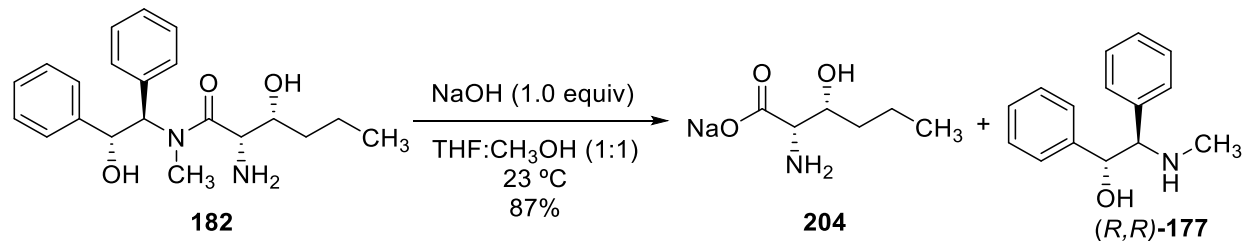
Hydrolysis of Aldol adduct **181**, to provide carboxylate **203**.



A 25-mL round bottom flask equipped with a stir bar was charged with aldol adduct **181** (700 mg, 1.89 mmol, 1 equiv). A 1:1 mixture of tetrahydrofuran:methanol (7.6 mL) was added, followed by aqueous sodium hydroxide solution (1.0 M, 1.89 mL, 1.89 mmol, 1 equiv). Reaction progress was monitored by the consumption of starting material by TLC (5% methanol–ethyl acetate + 0.5% saturated aqueous ammonium hydroxide solution). After 4 h, reaction mixture was concentrated and the residue was suspended in water (20 mL) and washed with dichloromethane (2 × 20 mL). The combined organic washes were back-extracted with water (20 mL) and the aqueous extract was added to the aqueous phase. The collective aqueous phase was once again extracted with dichloromethane (10 mL) and the organic extract was added to the organic phase. The organic phase was dried over sodium sulfate. The dried organic phase was filtered and the filtrate was concentrated to recover *(R,R)*-pseudoephedrine (428 mg, 100%, >95% purity), which matched previously reported data.^{110b} The aqueous layers were combined and concentrated in vacuo to afford the sodium carboxylate **203** as a white solid (329 mg, 95%). The enantiomeric excess of this product was determined to be $\geq 98\%$ by ¹H NMR comparison of the corresponding *(R)*- and *(S)*- MTPA amides.¹³¹ ¹H NMR (500 MHz, CD₃OD), δ : 3.61 (d, 1H, $J = 2.4$ Hz), 3.38 (d, 1H, $J = 2.4$ Hz), 0.97 (s, 9H). ¹³C NMR (125 MHz, CD₃OD), δ : 182.3, 79.9, 57.5, 36.4, 27.1. FTIR (neat), cm⁻¹: 3362 (br), 1620 (s), 1377 (s), 1316 (s), 1017 (s), 934 (s); HRMS (ESI): Calcd for (C₇H₁₅NO₃ + Na)⁺: 184.0944; Found: 184.0948.

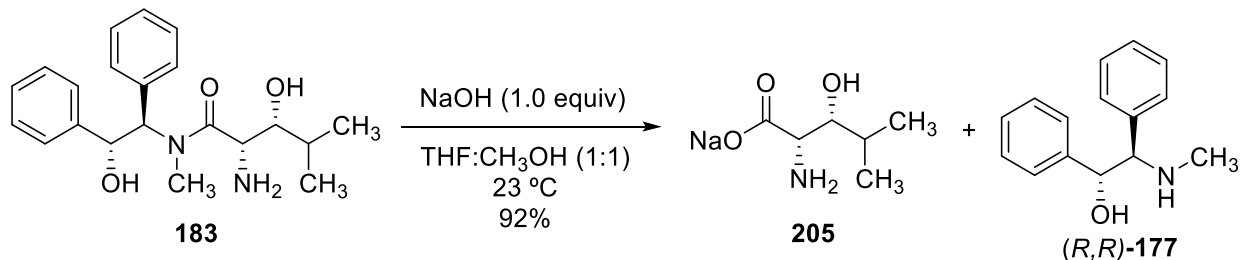
¹³¹ Parker, D. *Chem. Rev.* **1991**, *91*, 1441–1457.

Hydrolysis of Aldol adduct **182**, to provide carboxylate **204**.



A 25-mL round bottom flask equipped with a stir bar was charged with aldol adduct **182** (200 mg, 0.561 mmol, 1 equiv). A 1:1 mixture of tetrahydrofuran:methanol (2.2 mL) was added, followed by aqueous sodium hydroxide solution (1.0 M, 0.56 mL, 0.56 mmol, 1 equiv). Reaction progress was monitored by the consumption of starting material by TLC (5% methanol–ethyl acetate + 0.5% saturated aqueous ammonium hydroxide solution). After 4 h, reaction mixture was concentrated and the residue was suspended in water (6 mL) and washed with dichloromethane (2 × 6 mL). The combined organic washes were back-extracted with water (6 mL) and the aqueous extract was added to the aqueous phase. The collective aqueous phase was once again extracted with dichloromethane (3 mL) and the organic extract was added to the organic phase. The organic phase was dried over sodium sulfate. The dried organic phase was filtered and the filtrate was concentrated to recover *(R,R)*-pseudoephedrine (120 mg, 94%, >95% purity), which matched previously reported data.^{110b} The aqueous layers were combined and concentrated in vacuo to afford the sodium carboxylate **204** as a white solid (83 mg, 87%). The enantiomeric excess of this product was determined to be $\geq 98\%$ by ¹H NMR comparison of the corresponding *(R)*- and *(S)*- MTPA amides.¹³¹ ¹H NMR (500 MHz, CD₃OD), δ : 3.73 (m, 1H), 3.12 (d, 1H, $J = 4.4$ Hz), 1.57–1.48 (m, 2H), 1.47–1.33 (m, 2H), 3.12 (t, 3H, $J = 7.3$ Hz). ¹³C NMR (125 MHz, CD₃OD), δ : 181.2, 74.2, 61.7, 37.1, 20.3, 14.4. FTIR (neat), cm⁻¹: 3271 (br), 2957 (s), 2872 (s), 1604 (s), 1416 (s), 957 (s), 721 (s), 687 (s); HRMS (ESI): Calcd for (C₆H₁₃NO₃ + Na)⁺: 170.0788; Found: 170.0796.

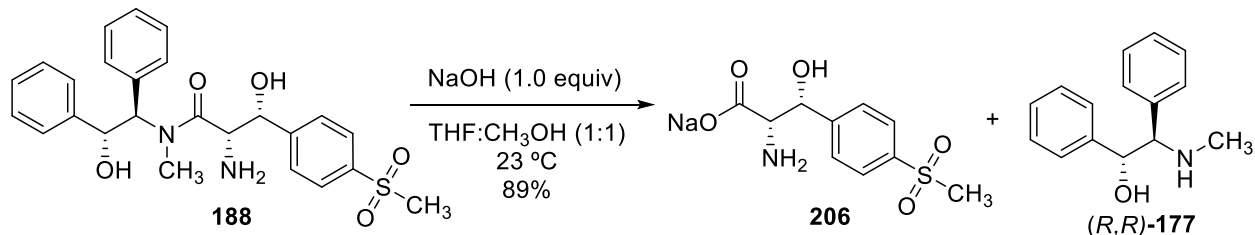
Hydrolysis of Aldol adduct **183**, to provide carboxylate **205**.



A 5-mL round bottom flask equipped with a stir bar was charged with aldol adduct **183** (42 mg, 0.118 mmol, 1 equiv). A 1:1 mixture of tetrahydrofuran:methanol (0.47 mL) was added, followed by aqueous sodium hydroxide solution (1.0 M, 0.12 mL, 0.12 mmol, 1 equiv). Reaction progress was monitored by the consumption of starting material by TLC (5% methanol–ethyl acetate + 0.5% saturated aqueous ammonium hydroxide solution). After 6 h, reaction mixture was concentrated and the residue was suspended in water (2 mL) and washed with dichloromethane (2 × 4 mL). The combined organic washes were back-extracted with water (4 mL) and the aqueous extract was added to the aqueous phase. The collective aqueous phase was once again extracted with dichloromethane (2 mL) and the organic extract was added to the organic phase. The organic phase was dried over sodium sulfate. The dried organic phase was filtered and the filtrate was concentrated to recover *(R,R)*-pseudoephedrine (24.7 mg, 92%, >95% purity), which matched previously reported data.^{110b} The aqueous layers were combined and concentrated in vacuo to afford the sodium carboxylate **205** as a white solid (18.4mg, 92%). The enantiomeric excess of this product was determined to be $\geq 98\%$ by ¹H NMR comparison of the corresponding (*R*)- and (*S*)- MTPA amides.¹³¹ ¹H NMR (500 MHz, CD₃OD), δ : 3.51 (dd, 1H, $J = 7.3$ Hz, 3.9 Hz), 3.30 (d, 1H, $J = 3.9$ Hz), 1.78 (app sxt, 1H, $J = 6.8$ Hz), 1.00 (d, 1H, $J = 6.4$ Hz), 0.95 (d, 1H, $J = 6.8$ Hz). ¹³C NMR (125 MHz, CD₃OD), δ : 181.1, 79.4, 59.3, 31.8,

20.1, 18.9. FTIR (neat), cm^{-1} : 3374 (br), 3140 (m), 2959 (s), 1586 (s), 1416 (s), 1063 (s), 934 (s), 700 (s); HRMS (ESI): Calcd for $(\text{C}_6\text{H}_{13}\text{NO}_3 + \text{Na})^+$: 170.0788; Found: 170.0796.

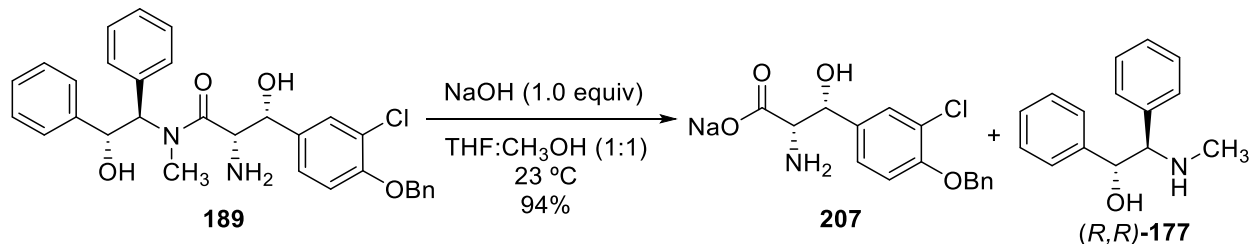
Hydrolysis of Aldol adduct **188**, to provide carboxylate **206**.



A 25-mL round bottom flask equipped with a stir bar was charged with aldol adduct **188** (300 mg, 0.640 mmol, 1 equiv). A 1:1 mixture of tetrahydrofuran:methanol (5.8 mL) was added and the vessel was cooled in an ice-water bath. Aqueous sodium hydroxide solution (1.0 M, 0.640 mL, 0.640 mmol, 1 equiv) was added. After 5 minutes, the cooling bath was removed and stirring was continued at 23 °C. Reaction progress was monitored by the consumption of starting material by TLC (10% methanol–dichloromethane + 0.5% saturated aqueous ammonium hydroxide solution). After 3.5 h, reaction mixture was concentrated and the residue was suspended in water (5 mL) and washed with dichloromethane (4 × 5 mL). The first wash with dichloromethane was not shaken vigorously in order to prevent the formation of an emulsion. The organic washes were combined and dried over sodium sulfate. The dried organic phase was filtered and the filtrate was concentrated to recover (*R,R*)-pseudoephedrine (145 mg, 100%, >95% purity), which matched previously reported data.^{110b} The aqueous layers were combined and concentrated in vacuo to afford the sodium carboxylate **206** as a white solid (167 mg, 93%). The enantiomeric excess of this product was determined to be ≥98% by ¹H NMR comparison of the corresponding (*R*)- and (*S*)- MTPA amides.¹³¹ ¹H NMR (500 MHz, CD₃OD), δ: 7.91 (d, 2H, *J* = 7.8 Hz), 7.69 (d, 2H, *J* = 7.8 Hz), 5.07 (d, 1H, *J* = 4.4 Hz), 3.40 (d, 1H, *J* = 4.4 Hz), 3.10 (s, 3H). ¹³C NMR (125 MHz, CD₃OD), δ: 179.5, 151.1, 140.6, 128.4, 128.2, 75.6, 63.4, 44.5.

FTIR (neat), cm^{-1} : 3370 (br), 2930 (m), 2074 (s), 1591 (s), 1290 (s), 1148 (s), 542 (s); HRMS (ESI): Calcd for $(\text{C}_{10}\text{H}_{13}\text{NO}_5\text{S} + \text{Na})^+$: 282.0412; Found: 282.0405.

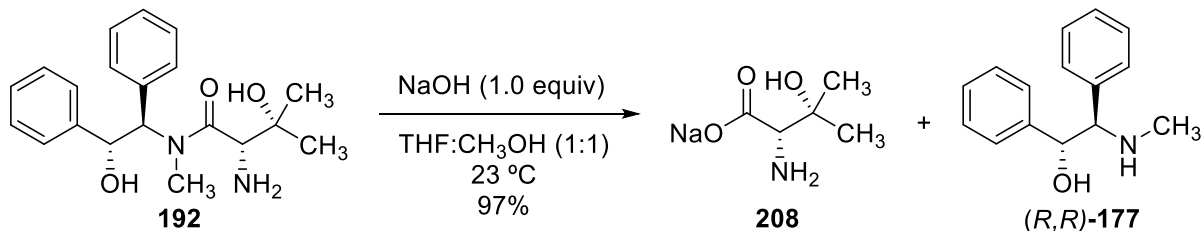
Hydrolysis of Aldol adduct **189**, to provide carboxylate **207**.



A 100-mL round bottom flask equipped with a stir bar was charged with aldol adduct **189** (230 mg, 0.433 mmol, 1 equiv). A 1:1 mixture of tetrahydrofuran:methanol (2.1 mL) was added and the vessel was cooled in an ice-water bath. Aqueous sodium hydroxide solution (1.0 M, 0.433 mL, 0.433 mmol, 1 equiv) was added. After 5 minutes, the cooling bath was removed and stirring was continued at 23 °C. Reaction progress was monitored by the consumption of starting material by TLC (10% methanol–dichloromethane + 0.5% saturated aqueous ammonium hydroxide solution). After 20 h, reaction mixture was concentrated and the residue was suspended in water (50 mL) and washed with ether (4 × 50 mL). The first wash with ether was not shaken vigorously in order to prevent the formation of an emulsion. The organic washes were combined and dried over sodium sulfate. The dried organic phase was filtered and the filtrate was concentrated to recover (R,R) -pseudoephedrine (98 mg, 100%, >95% purity), which matched previously reported data.^{110b} The aqueous phase was then washed with dichloromethane (2 × 50 mL). The first wash with dichloromethane was not shaken vigorously in order to prevent the formation of an emulsion. The organic washes were discarded. The remaining aqueous phase was concentrated in vacuo to afford the sodium carboxylate as a white solid (140 mg, 94%). The enantiomeric excess of this product was determined to be $\geq 98\%$ by ¹H NMR comparison of the corresponding (R) - and (S) - MTPA amides.¹³¹ Due to poor solubility in several solvents, this product was characterized as its amine salt: To carboxylate **207** (45.5 mg, 0.132 mmol, 1 equiv)

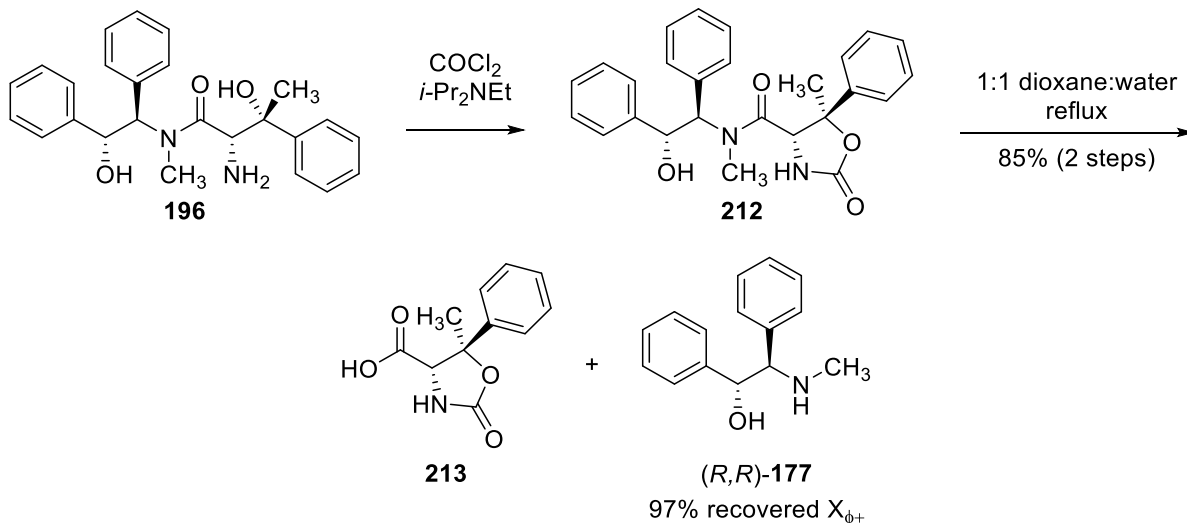
in CD₃OD (0.3 mL) in an NMR test tube was added 1.0 M deuterium chloride solution (0.264 mL, 0.264 mmol, 2 equiv) and the amine salt was characterized. ¹H NMR (500 MHz, CD₃OD), δ: 7.55 (d, 1H, *J* = 2 Hz), 7.47 (d, 2H, *J* = 7.3 Hz), 7.39–7.31 (m, 4H), 7.17 (d, 1H, *J* = 8.3 Hz), 5.24 (d, 1H, *J* = 4.4 Hz), 5.21 (s, 2H), 4.14 (d, 1H, *J* = 4.4 Hz). ¹³C NMR (125 MHz, CD₃OD), δ: 170.2, 155.1, 137.6, 133.7, 129.5, 129.1, 129.1, 128.3, 127.0, 124.1, 115.6, 71.8, 71.0, 60.1. FTIR (neat), cm⁻¹: 3327 (br), 3034 (m), 2926 (m), 1605 (s), 1256 (s), 1059 (s), 696 (s); HRMS (ESI): Calcd for (C₁₆H₁₆ClNO₄ + H)⁺: 322.0846; Found: 322.0861.

Hydrolysis of Aldol adduct **192**, to provide carboxylate **208**.



A 25-mL round bottom flask equipped with a stir bar was charged with aldol adduct **192** (250 mg, 0.73 mmol, 1 equiv). A 1:1 mixture of tetrahydrofuran:methanol (3.65 mL) was added, followed by aqueous sodium hydroxide solution (1.0 M, 0.73 mL, 0.73 mmol, 1 equiv). Reaction progress was monitored by the consumption of starting material by TLC (10% methanol–dichloromethane + 0.5% saturated aqueous ammonium hydroxide solution). After 3 d, reaction mixture was concentrated and the residue was suspended in water (10 mL) and washed with dichloromethane (2 × 10 mL). The combined organic washes were back-extracted with water (2 mL) and the aqueous extract was added to the aqueous phase. The collective aqueous phase was once again extracted with dichloromethane (5 mL) and the organic extract was added to the organic phase. The organic phase was dried over sodium sulfate. The dried organic phase was filtered and the filtrate was concentrated to recover *(R,R)*-pseudoephedrine (162 mg, 98%, >95% purity), which matched previously reported data.^{110b} The aqueous layers were combined and concentrated in vacuo to afford the sodium carboxylate **208** as a white solid (110 mg, 97%). The enantiomeric excess of this product was determined to be ≥98% by ¹H NMR comparison of the corresponding *(R)*- and *(S)*- MTPA amides.¹³¹ ¹H NMR (500 MHz, CD₃OD), δ: 3.12 (br s, 1H), 1.21 (s, 6H). ¹³C NMR (125 MHz, CD₃OD), δ: 180.7, 72.9, 65.2, 26.9, 25.6. FTIR (neat), cm⁻¹: 3362 (br), 2972 (m), 1570 (s), 1408 (s), 1165 (s), 957 (s), 741 (s), 590 (s); HRMS (ESI): Calcd for (C₅H₁₁NO₃ + Na)⁺: 156.0631; Found: 156.0635.

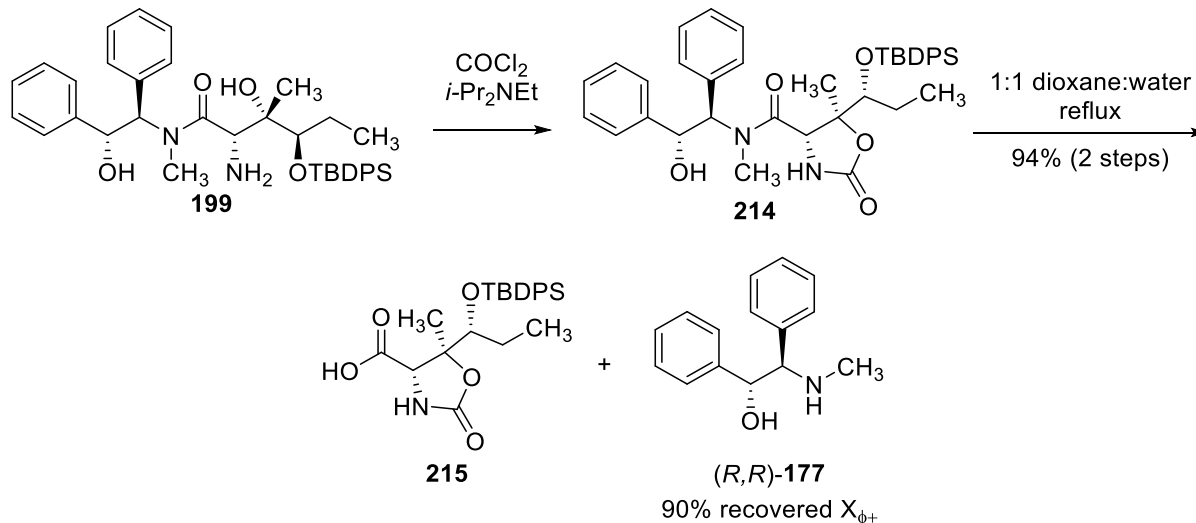
Protection and Neutral Hydrolysis of Aldol Adduct **196**.



Aldol adduct **196** (210 mg, 0.519 mmol, 1 equiv) was dissolved in dichloromethane (5.2 mL), and diisopropylethylamine (0.165 mL, 1.56 mmol, 3 equiv) was added. The reaction vessel was cooled to $-78\text{ }^\circ\text{C}$ in a dry ice-acetone cooling bath and a solution of phosgene in toluene (15% w/w, 0.665 mL, 0.571 mmol, 1.1 equiv) was added dropwise. Reaction progress was monitored by the consumption of starting material by TLC (10% methanol–dichloromethane + 1% saturated aqueous ammonium hydroxide solution, plate developed twice). After 30 minutes, 1 M aqueous hydrochloric acid solution (10 mL) was added, and the reaction vessel was allowed to warm to $23\text{ }^\circ\text{C}$ with vigorous stirring. The layers were separated, and the aqueous layer was extracted with dichloromethane ($2 \times 10\text{ mL}$). The combined organic layers were washed sequentially with 1 M aqueous hydrochloric acid solution (10 mL) and saturated aqueous sodium chloride solution (10 mL). The washed organic phase was dried over a pad of sodium sulfate and the dried organic phase was filtered. The filtrate was concentrated to provide the crude carbamate as a white solid (240 mg). The crude product from this reaction was carried without further purification.

The carbamate (223 mg, 0.519 mmol, 1 equiv) was suspended in 1:1 dioxane:water (10 mL), placed in an oil heating bath, and brought to a vigorous reflux. Reaction progress was monitored by the consumption of starting material by TLC (10% methanol–dichloromethane + 1% saturated aqueous ammonium hydroxide solution). After 24 h, the reaction vessel was allowed to cool to 23 °C and the reaction mixture was concentrated to ~2 mL in vacuo. The resulting suspension was dissolved in water (8 mL) and ether (10 mL), and was stirred vigorously while the pH was adjusted to ~13-14 with 2 M aqueous sodium hydroxide solution. The mixture was transferred to a separatory funnel (quantitated with 2 mL water and 2 mL ether), and the layers were separated. The aqueous layer was washed with diethyl ether (1 × 10 mL), and the combined ether layers were dried through a pad of sodium sulfate and concentrated to recover pseudoephedrine (115 mg, 97%, >95% purity), which matched previously reported data.^{110b} The aqueous layers were acidified to pH 2–3 with 1 M aqueous hydrochloric acid, and the suspension was extracted with dichloromethane (3 × 15 mL) and ethyl acetate (3 × 10 mL). The ethyl acetate layers were washed with 1 M aqueous hydrochloric acid (2 × 5 mL), and the two organic phases were concentrated separately. Each contained pure product **213** and were combined to yield acid **213** as a white solid (98 mg, 85%). TLC (10% methanol–dichloromethane + 1% acetic acid): $R_f = 0.10$ (UV, PMA). ¹H NMR (500 MHz, CD₃OD), δ : 7.51 (d, 2H, $J = 7.3$ Hz), 7.43–7.40 (m, 2H), 7.35–7.32 (m, 1H), 4.44 (s, 1H), 1.69 (s, 3H). ¹³C NMR (125 MHz, CD₃OD), δ : 172.2, 160.5, 145.6, 129.8, 129.2, 125.0, 85.6, 66.5, 25.3. FTIR (neat), cm⁻¹: 3308 (br), 2926 (m), 1732 (s), 1383 (s), 1217 (s), 980 (m), 764 (s) 698 (s); HRMS (ESI): Calcd for (C₁₁H₁₁NO₄ + Na)⁺: 244.0580; Found: 244.0585.

Protection and Neutral Hydrolysis of Aldol Adduct **199**.



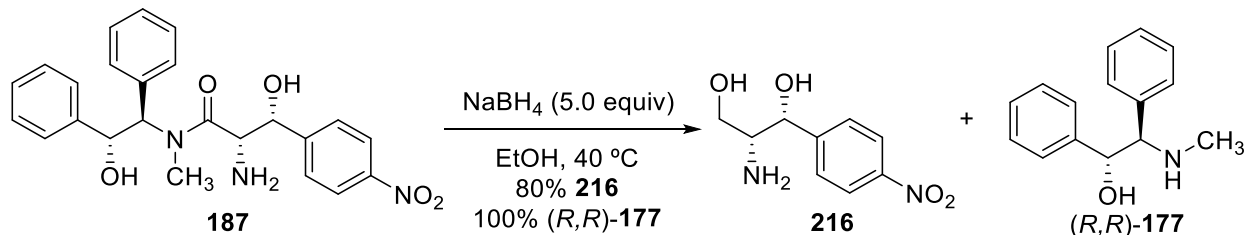
Aldol adduct **199** (28.3 g, 45.3 mmol, 1 equiv) was dissolved in dichloromethane (850 mL), and diisopropylethylamine (23.7 mL, 136 mmol, 3.0 equiv) was added. The reaction vessel was cooled to $-78\text{ }^\circ\text{C}$ in a dry ice-acetone cooling bath and a solution of phosgene in toluene (15% w/w, 37.2 mL, 52.1 mmol, 1.15 equiv) was added dropwise. Reaction progress was monitored by the consumption of starting material by TLC (5% methanol–dichloromethane + 1% saturated aqueous ammonium hydroxide solution). After 30 minutes, half saturated aqueous ammonium chloride solution (800 mL) was added, and the reaction vessel was allowed to warm to $23\text{ }^\circ\text{C}$ with vigorous stirring. The layers were separated, and the aqueous layer was extracted with dichloromethane ($2 \times 250\text{ mL}$). The combined organic layers were washed sequentially with 1 M aqueous hydrochloric acid solution ($2 \times 500\text{ mL}$) and saturated aqueous sodium chloride solution (500 mL). The washed organic phase was dried over a pad of sodium sulfate and the dried organic phase was filtered. The filtrate was concentrated to provide the carbamate **214** as a white solid (29.5 g, 100%). Mp = $128\text{--}130\text{ }^\circ\text{C}$. TLC (5% methanol–dichloromethane): $R_f = 0.28$ (UV, PMA). $^1\text{H NMR}$ (500 MHz, CDCl_3), δ : 7.71–7.66 (m, 4H), 7.43–7.32 (m, 8H), 7.23–7.14 (m, 8H), 6.13 (d, 1H, $J = 10.1\text{ Hz}$), 6.02 (br s, 1H), 5.25 (d, 1H, $J = 10.1\text{ Hz}$), 4.74 (s,

1H), 4.16 (br s, 1 H), 3.81 (dd, 1H, $J = 6.4$ Hz, 4.1 Hz), 2.83 (s, 3H), 1.65–1.58 (m, 1H), 1.56–1.51 (m, 1H), 1.15 (s, 3 H), 1.03 (s, 9H). 0.60 (t, 3H, $J = 7.3$ Hz). ^{13}C NMR (125 MHz, CDCl_3), δ : 171.1, 159.4, 141.0, 136.1, 135.8, 135.7, 133.8, 132.4, 129.9, 129.7, 129.1, 128.3, 127.8, 127.7, 127.5, 87.2, 78.3, 71.9, 63.0, 57.7, 30.7, 27.0, 25.7, 19.6, 16.9, 11.3. FTIR (neat), cm^{-1} : 3341 (br), 3070 (m), 2940 (s), 2859 (m), 1759 (s), 1633 (s), 1103 (s) 700 (s); HRMS (ESI): Calcd for $(\text{C}_{39}\text{H}_{46}\text{N}_2\text{O}_5\text{Si} + \text{H})^+$: 651.3249; Found: 651.3244.

Carbamate **214** (250 mg, 0.384 mmol, 1 equiv) was suspended in 1:1 dioxane:water (25 mL) in a 50-mL round-bottom flask. The vessel was immersed in an oil bath and the suspension was brought to reflux. After 44 h, the reaction vessel was allowed to cool to 23 °C and the resulting suspension was evaporated under reduced pressure. The residue was partitioned between 1 M aqueous hydrochloric acid solution (20 mL) and ether (20 mL), and the layers were mixed vigorously and separated. The aqueous layer was extracted with ether (2×20 mL), and the combined organic layers were washed with 1 M aqueous hydrochloric acid solution (20 mL), saturated aqueous sodium chloride solution (20 mL), and the washed organic solution was dried with sodium sulfate. The dried solution was filtered and the filtrate was concentrated to provide acid **215** as a white solid (160 mg, 94%). The product was found to contain $\leq 8\%$ of an impurity that was identified as TBDPS-OH. TLC (10% methanol–dichloromethane + 1% acetic acid): $R_f = 0.50$ (UV, PMA). ^1H NMR (500 MHz, CD_3OD), δ : 7.77–7.67 (m, 4H), 7.47–7.33 (m, 6H), 6.98 (br s, 1H), 4.78 (s, 1H), 3.76 (t, 1H, $J = 5.3$ Hz), 1.69–1.57 (m, 1H), 1.50–1.38 (m, 4H), 1.05 (s, 9H), 0.53 (t, 3H, $J = 7.6$ Hz). ^{13}C NMR (125 MHz, CD_3OD), δ : 173.0, 160.0, 136.1, 135.8, 134.0, 132.3, 129.9, 129.7, 127.7, 127.5, 88.3, 78.9, 58.6, 26.9, 25.5, 19.5, 19.0, 11.2. FTIR (neat), cm^{-1} : 3267 (br), 2932 (m), 2889 (m), 1744 (s), 1688 (s), 1219 (m), 1111 (s) 907 (s); HRMS (ESI): Calcd for $(\text{C}_{24}\text{H}_{31}\text{NO}_5 + \text{H})^+$: 442.2044; Found: 442.2058.

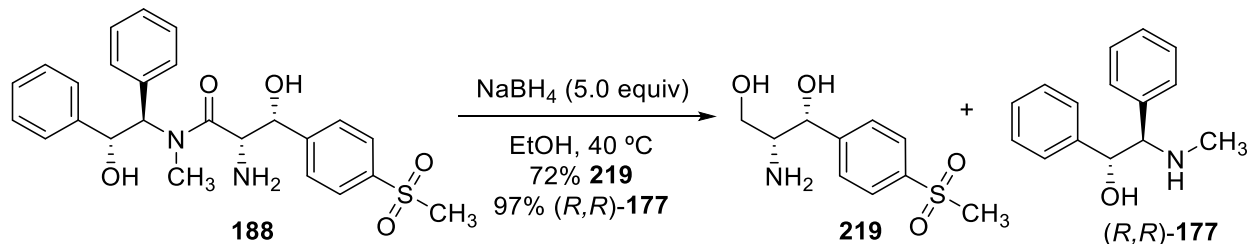
The aqueous layers were combined and were brought to pH 14 by the addition of 2 M sodium hydroxide solution (50 mL). The resulting suspension was extracted with dichloromethane (2×20 mL). The organic phases were combined and the resulting solution was washed with saturated aqueous sodium chloride solution (15 mL) and dried over sodium sulfate. The dried solution was filtered and the filtrate was concentrated to provide pseudoephedrine (79 mg, 90%), which matched previously reported data.^{110b}

Reduction of Aldol Adduct **187** to Provide Amino Diol **216** and Pseudoephedrine (*R,R*)-**177**.



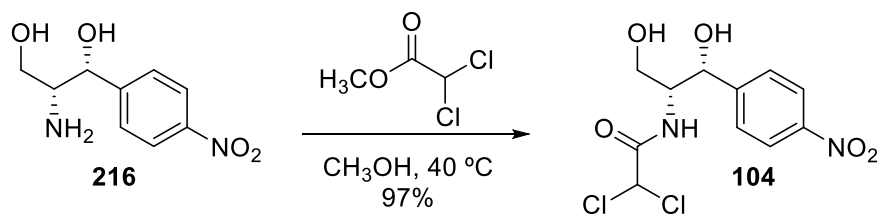
A 100 mL round bottom flask equipped with a stir bar was charged with aldol adduct **187** (420 mg, 0.964 mmol, 1 equiv). 200-Proof ethanol (19.3 mL) was added, followed by sodium borohydride (182 mg, 4.82 mmol, 5 equiv) in one portion. The reaction vessel was placed in an oil heating bath and warmed to 40 °C. Reaction progress was monitored by the consumption of starting material by TLC (10% methanol–dichloromethane + 0.5% saturated aqueous ammonium hydroxide solution). After 15 h, the reaction mixture was allowed to cool to 23 °C and saturated aqueous ammonium chloride solution was added carefully until gas evolution ceased (~1.5 mL). The reaction mixture was diluted with methanol (5 mL) and then concentrated in vacuo and loaded directly onto a column. The reaction mixture was purified by column chromatography (5→15% methanol–dichloromethane + 1% saturated aqueous ammonium hydroxide solution) to provide both (*R,R*)-pseudoephedrine (219 mg, 100%, >95% purity) which matched previously reported data,^{110b} and amino diol **216** (163 mg, 80%). ¹H NMR (500 MHz, CD₃OD), δ: 8.22 (d, 2H, *J* = 8.8 Hz), 7.63 (d, 2H, *J* = 8.8 Hz), 4.79 (d, 1H, *J* = 5.9 Hz), 3.53 (dd, 1H, *J* = 10.7 Hz, 4.9 Hz), 3.39 (dd, 1H, *J* = 11.2 Hz, 6.4 Hz), 3.39 (dd, 1H, *J* = 11.2 Hz, 5.4 Hz). ¹³C NMR (125 MHz, CD₃OD), δ: 152.3, 148.7, 128.6, 124.3, 74.0, 74.0, 59.8. FTIR (neat), cm⁻¹: 3376 (br), 2963 (m), 2914 (m), 1514 (s), 1344 (s), 835 (s), 700 (s); HRMS (ESI): Calcd for (C₉H₁₂N₂O₄ + H)⁺: 213.0870; Found: 213.0875.

Reduction of Aldol Adduct **188** to Provide Amino Diol **219** and Pseudoephedrine (*R,R*)-**177**.



A 100 mL round bottom flask equipped with a stir bar was charged with aldol adduct **188** (454 mg, 0.969 mmol, 1 equiv). 200-Proof ethanol (19.4 mL) was added, followed by sodium borohydride (183 mg, 4.84 mmol, 5 equiv) in one portion. The reaction vessel was placed in an oil heating bath and warmed to 40 °C. Reaction progress was monitored by the consumption of starting material by TLC (10% methanol–dichloromethane + 0.5% saturated aqueous ammonium hydroxide solution). After 8 h, the reaction mixture was allowed to cool to 23 °C and saturated aqueous ammonium chloride solution was added carefully until gas evolution ceased (~1.5 mL). The reaction mixture was diluted with methanol (5 mL) and then concentrated in vacuo and loaded directly onto a column. The reaction mixture was purified by column chromatography (10→30% methanol–dichloromethane + 1% saturated aqueous ammonium hydroxide solution) to provide both (*R,R*)-pseudoephedrine (213 mg, 97%, >95% purity) which matched previously reported data,^{110b} and amino diol **219** (172 mg, 72%). ¹H NMR (500 MHz, CD₃OD), δ: 7.94 (d, 2H, *J* = 8.8 Hz), 7.66 (d, 2H, *J* = 8.3 Hz), 4.78 (d, 1H, *J* = 5.9 Hz), 3.53 (dd, 1H, *J* = 10.7 Hz, 4.9 Hz), 3.39 (dd, 1H, *J* = 11.2 Hz, 6.4 Hz), 3.12 (s, 3H), 3.39 (dd, 1H, *J* = 11.2 Hz, 5.9 Hz). ¹³C NMR (125 MHz, CD₃OD), δ: 151.0, 141.0, 128.6, 128.4, 74.0, 63.8, 59.8, 44.4. FTIR (neat), cm⁻¹: 3349 (br), 2926 (m), 1707 (m), 1302 (s), 1148 (s), 1051 (s), 768 (s), 542 (s); HRMS (ESI): Calcd for (C₁₀H₁₅NO₄S + Na)⁺: 268.0614; Found: 268.0624.

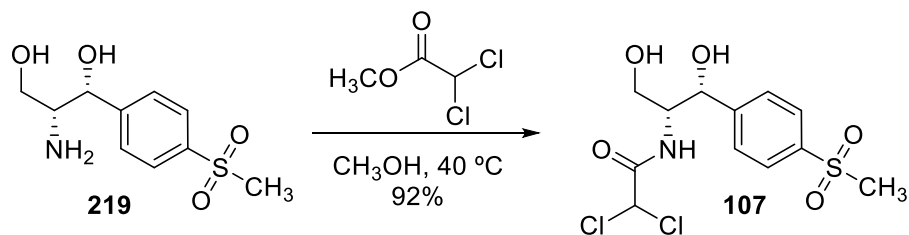
Acylation of Amino Diol **216**: The Synthesis of Chloramphenicol (**104**).



A 25 mL round bottom flask equipped with a stir bar was charged with amino diol **216** (143 mg, 0.674 mmol, 1 equiv). Methanol (2.7 mL) was added, followed by methyl dichloroacetate (0.21 mL, 2.02 mmol, 3 equiv). The reaction vessel was placed in an oil heating bath and warmed to 40 °C, at which time complete dissolution of the starting material was achieved. Reaction progress was monitored by the consumption of starting material by TLC (10% methanol–dichloromethane + 0.5% saturated aqueous ammonium hydroxide solution). After 9 h, the reaction mixture was allowed to cool to 23 °C and the reaction mixture was concentrated in vacuo, providing the title compound as a light yellow solid (211 mg, 97%) which corresponded with previously reported data.¹³²

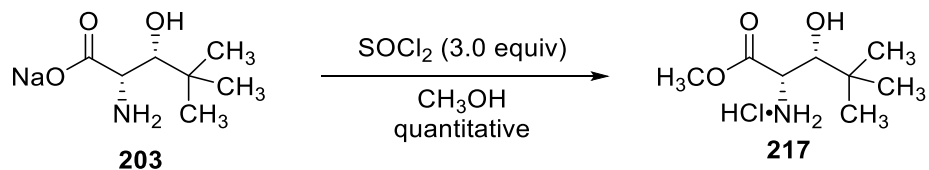
¹³² C. R. Mateus, F. Coelho, *J. Braz. Chem. Soc.* **2005**, *16*, 386–396.

Acylation of Amino Diol **219**: The Synthesis of Thiamphenicol (**107**).



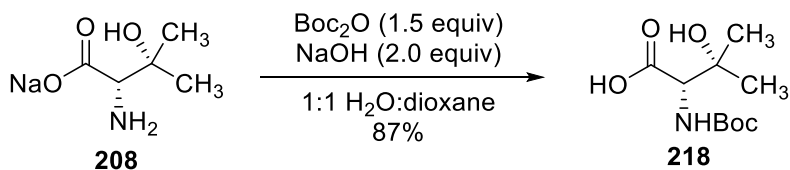
A 25 mL round bottom flask equipped with a stir bar was charged with amino diol **219** (153 mg, 0.624 mmol, 1 equiv). Methanol (2.5 mL) was added, followed by methyl dichloroacetate (0.190 mL, 1.87 mmol, 3 equiv). The reaction vessel was placed in an oil heating bath and warmed to $40\text{ }^\circ\text{C}$, at which time complete dissolution of the starting material was achieved. Reaction progress was monitored by the consumption of starting material by TLC (10% methanol–dichloromethane + 0.5% saturated aqueous ammonium hydroxide solution). After 16 h, the reaction mixture was allowed to cool to $23\text{ }^\circ\text{C}$ and the reaction mixture was concentrated in vacuo. The residue was purified by column chromatography (10% methanol–dichloromethane), providing thiamphenicol as a white solid (204 mg, 92%) which matched previously reported data.¹³²

Functionalization of carboxylate **203** to provide the ester hydrochloride **217**.



A 25-mL round bottom flask equipped with a stir bar and a reflux condenser was charged with carboxylate **203** (100 mg, 0.546 mmol, 1 equiv). Methanol (2.6 mL) was added and the reaction vessel was placed in an ice water cooling bath. Thionyl chloride (0.120 mL, 1.64 mmol, 3 equiv) was added dropwise and then the cooling bath was removed. The reaction vessel was placed in an oil heating bath and brought to reflux. Reaction progress was monitored by the consumption of starting material by ¹H NMR (in CD₃OD) analysis of aliquots removed from the reaction mixture. After 4 h, reaction mixture was allowed to cool to 23 °C and concentrated in vacuo. The crude residue was taken up in chloroform (2 mL) and filtered through a pad of Celite. The organic phase was concentrated to afford the ester hydrochloride **217** as a yellow oil in quantitative yield. ¹H NMR (500 MHz, CD₃OD), δ: 4.14 (d, 1H, *J* = 2.8 Hz), 3.86 (s, 3H), 3.78 (d, 1H, *J* = 2.8 Hz), 0.99 (s, 9H). ¹³C NMR (125 MHz, CD₃OD), δ: 171.0, 76.5, 54.7, 53.9, 36.3, 26.1. FTIR (neat), cm⁻¹: 3227 (br), 2959 (s), 2874 (m), 1746 (s), 1441 (s), 1229 (s), 1018 (s): HRMS (ESI): Calcd for (C₈H₁₇NO₃ + Na)⁺: 198.1101; Found: 198.1101.

Boc protection of amino carboxylate **208**.

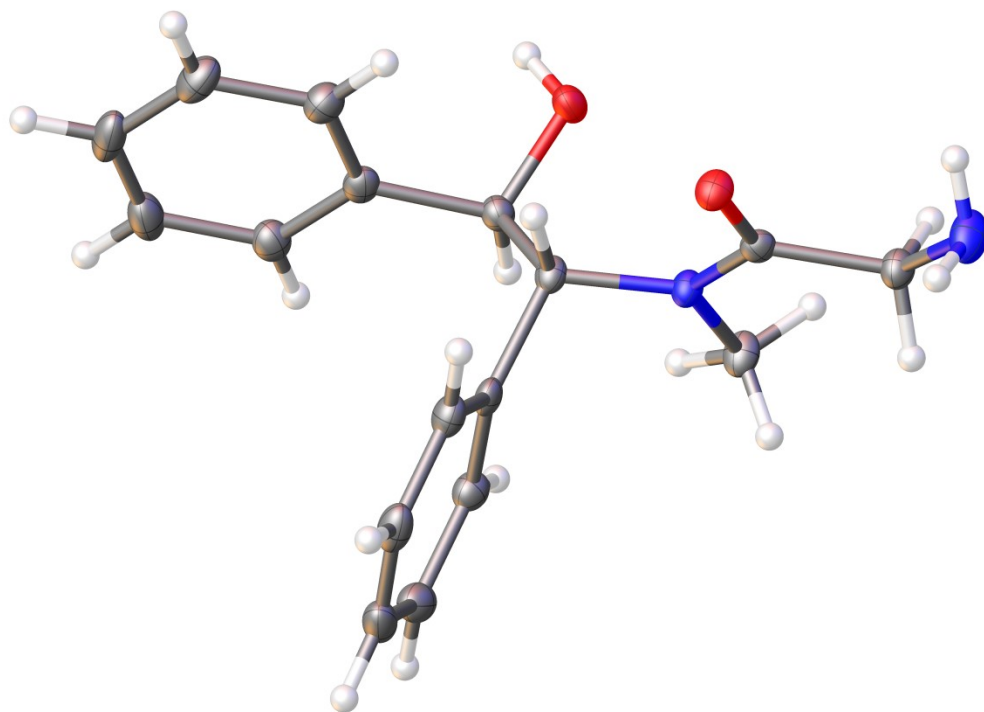
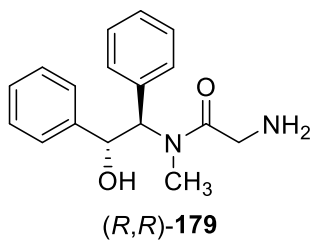


A 25-mL round bottom flask equipped with a stir bar was charged with carboxylate **25** (110 mg, 0.709 mmol, 1 equiv). A 1:1 mixture of water:1,4-dioxane (6.0 mL) was added and the reaction vessel was placed in an ice water cooling bath. Aqueous sodium hydroxide solution (1.0 M, 1.42 mL, 1.42 mmol, 2 equiv) was added, followed by di-*tert*-butyl dicarbonate (2.47 mL, 1.06 mmol, 1.5 equiv). The cooling bath was removed after 5 minutes and the vessel continued to stir at 23 °C. Reaction progress was monitored by the consumption of starting material by ¹H NMR (in CD₃OD) analysis of aliquots removed from the reaction mixture. After 20 h, water (5 mL) was added and the mixture was washed with one portion of ether (20 mL). The aqueous phase was then placed in an ice-water cooling bath and 1 M aqueous hydrochloric acid solution was added dropwise to pH 2. The acidified aqueous phase was then extracted with ethyl acetate (3 × 25 mL). The organic extracts were combined and were dried over sodium sulfate. The dried organic phase was filtered and the filtrate was concentrated to provide the *N*-Boc-protected acid **29** (144 mg, 87%) as a light yellow oil which matched previously reported data.¹³³

¹³³ J. E. Dettwiler, W. D. Lubell, *J. Org. Chem.* **2003**, 68, 177–179.

X-ray Crystallographic Laboratory Structure Report

Shao-Liang Zheng, Harvard University



X-Ray Crystallography

A crystal mounted on a diffractometer was collected data at 100 K. The intensities of the reflections were collected by means of a Bruker APEX II DUO CCD diffractometer ($\text{CuK}\alpha$ radiation, $\lambda=1.54178 \text{ \AA}$), and equipped with an Oxford Cryosystems nitrogen flow apparatus. The collection method involved 1.0° scans in ω at 30° , 55° , 80° and 115° in 2θ . Data integration down to 0.84 \AA resolution was carried out using SAINT V8.30 A¹³⁴ with reflection spot size optimization. Absorption corrections were made with the program SADABS.¹³⁴ The structure was solved by the direct methods procedure and refined by least-squares methods against F^2 using SHELXS-2013 and SHELXL-2013⁶⁶ with OLEX 2 interface.¹³⁵ Non-hydrogen atoms were refined anisotropically, and hydrogen atoms were allowed to ride on the respective atoms. Crystal data as well as details of data collection and refinement are summarized in Table E3. The Ortep plots produced with SHELXL-2013 program, and the other drawings were produced with Accelrys DS Visualizer 2.0.⁶⁷

¹³⁴ Bruker AXS APEX II, Bruker AXS, Madison, Wisconsin, 2013.

¹³⁵ O. V. Dolomanov, L. J. Bourhis, R. J. Gildea, J. A. K. Howard and H. Puschmann, *J. Appl. Cryst.* **2009**, *42*, 339–341.

Table E3: Experimental details.

Crystal data	
Chemical formula	C ₁₇ H ₂₀ N ₂ O ₂
M_r	284.35
Crystal system, space group	Orthorhombic, $P2_12_12_1$
Temperature (K)	100
a, b, c (Å)	6.7671 (2), 14.6871 (3), 14.9526 (3)
V (Å ³)	1486.12 (6)
Z	4
Radiation type	Cu $K\alpha$
μ (mm ⁻¹)	0.67
Crystal size (mm)	0.28 × 0.24 × 0.16
Data collection	
Diffractometer	Bruker D8 goniometer with CCD area detector diffractometer
Absorption correction	Multi-scan <i>SADABS</i>
T_{\min}, T_{\max}	0.693, 0.753
No. of measured, independent and observed [$I > 2\sigma(I)$] reflections	36350, 2592, 2570
R_{int}	0.028
$(\sin \theta/\lambda)_{\text{max}}$ (Å ⁻¹)	0.596
Refinement	
$R[F^2 > 2\sigma(F^2)], wR(F^2), S$	0.024, 0.062, 1.08
No. of reflections	2592
No. of parameters	204
No. of restraints	0
H-atom treatment	H atoms treated by a mixture of independent and constrained refinement
$\Delta\rho_{\text{max}}, \Delta\rho_{\text{min}}$ (e Å ⁻³)	0.19, -0.14
Absolute structure	Flack x determined ¹³⁶ using 1046 quotients [(I+)-(I-)]/[(I+)+(I-)].
Absolute structure parameter	0.02 (4)

Computer programs: *APEX2* v2013.4.1 (Bruker-AXS, 2013), *SAINT* 8.30A (Bruker-AXS, 2012), *SHELXS2013* (Sheldrick, 2013), *SHELXL2013* (Sheldrick, 2013), Bruker *SHELXTL* (Sheldrick, 2013).

¹³⁶ Parsons and Flack, *Acta Cryst* **2004**, *A60*, s61.

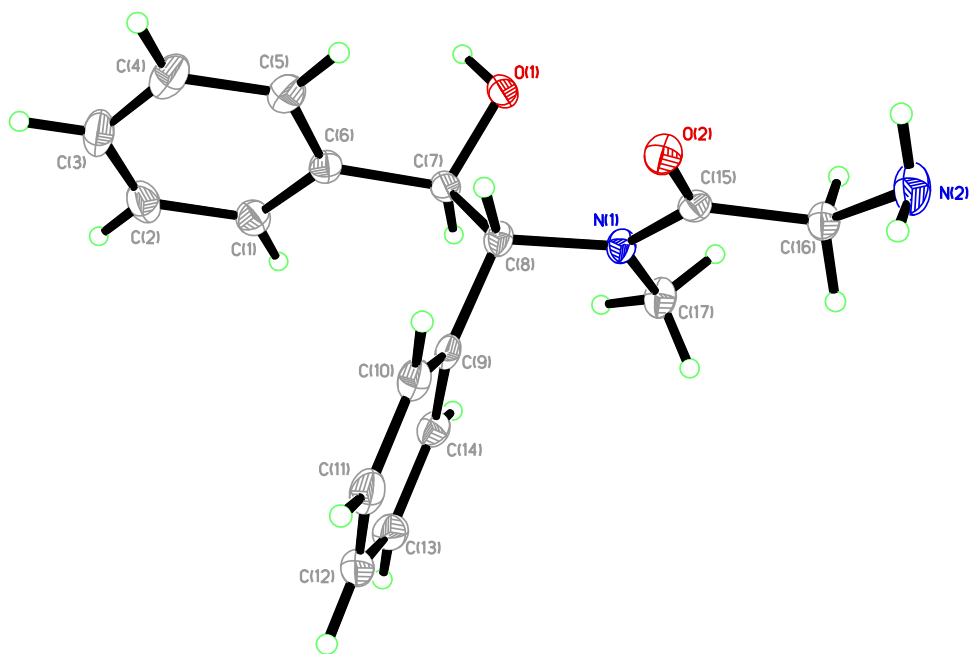


Figure E5: Perspective views showing 50% probability displacement.

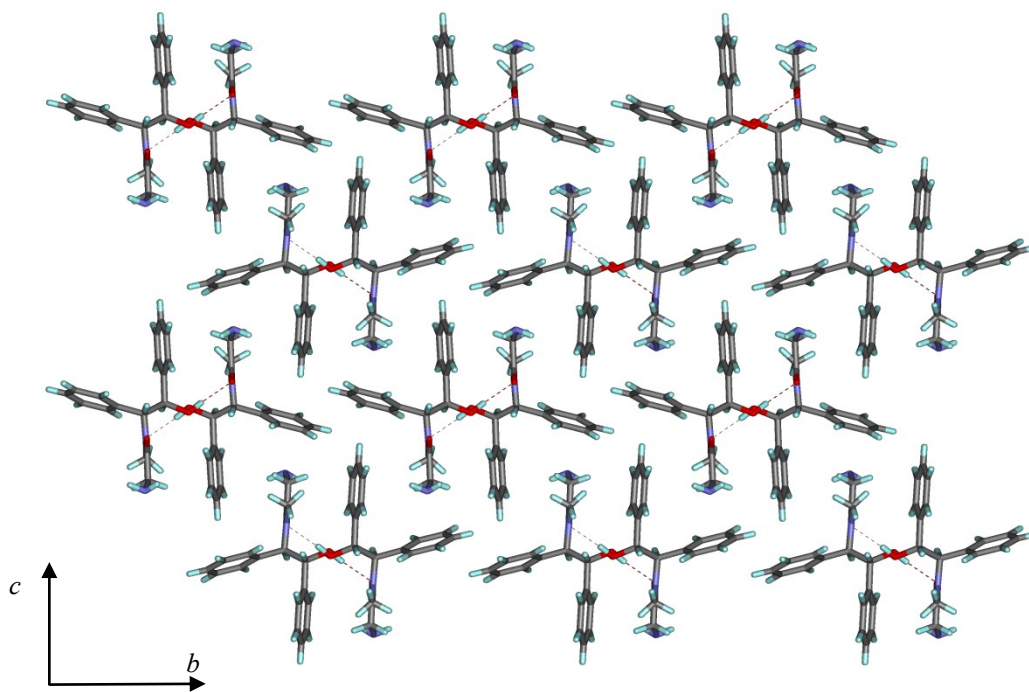
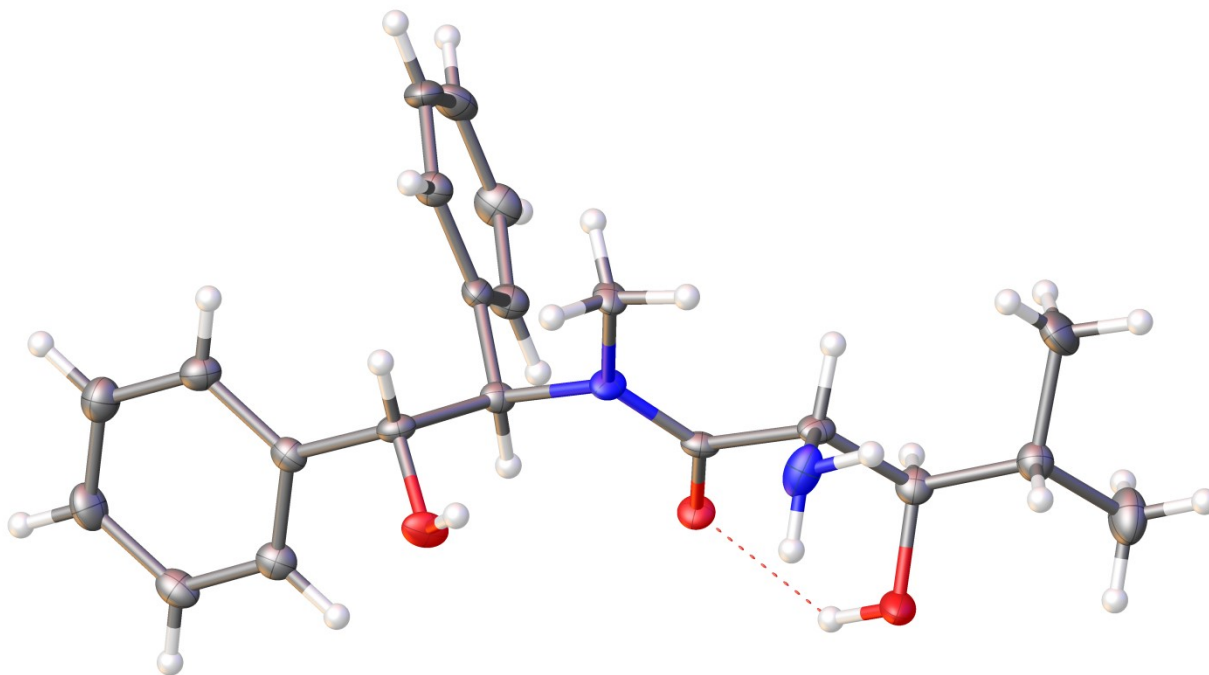
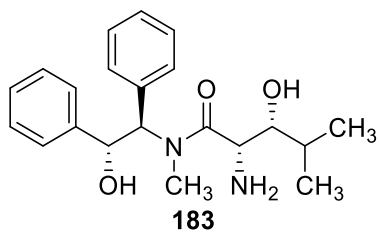


Figure E6: Three-dimensional supramolecular architecture viewed along the *a*-axis direction.

X-ray Crystallographic Laboratory Structure Report

Shao-Liang Zheng, Harvard University



X-Ray Crystallography

A crystal mounted on a diffractometer was collected data at 100 K. The intensities of the reflections were collected by means of a Bruker APEX II DUO CCD diffractometer ($\text{Cu}_{\text{K}\alpha}$ radiation, $\lambda=1.54178 \text{ \AA}$), and equipped with an Oxford Cryosystems nitrogen flow apparatus. The collection method involved 1.0° scans in ω at 30° , 55° , 80° and 115° in 2θ . Data integration down to 0.84 \AA resolution was carried out using SAINT V8.30 A¹³⁴ with reflection spot size optimization. Absorption corrections were made with the program SADABS.¹³⁴ The structure was solved by the direct methods procedure and refined by least-squares methods against F^2 using SHELXS-2013 and SHELXL-2013⁶⁶ with OLEX 2 interface.¹³⁵ Non-hydrogen atoms were refined anisotropically, and hydrogen atoms were allowed to ride on the respective atoms. Crystal data as well as details of data collection and refinement are summarized in Table E4. The Ortep plots produced with SHELXL-2013 program, and the other drawings were produced with Accelrys DS Visualizer 2.0.⁶⁷

Table E4: Experimental details.

Crystal data	
Chemical formula	C ₂₁ H ₂₈ N ₂ O ₃
M_r	356.45
Crystal system, space group	Monoclinic, $P2_1$
Temperature (K)	100
a, b, c (Å)	12.4892 (4), 6.1263 (2), 12.4919 (4)
β (°)	93.300 (2)
V (Å ³)	954.20 (5)
Z	2
Radiation type	Cu $K\alpha$
μ (mm ⁻¹)	0.66
Crystal size (mm)	0.18 × 0.03 × 0.02
Data collection	
Diffractometer	Bruker D8 goniometer with CCD area detector diffractometer
Absorption correction	Multi-scan <i>SADABS</i>
T_{\min}, T_{\max}	0.490, 0.753
No. of measured, independent and observed [$I > 2\sigma(I)$] reflections	14252, 3128, 3115
R_{int}	0.063
$(\sin \theta/\lambda)_{\text{max}}$ (Å ⁻¹)	0.596
Refinement	
$R[F^2 > 2\sigma(F^2)], wR(F^2), S$	0.044, 0.110, 1.04
No. of reflections	3128
No. of parameters	255
No. of restraints	1
H-atom treatment	H atoms treated by a mixture of independent and constrained refinement
$\Delta\rho_{\text{max}}, \Delta\rho_{\text{min}}$ (e Å ⁻³)	0.29, -0.22
Absolute structure	Flack x determined ¹³⁶ using 1312 quotients [(I+)-(I-)]/[(I+)+(I-)].
Absolute structure parameter	-0.3 (3)

Computer programs: *APEX2* v2013.4.1 (Bruker-AXS, 2013), *SAINT* 8.30A (Bruker-AXS, 2012), *SHELXS2013* (Sheldrick, 2013), *SHELXL2013* (Sheldrick, 2013), Bruker *SHELXTL* (Sheldrick, 2013).

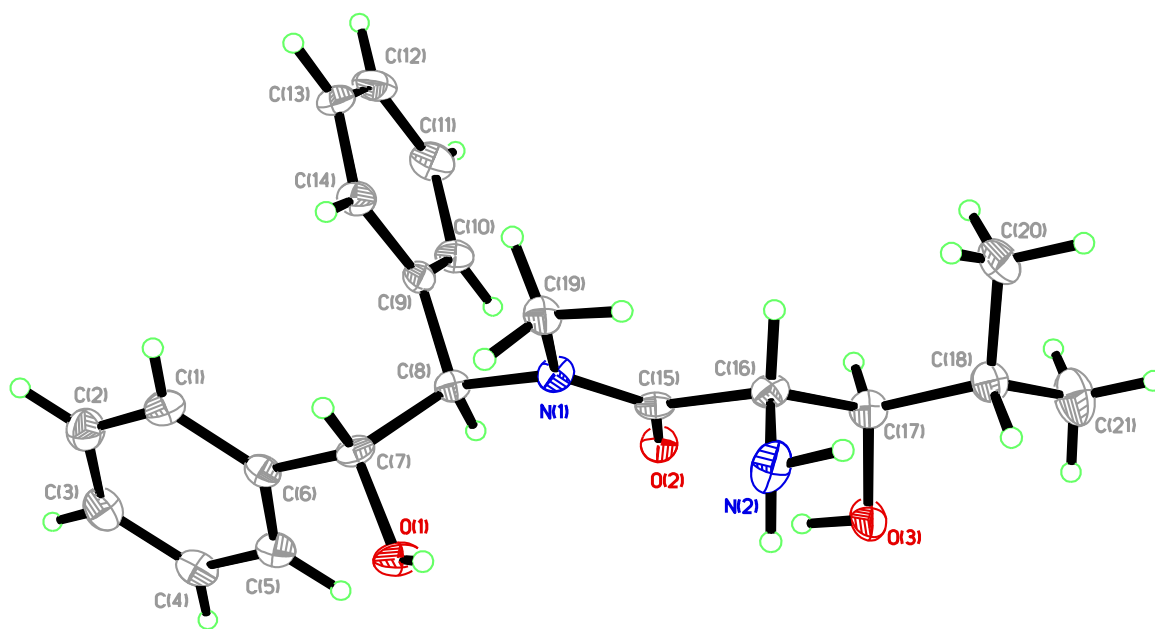


Figure E7: Perspective views showing 50% probability displacement.

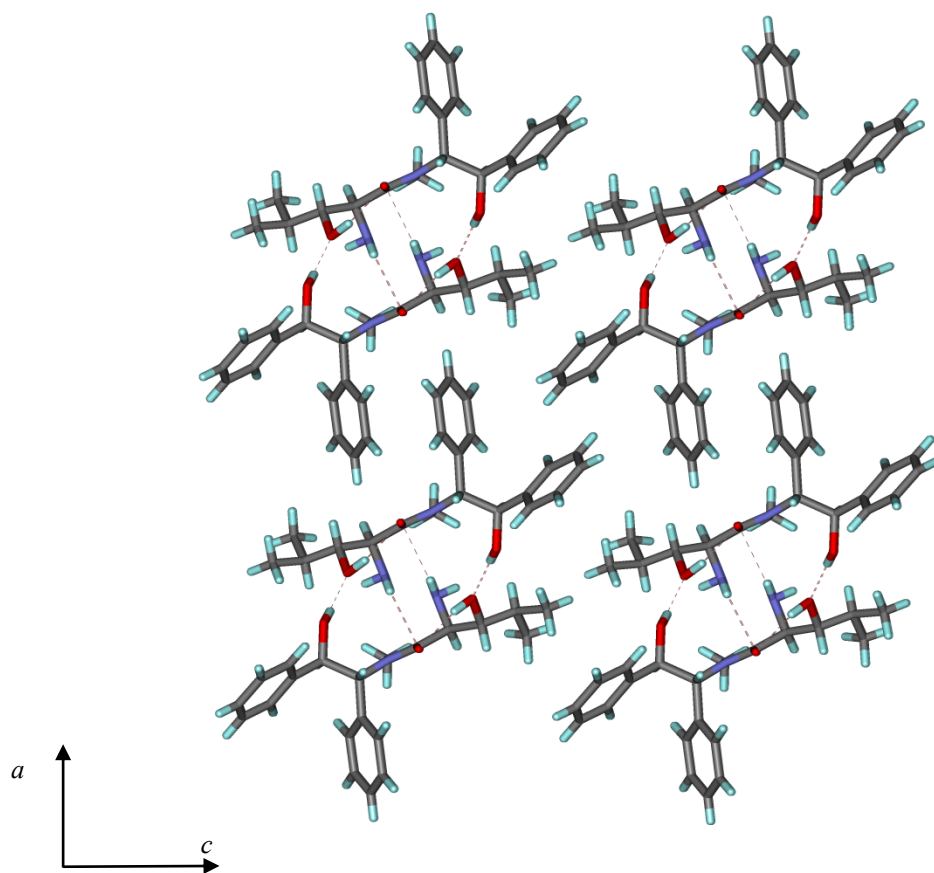
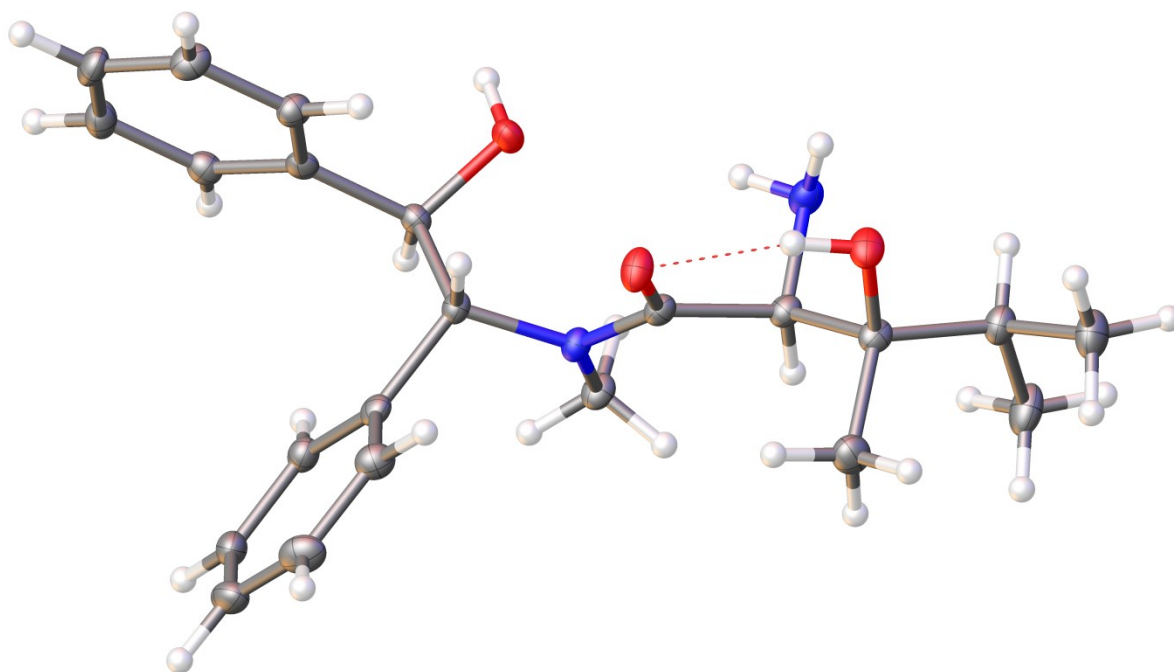
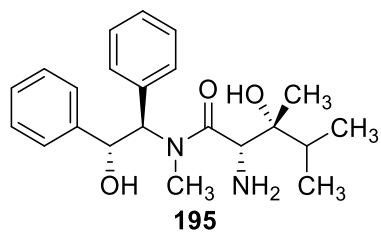


Figure E8: Three-dimensional supramolecular architecture viewed along the *b*-axis direction.

X-ray Crystallographic Laboratory Structure Report

Shao-Liang Zheng, Harvard University



X-Ray Crystallography

A crystal mounted on a diffractometer was collected data at 100 K. The intensities of the reflections were collected by means of a Bruker APEX II DUO CCD diffractometer ($\text{Cu}_{\text{K}\alpha}$ radiation, $\lambda=1.54178 \text{ \AA}$), and equipped with an Oxford Cryosystems nitrogen flow apparatus. The collection method involved 1.0° scans in ω at 30° , 55° , 80° and 115° in 2θ . Data integration down to 0.84 \AA resolution was carried out using SAINT V8.30 A¹³⁴ with reflection spot size optimization. Absorption corrections were made with the program SADABS.¹³⁴ The structure was solved by the direct methods procedure and refined by least-squares methods against F^2 using SHELXS-2013 and SHELXL-2013⁶⁶ with OLEX 2 interface.¹³⁵ Non-hydrogen atoms were refined anisotropically, and hydrogen atoms were allowed to ride on the respective atoms. Crystal data as well as details of data collection and refinement are summarized in Table E5. The Ortep plots produced with SHELXL-2013 program, and the other drawings were produced with Accelrys DS Visualizer 2.0.⁶⁷

Table E5: Experimental details.

Crystal data	
Chemical formula	C ₂₂ H ₃₂ N ₂ O ₄
M_r	388.49
Crystal system, space group	Monoclinic, $P2_1$
Temperature (K)	100
a, b, c (Å)	10.0576 (2), 7.5081 (2), 14.2721 (3)
β (°)	100.2676 (8)
V (Å ³)	1060.48 (4)
Z	2
Radiation type	Cu $K\alpha$
μ (mm ⁻¹)	0.67
Crystal size (mm)	0.20 × 0.14 × 0.10
Data collection	
Diffractometer	Bruker D8 goniometer with CCD area detector diffractometer
Absorption correction	Multi-scan <i>SADABS</i>
T_{\min}, T_{\max}	0.549, 0.753
No. of measured, independent and observed [$I > 2\sigma(I)$] reflections	26005, 3570, 3547
R_{int}	0.050
$(\sin \theta/\lambda)_{\text{max}}$ (Å ⁻¹)	0.594
Refinement	
$R[F^2 > 2\sigma(F^2)], wR(F^2), S$	0.035, 0.090, 1.02
No. of reflections	3570
No. of parameters	281
No. of restraints	1
H-atom treatment	H atoms treated by a mixture of independent and constrained refinement
$\Delta\rho_{\text{max}}, \Delta\rho_{\text{min}}$ (e Å ⁻³)	0.17, -0.20
Absolute structure	Flack x determined ¹³⁶ using 1570 quotients [(I+)-(I-)]/[(I+)+(I-)].
Absolute structure parameter	-0.10 (15)

Computer programs: *APEX2* v2013.4.1 (Bruker-AXS, 2013), *SAINT* 8.30A (Bruker-AXS, 2012), *SHELXS2013* (Sheldrick, 2013), *SHELXL2013* (Sheldrick, 2013), Bruker *SHELXTL* (Sheldrick, 2013).

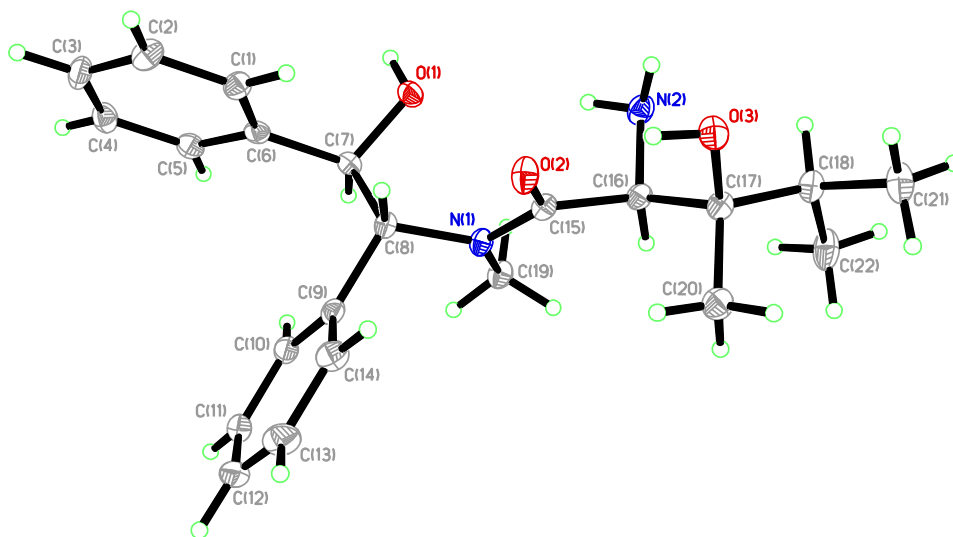


Figure E9: Perspective views showing 50% probability displacement.

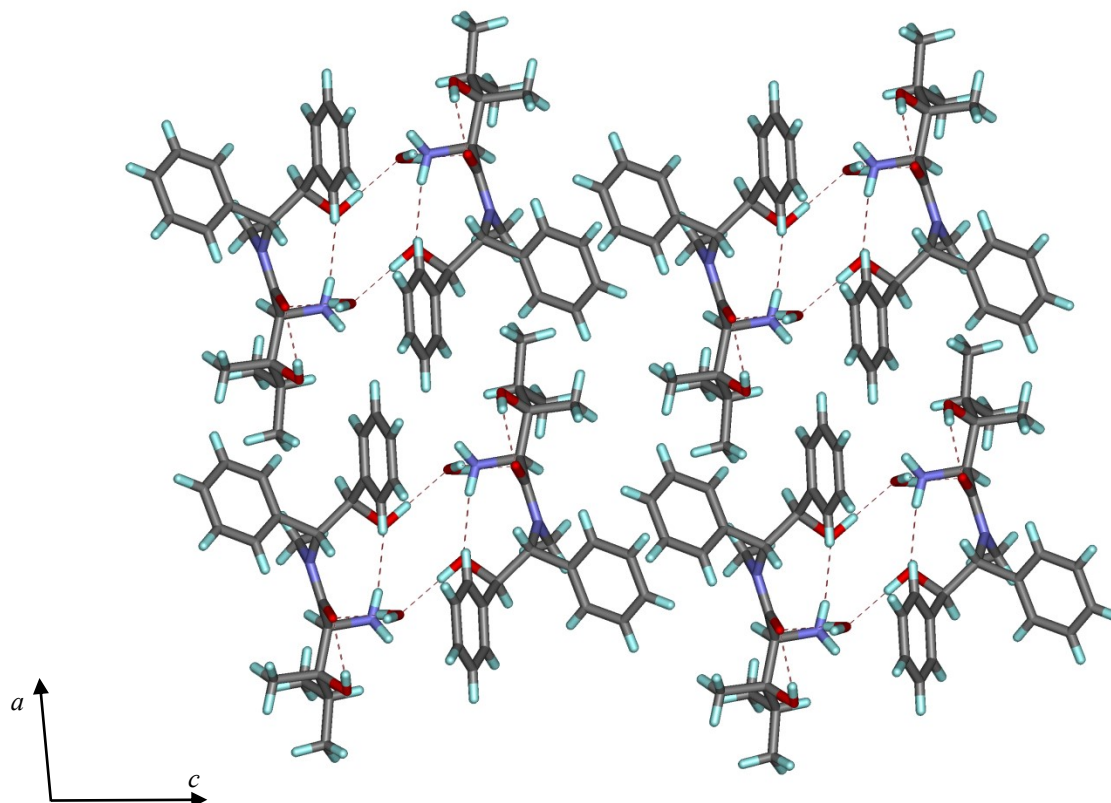


Figure E10: Three-dimensional supramolecular architecture viewed along the *b*-axis direction.

Chapter 4

Synthesis of Monobactams through the Aldolization of Pseudoephedrine Glycinamide

Monocyclic β -Lactams (Monobactams)

Monocyclic β -lactams, also known as monobactams, are a class of antibacterial agents that primarily target Gram-negative pathogens. Like other β -lactam antibiotics, monobactams bind to penicillin-binding protein 3, inhibiting cell wall synthesis and causing cell death. Weakly bioactive natural monocyclic β -lactams **220** and **221** were isolated simultaneously in 1981 at Takeda Pharmaceuticals¹³⁷ in Japan and Squibb¹³⁸ in the United States (Figure 4.1). Inspired by the potential these molecules possessed, multiple research platforms were launched toward the study of additional monobactams through both semi-synthetic¹³⁹ and fully synthetic methods.¹⁴⁰

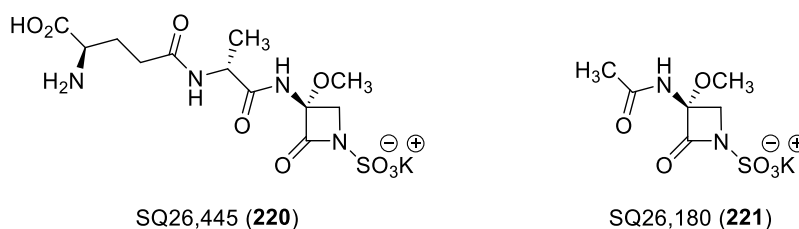


Figure 4.1: Naturally occurring monocyclic β -lactam antibiotics.

¹³⁷ Imada, A.; Kitano, K.; Muroi, M.; Asai, M. *Nature* **1981**, *289*, 590–591.

¹³⁸ Sykes, R. B.; Cimarusti, C. M.; Bonner, D. P.; Bush, K.; Floyd, D. M.; Georgopapadakou, N. H.; Koster, W. H.; Liu, W. C.; Parker, W. L.; Principe, P. A.; Rathnum, M. L.; Slusarchyk, W. A.; Trejo, W. H.; Wells, J. S. *Nature* **1981**, *291*, 489–491.

¹³⁹ Selected examples of semi-synthetic methods, see: (a) Cimarusti, C. M.; Bonner, D. P.; Bruer, H.; Chang, H.W.; Fritz, A. W.; Floyd, D. M.; Kissick, T.P.; Koster, W. H.; Kronenthal, D.; Massa, F.; Mueller, R. H.; Pluscec, J.; Slusarchyk, W.A.; Sykes, R.B.; Weaver, E.R. *Tetrahedron* **1983**, *39*, 2577–2589. (b) Matsuo, T.; Sugawara, T.; Masuya, H.; Kawano, Y.; Noguchi, N.; Ochiai, M. *Chem. Pharm. Bull.* **1983**, *31*, 1874–1884. (c) Matsuo, T.; Masuya, H.; Sugawara, T.; Kawano, Y.; Noguchi, N.; Ochiai, M. *Chem. Pharm. Bull.* **1983**, *31*, 2200–2208. (d) Arnould, J.; Boutron, P.; Pasquet, M. *Eur. J. Med. Chem.* **1992**, *27*, 131–140.

¹⁴⁰ For a review, see Thomas, R. C. Synthetic Aspects of Monocyclic β -Lactam Antibiotics. In *Recent Progress in the Chemical Synthesis of Antibiotics*, Lukacs, G., Ohno, M., Eds.; Springer-Verlag: Berlin, Heidelberg, 1990; 533–564, and references cited therein.

Later in 1981, Squibb scientists reported the synthesis of compound SQ 26,776, later renamed aztreonam (**103**), a potent Gram-negative antibiotic agent (Figure 4.2).¹⁴¹ Aztreonam was discovered by screening monocyclic β -lactam cores with varied substitution patterns at C4, as well as by investigation of common cephalosporin acyl side chains on the C3-amine and the identity of the activating group on the lactam nitrogen.¹⁴² Critical for the resulting biological activity of monobactams, these three parameters can be tuned to promote Gram-positive, Gram-negative or, in some cases, broad spectrum antibacterial activity.¹⁴³ Aztreonam itself was optimized for Gram-negative antibiotic activity, especially against virulent *Pseudomonas aeruginosa*, a naturally antibiotic-resistant species responsible for nosocomial infections. The most lucrative monobactam to date, aztreonam was approved by the FDA in 1986 for use against Gram-negative bacteria, but nowadays aztreonam resistance has become commonplace, even in *P. aeruginosa* isolates.

Shortly after the discovery of aztreonam, Takeda researchers in collaboration with Hoffman-La Roche scientists reported the synthesis of their own monocyclic β -lactam antibiotic, carumonam (**222**), also known as AMA-1080 (Figure 4.2).¹⁴⁴ Structurally, aztreonam and

¹⁴¹ (a) Sykes, R. B.; Bonner, D. P.; Bush, K.; Georgopapadakou, N. H. *Antimicrob. Agents Chemother.* **1982**, *21*, 85–92. (b) Georgopapadakou, N. H.; Smith, S. A.; Sykes, R. B. *Antimicrob. Agents Chemother.* **1982**, *21*, 950–956. For an overview of the development of aztreonam, see: Sykes, R. B.; Bonner, D. P. *Rev. Infect. Dis.* **1985**, *7 Suppl 4*, S579–S593. For an overview on aztreonam's biological activity, see: Tunkel, A. R.; Scheld, W. M. *Infect. Control Hosp. Epidemiol.* **1990**, *11*, 486–494.

¹⁴² (a) Sykes, R. B.; Bonner, D. P.; Bush, K.; Georgopapadakou, N. H.; Wells, J. S. *J. Antimicrob. Chemother.* **1981**, *8, Suppl. E*, 1–16. (b) Breuer, H.; Cimarusti, C. M.; Denzel, T.; Koster, W. H.; Slusarchyk, W. A.; Treuner, U. D. *J. Antimicrob. Chemother.* **1981**, *8, Suppl. E*, 21–28.

¹⁴³ Bonner, D. P.; Sykes, R. B. *J. Antimicrob. Chemother.* **1984**, *14*, 313–327.

¹⁴⁴ For the synthesis of carumonam, see: (a) Sendai, M.; Hashiguchi, S.; Tomimoto, M.; Kishimoto, S.; Matsuo, T.; Kondo, M.; Ochiai, M. *J. Antibiot.* **1985**, *38*, 346–371. (b) Sendai, M.; Hashiguchi, S.; Tomimoto, M.; Kishimoto, S.; Matsuo, T.; Ochiai, M. *Chem. Pharm. Bull.* **1985**, *33*, 3798–3810. (c) Wei, C. C.; De Bernardo, S.; Teng, J. P.; Borgese, J.; Weigele, M. *J. Org. Chem.* **1985**, *50*, 3462–3467. (d) Manchand, P. S.; Luk, K.-C.; Belica, P. S.; Choudhry, S. C.; Wei, C. C. *J. Org. Chem.* **1988**, *53*, 5507–5512. For the biological activity of carumonam, see: (e) Imada, A.; Kondo, M.; Okonogi, K.; Yukishige, K.; Kuno, M. *Antimicrob. Agents Chemother.* **1985**, *27*, 821–827.

carumonam are quite similar, except for a slight modification of the acyl side chain and the substituent at C4 (and its stereochemical configuration). While it was approved in Japan in the mid- to late-1980s for use against Gram-negative bacterial infections and marketed under the name “amasulin,” carumonam is not widely prescribed in the United States.

After the successful development of aztreonam, the Squibb chemists continued to evaluate additional monobactam candidates for improved potencies and pharmacokinetic profiles, thereby arriving at tigemonam (**223**) in 1988 (Figure 4.2).¹⁴⁵ Tigemonam possesses an acyl side chain identical to carumonam, an *O*-sulfonic acid β -lactam activating group, and two methyl groups at the C4-position. While tigemonam (**223**) was a promising candidate, its development as a new antibiotic stalled in the early 1990s and was eventually discontinued.

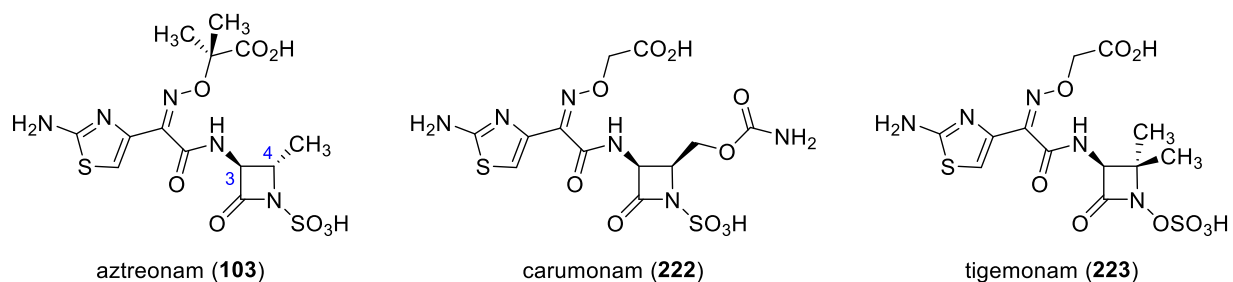


Figure 4.2: The structures of aztreonam (**103**), carumonam (**222**) and tigemonam (**223**).

¹⁴⁵ (a) Sykes, R. B.; Koster, W. H.; Bonner, D. P. *J. Clin. Pharmacol.* **1988**, *28*, 113–119. (b) Tanaka, S. K.; Summerill, R. A.; Minassian, B. F.; Bush, K.; Visnic, D. A.; Bonner, D. P.; Sykes, R. B. *Antimicrob. Agents Chemother.* **1987**, *31*, 219–225. (c) Clark, J. M.; Olsen, S. J.; Weinberg, D. S.; Dalvi, M.; Whitney, R. R.; Bonner, D. P.; Sykes, R. B. *Antimicrob. Agents Chemother.* **1987**, *31*, 226–229. (d) Chin, N.-X.; Neu, H. C. *Antimicrob. Agents Chemother.* **1988**, *32*, 84–91. (e) Fuchs, P. C.; Jones, R. N.; Barry, A. L. *Antimicrob. Agents Chemother.* **1988**, *32*, 346–349. (f) Rylander, M.; Gezelius, L.; Norrby, S. R. *J. Antimicrob. Chemother.* **1988**, *22*, 307–313. (g) Brown, J.; Yang, Y.; Livermore, D. M. *J. Antimicrob. Chemother.* **1989**, *23*, 201–207. (h) Nélet, F.; Gutmann, L.; Kitzis, M. D.; Acar, J. F. *J. Antimicrob. Chemother.* **1989**, *24*, 173–181. (i) van Ogtrop, M. L.; Mattie, H.; Guiot, H. F.; van Strijen, E.; Sekh, B. R.; van Furth, R. *Antimicrob. Agents Chemother.* **1991**, *35*, 417–422.

Twenty years later, there is renewed interest in monocyclic β -lactam antibiotics, sparked by Basilea's development of BAL30072 (**224**) in 2010¹⁴⁶ and continued by Pfizer's report of MB-1 (**225**) in 2012 (Figure 4.3).¹⁴⁷ Both of these molecules feature a 1,5-dihydroxy-4-pyridone substituent, a siderophore¹⁴⁸ presumed to improve cell penetration by taking advantage of iron transport mechanisms.¹⁴⁹ BAL30072 is currently in Phase I clinical trials to treat multidrug-resistant Gram-negative pathogens, alone and in combination with meropenem, a carbapenem. Pfizer's MB-1 (**225**) is currently undergoing *in vivo* pre-clinical trials, but there is a recent report of unexpected variability between *in vitro* and *in vivo* efficacies.¹⁵⁰

¹⁴⁶ (a) Mushta, S.; Warner, M.; Livermore, D. *J. Antimicrob. Chemother.* **2010**, *65*, 266–270. (b) Page, M. G. P.; Dantier, C.; Desaeubre, E. *Antimicrob. Agents Chemother.* **2010**, *54*, 2291–2302. (c) Russo, T. A.; Page, M. G. P.; Beanan, J. M.; Olson, R.; Hujer, A. M.; Hujer, K. M.; Jacobs, M.; Bajaksouzian, S.; Endimiani, A.; Bonomo, R. A. *J. Antimicrob. Chemother.* **2011**, *66*, 867–863. (d) Mima, T.; Kvitko, B. H.; Rholl, D. A.; Page, M. G. P.; Desarbre, E. Schweizer, H. P. *Int. J. Antimicrob. Agents* **2011**, *38*, 157–159. (e) Higgins, P. G.; Stefanik, D.; Page, M. G. P.; Hackel, M.; Seifert, H. *J. Antimicrob. Chemother.* **2012**, *67*, 1167–1169. (f) Hofer, B.; Dantier, C.; Gebhardt, K.; Desarbre, E.; Schmitt-Hoffmann, A.; Page, M. G. P. *J. Antimicrob. Chemother.* **2013**, *68*, 1120–1129. (g) Mushta, S.; Woodford, N.; Hope, R.; Adkin, R.; Livermore, D. M. *J. Antimicrob. Chemother.* **2013**, *68*, 1601–1608. (h) van Delden, C.; Page, M. G. P.; Köhler, T. *Antimicrob. Agents Chemother.* **2013**, *57*, 2095–2102. (i) Hornsey, M.; Phee, L.; Stubbings, W.; Wareham, D. W. *Int. J. Antimicrob. Agents* **2013**, *42*, 343–346. (j) Landman, D.; Singh, M.; El-Imad, B.; Miller, E.; Win, T.; Quale, J. *Int. J. Antimicrob. Agents* **2014**, *43*, 527–532.

¹⁴⁷ (a) Mitton-Fry, M. J.; Arcari, J. T.; Brown, M. F.; Casavant, J. M.; Finegan, S. M.; Flanagan, M. E.; Gao, H.; George, D. M.; Gerstenberger, B. S.; Han, S.; Hardink, J. R.; Harris, T. M.; Hoang, T.; Huband, M. D.; Irvine, R.; Lall, M. S.; Lemmon, M. M.; Li, C.; Lin, J.; McCurdy, S. P.; Mueller, J. P.; Mullins, L.; Niosi, M.; Noe, M. C.; Pattavina, D.; Penzien, J.; Plummer, M. S.; Risley, H.; Schuff, B. P.; Shanmugasundaram, V.; Starr, J. T.; Sun, J.; Winton, J.; Young, J. A. *Bioorg. Med. Chem. Lett.* **2012**, *22*, 5989–5994. (b) Brown, M. F.; Mitton-Fry, M. J.; Arcari, J. T.; Barham, R.; Casavant, J.; Gerstenberger, B. S.; Han, S.; Hardink, J. R.; Harris, T. M.; Hoang, T.; Huband, M. D.; Lall, M. S.; Lemmon, M. M.; Li, C.; Lin, J.; McCurdy, S. P.; McElroy, E.; McPherson, C.; Marr, E. S.; Mueller, J. P.; Mullins, L.; Nikitenko, A. A.; Noe, M. C.; Penzien, J.; Plummer, M. S.; Schuff, B. P.; Shanmugasundaram, V.; Starr, J. T.; Sun, J.; Tomaras, A.; Young, J. A.; Zaniewski, R. P. *J. Med. Chem.* **2013**, *56*, 5541–5552.

¹⁴⁸ Siderophores, from the Greek for “iron carriers,” are small molecules with high affinities for iron secreted by bacteria and fungi with the purpose of scavenging iron from the environment. For a review on the chemistry and biology of siderophores, see Hider, R. C.; Kong, X. *Nat. Prod. Rep.* **2010**, *27*, 637–657.

¹⁴⁹ Page, M. G. P. *Ann. N. Y. Acad. Sci.* **2013**, *1227*, 115–126.

¹⁵⁰ Tomaras, A. P.; Carndon, J. L.; McPherson, C. J.; Nicolau, D. P. *Antimicrob. Agents Chemother.* **2015**, *59*, 2439–2442.

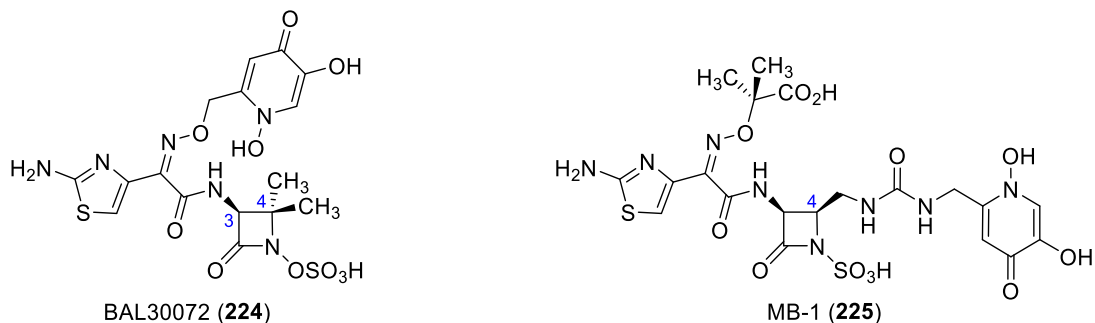


Figure 4.3: Current generation of monobactam antibiotics.

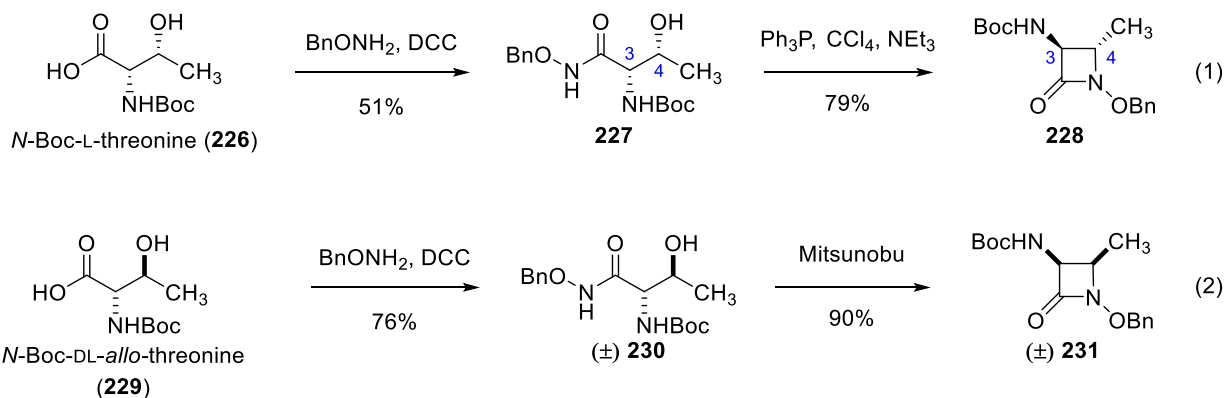
Synthetic Methods

Both semi-synthetic and fully synthetic methodologies have been employed in the production of monobactams and related compounds. In the initial stages of development, it was demonstrated that semi-synthetic means required greater effort while producing only a narrow scope of accessible scaffolds.¹⁵¹ The limitations of semi-synthesis, coupled with the ingenuity of academic and industrial chemists, inspired multiple fully synthetic avenues to monocyclic β -lactam structures.¹⁵²

¹⁵¹ Cimarusti, C. M.; Applegate, H. E.; Chang, H. W.; Floyd, D. M.; Koster, W. H.; Slusarchyk, W. A.; Young, M. G. *J. Org. Chem.* **1982**, *47*, 179–180.

¹⁵² Selected industrial examples include: (a) Skotnicki, J.; Commons, T.; Rees, R.; Speth, J. *J. Antibiot.* **1983**, *36*, 1201–1204. (b) Kishimoto, S.; Sendai, M.; Tomimoto, M.; Hashiguchi, S.; Matsuo, T.; Ochiai, M. *Chem. Pharm. Bull.* **1984**, *32*, 2646–2659. (c) Mewshaw, R.; Commons, T. *J. Antibiot.* **1987**, *40*, 1563–1571. (d) Yamashita, H.; Minami, N.; Sakakibara, K.; Kobayashi, S.; Ohno, M.; Hamada, M.; Umezawa, H. *J. Antibiot.* **1987**, *40*, 1716–1732. (e) Yamashita, H.; Minami, N.; Sakakibara, K.; Kobayashi, S.; Ohno, M. *Chem. Pharm. Bull.* **1988**, *36*, 469–480. Selected academic examples include: (f) Shibuya, M.; Jinbo, Y.; Kubota, S. *Chem. Pharm. Bull.* **1984**, *32*, 1303–1312. (g) Guanti, G.; Banfi, L.; Narisano, E. *Synthesis*, **1985**, *6/7*, 609–611. (h) Evans, D. A.; Williams, J. M. *Tetrahedron Lett.* **1988**, *29*, 5065–5068. (i) Fernández-Resa, P.; Herranz, R.; Conde, S.; Arribas, E. *J. Chem. Soc. Perkin Trans. 1*, **1989**, 67–71. (j) Hegedus, L.; Imwinkelried, R.; Alarid-Sargent, M.; Dvorak, D.; Satoh, Y. *J. Am. Chem. Soc.* **1990**, *112*, 1109–1117. (k) Cainelli, G.; Panunzio, M.; Bandini, E.; Martelli, G.; Spunta, G.; DaCol, M. *Tetrahedron*, **1995**, *51*, 5067–5072. (l) Ageno, G.; Banfi, L.; Cascio, G.; Guanti, G.; Manghisi, E.; Riva, R.; Rocca, V. *Tetrahedron*. **1995**, *51*, 8121–8134. (m) Palomo, C.; Aizpurua, J.; Garcia, J.; Galarza, R.; Legido, M.; Urchegui, R.; Roman, P.; Luque, A.; Server-Carrio, J.; Linden, A. *J. Org. Chem.* **1997**, *62*, 2070–2079. For a recent review on the syntheses of azetidinones, see: (n) Brandi, A.; Cicchi, S.; Cordero, F. M. *Chem. Rev.* **2008**, *108*, 3988–4035.

The strategy of highest utility was developed by Dr. Marvin Miller at the University of Notre Dame, who pioneered access to β -lactams from amino acid starting materials.¹⁵³ Using threonine as a sample substrate, Miller demonstrated that β -lactams could be formed in a stereospecific manner (Scheme 4.1). *N*-Boc-L-threonine (**226**) was converted into hydroxamate **227** by treatment with *O*-benzyl hydroxylamine and DCC. Hydroxamate **227** cyclized to give β -lactam **228** under Mitsunobu (PPh_3 , DEAD) or modified Appel (PPh_3 , CCl_4 , NEt_3) conditions (Scheme 4.1, equation 1). Subjection of *N*-Boc-DL-*allo*-threonine (**229**) to the same sequence of reactions afforded β -lactam **231**, a diastereomer of **228** (Scheme 4.1, equation 2). The hydroxamate functionality was essential for successful cyclization; the increased acidity of the N–H bond facilitated conversion into a better tethered nucleophile for an intramolecular Mitsunobu-type reaction.



Scheme 4.1: Miller methodology for the synthesis of β -lactams.

Miller noted, “The retention of configuration at C₃ and the clean inversion at C₄ during this cyclization implied that essentially any chiral β -lactam could be made by simply choosing the

¹⁵³ (a) Miller, M. J.; Mattingly, P. G.; Morrison, M.A.; Kerwin, Jr., J. F. *J. Am. Chem. Soc.* **1980**, *102*, 7026–7032. (b) Miller, M. J.; Bajwa, J. S.; Mattingly, P. G.; Peterson, K. *J. Org. Chem.* **1982**, *47*, 4928–4933. (c) Mattingly, P. G.; Miller, M. J.; Cooper, R. D. G.; Daugherty, B. W. *J. Org. Chem.* **1983**, *48*, 3556–3559. (d) Miller, M. J.; Mattingly, P. G. *Tetrahedron* **1983**, *39*, 2563–2570. (e) Miller, M. J.; Biswas, A.; Krook, M. A. *Tetrahedron* **1983**, *39*, 2571–2575. (f) Krook, M. A.; Miller, M. J. *J. Org. Chem.* **1985**, *50*, 1126–1128. (g) Woulfe, S. R.; Miller, M. J. *J. Med. Chem.* **1985**, *28*, 1447–1453. (h) Woulfe, S. R.; Miller, M. J. *J. Org. Chem.* **1986**, *51*, 3133–3139.

appropriate chiral starting β -hydroxy acid.”¹⁵⁴ With the reliability and predictability of this method, in many cases, access to the chiral β -hydroxy acid starting material was the limiting factor for a desired transformation.

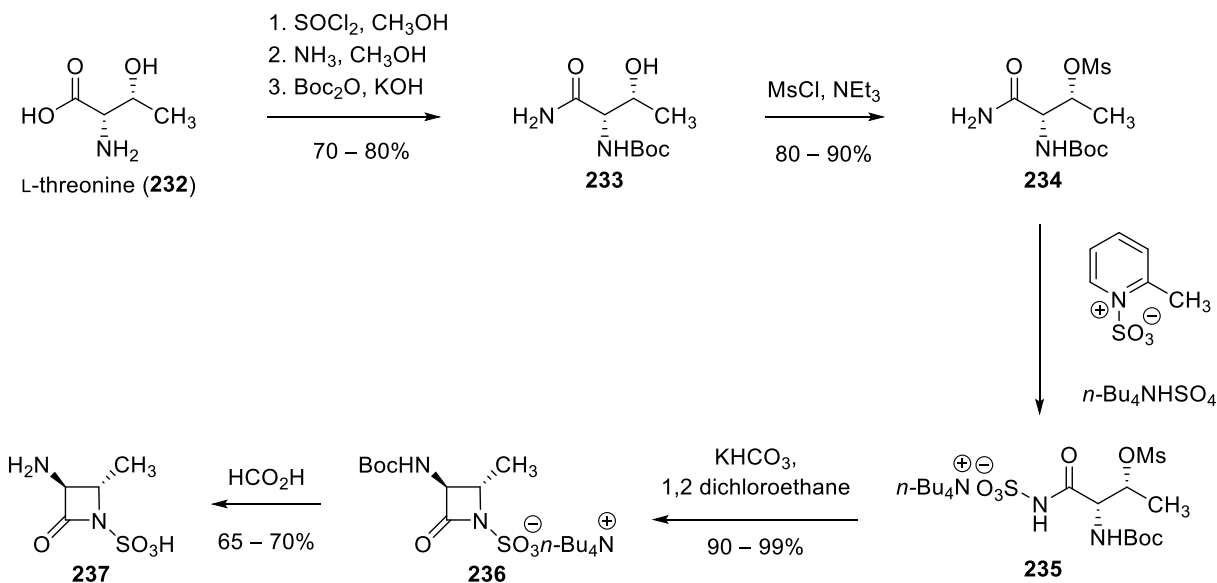
Synthesis of the Aztreonam Core and Other Monobactam Cores

Utilizing Miller’s methodology as a guide, the Squibb chemists optimized their synthetic approach to the β -lactam core of aztreonam (Scheme 4.2).¹⁵⁵ Conversion of threonine (**232**) into amide **233** was effected by sequential treatment with thionyl chloride, ammonia (to form the amide), and di-*tert*-butyl dicarbonate with potassium hydroxide. The secondary alcohol of **233** was transformed into mesylate **234** in $\geq 80\%$ yield, and the amide of **234** was transformed into acyl sulfamate **235**, a cyclization precursor. Functionalization of nitrogen at this stage circumvents later functional group manipulations. Cyclization of **235** occurred upon exposure to a mild base, potassium bicarbonate, affording β -lactam **236** in $\geq 90\%$ yield. Removal of the *tert*-butyl carbamate gave aztreonam β -lactam core **237** in $\geq 65\%$ yield. The core **237** was converted into aztreonam (**103**) in two additional steps (not shown).¹⁵⁶

¹⁵⁴ Miller, M. *Acc. Chem. Res.* **1986**, *19*, 49–56.

¹⁵⁵ Floyd, D. M.; Fritz, A. W.; Cimarusti, C. M. *J. Org. Chem.* **1982**, *47*, 176–178.

¹⁵⁶ Singh, J.; Denzel, T. W.; Fox, R.; Kissick, T. P.; Herter, R.; Wurdinger, J.; Schierling, P.; Papaioannou, C. G.; Moniot, J. L.; Mueller, R. H.; Cimarusti, C. M. *Org. Process Res. Dev.* **2002**, *6*, 863–868.



Scheme 4.2: Synthesis of **237**, the β -lactam core of aztreonam.

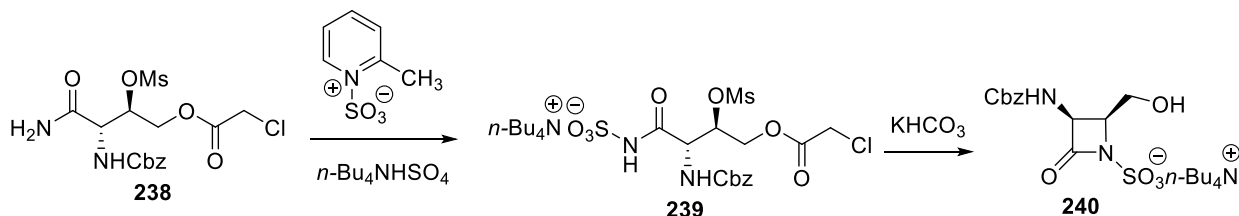
Other clinically relevant monocyclic β -lactams could be accessed using Miller's cyclization chemistry, with Squibb modifications if necessary, albeit using different cyclization precursors (Scheme 4.3). Carumonam core **240** was the product of a base-promoted cyclization of acyl sulfamate **239** (Scheme 4.3, **A**).^{144b} Tigemonam and BAL30072 share a common core synthesized from *N*-Boc-3-hydroxy-L-valine (**218**). Proving the timeless nature of high-quality chemistry, the Basilea chemists constructed the core of BAL30072 in the mid-2000s based on work published in the 1980s (Scheme 4.3, **B**).¹⁵⁷

While carumonam and Pfizer compound MB-1 (**225**) share a common carbon core, the Pfizer researchers utilized a different strategy to access the core of β -lactam **225** in 2012. Compound **246** was accessed employing methodology originally disclosed by Takeda chemists toward the synthesis of carumonam, that involved a [2+2] cycloaddition between imine **243** and a ketene derived from phthalimidoacetyl chloride (Scheme 4.3, **C**).^{152b} While this cycloaddition

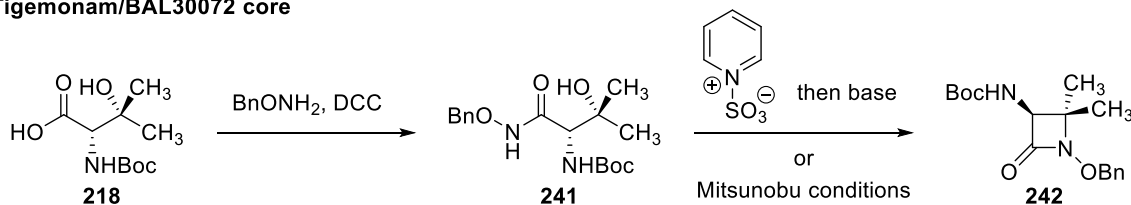
¹⁵⁷ Desarbre, E.; Gaucher, B.; Page, M. G. P.; Roussel, P. Useful Combinations of Monobactam Antibiotics with Beta-Lactamase Inhibitors. Eur. Pat. Appl. WO2007065288, 2007.

strategy allowed the production of hundreds of grams of *cis*-cycloadduct **244**, the route required a resolution of stereoisomers, resulting in a significant loss of material, and required additional protecting group interchanges.

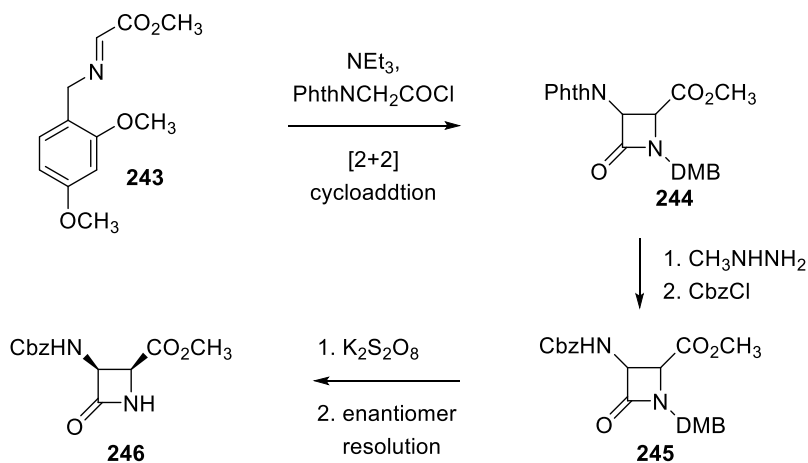
A. Carumonam core



B. Tigemonam/BAL30072 core



C. Pfizer compound MB-1 (1st generation carumonam core)



Scheme 4.3: Syntheses of the cores of the clinically relevant monobactams.

These methodologies are highly useful and allow access to a variety of β -lactams; however their scope is still limited by the availability of chiral β -hydroxy- α -amino acid starting materials. For example, the C4-position of the monobactams is traditionally monosubstituted (in either an

(*R*)- or (*S*)- configuration) and the prepared disubstituted compounds (e.g. tigemonam and BAL30072) have identical, methyl substituents. Access to differentially substituted monocyclic β -lactams is thus limited. These novel compounds hold potential to further the investigation of SAR of the monobactams, strengthen target binding to PBP3, and overcome common bacterial resistance mechanisms (such as β -lactamases).

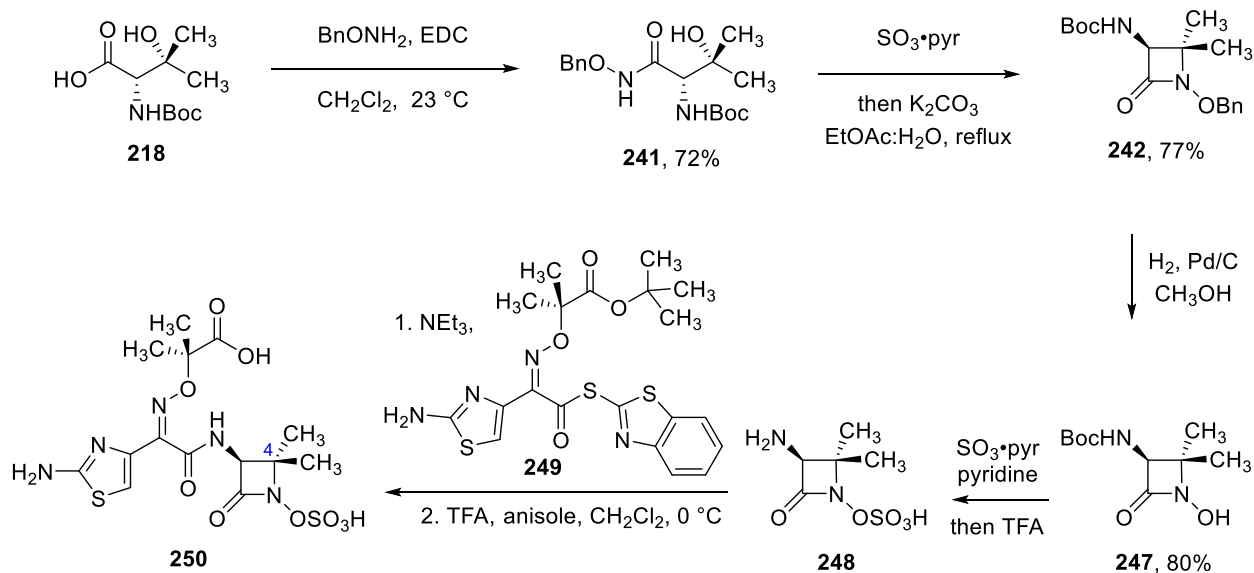
Synthesis of C4-Disubstituted Monocyclic β -Lactams

In the previous chapter, I detailed a strategy that provides an approach to β,β' -disubstituted- β -hydroxy- α -amino acids. Application of the *N*-Boc-protected derivatives toward the synthesis of monobactams, using predictable and precedented methods, would result in the stereocontrolled production of differentially C4 substituted monobactam antibiotics.

To validate this approach, I targeted aztreonam–tigemonam hybrid **250**,¹⁵⁸ starting from *N*-Boc amino acid **218** (which was obtained by aldolization of (*R,R*)-pseudoephedrine glycinamide with acetone and subsequent auxiliary cleavage and amine protection). *N*-Boc-3-hydroxy-L-valine (**218**) was converted into hydroxamate **241** in 72% yield upon treatment with *O*-benzyl hydroxylamine and EDC (Scheme 4.4). Cyclization of hydroxamate **241** proceeded after addition of the SO₃•pyridine complex and K₂CO₃, and heating the reaction mixture to reflux, affording β -lactam **242** in 77% yield. The benzyl ether was reductively cleaved by subjection to hydrogenolysis conditions, giving *N*-hydroxy β -lactam **247** in 80% yield. The *O*-sulfonic acid was introduced by additional treatment with the SO₃•pyridine complex, and the *tert*-butyl carbamate was removed with strong acid, yielding β -lactam **248**. The aztreonam acyl side chain was introduced by coupling **249** with core **248** in the presence of triethylamine. Saponification of the *tert*-butyl ester of the side chain was effected upon brief treatment with

¹⁵⁸ Bush, K.; Liu, F. Y.; Smith, S. A. *Dev. Ind. Microbiol.* **1987**, *27*, 153–164.

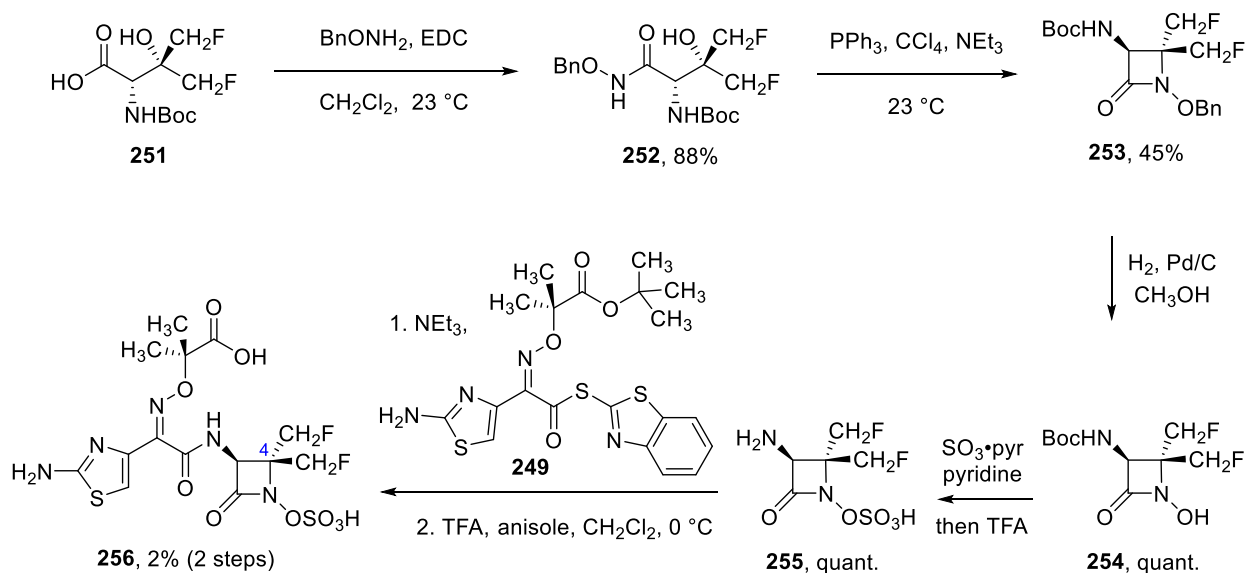
TFA in the presence of anisole (as a *tert*-butyl cation scavenger) at 0 °C, producing aztreonam–tigemonam hybrid **250**. This target molecule served as the basis for comparison, along with aztreonam, in the analysis of biological activity.



Scheme 4.4: Synthesis of aztreonam–tigemonam hybrid **250**.

Utilizing the same synthetic strategy, I synthesized C4-bisfluoromethyl monobactam analog **256** (Scheme 4.5). *N*-Boc amino acid **251** was transformed into hydroxamate **252** in 88% yield upon treatment with *O*-benzyl hydroxylamine and EDC. Cyclization of hydroxamate **252** under identical conditions for **241** was unsuccessful. Presumably, the tertiary alcohol was not transformed into the intermediate sulfonate (not shown) due to the strongly electron withdrawing nature of the nearby fluoromethyl substituents. However, β-lactam **253** was accessed in 45% yield by reaction with PPh₃, CCl₄ and NEt₃. The benzyl ether was reductively cleaved upon treatment with H₂ and Pd/C, producing *N*-hydroxy β-lactam **254** in quantitative yield. Comparable to the dimethyl substrate **247**, the *O*-sulfonic acid was added by treatment with SO₃·pyridine complex and the *tert*-butyl carbamate was cleaved upon exposure to strong acid, yielding β-lactam **255**. Introduction of the acyl side chain and saponification of the *tert*-

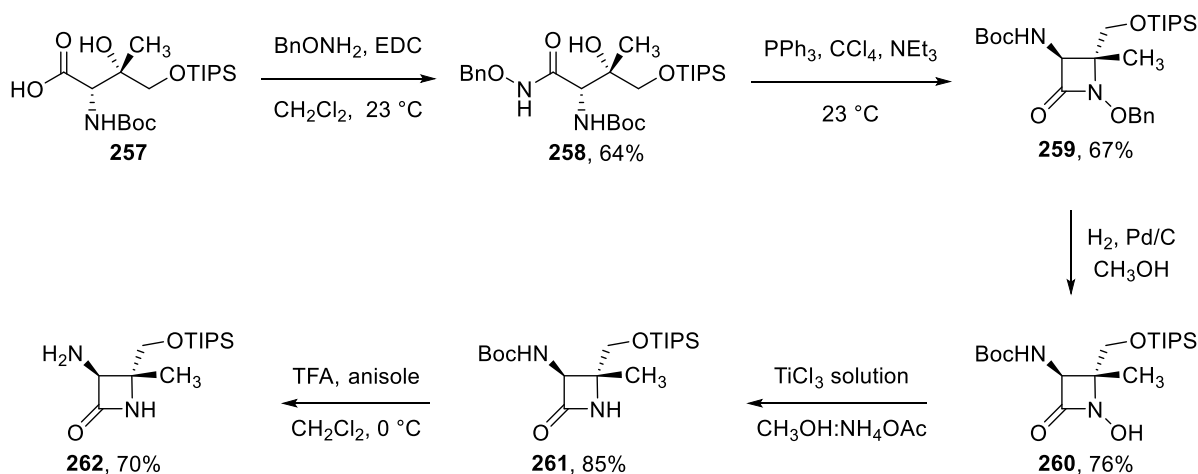
butyl ester were effected analogously to compound **248**, but delivered **256** in rather disappointing 2% yield. This low yield presumably arose from the facile cleavage of the *O*-sulfonic acid functionality or the inherent instability of **256** imparted by the two fluoromethyl substituents.¹⁵⁹ In light of this, I decided to pursue *N*-sulfonic acid monobactams instead of additional *O*-sulfonic acid derivatives.



Synthesis of C4-disubstituted monobactams **250** and **256** validated this synthetic strategy, but in both cases, the two substituents were identical. To demonstrate the enabling capabilities of the newly developed aldol methodology in the synthesis of monobactam antibiotics, I targeted β -lactam core **262**, with asymmetric substitution at the C4-position consisting of a smaller methyl group and a larger synthetic handle in the form of a silyl-protected hydroxymethyl functionality (Scheme 4.6). *N*-Boc amino acid **257** was isolated from a one-pot reaction involving basic

¹⁵⁹ C4-Fluoromethyl aztreonam and related compounds have been synthesized and their antibacterial efficacies have been evaluated. These compounds were shown to demonstrate similar bioactivity to aztreonam and possess greater stability toward β -lactamases. See: Matsuda, K.; Nakagawa, S.; Nakano, F.; Inoue, M.; Mitsuhashi, S. *J. Antimicrob. Chemother.* **1987**, *19*, 753–760. C4-Trifluoromethyl aztreonam has also been synthesized and shown to decompose in physiological buffers. See Ref. 152g. We therefore surmised that the stability of bisfluoromethyl monobactam **256** lies between that of C4-fluoromethyl aztreonam and C4-trifluoromethyl aztreonam.

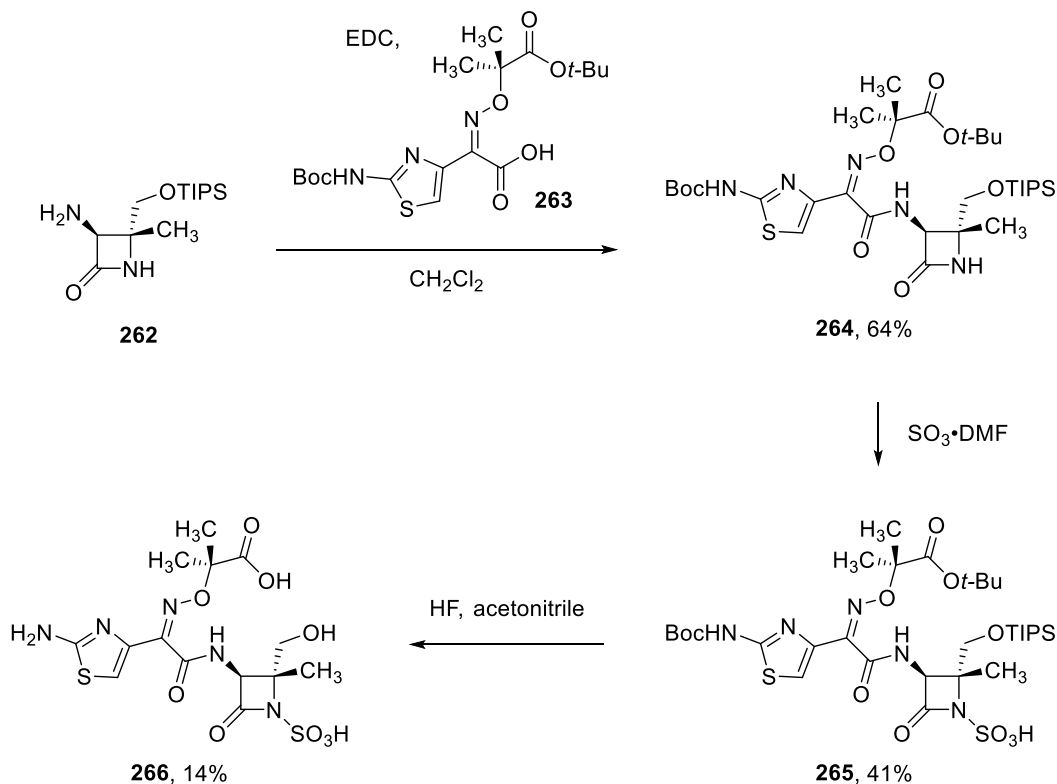
hydrolysis of aldol adduct **198** with sodium hydroxide, followed by *N*-Boc protection with di-*tert*-butyl dicarbonate and additional sodium hydroxide. Treatment of *N*-Boc acid **257** with *O*-benzyl hydroxylamine in the presence of EDC afforded hydroxamate **258** in 64% yield. Cyclization was effected by PPh₃, CCl₄, and NEt₃, producing β-lactam **259** in 67% yield. The benzyl ether was removed under reducing conditions (H₂, Pd/C), affording *N*-hydroxyl β-lactam **260** in 76% yield. At this point the stereochemical configuration was determined by nOe NMR experiments and was consistent with predictions based on Miller's method (invertive cyclization). Using conditions developed by Miller in 1980, I reductively cleaved the N–O bond by treatment with a solution of titanium trichloride in buffered methanol,¹⁶⁰ obtaining β-lactam **261** in 85% yield. At this point, I decided to attach the acyl side chain on the C3-amine, thereby accessing a common intermediate amenable to late-stage diversification. Therefore, I treated β-lactam **261** with TFA in the presence of anisole at 0 °C, and obtained β-lactam core **262** in 70% yield.



Scheme 4.6: Synthesis of **262**, a C4-differentially substituted β-lactam core.

¹⁶⁰ Mattingly, P. G.; Miller, M. J. *J. Org. Chem.* **1980**, *45*, 410–415.

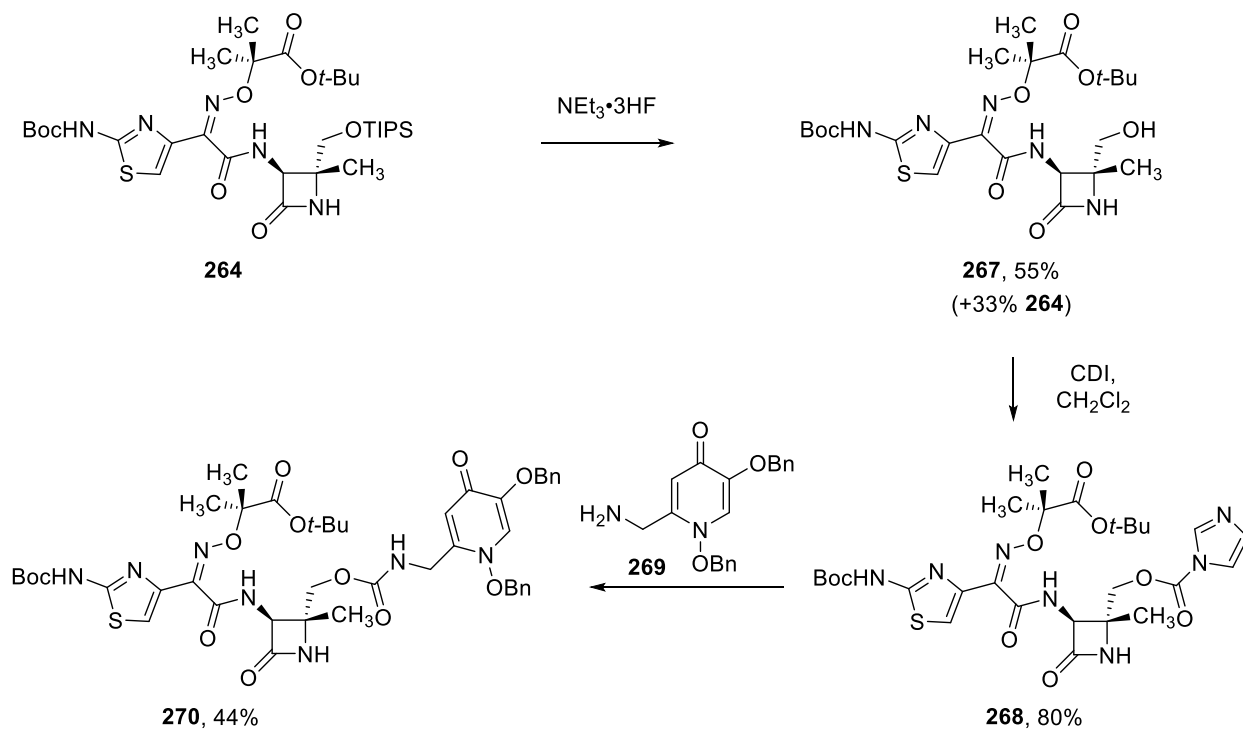
Next, the side chain was attached onto β -lactam core **262** (Scheme 4.7). Standard peptide coupling conditions (amine **262**, acid **263**, and EDC), delivered *N*-acylated product **264** in 64% yield. Treatment of **264** with the $\text{SO}_3 \cdot \text{DMF}$ complex afforded *N*-sulfonic acid **265** in 41% yield, which, upon global deprotection with HF, gave C4-differentially substituted monocyclic β -lactam **266** in 14% yield.



Scheme 4.7: Synthesis of 4-hydroxymethyl-4-methyl monobactam **266**.

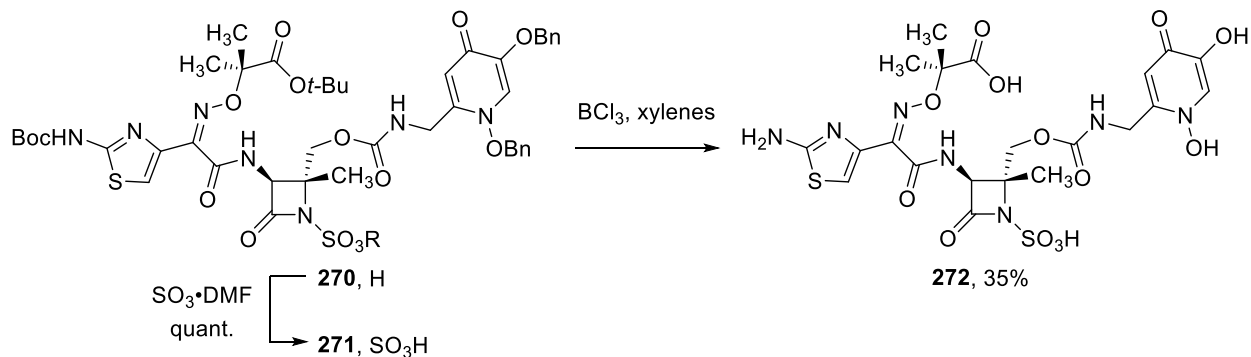
Additionally, I wanted to explore the use of the hydroxymethyl substituent at the C4-position as a handle to introduce additional functionality, such as a siderophore (Scheme 4.8). For that reason, I removed the TIPS group from *N*-acylated product **264** by treatment with $\text{NEt}_3 \cdot 3\text{HF}$, and obtained alcohol **267** in 55% yield, along with 33% of **264**. The alcohol **267** was transformed into intermediate carbamate **268** in 80% yield by reaction with CDI. I then introduced a 1,5-dibenzyloxy-4-pyridone moiety by treatment of **268** with amine **269**,^{147b} obtaining carbamate **270**

in 44% yield. The low yield presumably arose from the steric bulk near the C4-position. Attempts to effect carbamate **270** formation by a one-pot procedure were unsuccessful.



Scheme 4.8: Synthesis of intermediate monobactam **270**.

With **270** in hand, I was two transformations away from a final compound **272** (Scheme 4.9). The *N*-sulfonic acid was introduced by subjecting **270** to $\text{SO}_3 \cdot \text{DMF}$ complex, quantitatively delivering compound **271**. Global deprotection of the two benzyl ethers, the *tert*-butyl carbamate and the *tert*-butyl ester was effected upon treatment of **271** with BCl_3 in xylenes, affording siderophore-conjugated monocyclic β -lactam **272** in 35% yield. Synthesis of this compound was particularly exciting due to its unprecedented asymmetric C4-stereocenter and successful incorporation of a siderophore that potentially could improve cell penetration.



Scheme 4.9: Synthesis of siderophore monobactam **272**.

In total, I prepared four fully synthetic C4-disubstituted monocyclic β -lactams. These included aztreonam–tigemonam hybrid **250**, a benchmark standard; bisfluoromethyl monobactam **256**, an otherwise inaccessible scaffold; hydroxymethyl monobactam **266**, an asymmetric C4-disubstituted standard; and monobactam **272**, a siderophore-conjugated compound.

Antibacterial Activity

The compounds **250**, **256**, **266**, and **272** were tested for antibacterial activity. Determination of minimum inhibitory concentration (MIC) values, a measure of antibiotic potency, was performed at the University of North Texas Health Sciences Center (UNT-HSC). Aztreonam was used as a standard and the results are summarized in Table 4.1. Aztreonam–tigemonam hybrid **250** displayed improved biological activity compared with aztreonam against Gram-positive (*S. pneumonia* and *S. pyogenes*) bacterial strains and similar activity against Gram-negative pathogens. The bisfluoromethyl monobactam **256** demonstrated weak potency against only *H. influenzae* strains, presumably due to the facile cleavage of the activating group on the β -lactam (thereby reducing the compound's inherent potency) or the intrinsic instability imparted by the two fluoromethyl substituents. Hydroxymethyl monobactam **266** did not display any

antibacterial activity. Lastly, siderophore-conjugated monobactam **272** demonstrated no antibiotic activity against Gram-positive bacterial strains and poor bioactivity against roughly half of the Gram-negative strains tested.

Table 4.1: Minimum Inhibitory Concentrations for Monobactams 250, 256, 266 and 272.

	Species	Genotype	250	256	266	272	AZR
Gram-positive	<i>S. aureus</i>	ATCC 29213	> 32	> 32	>32	>32	> 32
	<i>S. aureus</i>	BAA-1556 (USA300)	> 32	> 32	>32	>32	> 32
	<i>S. aureus</i>	NRS710 (USA100, Erythro > 8)	> 32	> 32	>32	>32	> 32
	<i>S. aureus</i>	TP 506 (<i>erm A</i>)	> 32	> 32	>32	>32	> 32
	<i>S. aureus</i>	NRS22 (USA600, GISA)	> 32	> 32	>32	>32	> 32
	<i>S. pneumoniae</i>	ATCC 49619	0.5	> 32	>32	>32	0.5
	<i>S. pneumoniae</i>	TP 160 (<i>mef A</i>)	> 32	> 32	>32	>32	> 32
	<i>S. pneumoniae</i>	TP 1517 (<i>mef A</i>)	16	32	>32	>32	> 32
	<i>S. pneumoniae</i>	TP 1579 (<i>erm B</i> + <i>tet(M,O)</i>)	16	> 32	>32	>32	> 32
	<i>S. pneumoniae</i>	TP 1537 (<i>erm B</i> + <i>mef A</i>)	> 32	> 32	>32	>32	> 32
	<i>S. pyogenes</i>	ATCC 19615	2	> 32	>32	>32	16
	<i>S. pyogenes</i>	Macrolide-resistant	2	> 32	>32	>32	16
	<i>E. faecalis</i>	ATCC 29212	> 32	> 32	>32	>32	> 32
	<i>E. faecalis</i>	Vancomycin resistant	> 32	> 32	>32	>32	> 32
Gram-negative	<i>E. coli</i>	ATCC 25922	1	> 32	>32	16	< 0.0313
	<i>E. coli</i>	GUEST131 (NDM-1)	> 32	> 32	>32	16	> 32
	<i>E. coli</i>	TEM-1	ND	ND	>32	16	0.0625
	<i>E. coli</i>	CTX-M-4	ND	ND	>32	>32	2
	<i>A. baumannii</i>	ATCC 19606	8	> 32	>32	>32	16
	<i>A. baumannii</i>	imipenem-resistant	32	> 32	>32	>32	32
	<i>A. baumannii</i>	chromosomal class C	ND	ND	>32	>32	> 32
	<i>A. baumannii</i>	IMP-4	ND	ND	>32	>32	32
	<i>K. pneumoniae</i>	ATCC 10031	0.125	> 32	>32	2	< 0.0313
	<i>K. pneumoniae</i>	IHMA 658692; KPC-2	1	> 32	>32	>32	32
	<i>K. pneumoniae</i>	TEM-10	ND	ND	>32	>32	> 32
	<i>K. pneumoniae</i>	SHV-2	ND	ND	>32	>32	> 32
	<i>P. aeruginosa</i>	ATCC 27853	8	> 32	>32	16	8
	<i>P. aeruginosa</i>	HPA101-1477	ND	ND	>32	8	8
	<i>H. influenzae</i>	Erythro >4, Clarithro 8, Azithro 1	< 0.0313	4	>32	8	< 0.0313
	<i>H. influenzae</i>	ATCC 49247	0.0625	16	>32	32	0.125

MICs are reported as µg/mL. AZR = aztreonam.

Conclusions

I utilized the newly developed methodology (pseudophenamine glycinamide aldolizations with ketone electrophiles) to access to β,β' -disubstituted- β -hydroxy- α -amino acids. I elaborated these substrates to provide novel C4-disubstituted monobactam analogs, an underrepresented class of β -lactam antibiotics. Four C4-disubstituted monocyclic β -lactam antibiotic candidates were synthesized and their antibiotic activities were assessed. While the novel siderophore-conjugated monobactam **272** was shown to display poor antibacterial activity, aztreonam-tigemonam hybrid **250** demonstrated improved bioactivity against Gram-positive pathogens, as compared to aztreonam.

The antibacterial activity of the monobactams is a function of multiple structural components. As noted by the Squibb scientists who developed aztreonam (and later tigemonam), “Substitution at the 4-position of the monocyclic ring although capable of producing dramatic changes in biological activity, is highly unpredictable.”¹⁴³ The activating group on the β -lactam nitrogen, the C3-acyl side chain and the identity and configuration of substitution at C4 greatly impact potential biological activity. I have investigated three new scaffolds (and one known) and found that the *O*-sulfonic acid activating group can improve biological activity, at the expense of compound stability. Regarding the influence of C4-disubstitution (e.g. **266**, **272**), additional substrates are necessary before trends can be established. Therefore, continued production of monocyclic β -lactam scaffolds is warranted (and is enabled via our methodology) in order to further investigate SAR of monobactams, strengthen target affinity, and impart stability toward β -lactamases, potentially producing a new marketable monocyclic β -lactam antibiotic.

General Experimental Procedures

All reactions were performed in flame-dried glassware fitted with rubber septa under a positive pressure of argon, unless otherwise noted. Air- and moisture-sensitive liquids were transferred via syringe or stainless steel cannula. Solutions were concentrated by rotary evaporation below 35 °C. Analytical thin-layer chromatography (TLC) was performed using glass plates pre-coated with silica gel (0.25-mm, 60-Å pore size, 230–400 mesh, Merck KGA) impregnated with a fluorescent indicator (254 nm). TLC plates were visualized by exposure to ultraviolet light (UV), then were stained by submersion in a 10% solution of phosphomolybdic acid (PMA) in ethanol, followed by brief heating on a hot plate. Flash-column chromatography was performed as described by Still et al.,⁶⁰ employing silica gel (60 Å, standard grade) purchased from Dynamic Adsorbents. Tetrahydrofuran, dichloromethane, and ether were purified by the method of Pangborn et al.⁶¹

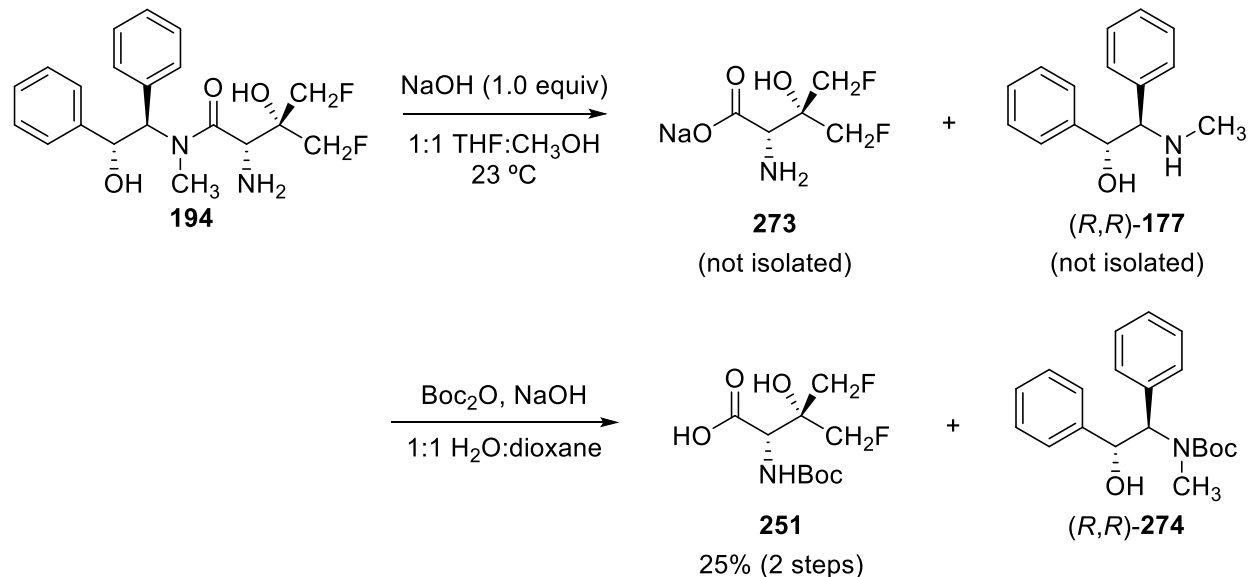
Instrumentation

Proton nuclear magnetic resonance (¹H NMR) spectra were recorded on Varian MERCURY 400 (400 MHz), Varian INOVA 500 (500 MHz), or Varian INOVA 600 (600 MHz) NMR spectrometers at 23 °C. Proton chemical shifts are expressed in parts per million (ppm, δ scale) and are referenced to residual protium in the NMR solvent (CHCl₃: δ 7.26, D₂HCO: δ 3.31). Data are represented as follows: chemical shift, multiplicity (s = singlet, d = doublet, t = triplet, q = quartet, dd = doublet of doublets, dt = doublet of triplets, sxt = sextet, m = multiplet, br = broad, app = apparent), integration, and coupling constant (*J* in Hertz (Hz)). Infrared (IR) spectra were obtained using a Shimadzu 8400S FT-IR spectrophotometer referenced to a polystyrene standard. Data are represented as follows: frequency of absorption (cm⁻¹), and

intensity of absorption (s = strong, m = medium, br = broad). HPLC retention times were acquired using a Beckman System Gold instrument equipped with a Chiracel OD-H column (5 mm particle size, 4.6 mm x 250 mm). High-resolution mass spectra were obtained at the Harvard University Mass Spectrometry Facility using a Bruker microTOF-QII mass spectrometer. LC–MS analysis was performed on an Agilent 1260 Infinity instrument equipped with a 6120 quadrupole LC–MS.

(For clarity, intermediates that have not been assigned numbers in the text are numbered sequentially in the Supporting Information beginning with 273.)

One pot, two step synthesis of *N*-Boc acid **251** from aldol adduct **194**.

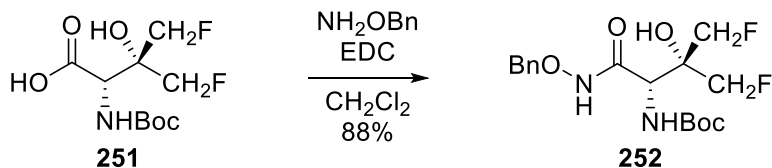


A 25-mL round bottom flask equipped with a stir bar was charged with aldol adduct **194** (616 mg, 1.63 mmol, 1 equiv). A 1:1 mixture of tetrahydrofuran:methanol (6.4 mL) was added, followed by aqueous sodium hydroxide solution (1.0 M, 1.63 mL, 1.63 mmol, 1 equiv). Reaction progress was monitored by the consumption of starting material by TLC (10% methanol–dichloromethane + 0.5% saturated aqueous ammonium hydroxide solution). After 4 d, the reaction mixture was concentrated to dryness and the residue was dissolved in a 1:1 mixture of water:1,4-dioxane (15 mL). The reaction vessel was placed in an ice-water cooling bath. Aqueous sodium hydroxide solution (1.0 M, 4.88 mL, 4.88 mmol, 3 equiv) was added, followed by di-*tert*-butyl dicarbonate (1.13 mL, 4.88 mmol, 3 equiv). The cooling bath was removed after 5 minutes and the vessel continued to stir at 23 °C. Reaction progress was monitored by the consumption of starting material by LC–MS analysis of aliquots removed from the reaction mixture. After 16 h, water (30 mL) was added and the mixture was washed with three portions of ether (30 mL). The ethereal extracts were combined and back-extracted with 0.5 M aqueous sodium hydroxide solution (20 mL). The ethereal extracts were dried over sodium sulfate and

filtered. The filtrate was concentrated to provide *N*-Boc-pseudoephedrine (*R,R*)-**274** in quantitative yield.

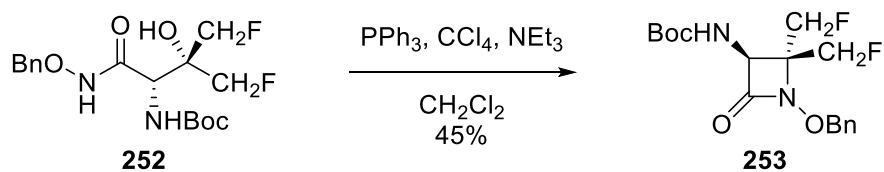
The basic aqueous phases were combined, the resulting solution was cooled in an ice-water cooling bath, and 1 M aqueous hydrochloric acid solution was added dropwise until the pH of the solution was ~2. The acidified aqueous phase was then extracted with ethyl acetate (3 × 25 mL). The organic extracts were combined and were dried over sodium sulfate. The dried organic solution was filtered and the filtrate was concentrated to provide crude *N*-Boc-protected acid. The crude material was purified via flash-column chromatography (2→5% methanol–dichloromethane + 1% acetic acid) to give *N*-Boc-protected acid **251** (110 mg, 25%) as an off-white foam. TLC (10% methanol–dichloromethane): $R_f = 0.15$ (UV, PMA). $^1\text{H NMR}$ (500 MHz, CD_3OD), δ : 4.66–4.46 (m, 3H), 4.41 (s, 1H), 4.37 (s, 1H), 1.46 (s, 9H). FTIR (neat), cm^{-1} : 3339 (br), 2980 (m), 1694 (s), 1394 (s), 1161 (s), 1024 (s); HRMS (ESI): Calcd for $(\text{C}_{10}\text{H}_{17}\text{F}_2\text{NO}_5 + \text{Na})^+$: 292.0967; Found: 292.0954.

Hydroxamate **252**.



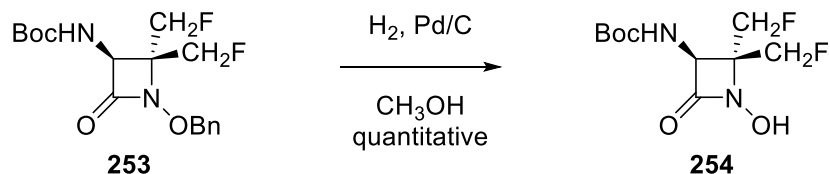
To a 25-mL round bottom flask equipped with a stir bar was added the *N*-Boc acid **251** (100 mg, 0.370 mmol, 1 equiv) and dry dichloromethane (3.70 mL). *O*-Benzylhydroxylamine (52.0 μL , 0.430 mmol, 1.15 equiv) was added, followed by EDC (78.0 mg, 0.410 mmol, 1.1 equiv) in one portion. Reaction progress was monitored by the consumption of starting material by LC–MS analysis of aliquots removed from the reaction mixture. After 14 h, additional dichloromethane (10 mL) was added and the reaction mixture was washed sequentially with water (15 mL) and saturated aqueous sodium chloride solution (15 mL). The organic phase was dried over sodium sulfate and was filtered. The filtrate was concentrated to provide crude material which was purified via flash-column chromatography (20 \rightarrow 40% ethyl acetate–hexanes) to provide the hydroxamate **252** (123 mg, 88%) as a white foam. TLC (20% ethyl acetate–hexanes): R_f = 0.55 (UV, PMA). ^1H NMR (600 MHz, CD_3OD), δ : 7.43 (d, 2H, J = 6.5 Hz), 7.38–7.34 (m, 3H), 4.47–4.37 (m, 4H), 4.21 (s, 1H), 1.45 (s, 9H). [*Note: Two proton signals are hidden under the residual water peak at δ 4.87.] FTIR (neat), cm^{-1} : 3273 (br), 2978 (m), 1674 (s), 1368 (s), 1163 (s), 1026 (s), 700 (s); HRMS (ESI): Calcd for $(\text{C}_{17}\text{H}_{24}\text{F}_2\text{N}_2\text{O}_5 - \text{H})^-$: 373.1581; Found: 373.1562.

β -Lactam **253**.



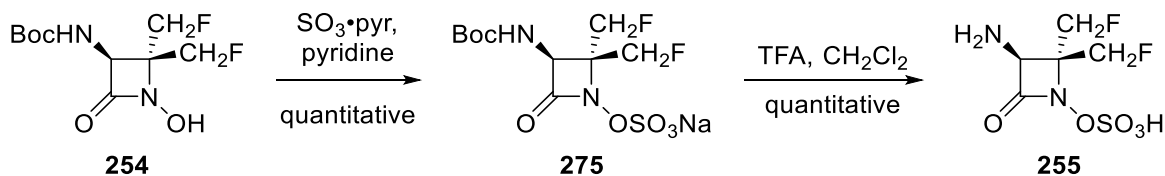
A 25-mL round bottom flask equipped with a stir bar was charged with hydroxamate **252** (123 mg, 0.329 mmol, 1 equiv). Dry acetonitrile (3.3 mL) was added, followed by carbon tetrachloride (190 μ L, 1.97 mmol, 6 equiv), triphenylphosphine (172 mg, 0.657 mmol, 2 equiv) and triethylamine (105 μ L, 0.756 mmol, 2.3 equiv). The reaction mixture continued to stir at 23 °C. After 2 h, the reaction mixture had darkened to brown in color. Reaction progress was monitored by the consumption of starting material by LC–MS analysis of aliquots removed from the reaction mixture. Upon complete consumption of the starting material, the reaction mixture was concentrated *in vacuo*. The residue was purified via flash-column chromatography (20% ethyl acetate–hexanes) to provide β -lactam **253** (53 mg, 45%). TLC (20% ethyl acetate–hexanes): R_f = 0.44 (UV, PMA). ¹H NMR (500 MHz, CD₃OD), δ : 7.45–7.38 (m, 5H), 5.01–4.96 (m, 2H), 4.84–4.70 (m, 3H), 4.62–4.43 (m, 2H), 1.44 (s, 9H). FTIR (neat), cm⁻¹: 3323 (br), 2980 (m), 2936 (m), 1790 (s), 1721 (s), 1163 (s), 1026 (s), 700 (s); HRMS (ESI): Calcd for (C₁₇H₂₂F₂N₂O₄ + Na)⁺: 379.1440; Found: 379.1437.

N-hydroxyl β -lactam **254**.



To a 10-mL round bottom flask equipped with a stir bar and charged with β -lactam **253** (53.0 mg, 0.149 mmol, 1 equiv) was added methanol (1.49 mL), followed by 10% palladium on carbon (16.0 mg). The reaction flask was then equipped with a balloon of hydrogen. An atmosphere of hydrogen was introduced by briefly evacuating the flask and backfilling with hydrogen gas. This process was repeated three times and the reaction mixture was stirred under an atmosphere of hydrogen at 23 °C. Reaction progress was monitored by the consumption of starting material by LC-MS analysis of aliquots removed from the reaction mixture. After 3 h, the reaction mixture was filtered through a pad of Celite on a fritted filter in order to remove the palladium. The methanolic filtrate was concentrated *in vacuo* to provide *N*-hydroxyl β -lactam **254** (40 mg) in quantitative yield and was used without further purification. TLC (5% methanol-dichloromethane): $R_f = 0.31$ (UV, PMA). ^1H NMR (600 MHz, CD_3OD), δ : 4.86–4.71 (m, 4H), 4.63 (s, 1H), 1.45 (s, 9H). HRMS (ESI): Calcd for $(\text{C}_{10}\text{H}_{16}\text{F}_2\text{N}_2\text{O}_4 + \text{Na})^+$: 289.0976; Found: 289.1013.

Monocyclic β -lactam core **255**.

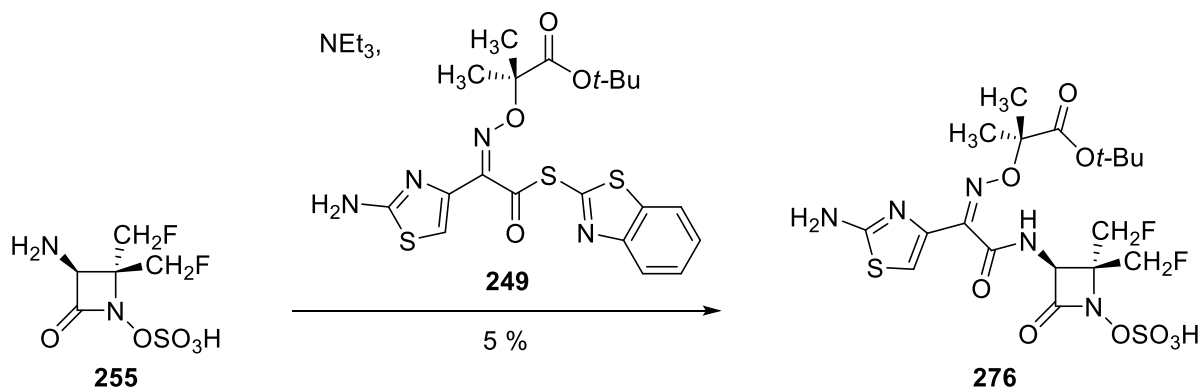


A 10-mL round bottom flask equipped with a stir bar was charged with *N*-hydroxyl β -lactam **254** (27.0 mg, 0.101 mmol, 1 equiv). Pyridine (254 μ L) was added and the reaction vessel was placed in an ice-water cooling bath. Sulfur trioxide-pyridine complex (21.0 mg, 0.132 mmol, 1.3 equiv) was added. The cooling bath was removed after 5 minutes and the vessel continued to stir at 23 °C. Reaction progress was monitored by the consumption of starting material by LC-MS analysis of aliquots removed from the reaction mixture. After 3 h, the reaction mixture was concentrated *in vacuo* to remove the pyridine and the residue was dissolved in methanol (2 mL). The *O*-sulfonic acid β -lactam solution in methanol was stirred with Dowex Marathon C Ion exchange beads for 15 min. The methanolic solution was filtered and the filtrate was concentrated to provide the *O*-sulfonic acid **275** (37.0 mg) in quantitative yield and was used without further purification.

A 10-mL round bottom flask equipped with a stir bar was charged with *O*-sulfonic acid **275** (37.0 mg, 0.101 mmol, 1 equiv), followed by dichloromethane (0.3 mL). The reaction vessel was placed in an ice-water cooling bath and a 1:1 mixture of trifluoroacetic acid:dichloromethane (0.7 mL) was added. Reaction progress was monitored by the consumption of starting material by LC-MS analysis of aliquots removed from the reaction mixture. After 20 min at 0 °C, the reaction mixture was concentrated to provide core **255** (25.0 mg) in quantitative yield as a white solid was used without further purification. ¹H NMR (600 MHz, CD₃OD), δ : 5.08 (dd, 1H, *J* = 11.5 Hz, 2.7 Hz), 5.00 (d, 1H, *J* = 11.5 Hz), 4.94–4.81 (m, 2H), 4.65 (s, 1H). [*Note: The

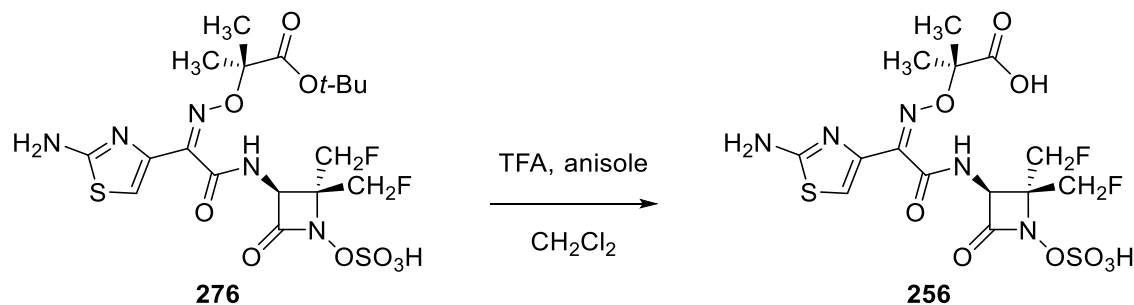
residual water peak at δ 4.87 obscures analysis of the multiplet at δ : 4.94–4.81]. HRMS (ESI):
Calcd for $(\text{C}_5\text{H}_8\text{F}_2\text{N}_2\text{O}_5\text{S} - \text{H})^-$: 245.0044; Found: 245.0073.

Amide **276**.



A 10-mL round bottom flask equipped with a stir bar was charged with core **255** (25.0 mg, 0.101 mmol, 1 equiv), followed by wet tetrahydrofuran (0.4 mL). The reaction vessel was placed in an ice-water cooling bath. Triethylamine (42.5 μL , 0.305 mmol, 3 equiv) was added and the cooling bath was removed after 5 minutes. The vessel continued to stir at 23 $^\circ\text{C}$ as **249** (73.0 mg, 0.152 mmol, 1.5 equiv) was added portion-wise. Reaction progress was monitored by the consumption of the core by LC–MS analysis of aliquots removed from the reaction mixture. After 2.5 h, ethyl acetate (10 mL) and water (10 mL) were added and the layers were separated. The organic layer was washed with 0.5 M aqueous hydrochloric acid solution (2×10 mL) and the aqueous extracts were combined and concentrated with no additional heating on the rotovap bath. The crude material was purified via reverse-phase HPLC (Agilent Extend-C18, 90:10 \rightarrow 70:30 water–acetonitrile + 0.1% formic acid, then 100% acetonitrile + 0.1% formic acid) to provide amide **276** (3.0 mg, 5%) as an off-white solid. ^1H NMR (600 MHz, CD_3OD), δ : 7.14 (s, 1H), 5.33 (s, 1H), 5.00–4.83 (m, 4H), 1.60 (s, 3H), 1.59 (s, 3H), 1.47 (s, 9H). HRMS (ESI): Calcd for $(\text{C}_{18}\text{H}_{25}\text{F}_2\text{N}_5\text{O}_9\text{S}_2 - \text{H})^-$: 556.0989; Found: 556.0985.

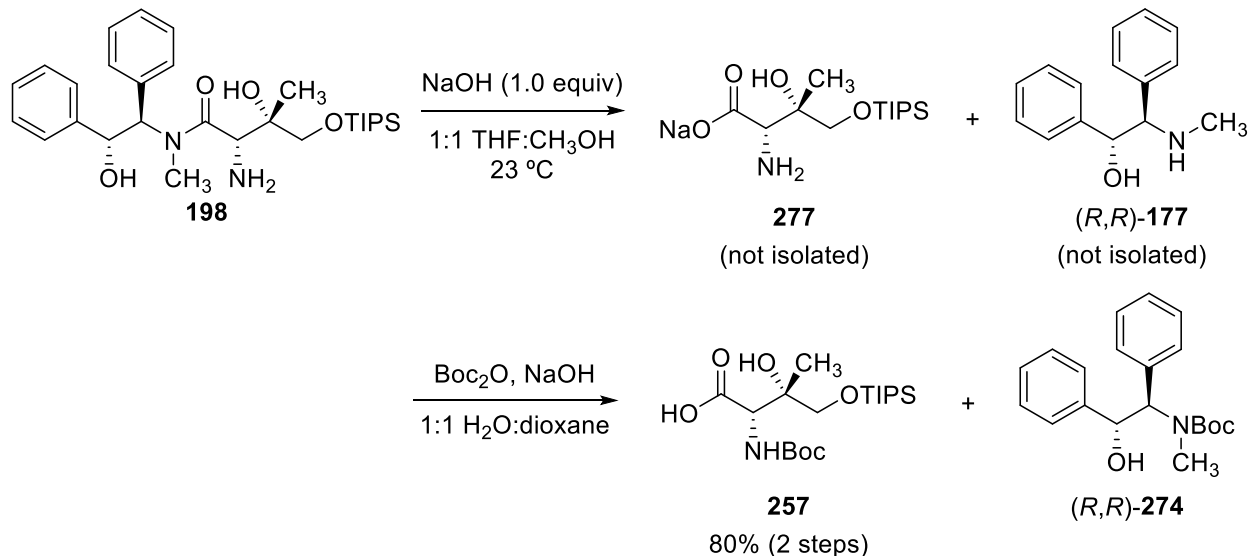
Bisfluoromethyl monobactam **256**.



A 10-mL round bottom flask equipped with a stir bar was charged with the coupled product **276** (3.0 mg, 5.4 μmol , 1 equiv), followed by dry dichloromethane (0.1 mL) and anisole (53 μL , 0.48 mmol, 90 equiv). The reaction vessel was placed in an ice-water cooling bath. Trifluoroacetic acid (83 μL , 1.1 mmol, 200 equiv) was added and the vessel continued to stir at 0 $^\circ\text{C}$ as reaction progress was monitored by the consumption of the starting material by LC–MS analysis of aliquots removed from the reaction mixture. After 30 min, additional trifluoroacetic acid (0.5 mL) was added and the reaction vessel continued to stir at 0 $^\circ\text{C}$. After 45 additional minutes, toluene (10 mL) was added and the reaction mixture was concentrated without additional heating on the rotovap bath. Water (2 mL) and hexanes (2 mL) were added and then layers were separated. A reverse-phase HPLC sample was prepared from the aqueous phase and the crude material was purified (Agilent Extend-C18, 90:10 \rightarrow 70:30 water–acetonitrile + 0.1% formic acid, then 100% acetonitrile + 0.1% formic acid)¹⁶¹ to provide *O*-sulfonic acid monobactam **256** (1.2 mg, 45%) as an off-white solid. HRMS (ESI): Calcd for $(\text{C}_{14}\text{H}_{17}\text{F}_2\text{N}_5\text{O}_9\text{S}_2 - \text{H})^-$: 500.0358; Found: 500.0469.

¹⁶¹ Care must be taken upon concentration of the aqueous fractions. Labile hydrolysis of the *O*-sulfonic acid occurs upon concentration of the HPLC fractions with formic acid present. Therefore, toluene was added to all desired fractions and the fractions were concentrated without additional heating on the rotovap bath.

One pot, two step synthesis of *N*-Boc acid **257** from aldol adduct **198**.

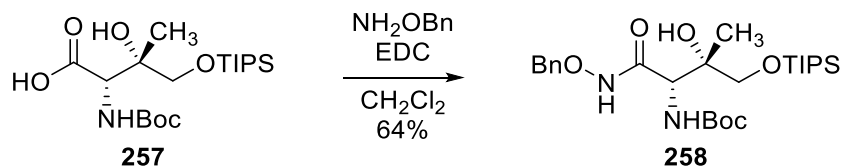


A 200-mL round bottom flask equipped with a stir bar was charged with aldol adduct **198** (3.55 g, 6.90 mmol, 1 equiv). A 1:1 mixture of tetrahydrofuran:methanol (30 mL) was added, followed by aqueous sodium hydroxide solution (1.0 M, 6.90 mL, 6.90 mmol, 1 equiv). Reaction progress was monitored by the consumption of starting material by TLC (10% methanol–dichloromethane + 0.5% saturated aqueous ammonium hydroxide solution). After 1 d, the reaction mixture was concentrated to dryness and the residue was dissolved in a 1:1 mixture of water:1,4-dioxane (50 mL). The reaction vessel was placed in an ice-water cooling bath. Aqueous sodium hydroxide solution (1.0 M, 20.7 mL, 20.7 mmol, 3 equiv) was added, followed by di-*tert*-butyl dicarbonate (4.81 mL, 20.7 mmol, 3 equiv). The cooling bath was removed after 5 minutes and the vessel continued to stir at 23 °C. Reaction progress was monitored by the consumption of starting material by LC–MS analysis of aliquots removed from the reaction mixture. After 16 h, water (90 mL) was added and the mixture was washed with three portions of ether (90 mL). The ethereal extracts were combined and back-extracted with 0.5 M aqueous

sodium hydroxide solution (50 mL). The ethereal extracts were dried over sodium sulfate and filtered. The filtrate was concentrated to provide *N*-Boc-pseudoephedrine in quantitative yield.

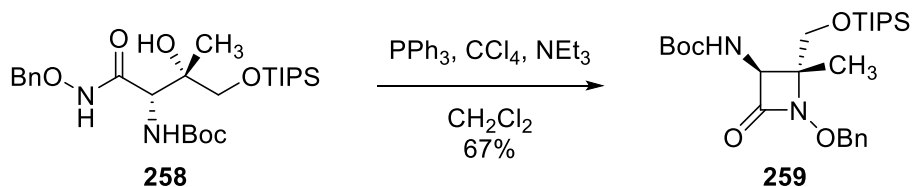
The basic aqueous phases were combined, the resulting solution was cooled in an ice-water cooling bath, and 1 M aqueous hydrochloric acid solution was added dropwise until the pH of the solution was ~2. The acidified aqueous phase was then extracted with ethyl acetate (3 × 75 mL). The organic extracts were combined and were dried over sodium sulfate. The dried organic solution was filtered and the filtrate was concentrated to provide *N*-Boc-protected acid **257** (2.23 g, 80%) as a clear oil. TLC (30% ethyl acetate–hexanes + 1% acetic acid): $R_f = 0.15$ (UV, PMA). $^1\text{H NMR}$ (3:1 ratio of rotamers; major rotamer reported, 600 MHz, CD_3OD), δ : 4.26 (s, 1H), 3.80 (d, 1H, $J = 9.4$ Hz), 3.45 (d, 1H, $J = 9.4$ Hz), 1.43 (s, 9H), 1.35 (s, 3H), 1.15–1.10 (m, 21H). FTIR (neat), cm^{-1} : 3331 (br), 2943 (m), 2866 (m), 1715 (s), 1368 (s), 1163 (s), 1101 (s), 683 (s); HRMS (ESI): Calcd for $(\text{C}_{19}\text{H}_{39}\text{NO}_6\text{Si} + \text{NH}_4)^+$: 423.2885; Found: 423.2887.

Hydroxamate **258**.



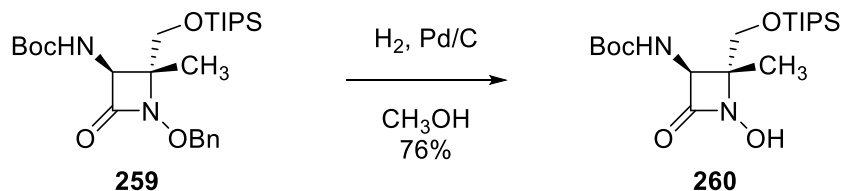
To a 200-mL round bottom flask equipped with a stir bar was added *N*-Boc acid **257** (2.23 g, 5.42 mmol, 1 equiv) and dry dichloromethane (54 mL). *O*-Benzylhydroxylamine (726 μ L, 6.24 mmol, 1.15 equiv) was added, followed by EDC (1.14 g, 5.97 mmol, 1.1 equiv) in one portion. Reaction progress was monitored by the consumption of starting material by LC–MS analysis of aliquots removed from the reaction mixture. After 1 h, additional dichloromethane (10 mL) was added and the reaction mixture was washed sequentially with water (25 mL) and saturated aqueous sodium chloride solution (25 mL). The organic phase was dried over sodium sulfate and was filtered. The filtrate was concentrated to provide crude material which was purified via flash-column chromatography (10 \rightarrow 30% ethyl acetate–hexanes) to provide hydroxamate **258** (1.77 g, 64%) as a white foam. TLC (33% ethyl acetate–hexanes): R_f = 0.55 (UV, PMA). ¹H NMR (600 MHz, CD₃OD), δ : 7.44 (d, 2H, J = 7.0 Hz), 7.38–7.33 (m, 3H), 4.06 (s, 1H), 3.81 (d, 1H, J = 9.4 Hz), 3.39 (d, 1H, J = 9.4 Hz), 1.43 (s, 9H), 1.27 (s, 3H), 1.15–1.09 (m, 21H). [*Note: Two proton signals are hidden under the residual water peak at δ 4.87.] FTIR (neat), cm⁻¹: 3431 (br), 3242 (br), 2943 (m), 2866 (m), 1674 (s) 1499 (s), 1167 (s), 1099 (s), 683 (s); HRMS (ESI): Calcd for (C₂₆H₄₆N₂O₆Si + K)⁺: 549.2757; Found: 549.2762.

β -Lactam **259**.



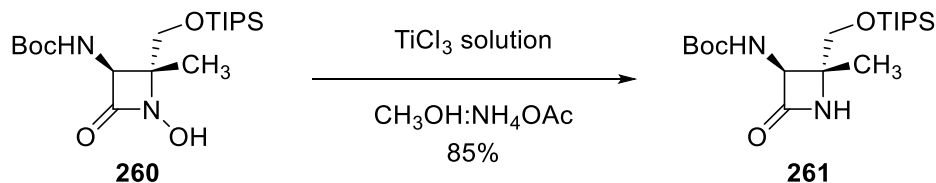
A 100-mL round bottom flask equipped with a stir bar was charged with hydroxamate **258** (1.74 g, 3.41 mmol, 1 equiv). Dry acetonitrile (34 mL) was added, followed by carbon tetrachloride (1.97 mL, 20.4 mmol, 6 equiv), triphenylphosphine (894 mg, 3.41 mmol, 1 equiv) and triethylamine (1.09 mL, 7.84 mmol, 2.3 equiv). The reaction mixture continued to stir at 23 °C; after 1 h, an additional portion of triphenylphosphine (295 mg, 0.124 mmol, 0.33 equiv) was added. Reaction progress was monitored by the consumption of starting material by LC–MS analysis of aliquots removed from the reaction mixture. After 2 h, the reaction mixture had darkened to brown in color and was concentrated *in vacuo*. The residue was purified via flash-column chromatography (5→50% ethyl acetate–hexanes) to provide β -lactam **259** (1.13 g, 67%). TLC (40% ethyl acetate–hexanes): R_f = 0.28 (UV, PMA). ¹H NMR (600 MHz, CD₃OD), δ : 7.43–7.41 (m, 2H), 7.39–7.35 (m, 3H), 5.04 (d, 1H, J = 11.2 Hz), 4.94 (d, 1H, J = 11.2 Hz), 4.77 (s, 1H), 3.93 (d, 1H, J = 11.2 Hz), 3.79 (d, 1H, J = 11.2 Hz), 1.44 (s, 9H), 1.15–1.11 (m, 3H), 1.10–1.08 (m, 18H), 0.97 (s, 3H). FTIR (neat), cm⁻¹: 3322 (br), 2926 (m), 2866 (m), 1770 (s) 1721 (s), 1167 (s), 1107 (s), 683 (s); HRMS (ESI): Calcd for (C₂₆H₄₄N₂O₅Si + K)⁺: 531.2651; Found: 531.2668.

N-hydroxyl β -lactam **260**.



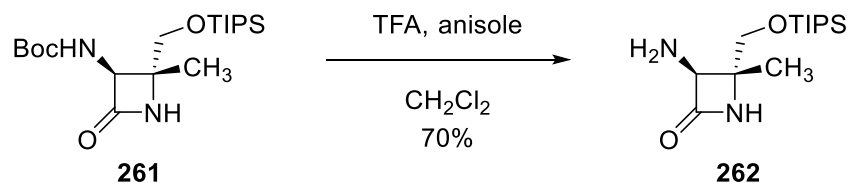
To a 100-mL round bottom flask equipped with a stir bar and charged with β -lactam **259** (1.10 g, 2.23 mmol, 1 equiv) was added methanol (45 mL), followed by 10% palladium on carbon (238 mg). The reaction flask was then equipped with a balloon of hydrogen. An atmosphere of hydrogen was introduced by briefly evacuating the flask and backfilling with hydrogen gas. This process was repeated three times and the reaction mixture was stirred under an atmosphere of hydrogen at 23 °C. Reaction progress was monitored by the consumption of starting material by LC-MS analysis of aliquots removed from the reaction mixture. After 2 h, the reaction mixture was filtered through a pad of Celite on a fritted filter in order to remove the palladium. The methanolic filtrate was concentrated and purified via flash-column chromatography (1 \rightarrow 4% methanol-dichloromethane) to provide the *N*-hydroxyl β -lactam **260** (683 mg, 76%) as a white foam. TLC (10% methanol-dichloromethane): R_f = 0.31 (UV, PMA). ¹H NMR (600 MHz, CD₃OD), δ : 4.81 (s, 1H), 3.96 (d, 1H, J = 11.2 Hz), 3.82 (d, 1H, J = 11.2 Hz), 1.45 (s, 9H), 1.17–1.13 (m, 6H), 1.12–1.11 (m, 18H). FTIR (neat), cm⁻¹: 3312 (br), 2942 (m), 2866 (m), 1761 (s), 1713 (s), 1165 (s), 1111 (s), 802 (s); HRMS (ESI): Calcd for (C₁₉H₃₈N₂O₅Si + H)⁺: 403.2623; Found: 406.2639.

N-H β -lactam **261**.



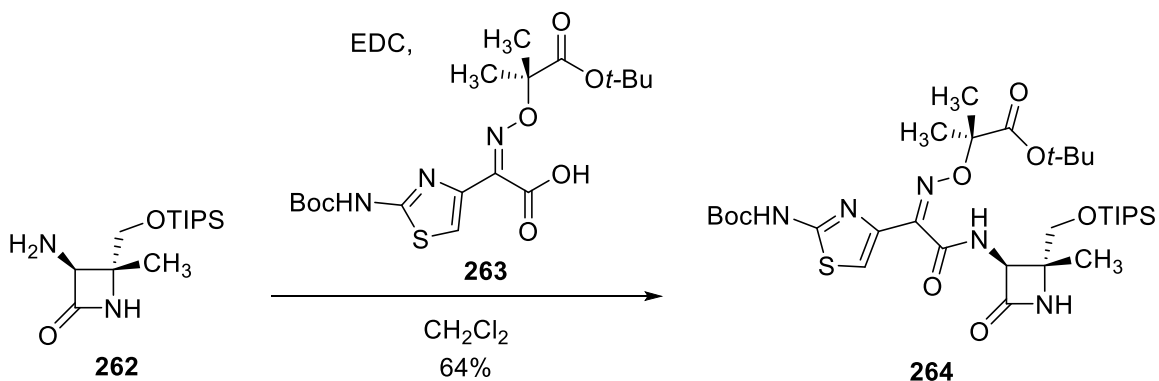
To a 25-mL round bottom flask equipped with a stir bar and charged with *N*-hydroxyl β -lactam **260** (103 mg, 0.256 mmol, 1 equiv) was added a 3:2 mixture of methanol:4.5 M aqueous ammonium acetate solution (3.65 mL). Argon gas was bubbled through the homogeneous solution for 15 minutes before a solution of titanium trichloride (0.500 mL, ~10 wt.% in 20-30 wt. % hydrochloric acid solution) was added at 23 °C. Reaction progress was monitored by the consumption of starting material by TLC and LC-MS analysis of aliquots removed from the reaction mixture. After 5 h, saturated aqueous sodium chloride solution (18 mL) and 2:1 ethyl acetate:tetrahydrofuran (18 mL) were added. The layers were separated and the organic phase was washed sequentially with saturated aqueous sodium bicarbonate solution (20 mL), water (20 mL), and saturated aqueous sodium chloride solution (20 mL). The organic phase was dried over sodium sulfate and was filtered. The filtrate was concentrated to provide crude material which was purified via flash-column chromatography (1 \rightarrow 4% methanol-dichloromethane) to provide the *N*-H β -lactam **261** (84 mg, 85%) as a white foam. TLC (10% methanol-dichloromethane): R_f = 0.38 (UV, PMA). ¹H NMR (600 MHz, CD₃OD), δ : 4.79 (s, 1H), 3.81–3.78 (m, 2H), 1.45 (s, 9H), 1.22 (s, 3H), 1.17–1.13 (m, 3H), 1.12–1.10 (m, 18H). FTIR (neat), cm⁻¹: 3304 (br), 2928 (m), 2866 (m), 1761 (s) 1721 (s), 1169 (s), 683 (s); HRMS (ESI): Calcd for (C₁₉H₃₈N₂O₄Si + H)⁺: 387.2688; Found: 387.2674.

Amine **262**.



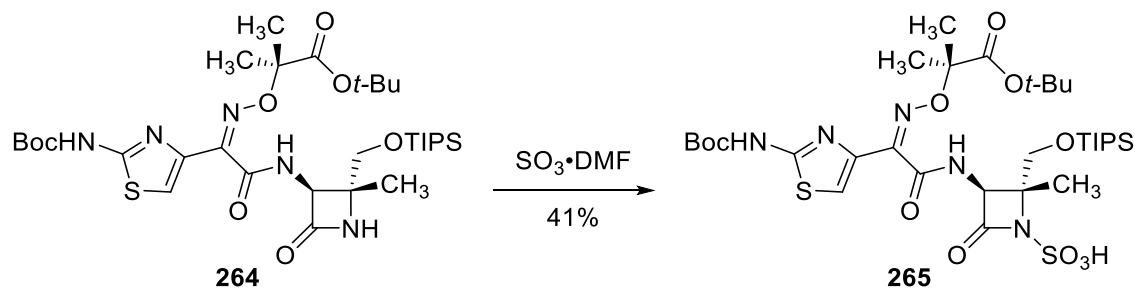
A 10-mL round bottom flask equipped with a stir bar was charged with *N*-H β-lactam **261** (58.0 mg, 0.150 mmol, 1 equiv), followed by dichloromethane (1.5 mL) and anisole (410 μL, 3.75 mmol, 25 equiv). The reaction vessel was placed in an ice-water cooling bath and trifluoroacetic acid (580 μL, 7.50 mmol, 50 equiv) was added. Reaction progress was monitored by the consumption of starting material by LC–MS analysis of aliquots removed from the reaction mixture. After 2 h at 0 °C, 1.0 M sodium hydroxide solution was added dropwise until pH ~14. The now basic aqueous phase was extracted with dichloromethane (3 × 7 mL). The organic extracts were combined, washed with saturated aqueous sodium chloride solution (15 mL), and dried over sodium sulfate. The dried organic solution was filtered and the filtrate was concentrated to provide the amine **262** (30.0 mg, 70%) as a clear film. TLC (10% methanol–dichloromethane): $R_f = 0.27$ (UV, PMA). ^1H NMR (600 MHz, CD_3OD), δ : 3.99 (s, 1H), 3.78–3.73 (m, 2H), 1.28 (s, 3H), 1.16–1.09 (m, 21H). FTIR (neat), cm^{-1} : 3314 (br), 2941 (m), 2866 (m), 1755 (s), 1724 (s), 1105 (s), 1059 (s), 712 (s), 681 (s); HRMS (ESI): Calcd for $(\text{C}_{14}\text{H}_{30}\text{N}_2\text{O}_2\text{Si} + \text{Na})^+$: 309.1969; Found: 309.1975.

N-acylated product **264**.



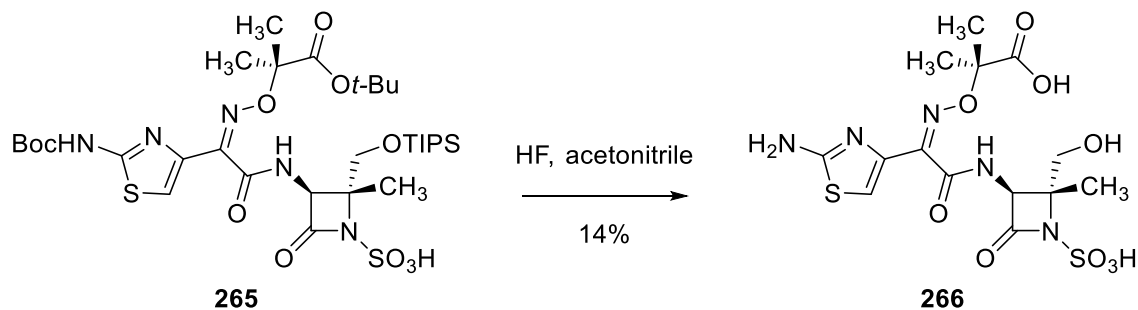
To a 10-mL round bottom flask equipped with a stir bar was added the amine **262** (30.0 mg, 1.05 mmol, 1 equiv) and dry dichloromethane (1.05 mL). Acid **263** (45.0 mg, 1.05 mmol, 1 equiv) was added, followed by EDC (21 mg, 1.10 mmol, 1.05 equiv) in one portion. Reaction progress was monitored by the consumption of starting material by LC–MS analysis of aliquots removed from the reaction mixture. After 1 h, additional dichloromethane (10 mL) was added and the reaction mixture was washed sequentially with water (25 mL), 1.0 M aqueous hydrochloric acid solution (25 mL), water (25 mL), and saturated aqueous sodium chloride solution (25 mL). The organic phase was dried over sodium sulfate and was filtered. The filtrate was concentrated to provide crude material which was purified via flash-column chromatography (1→10% methanol–dichloromethane) to provide amide **264** (47.0 mg, 64%) as a white foam. TLC (10% methanol–dichloromethane): $R_f = 0.33$ (UV, PMA). ^1H NMR (600 MHz, CD_3OD), δ : 7.33 (s, 1H), 5.21 (s, 1H), 3.90–3.85 (m, 2H), 1.54 (s, 9H), 1.52 (s, 3H), 1.50 (s, 3H), 1.48 (s, 9H), 1.32 (s, 3H), 1.19–1.15 (m, 3H), 1.14–1.11 (m, 18H). FTIR (neat), cm^{-1} : 3256 (br), 2942 (m), 2866 (m), 1755 (s), 1721 (s), 1553 (s), 1148 (s), 682 (s); HRMS (ESI): Calcd for $(\text{C}_{32}\text{H}_{55}\text{N}_5\text{O}_8\text{SSi} + \text{H})^+$: 698.3613; Found: 698.3617.

N-Sulfonic Acid **265**.



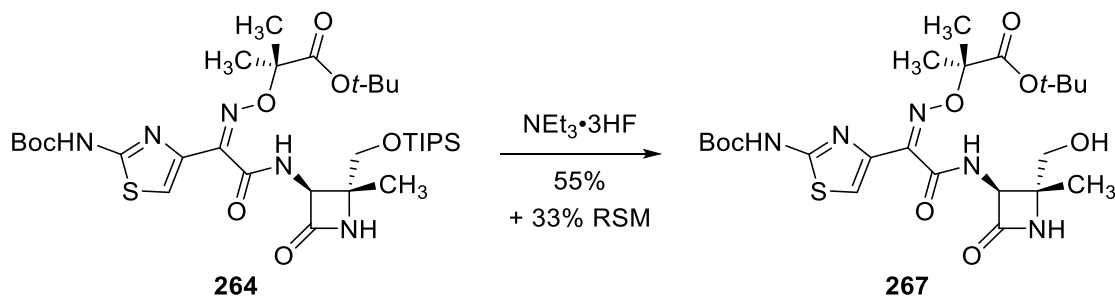
A 10-mL round bottom flask equipped with a stir bar was charged with amide **264** (13 mg, 19 μmol , 1 equiv). Dimethylformamide (0.2 mL) was added, followed by sulfur trioxide–dimethylformamide complex (29 mg, 190 μmol , 10 equiv) and the reaction mixture continued to stir at 23 °C. Reaction progress was monitored by the consumption of starting material by LC–MS analysis of aliquots removed from the reaction mixture. After 3 h, water (0.6 mL) was added, followed by ethyl acetate (0.5 mL) and half saturated aqueous sodium chloride solution (0.5 mL). The layers were separated and the aqueous phase was extracted with ethyl acetate (3 \times 2 mL). The combined organic extracts were washed sequentially with half saturated aqueous sodium chloride solution (5 mL) and saturated aqueous sodium chloride solution (5 mL). The washed organic phase was dried over sodium sulfate and the dried organic phase was filtered. The filtrate was concentrated to provide the *N*-sulfonic acid **265** (6.0 mg, 41%) which was used without further purification.

Hydroxymethyl monobactam **266**.



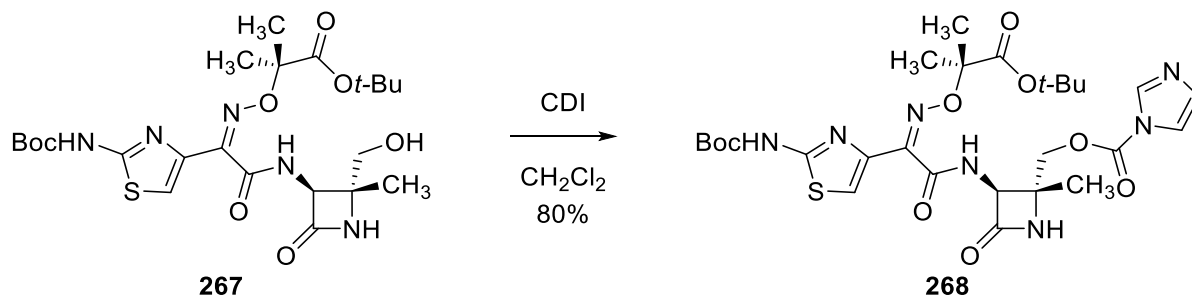
Concentrated aqueous hydrofluoric acid solution (48 wt%, 20 μ L) was added to a solution of the *N*-sulfonic acid **265** (6.0 mg, 7.7 μ mol, 1 equiv) in acetonitrile (0.5 mL) in a polypropylene reaction vessel at 23 $^{\circ}$ C. Reaction progress was monitored by the consumption of starting material by LC–MS analysis of aliquots removed from the reaction mixture. Upon consumption of the starting material and complete global deprotections, excess methoxytrimethylsilane (0.5 mL) was added to quench the hydrofluoric acid. The reaction mixture was concentrated and the residue was purified by reverse-phase HPLC (Agilent Extend-C18, 90:10 \rightarrow 10:90 water–acetonitrile + 0.1% formic acid) to afford hydroxymethyl monobactam **266** (0.5 mg, 14%). 1 H NMR (600 MHz, CD₃OD), δ : 6.86 (s, 1H), 5.26 (s, 1H), 4.05 (d, 1H, J = 12.4 Hz), 3.71 (d, 1H, J = 12.4 Hz), 1.57 (s, 3H), 1.54 (s, 3H), 1.46 (s, 3H). HRMS (ESI): Calcd for (C₁₄H₁₉N₅O₉S₂ + H)⁺: 466.0697; Found: 466.0711.

Alcohol **267**.



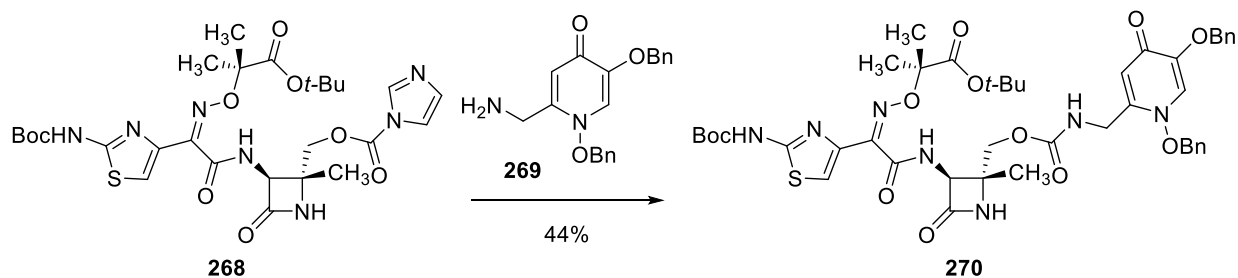
Amide **264** (40 mg, 57 μmol , 1 equiv) was dissolved in tetrahydrofuran (0.5 mL) in a polypropylene reaction tube. Excess triethylamine trihydrofluoride (93 μL , 570 μmol , 10 equiv) was added and the reaction mixture was stirred at 23 °C for 20 h. The reaction mixture was quenched with the addition of an aqueous potassium phosphate buffer solution (pH 7.0, 2 mL). Ethyl acetate (2 mL) was added and the layers were separated. The aqueous layer was extracted with ethyl acetate (2 \times 3 mL). The organic layers were combined and were washed with saturated aqueous sodium chloride solution (8 mL). The washed solution was dried over sodium sulfate and the dried solution was filtered. The filtrate was concentrated to provide crude material which was purified via flash-column chromatography (1 \rightarrow 4% methanol–dichloromethane) to recover starting amide **264** (13 mg, 33%) and to provide alcohol **267** (17 mg, 55%) as a clear film. TLC (10% methanol–dichloromethane): R_f = 0.25 (UV, PMA). ^1H NMR (600 MHz, CD_3OD), δ : 7.33 (s, 1H), 5.06 (s, 1H), 3.70–3.65 (m, 2H), 1.54 (s, 9H), 1.52 (s, 3H), 1.51 (s, 3H), 1.48 (s, 9H), 1.32 (s, 3H). FTIR (neat), cm^{-1} : 3283 (br), 2980 (m), 2936 (m), 1721 (s), 1553 (s), 1147 (s), 976 (s), 737 (s); HRMS (ESI): Calcd for $(\text{C}_{23}\text{H}_{35}\text{N}_5\text{O}_8\text{S} + \text{H})^+$: 542.2279; Found: 542.2301.

Carbamate **268**.



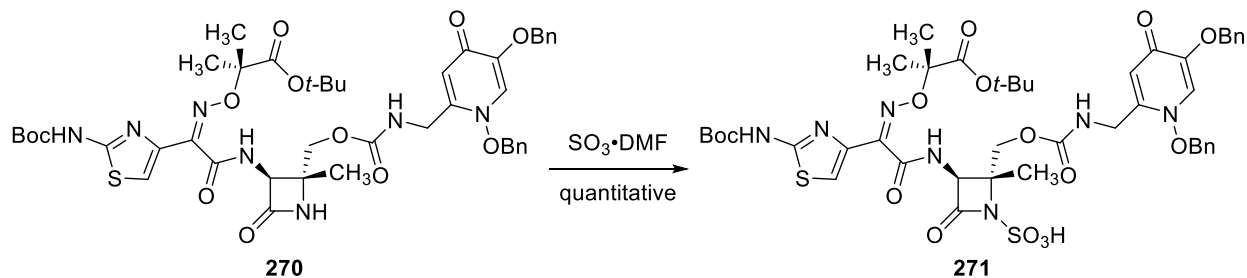
A 5-mL round bottom flask equipped with a stir bar was charged with carbonyldiimidazole (5.3 mg, 33 μ mol, 1.05 equiv), followed by dichloromethane (0.2 mL). A solution of alcohol **267** (17 mg, 31 μ mol, 1 equiv) in benzene (0.2 mL) was added. Reaction progress was monitored by the consumption of starting material by LC–MS analysis of aliquots removed from the reaction mixture. After 1 h, dichloromethane (3 mL) was added, followed by half saturated aqueous ammonium chloride solution (3 mL). The layers were separated and the organic phase was washed with an additional portion of half saturated aqueous ammonium chloride solution (3 mL). The washed solution was dried over sodium sulfate and the dried solution was filtered. The filtrate was concentrated to provide crude carbamate **268** (16 mg, 80%) which was used without further purification.

Carbamate **270**.



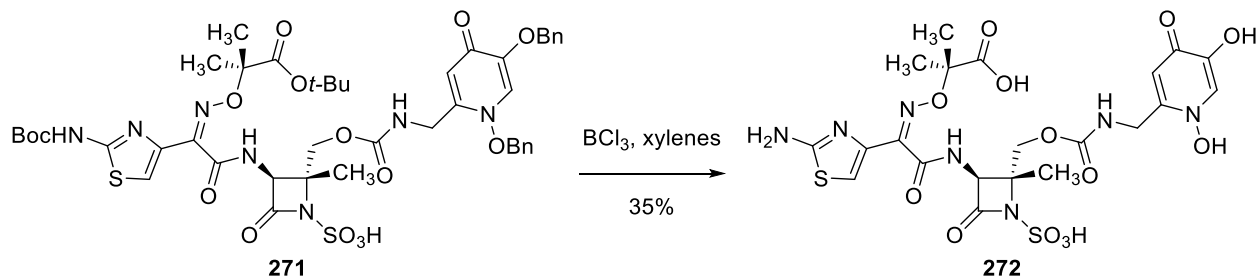
A 5-mL round bottom flask equipped with a stir bar was charged with carbamate **268** (16 mg, 25 μ mol, 1 equiv), followed by benzene (1 mL). Argon was bubbled through the reaction mixture for 10 minutes at 23 °C before amine **269** (17 mg, 50 μ mol, 2 equiv) was added. The reaction mixture was placed in a 50 °C oil bath and reaction progress was monitored by the consumption of starting material by LC–MS analysis of aliquots removed from the reaction mixture. After 18 h, the reaction flask containing a now green reaction mixture was removed from the oil bath and allowed to cool to 23 °C. The reaction mixture was concentrated and the residue was dissolved in dichloromethane (3 mL). The organic phase was washed sequentially with half saturated aqueous ammonium chloride solution (3 mL), water (3 mL) and saturated aqueous sodium chloride solution (3 mL). The washed solution was dried over sodium sulfate and the dried solution was filtered. The filtrate was concentrated to provide crude material which was purified via flash-column chromatography (1 \rightarrow 10% methanol–dichloromethane) to provide carbamate **270** (10 mg, 44%) as a green solid. TLC (10% methanol–dichloromethane): R_f = 0.30 (UV, PMA). ^1H NMR (600 MHz, CD_3OD), δ : 7.73 (s, 1H), 7.46–7.33 (m, 10H), 6.34 (s, 1H), 5.25 (s, 2H), 5.11 (s, 1H), 5.02 (s, 2H), 4.92 (s, 1H), 4.60 (br s, 4H), 4.38 (d, 1H, J = 11.7 Hz), 4.24–4.19 (m, 2H), 4.16 (d, 1H, J = 11.7 Hz), 1.53 (s, 9H), 1.52 (s, 3H), 1.50 (s, 3H), 1.47 (s, 9H), 1.37 (s, 3H). HRMS (ESI): Calcd for $(\text{C}_{44}\text{H}_{53}\text{N}_7\text{O}_{12}\text{S} + \text{H})^+$: 904.3546; Found: 904.3563.

N-Sulfonic Acid **271**.



A 10-mL round bottom flask equipped with a stir bar was charged with carbamate **271** (10 mg, 11 μmol , 1 equiv). Dimethylformamide (0.1 mL) was added, followed by sulfur trioxide–dimethylformamide complex (17 mg, 110 μmol , 10 equiv) and the reaction mixture continued to stir at 23 °C. Reaction progress was monitored by the consumption of starting material by LC–MS analysis of aliquots removed from the reaction mixture. After 45 min, water (0.6 mL) was added, followed by ethyl acetate (0.5 mL) and half saturated aqueous sodium chloride solution (0.5 mL). The layers were separated and the aqueous phase was extracted with ethyl acetate (3×2 mL). The combined organic extracts were washed sequentially with half saturated aqueous sodium chloride solution (5 mL) and saturated aqueous sodium chloride solution (5 mL). The washed organic phase was dried over sodium sulfate and the dried organic phase was filtered. The filtrate was concentrated to provide the *N*-sulfonic acid **271** (11 mg) as a green solid in quantitative yield and was carried forward without further purification. HRMS (ESI): Calcd for $(\text{C}_{44}\text{H}_{53}\text{N}_7\text{O}_{15}\text{S}_2 + \text{H})^+$: 984.3114; Found: 984.3137.

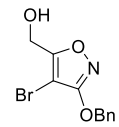
N-Sulfonic Acid Monobactam **272**.



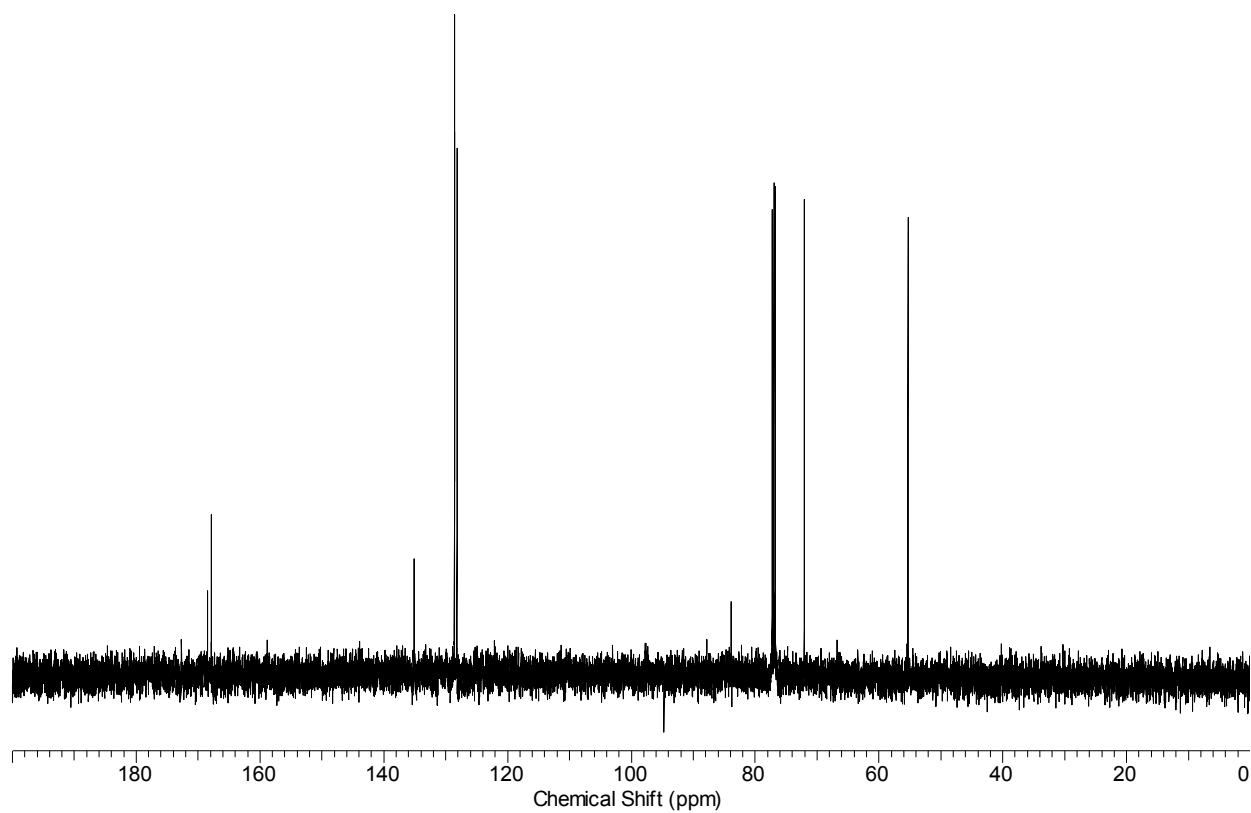
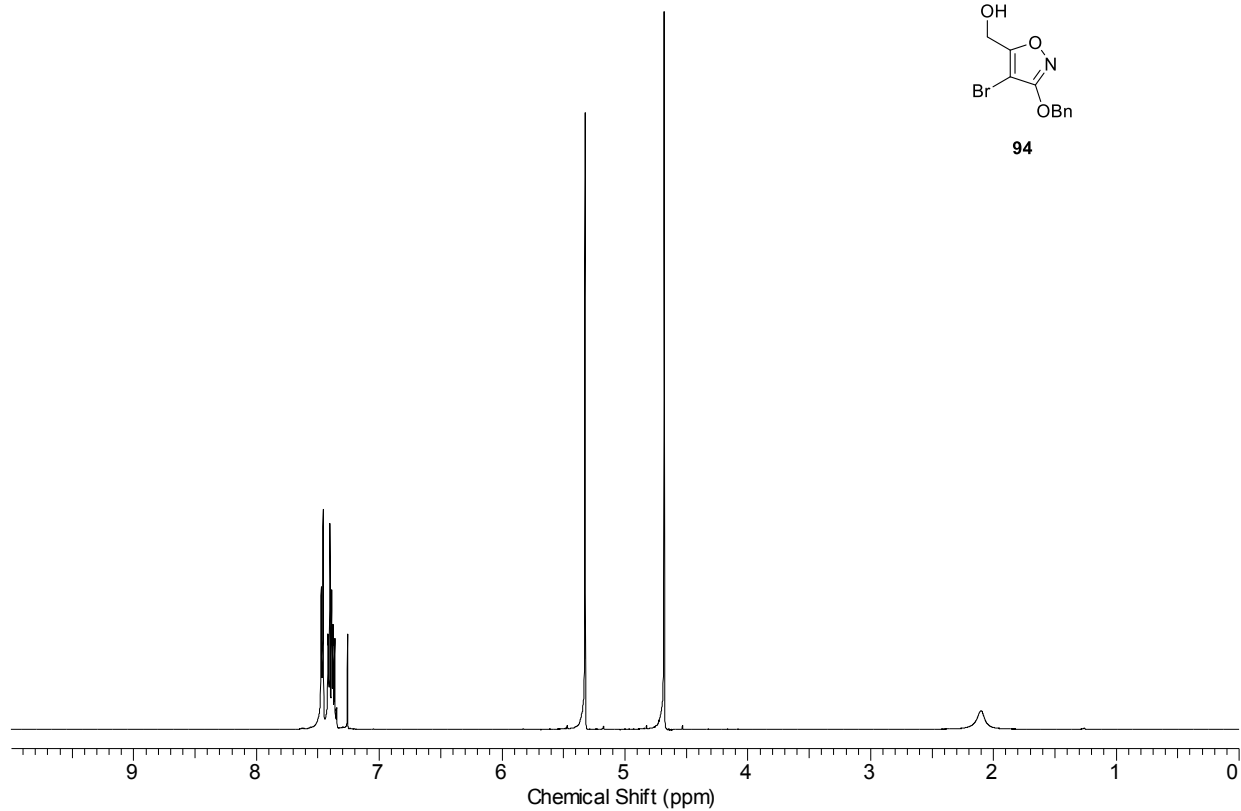
A 5-mL round bottom flask equipped with a stir bar was charged with the *N*-sulfonic acid **271** (11 mg, 11 μmol , 1 equiv), followed by dry dichloromethane (45 μL). Boron trichloride (1.0 M in *p*-xylenes, 78 μL , 78 μmol , 7 equiv) was added at 23 $^\circ\text{C}$. Reaction progress was monitored by LC–MS analysis of aliquots removed from the reaction mixture. After 90 min, water (0.3 mL) was added and the reaction mixture was concentrated. A reverse-phase HPLC sample was prepared from the residue and was purified (Agilent Extend-C18, 90:10 \rightarrow 10:90 water–acetonitrile + 0.1% formic acid) to afford *N*-sulfonic acid monobactam **272** (2.5 mg, 35%) as a light green solid. ^1H NMR (600 MHz, CD_3OD), δ : 8.20 (s, 1H), 7.19 (s, 1H), 7.19 (s, 1H), 5.29 (s, 1H), 4.71 (d, 1H, $J = 11.7$ Hz), 4.62 (d, 1H, $J = 17.3$ Hz), 4.46 (d, 1H, $J = 17.3$ Hz), 4.19 (d, 1H, $J = 11.7$ Hz), 1.64 (s, 3H), 1.63 (s, 3H), 1.51 (s, 3H). HRMS (ESI): Calcd for $(\text{C}_{21}\text{H}_{25}\text{N}_7\text{O}_{13}\text{S}_2 + \text{H})^+$: 648.1025; Found: 648.1035.

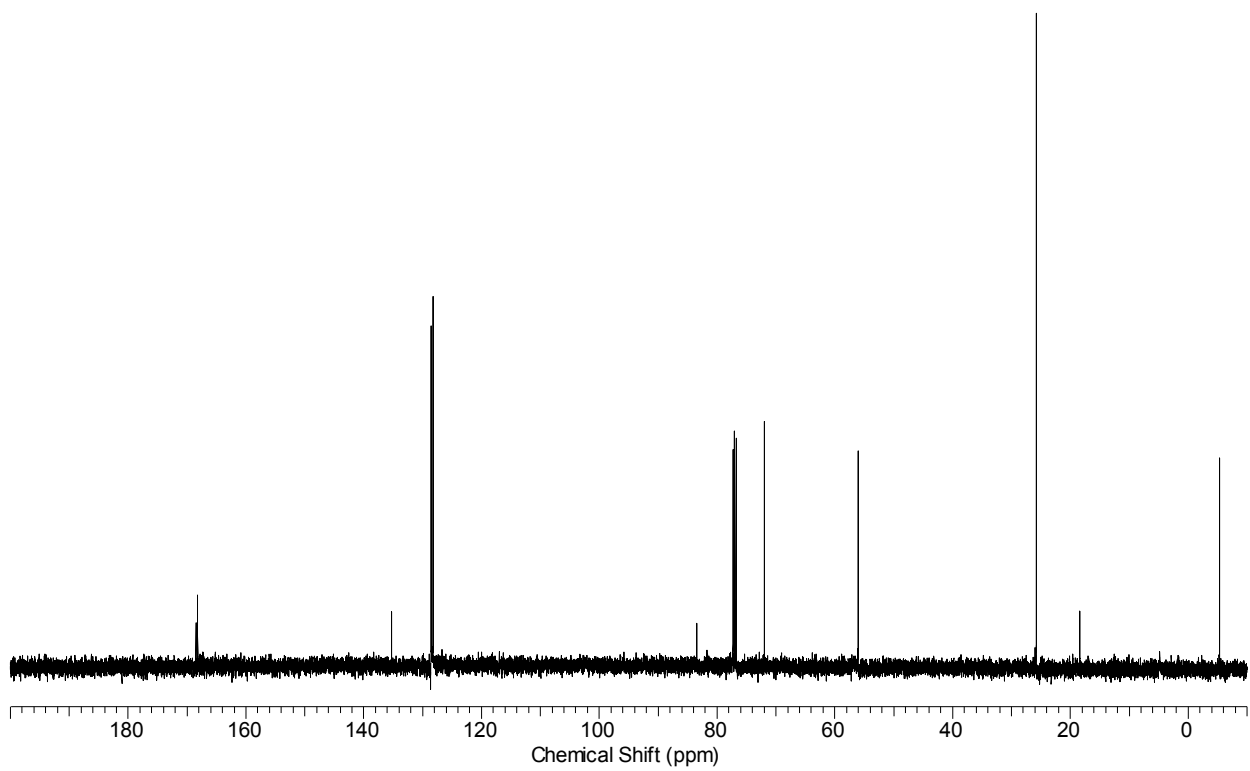
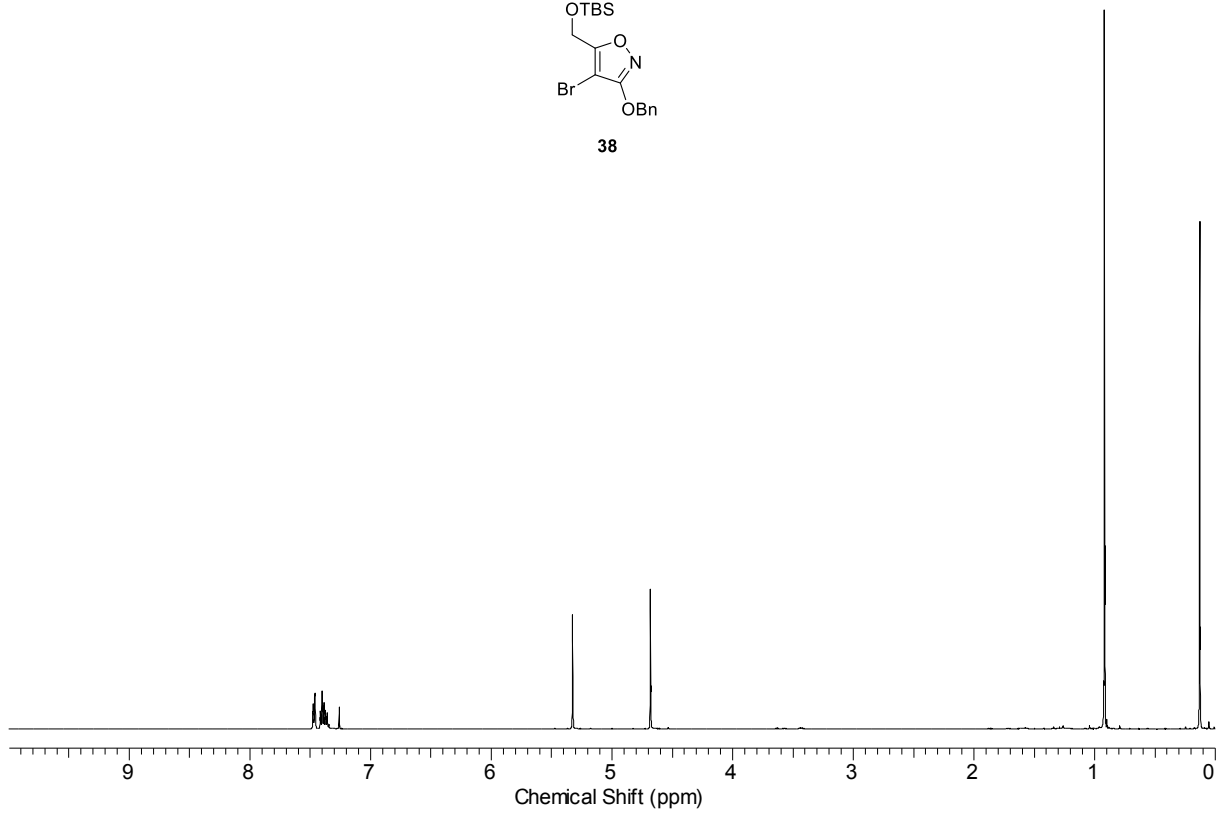
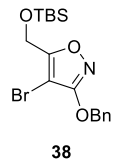
Appendix A

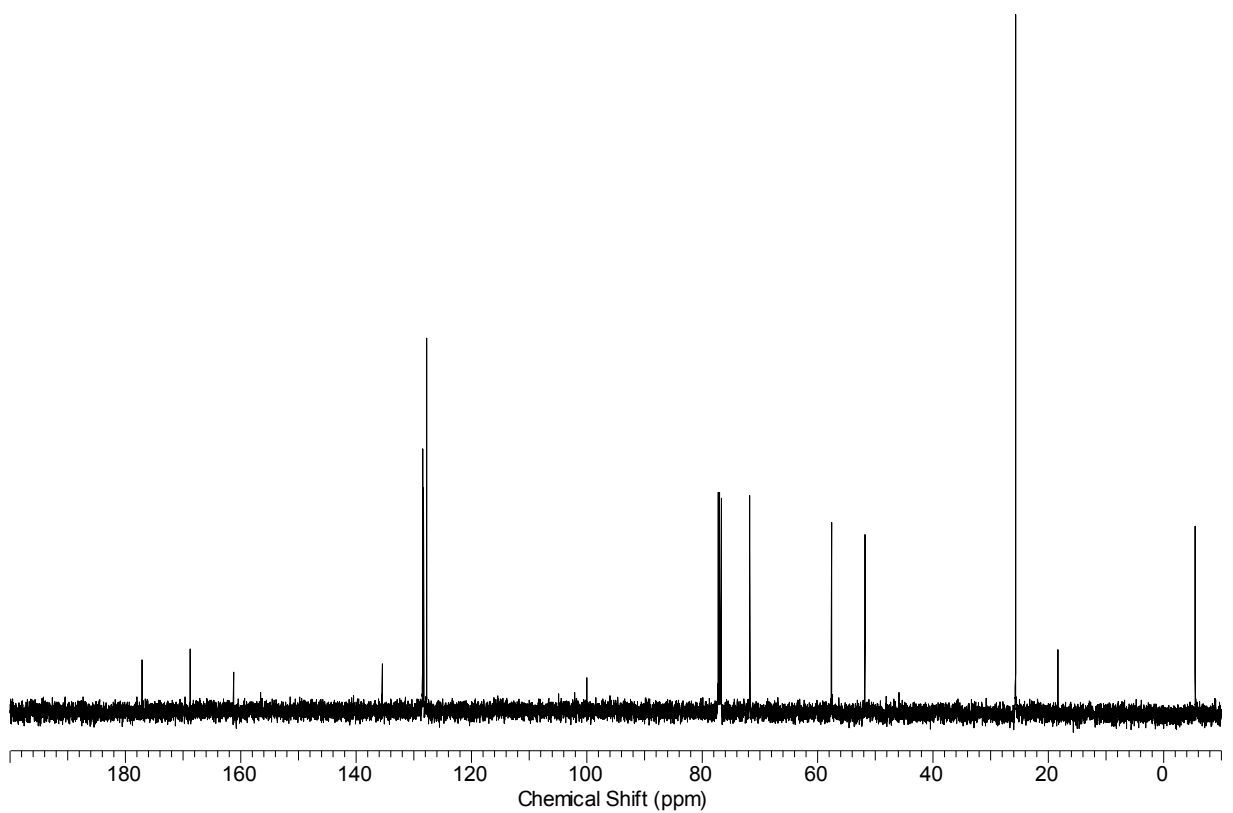
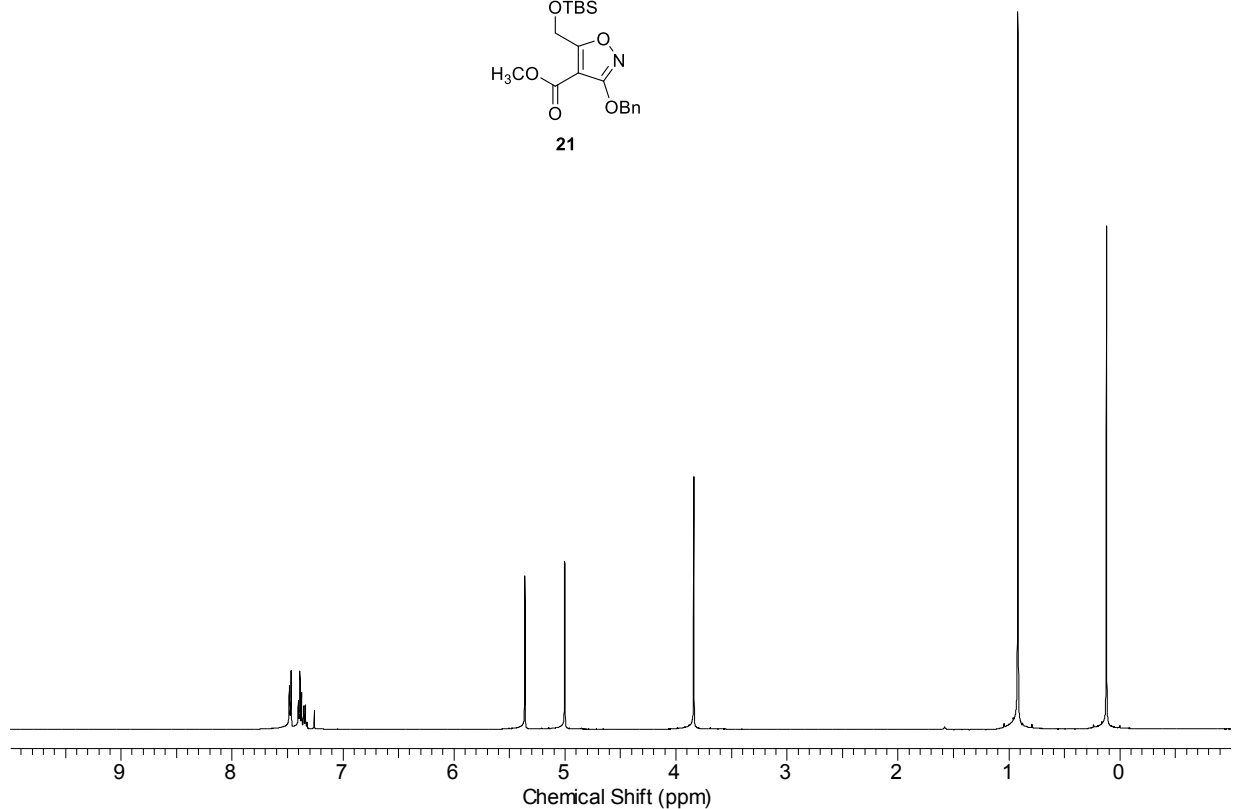
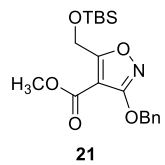
Catalog of Spectra

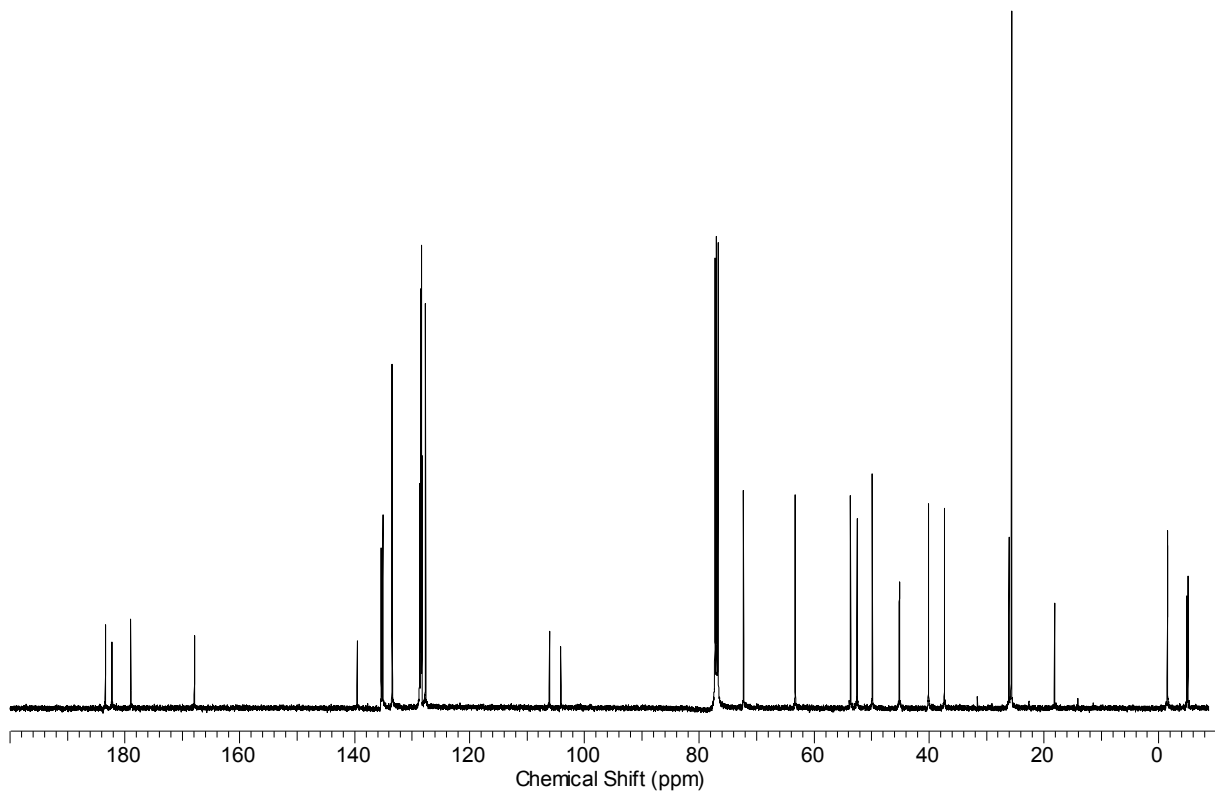
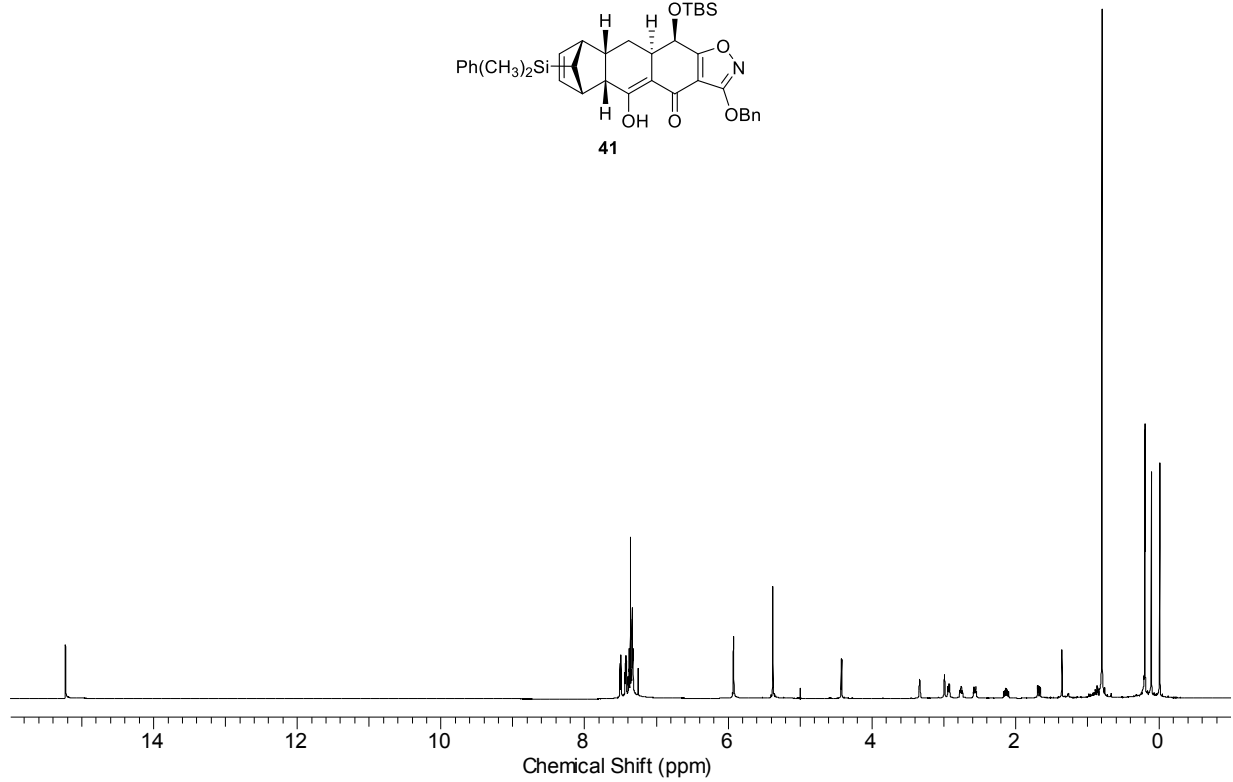
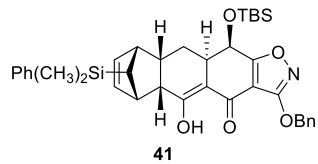


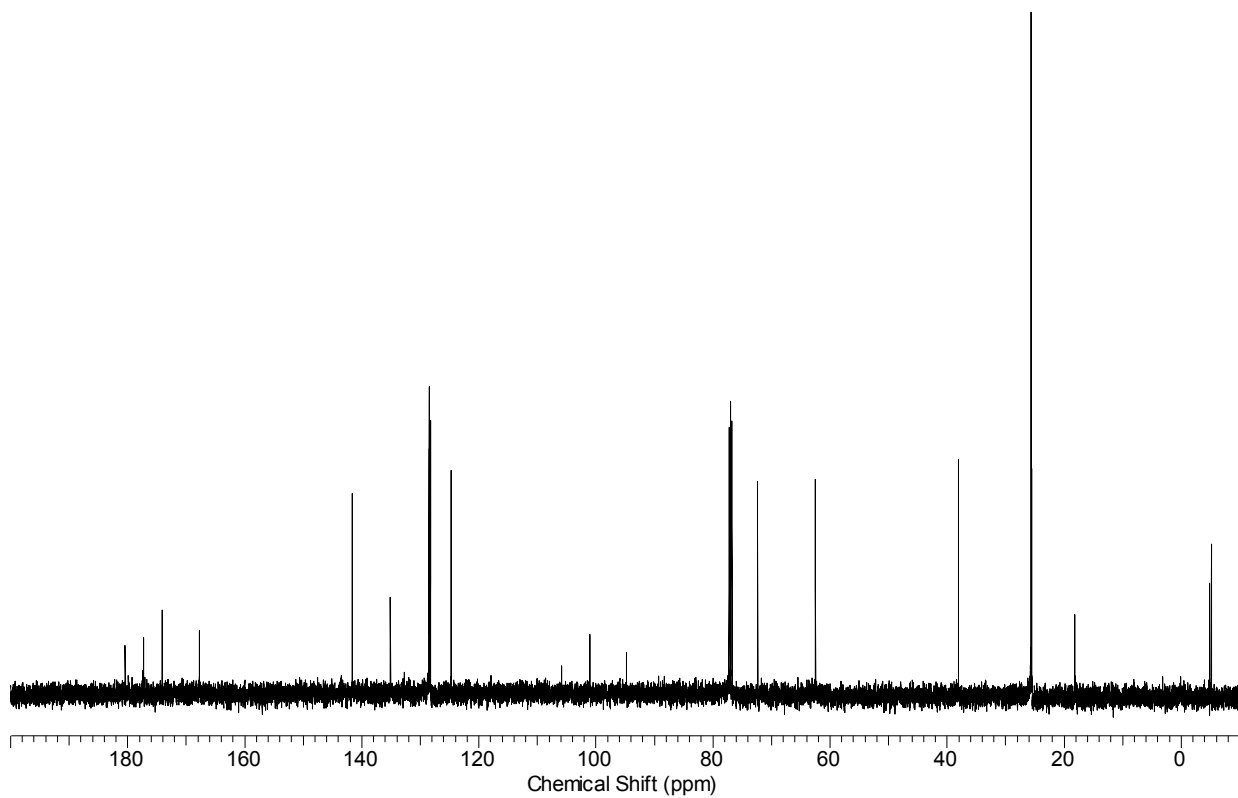
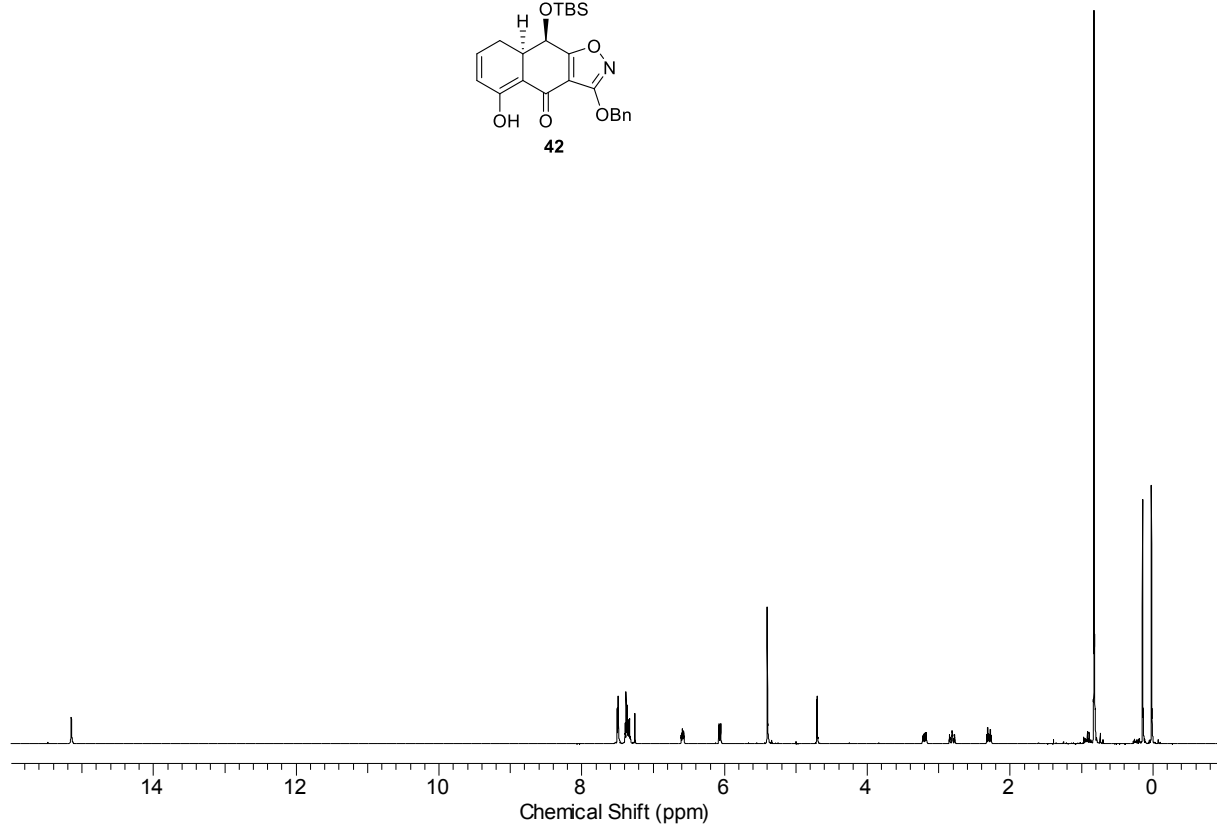
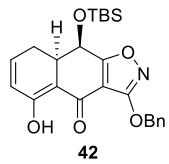
94

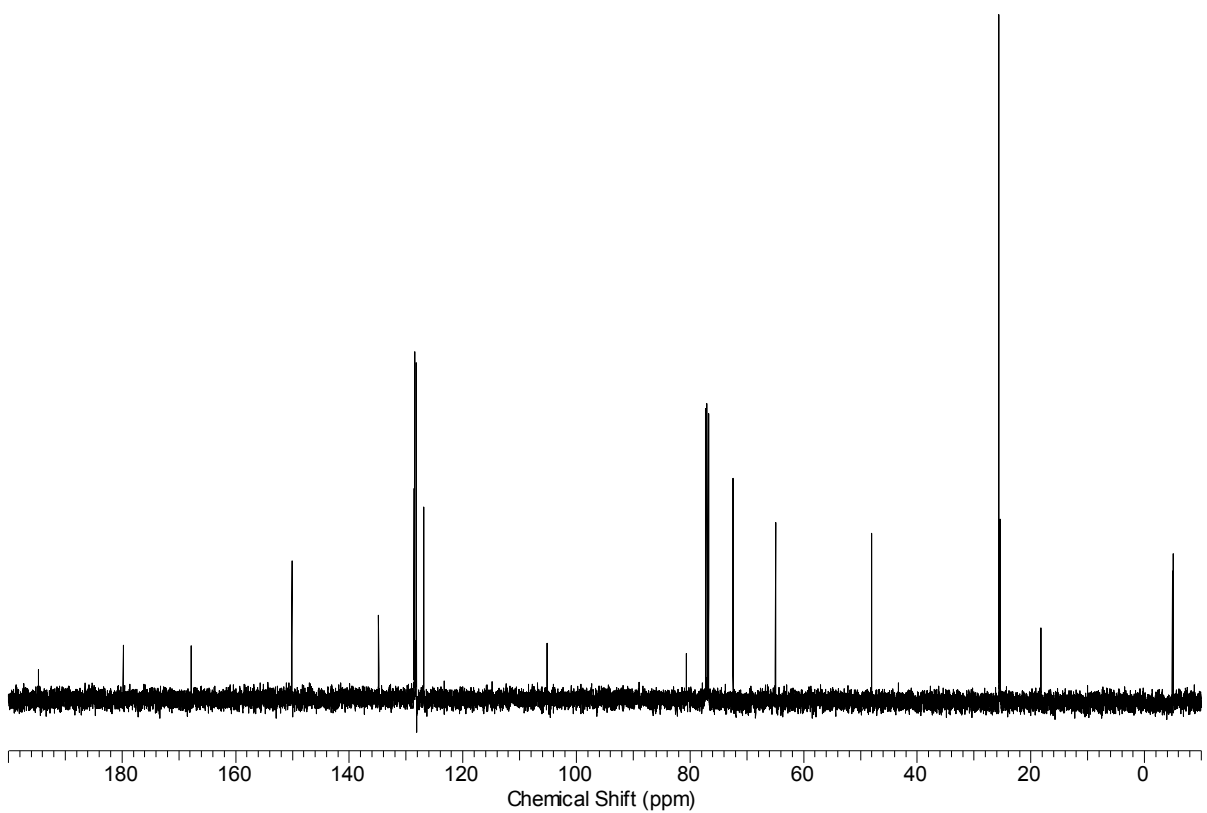
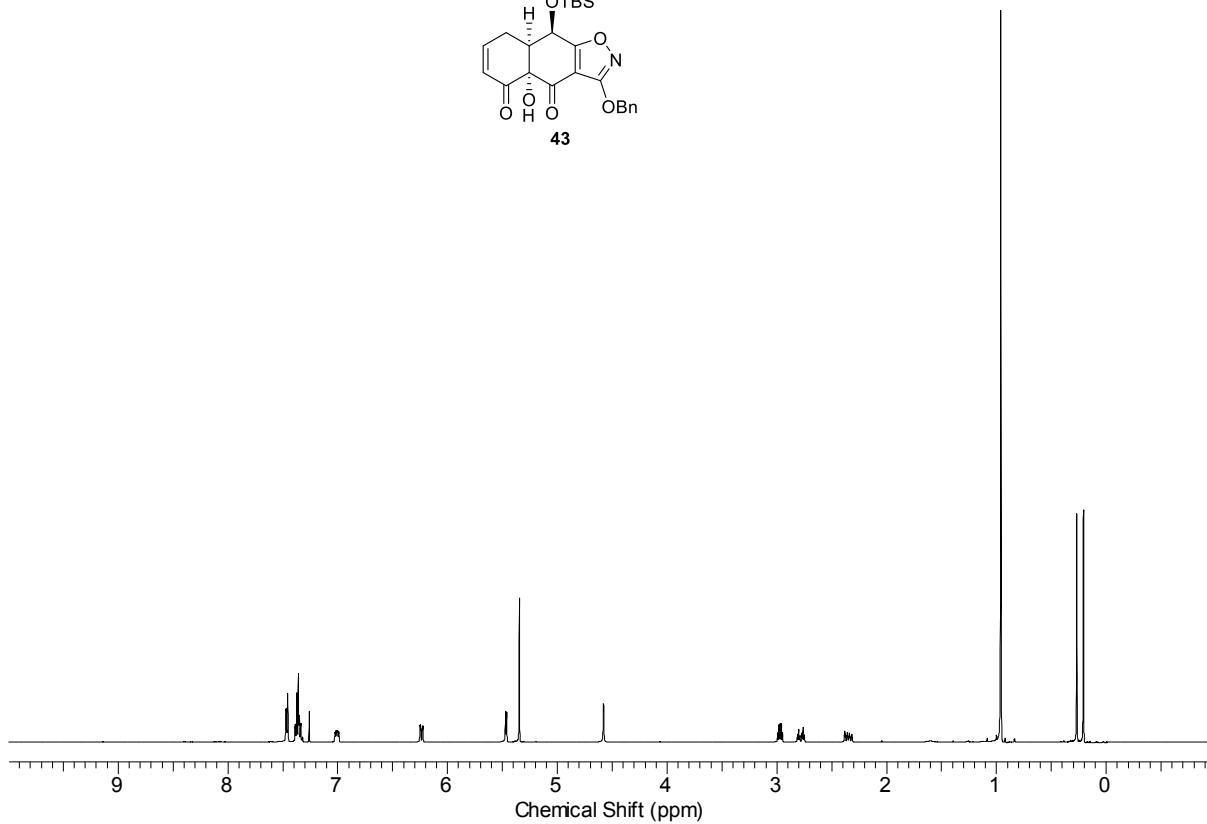
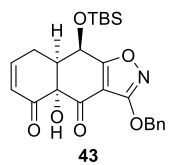


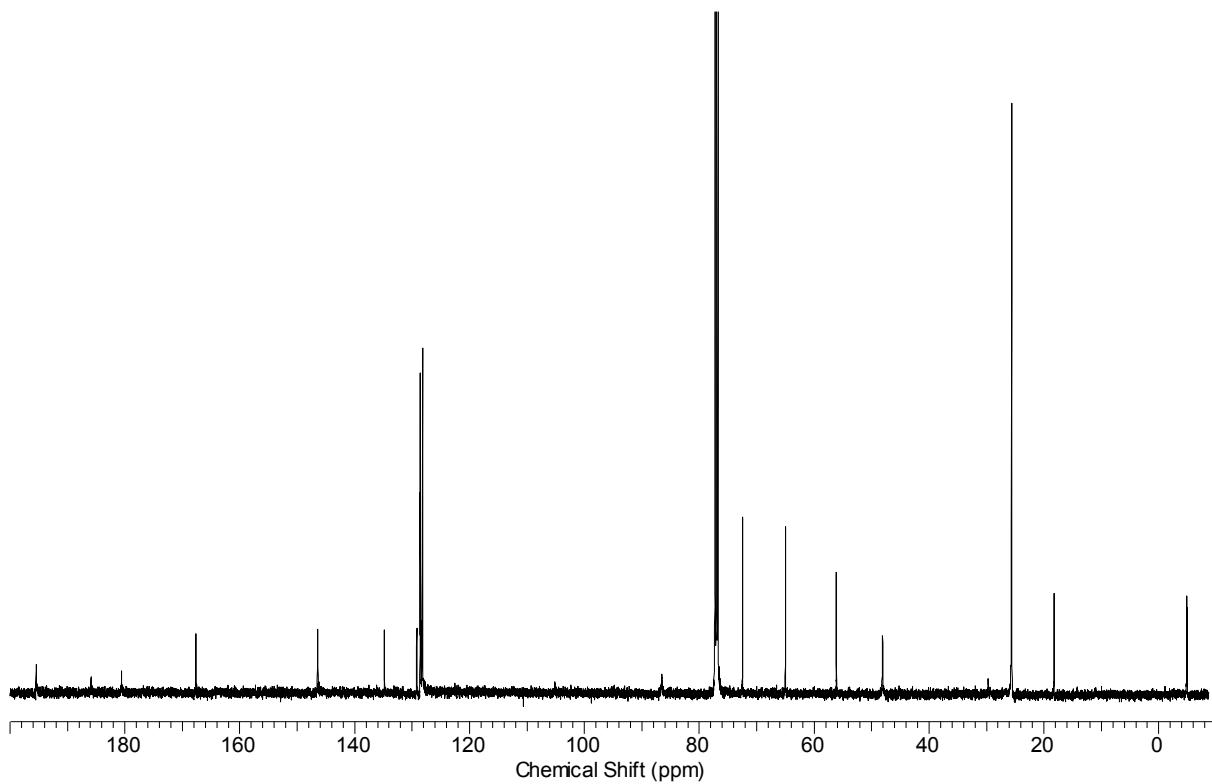
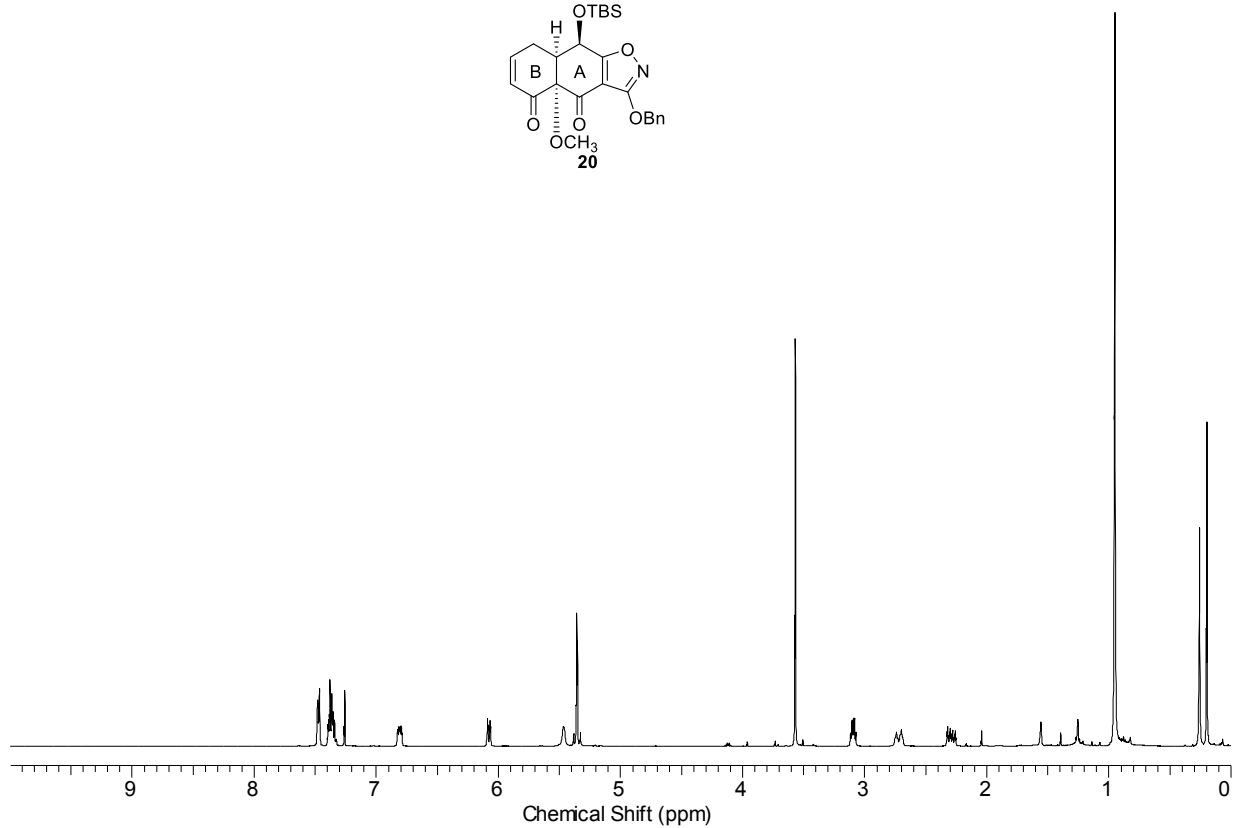
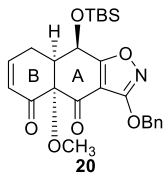


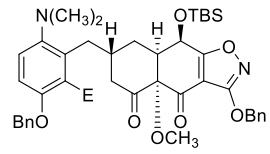






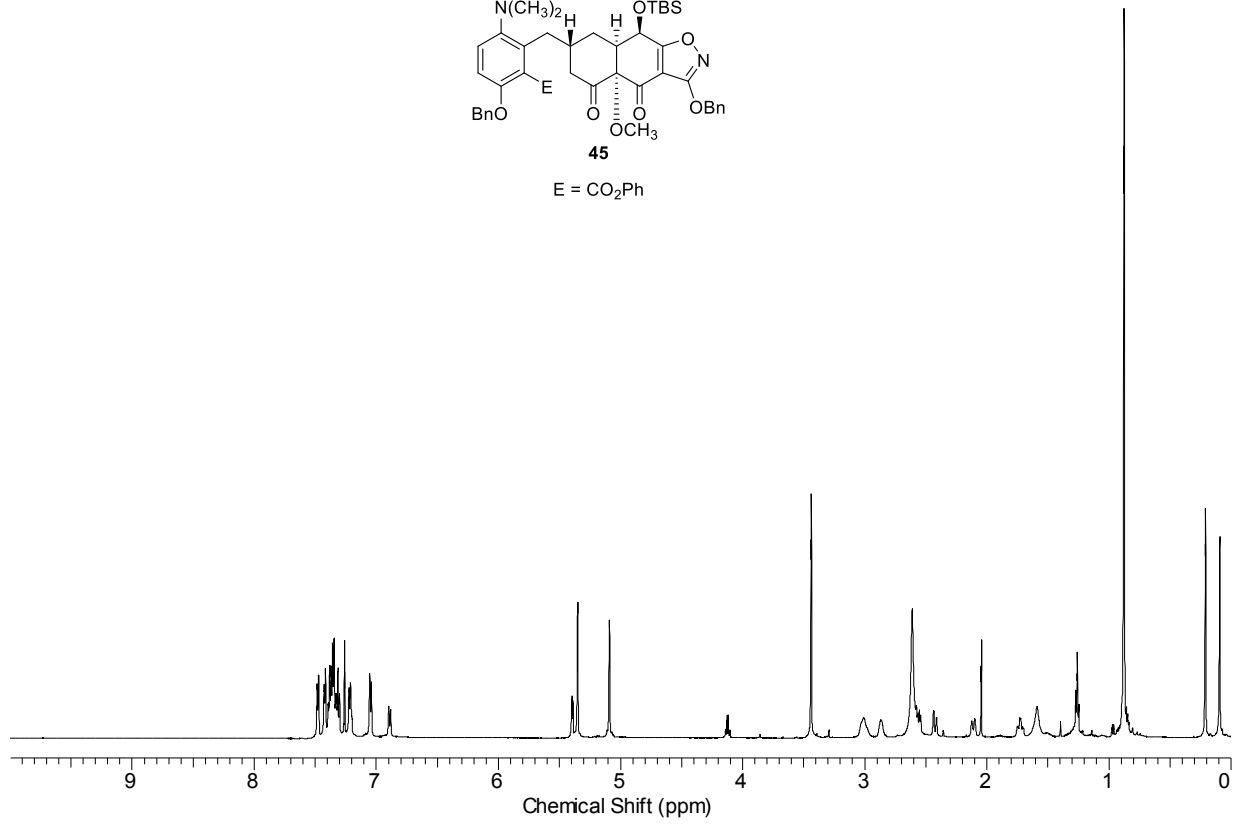


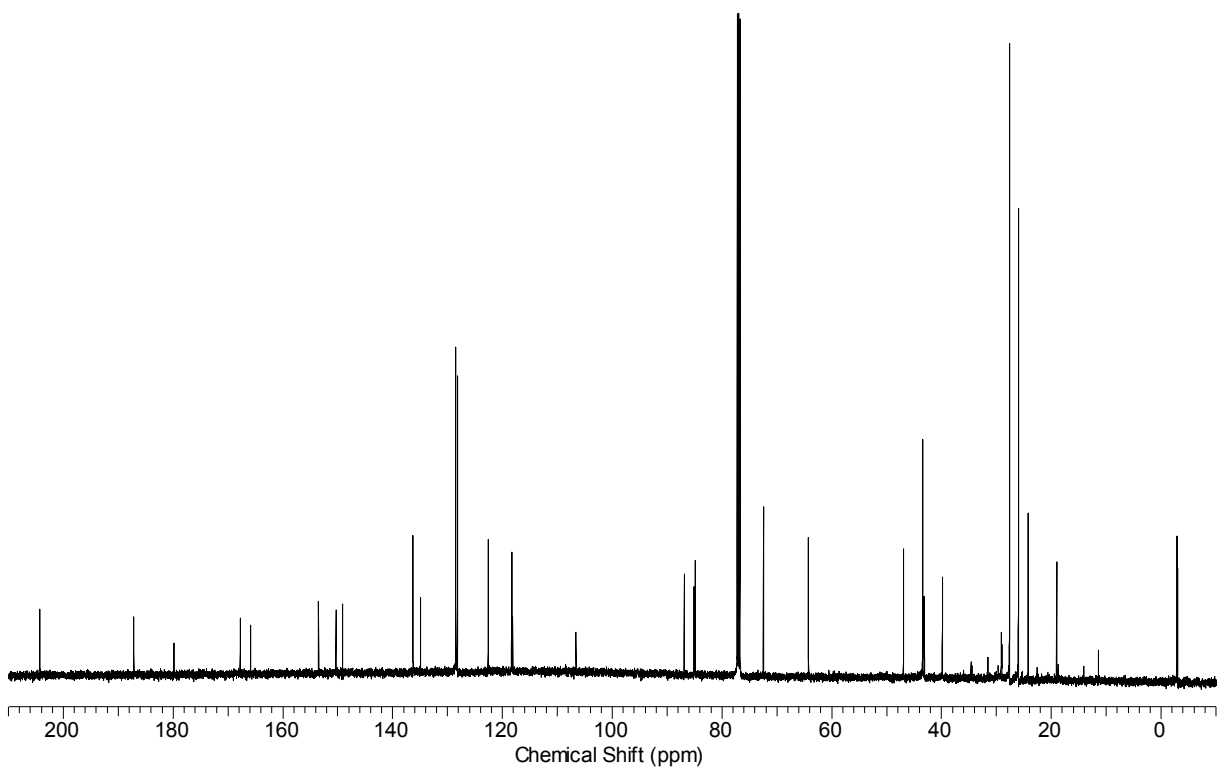
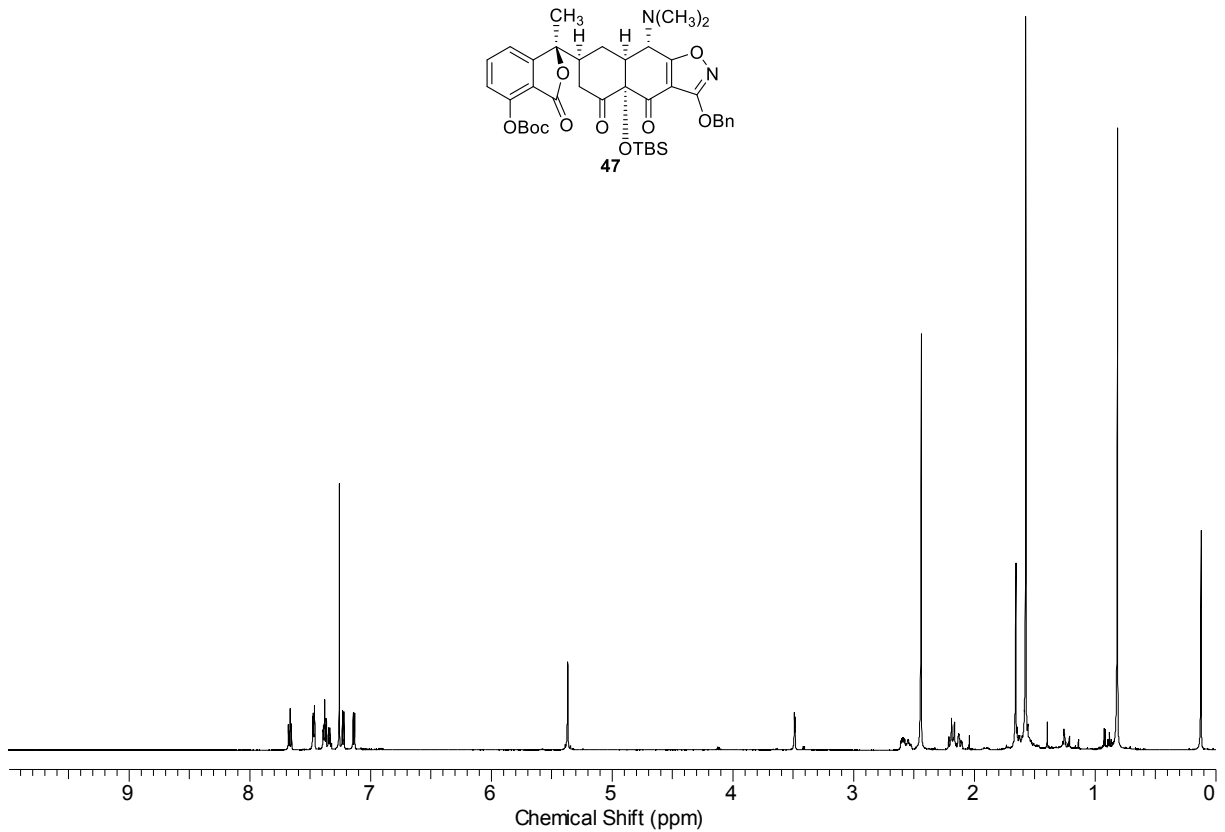
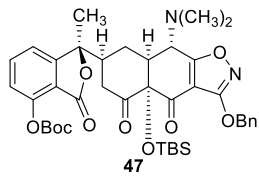


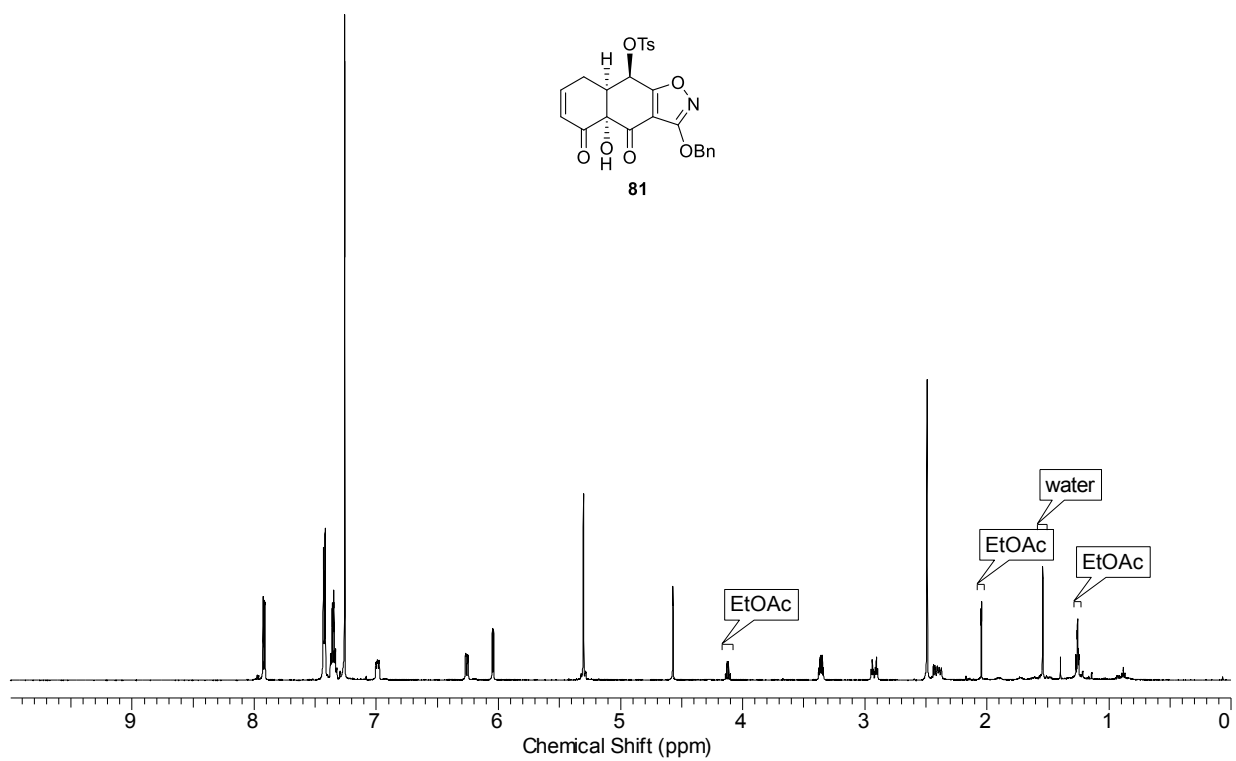
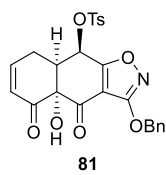
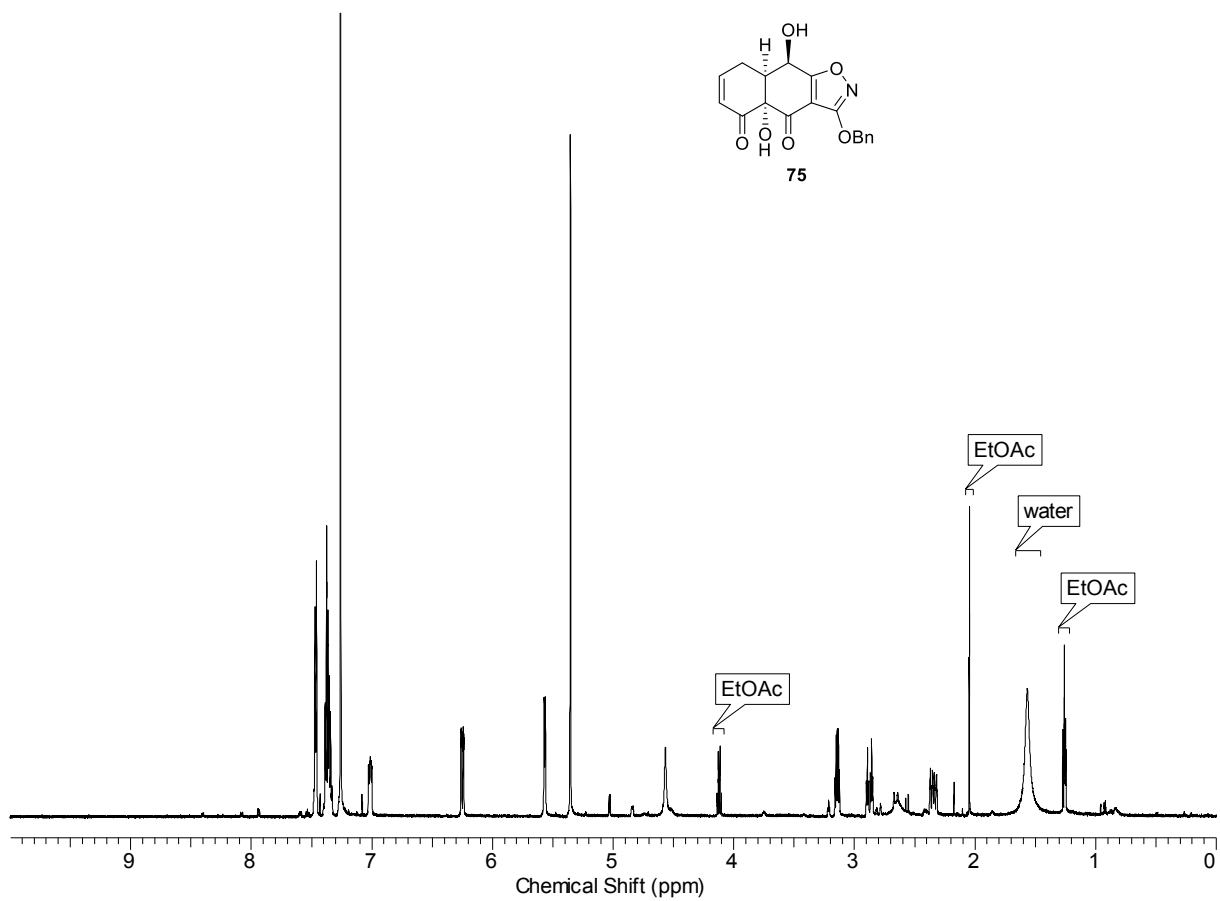
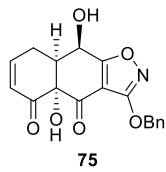


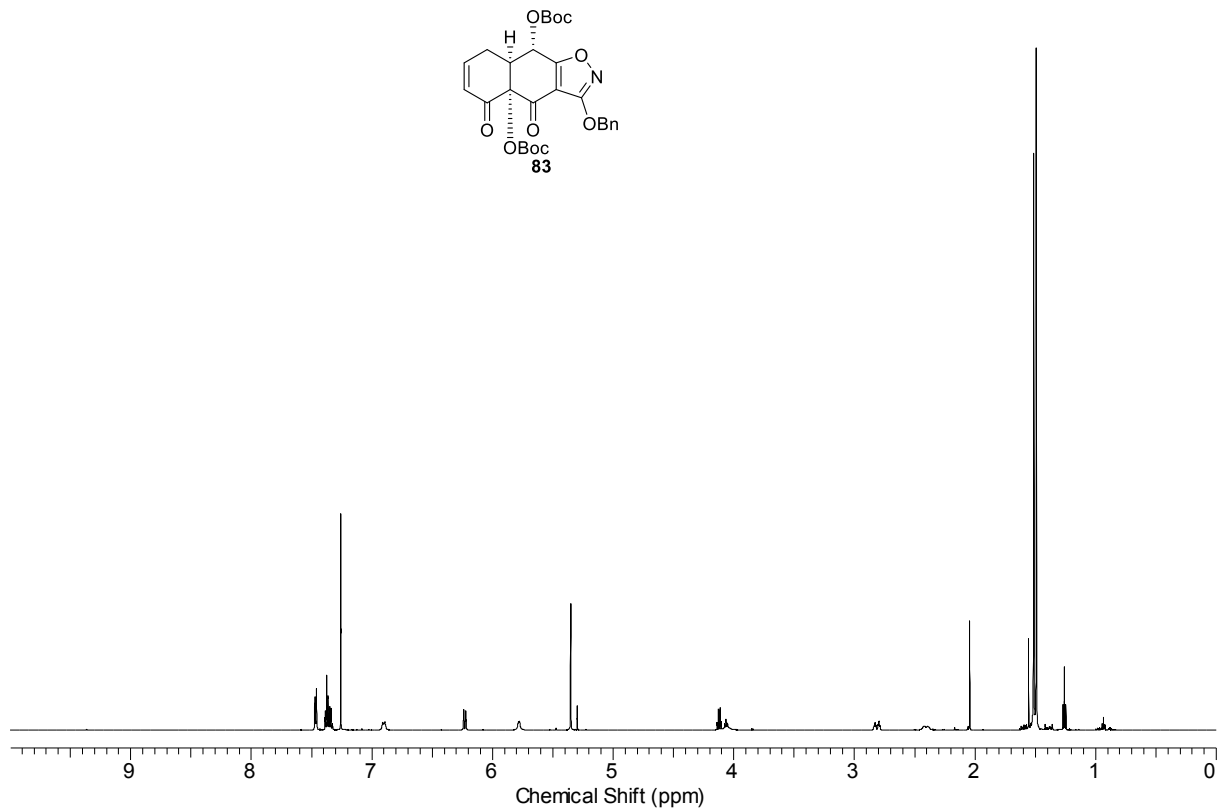
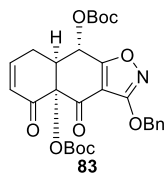
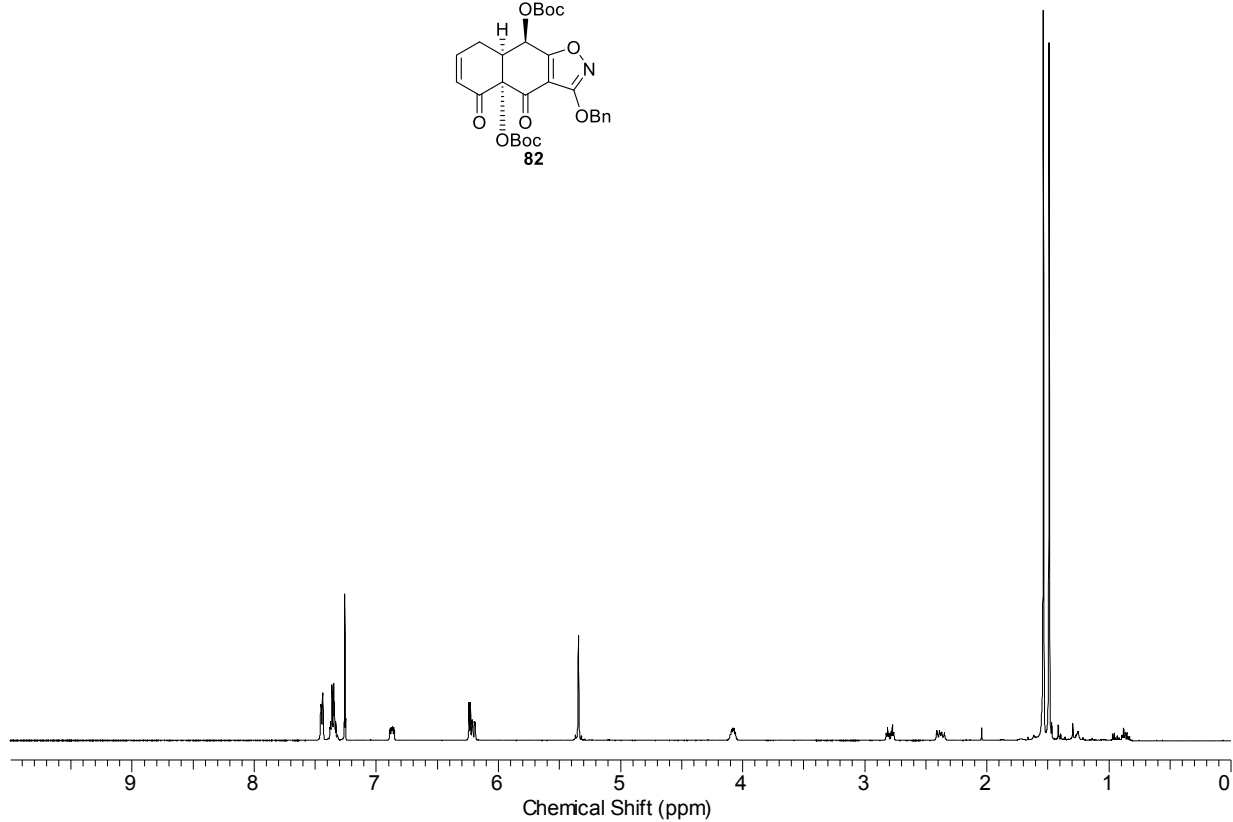
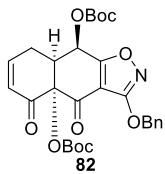
45

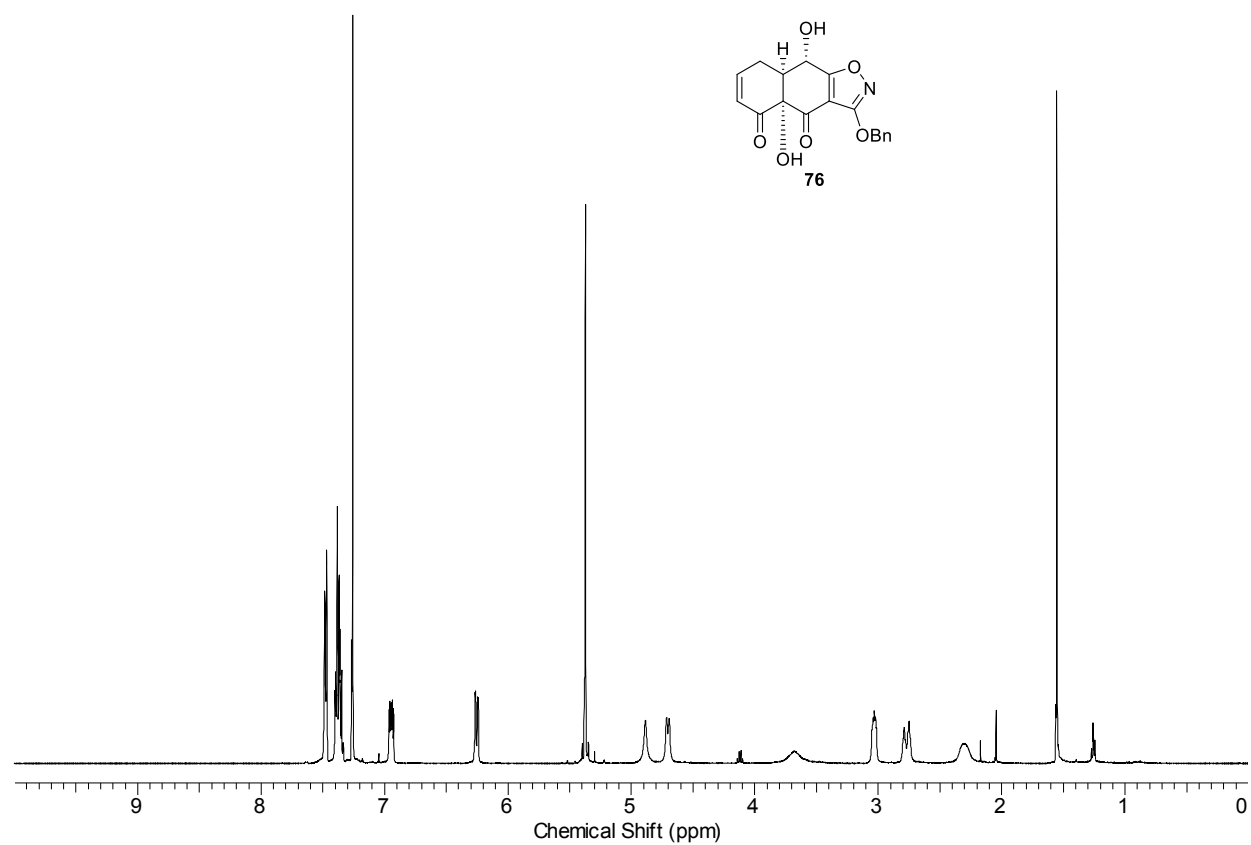
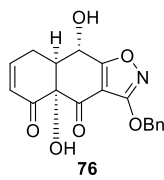
E = CO₂Ph

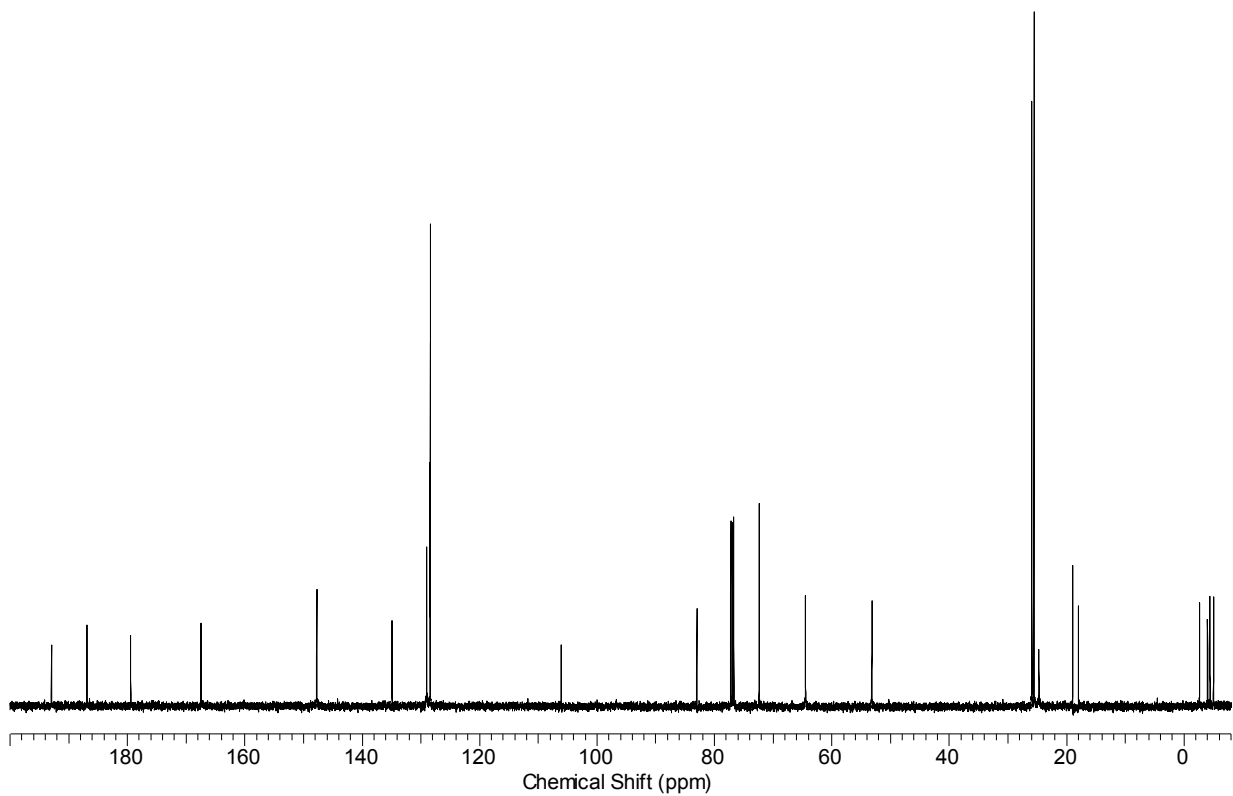
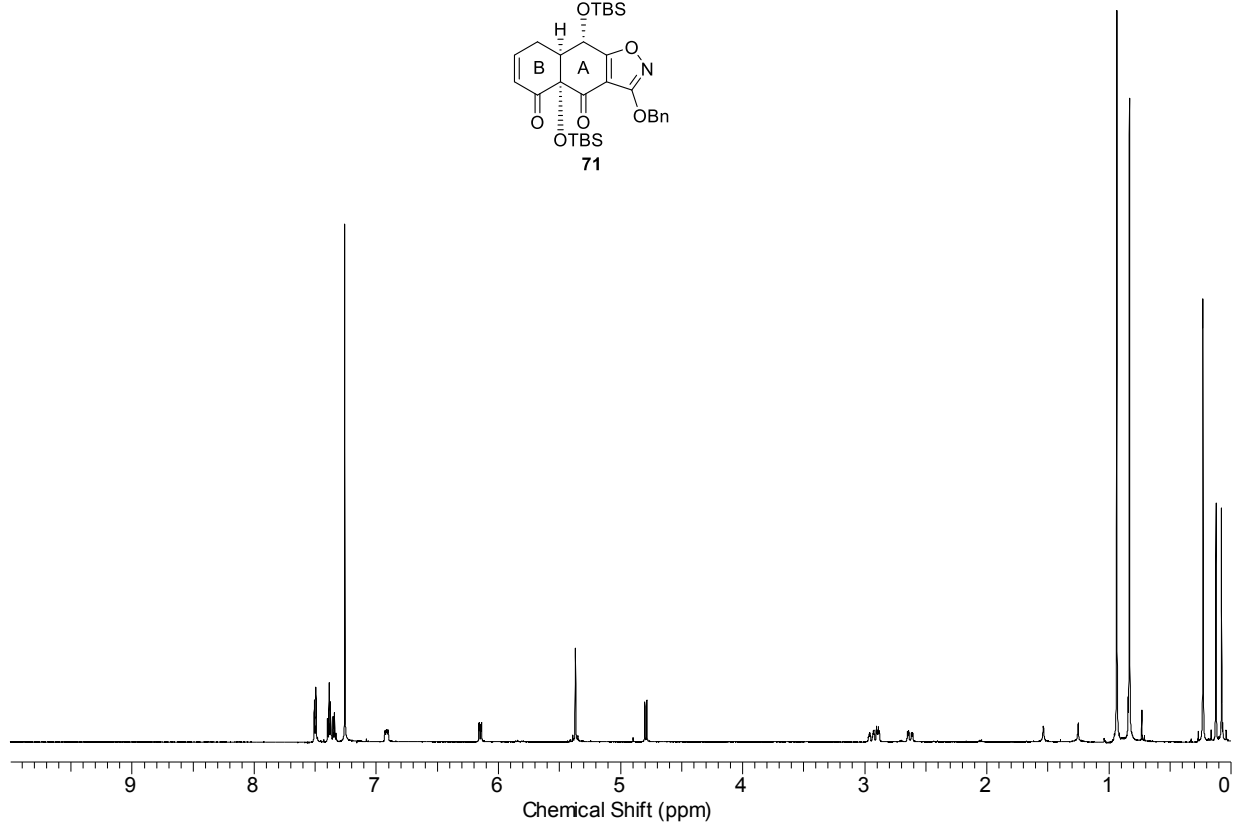
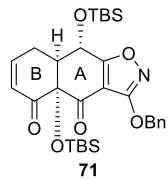


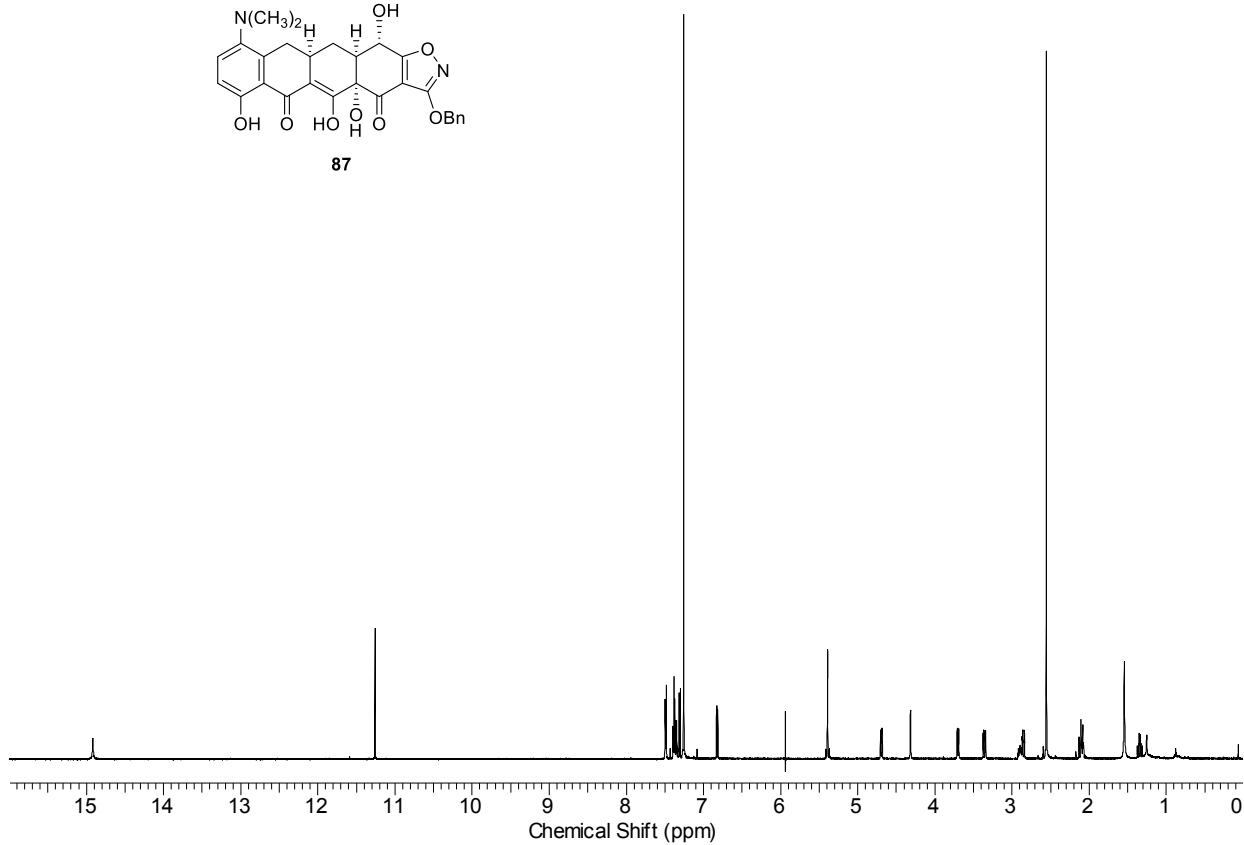
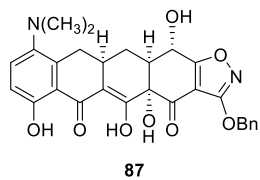
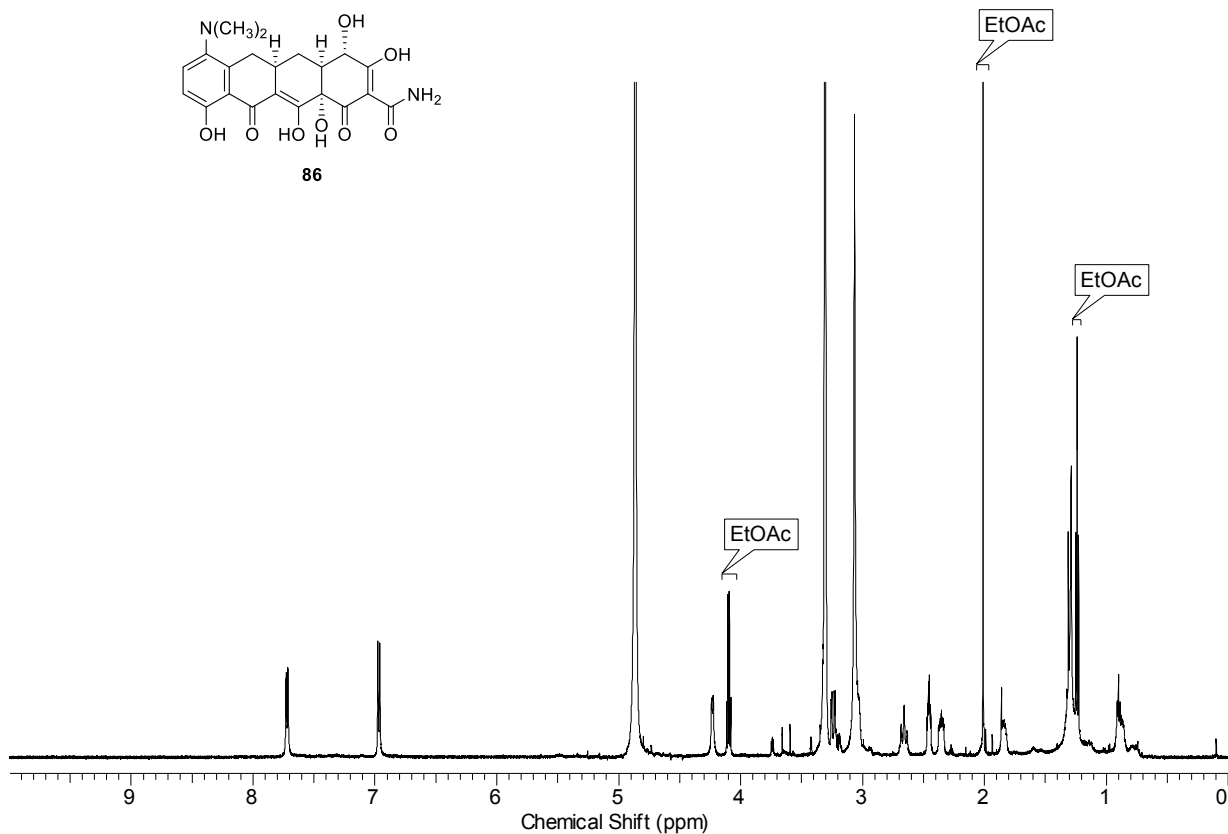
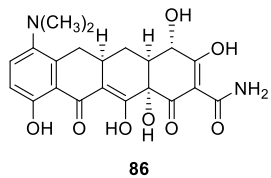


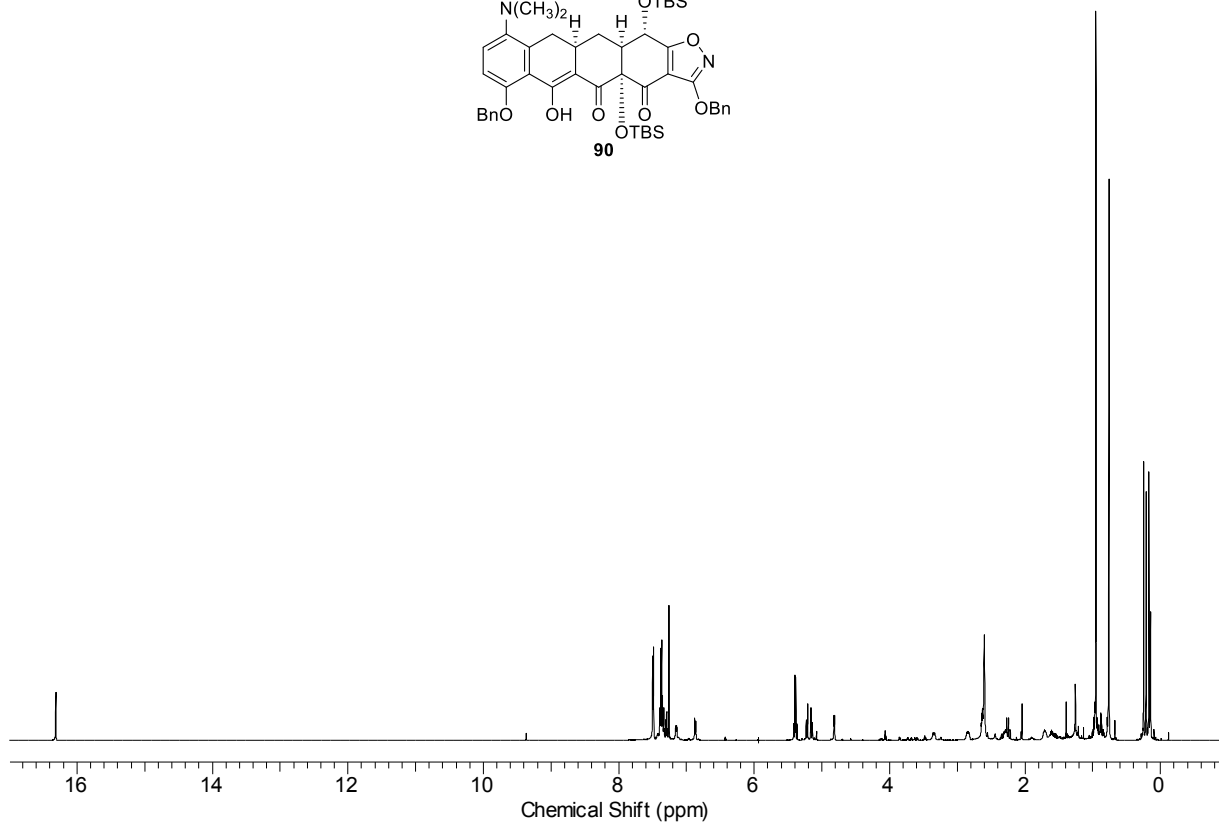
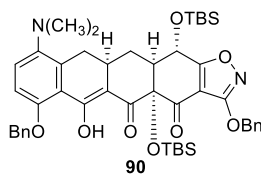
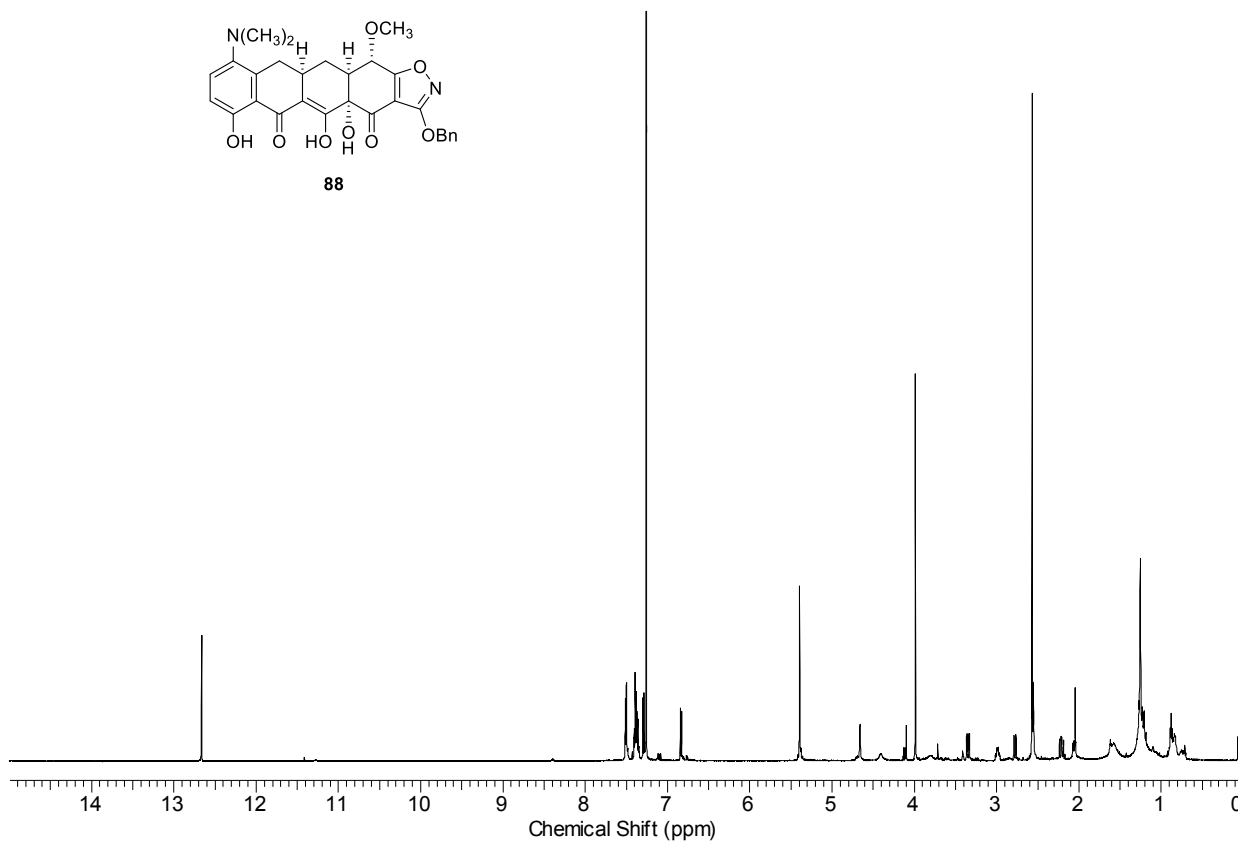
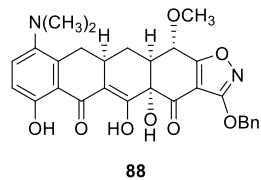


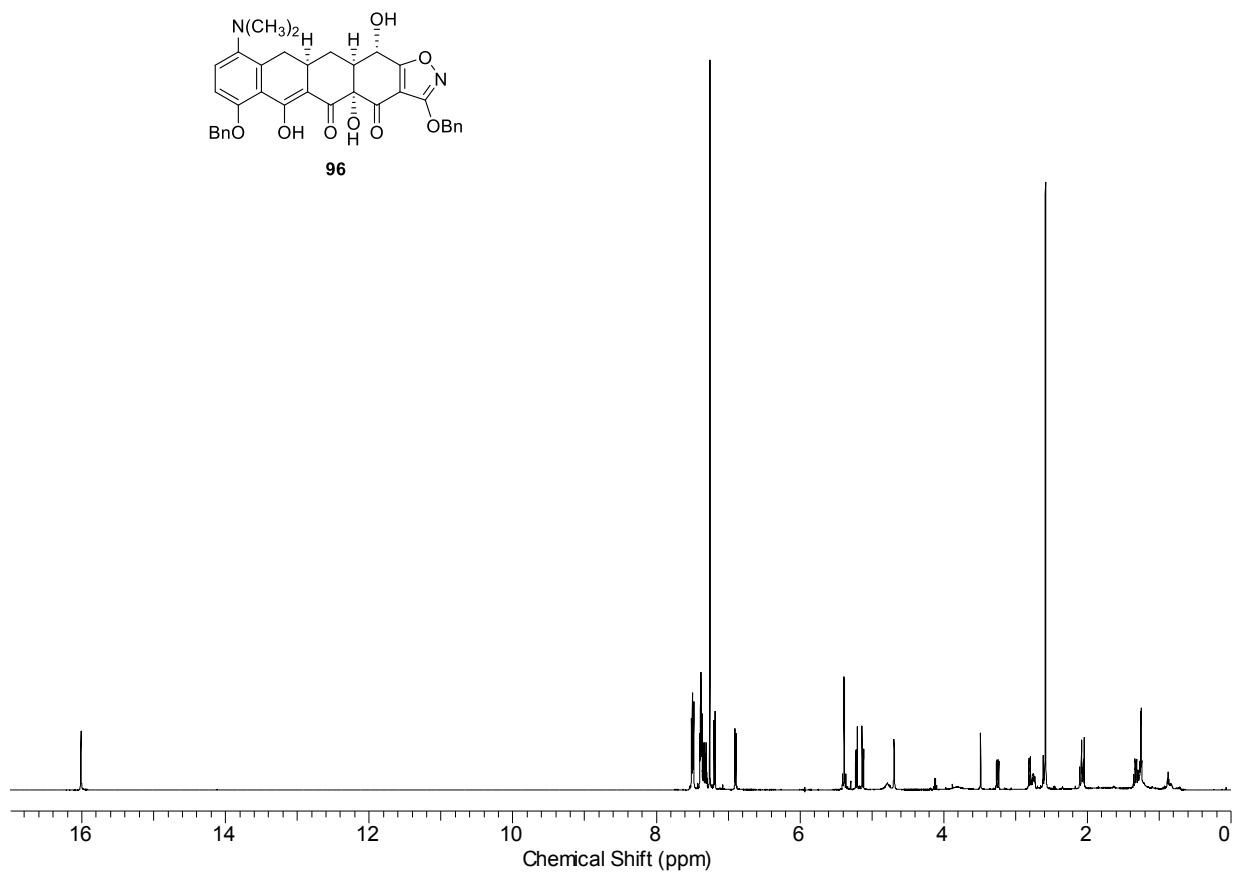
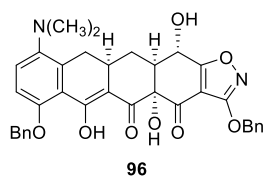
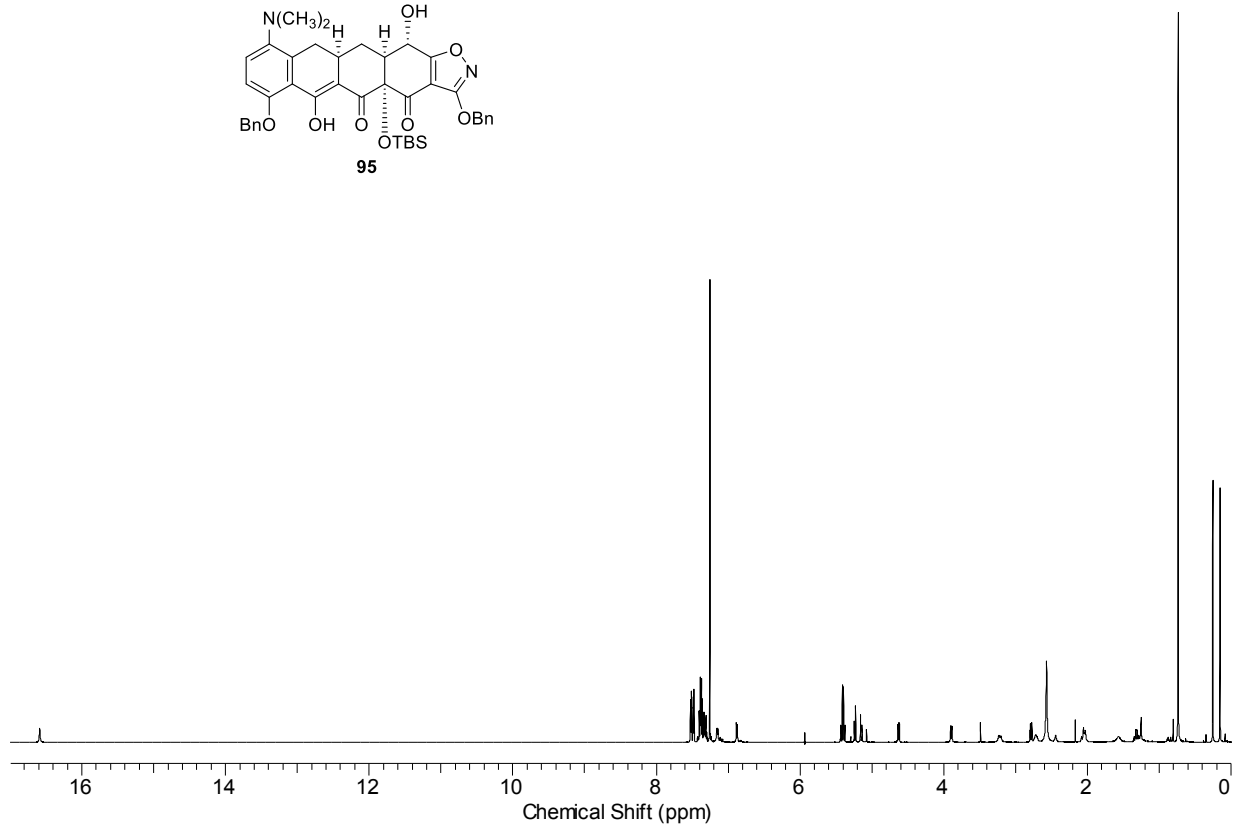
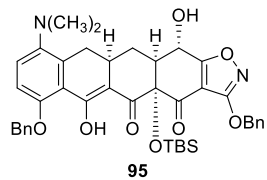


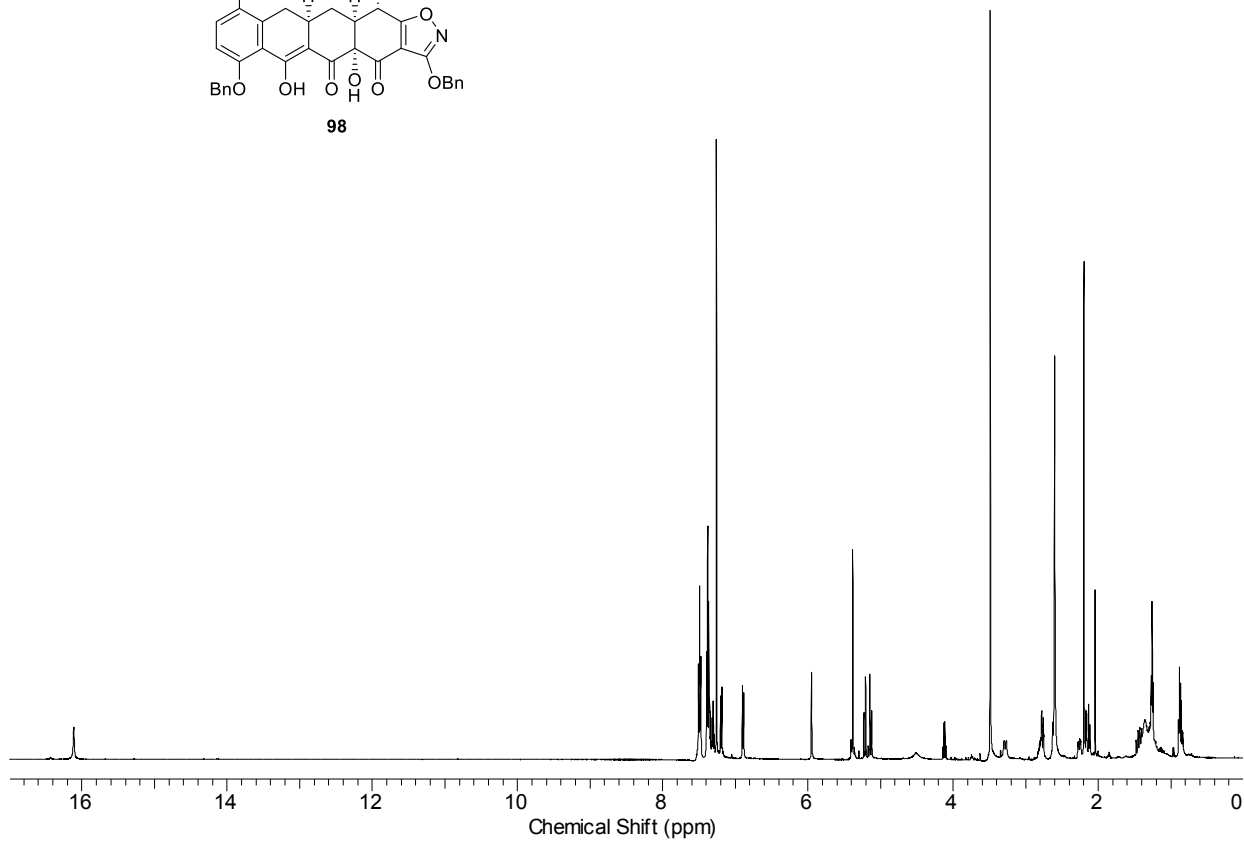
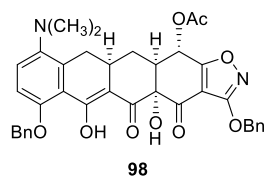
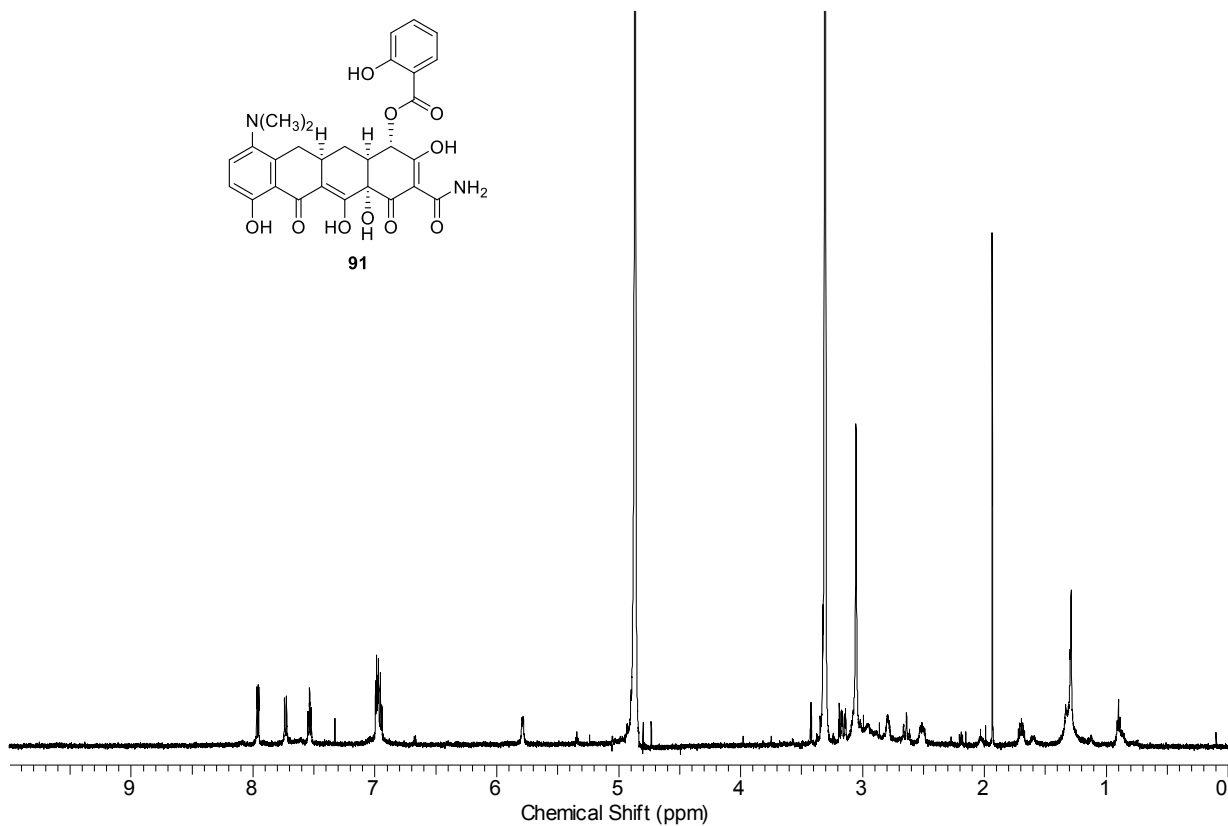
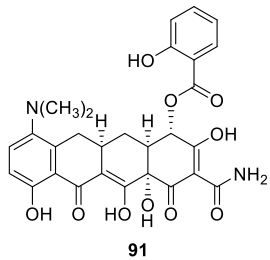


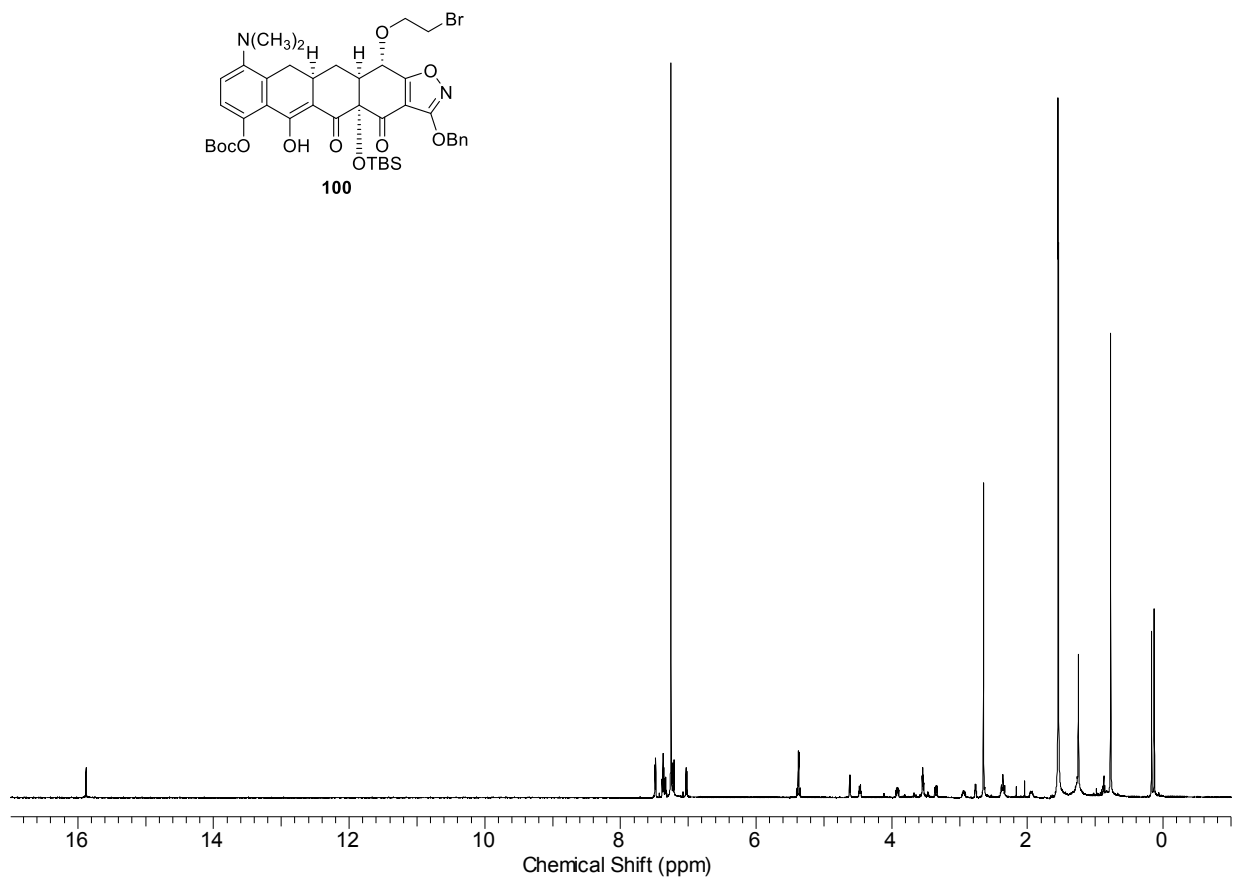
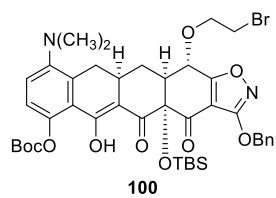
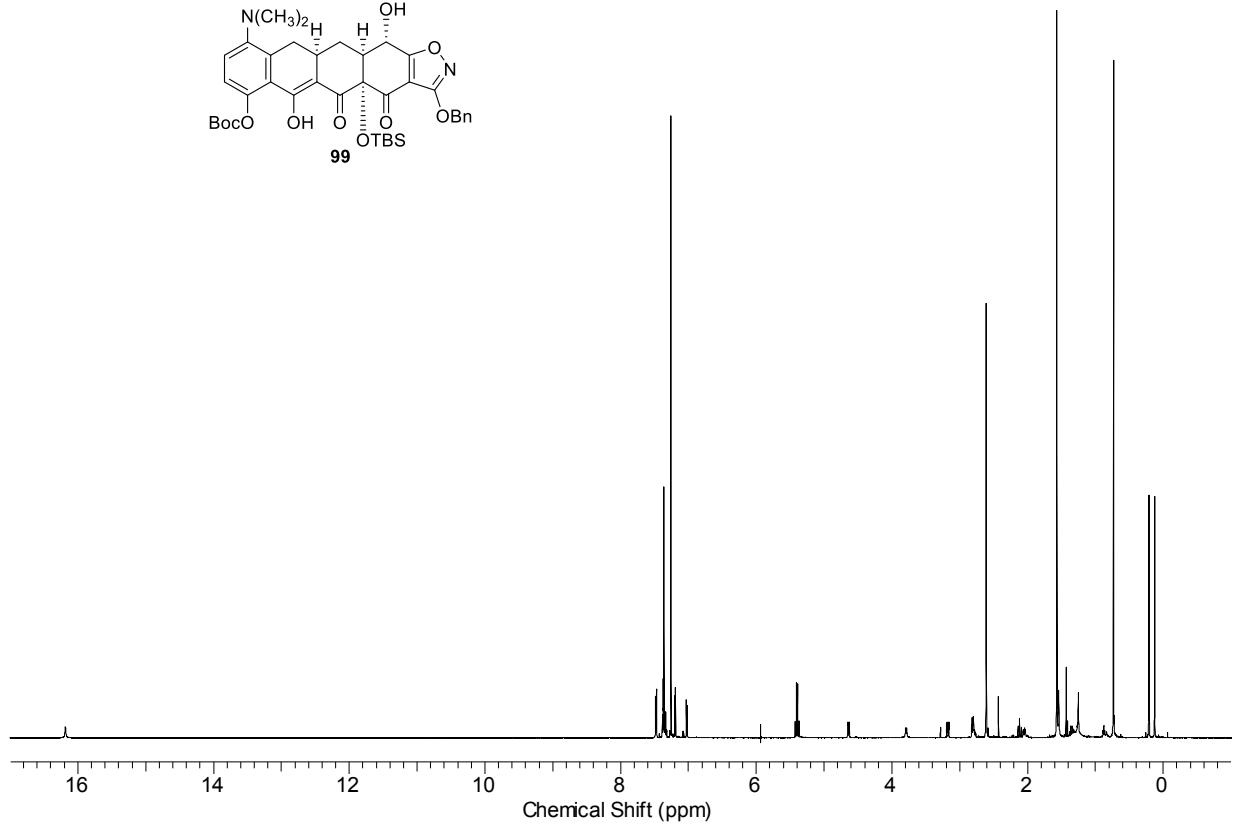
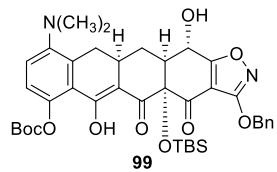


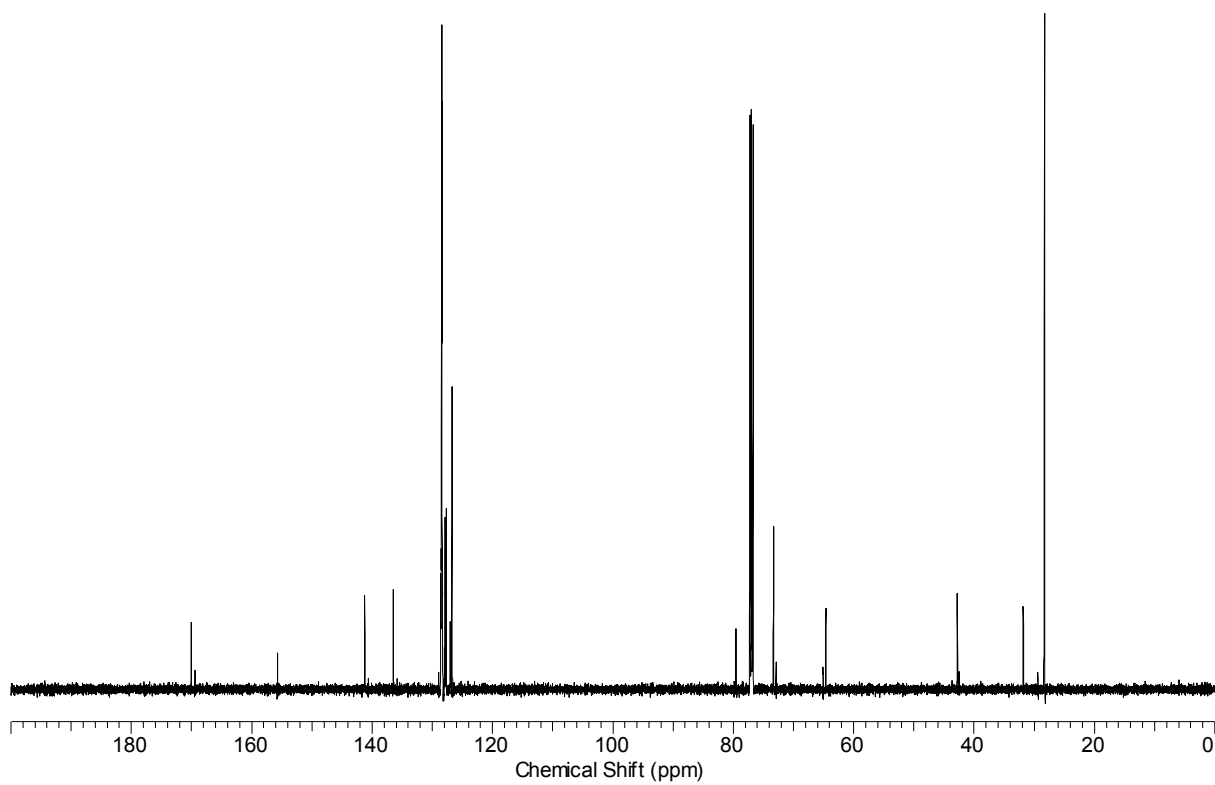
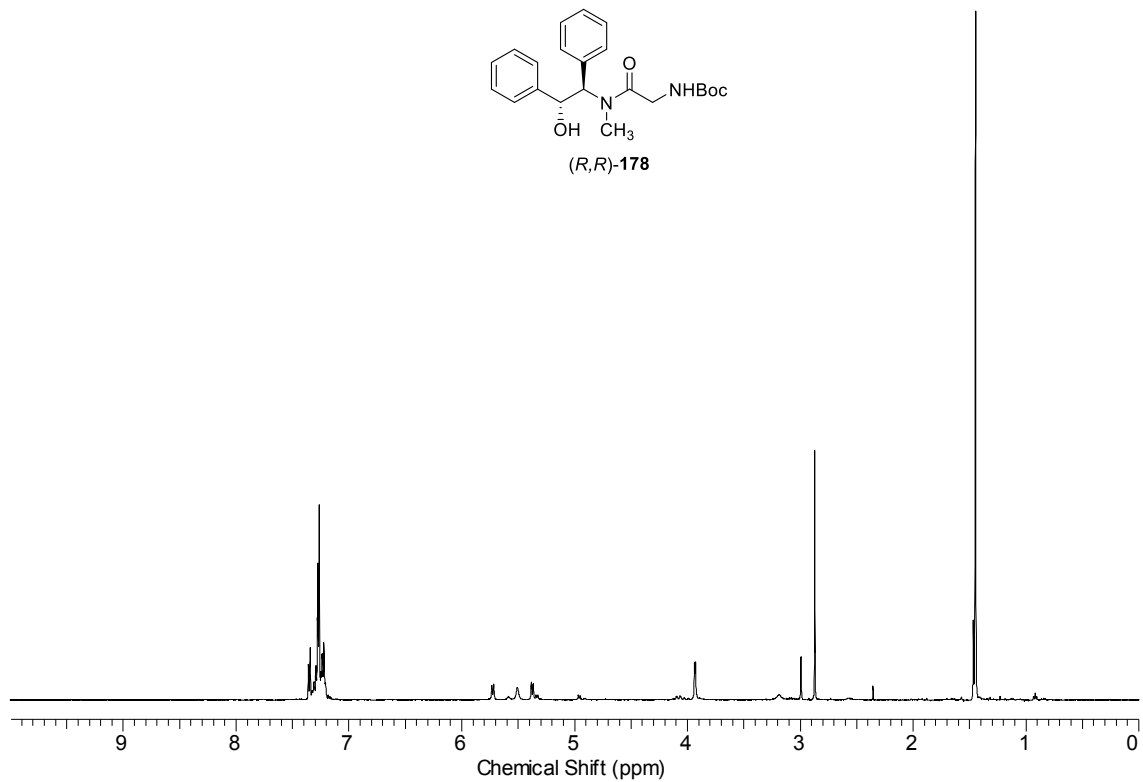
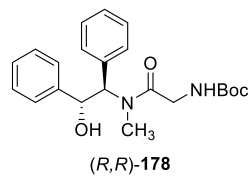


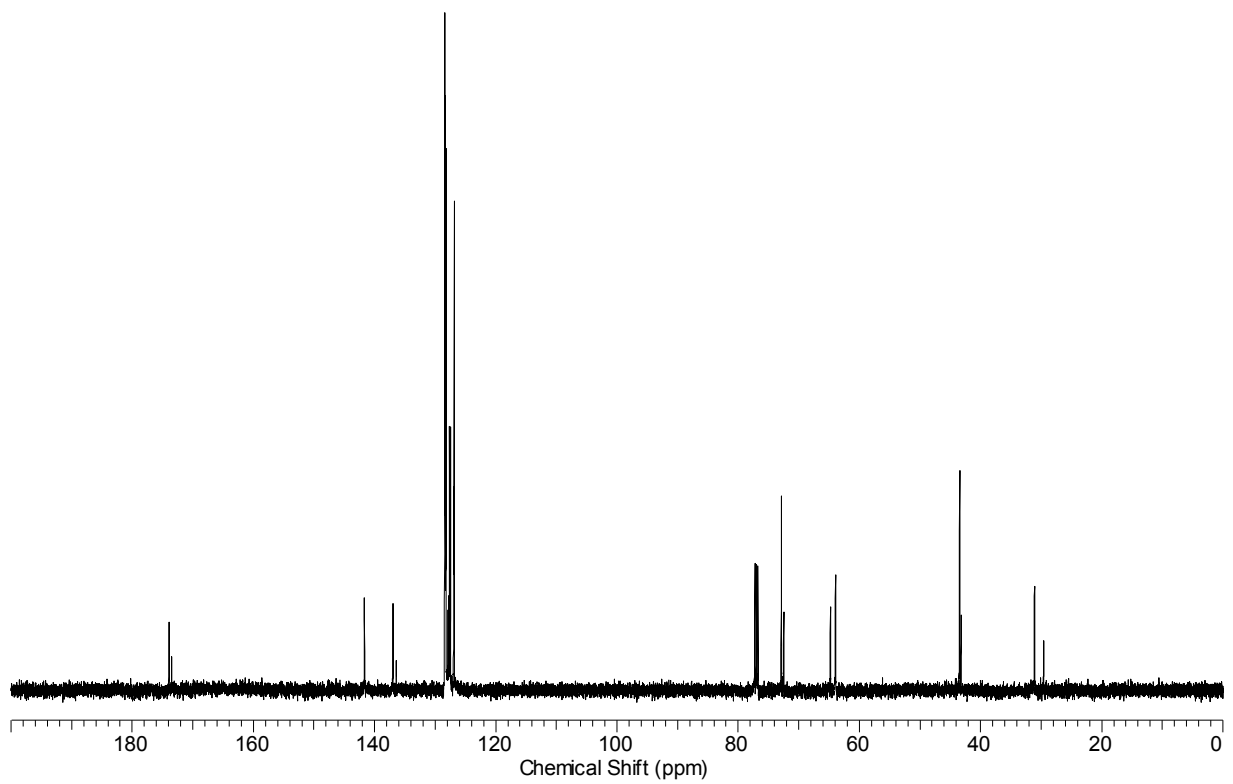
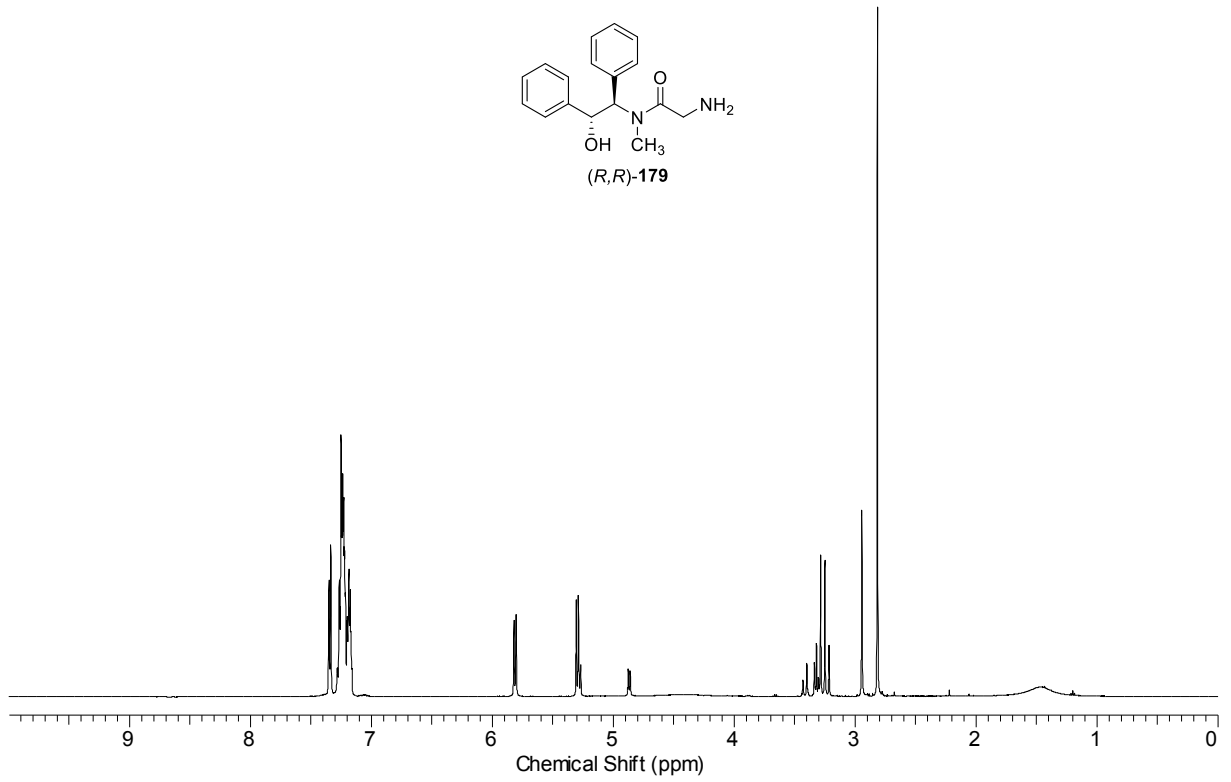
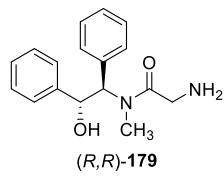


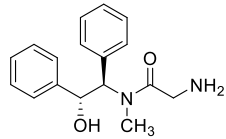












(*R,R*)-179

Saturation transfer experiments (1D gradient nOe)

